For Sandra.

The Measurement of the Rates of Hydroxyl Radical Reactions and the Prediction of Rate Constants in Alcohol Combustion.

by

Paul Graham Greenhill, B.Sc. (Hons.)

in the

Department of Chemistry

being a thesis submitted in fulfilment of the requirements

for the degree of

Doctor of Philosophy

University of Tasmania

July, 1986

This thesis contains no material which has been accepted for the award of any other higher degree or graduate diploma in any other tertiary institution, and to the best of my knowledge and belief, contains no material previously published or written by any other person, except where due reference is made in the text.

Abstract

Experimental studies on the reaction of OH with methanol and ethanol and theoretical studies on four of the reactions of the primary products of the reaction with methanol have been performed.

The rates of the reaction of OH ($X^2\pi$) with the alcohols methanol, ethanol and (D_3)methanol have been determined in the temperature ranges 250-800K , 250-460K, and at 293K respectively using the technique of flash photolysis-resonance absorption.

The results have been fitted to the following Arrhenius expressions:

$$k_{MeOH}(T) = (8.0 \pm 1.9) \times 10^{-12} \exp(-(664 \pm 88)K/T) \ cm^3s^{-1}$$

$$k_{CD_3OH}(293K) = (5.0 \pm 0.2) \times 10^{-13} \ cm^3s^{-1}$$

$$k_{EtOH}(T) = (12.5 \pm 2.4) \times 10^{-12} \exp(-(360 \pm 52)K/T) \ cm^3s^{-1}$$

The results obtained for the reaction with methanol are in agreement with some recent experiments. The results for the reaction with ethanol are approximately a factor of two higher than the only other determination of the temperature dependence, but are more in accord with some earlier room temperature measurements.

The methanol kinetic isotope effect k_H/k_D has been determined at room temperature and found to be 1.65. The presence of this effect indicates that the reaction at room temperature occurs largely by abstraction of the α-hydrogen.

The products of the pulsed photolysis of methanol and ethanol by a nitrogen flash lamp have been determined. Methanal (CH_2O) and the novel product dimethyl ether (CH_3OCH_3) were found from methanol. Ethanal (CH_3CHO) was the major product of ethanol photolysis with small amounts of CO, C_2H_2, as well as ethyl methyl ether($CH_3CH_2OCH_3$) and propanone (CH_3COCH_3).

Four of the reactions of the primary products have been studied by theoretical means in the temperature regime 300-2000K. The decomposition of the methoxy (CH_3O) and hydroxymethyl (CH_2OH) radicals have been investigated using RRKM theory with a Gorin model to describe the transition state. Fall off effects have been found to be important in the 1000K to 2000K region and corrections to the rate coefficients currently in use for these reactions have been determined to be necessary.

The recombination of H atoms with CH_3O and CH_2OH have been studied by a new technique based on transition state theory. These reactions are recombinations without barriers and proceed via a "simple fission" transition state. At large separation the transition states are described by a Gorin type hindered rotor model. However, as the separation decreases this model breaks down and an alternative is required.

We assume that the density of states calculated by microcanonical transition state theory must transform smoothly between large separation where the Gorin model is appropriate and the equilibrium geometry. The basis of the technique is the interpolation between the two well known regimes and choosing the contributions to the transition states using the variational criterium of minimisation of the sum of states.

The rate coefficients are then calculated by solution of the secular master equation.

The theory has been tested on the recombination of methyl radicals and reproduces the high pressure recombination rate coefficients to within a factor of two. It is considerably easier to perform than a normal transition state theory calculation and represents a useful technique for experimentalists and theoreticians wishing to predict rate constants for these types of reactions.

Acknowledgement.

I would like to express my sincere thanks to my supervisor, Dr. Barry O'Grady, for his help and guidance over the period since 1982. Without his perceptive comments and steady interest, much less would have been possible.

To Dr. Bob Gilbert also my sincere appreciation for the help given in the theoretical phases of the work. Thanks also for the several trips to Sydney and the provision of a bed and sustenance during those exhausting trips when even the beer came under scientific scrutiny.

To Kev, Mark, Tom, and the other students both here and in Sydney who enabled me to keep my sanity with occasional trips to the bar.

Thanks also to the staff of the department both technical and academic for their contributions whether it be electronic, mechanical, secretarial, glassblowing or just encouragement.

To my parents (both sets!), thank you for your encouragement and interest over the years.

Finally, but most importantly of all, to Sandra, my wife, for her patience and support (particularly her patience). The past three and a half years have been all the more pleasant and bearable since we have been together.

Chapter 1

Alcohol Combustion : An Overview.

Chapter 2

OH And Other Reactions Of Importance In Combustion.

Chapter 3

The Reaction Of OH With Methanol and Ethanol.

Chapter 4.

The Pulsed Photolysis Of Methanol and Ethanol.

CHAPTER 5

The Theoretical Prediction of CH_3O and CH_2OH Gas Phase Decomposition Rate Coefficients

Chapter 6.

Recombination Reactions: Variational Transition State Theory and The Gorin Model.

Appendices

Chapter 1

Alcohol Combustion : An Overview.

1.1 Introduction

The periodic nature of the "energy crises" has meant that research into alternative fuels has been periodic as well. Maximum effort has been expended at times when the crises are deepest. Out of this research only two fuels, methanol and ethanol, have emerged as viable alternatives to refined petroleum products. This is because they are generally readily obtainable and, in the case of ethanol, renewable from biomass sources.

1.2 History Of Alcohol Usage.

The first serious research into alcohol as a fuel was performed by Ricardo (1924) in 1922-24. This was prompted by the fear of an oil shortage as demand rose dramatically in the post war years but the shortage never eventuated and alcohol was never used to any great extent. However, the high anti-knock qualities of the alcohols were discovered at this time, a property which is desirable in any fuel.

Interest was not renewed until the oil crisis of the 1970's when the search for alternative fuels became very important again. The crisis did not reach the severity that many people feared but many lessons in conservation were learnt. Coupled with improvements in engine efficiency these advances once again slowed the urgency of the search for alternatives.

During this period many programs were instigated world wide, the most extensive being in Brazil where the government's objective was to achieve a level of 50% of automotive fuels from biomass sources. This has resulted in two forms of ethanol fuel being available as transport fuels to the general public; a 20% mixture with normal gasoline and a 95% azeotropic mixture with water. The former requires little engine modification but the latter requires quite extensive mechanical modification to the vehicle.

An approximately 10% mixture of ethanol with gasoline is also marketed in the U.S.A. as Gasahol and is also available in several other countries.

Methanol has not found the same degree of acceptance due to some properties which make it more difficult to handle as well as its corrosive nature. Its high vapour pressure at ambient temperatures provides storage problems overcoming evaporative loss and its solubility with water requires well controlled containment.

1.3 Sources Of Alcohols.

If continuing use is to be made of combustion as a major energy source then the fuel used must be readily and cheaply available and preferably renewable. Of the alcohols, ethanol is the most easily obtainable from the fermentation of sugar from sugar cane and sugar beet. The crops are readily cultivated and as such represent a highly renewable feedstock. The cane and beet crops are suitable for many agricultural areas but before they can be grown expressly for the purpose of ethanol production the infrastructure

for refining and sale must be created. Also the technical modifications of engines must be performed which requires a change of strategy by vehicle manufacturers.

At the present time the cost of production of ethanol from sugar is approximately 3 to 4 times that of the cost of petrol. The price difference means that the benefits of (possible) self sufficiency must be weighed against the increased internal economic cost.

Methanol is the other logical candidate but its production is more complex being the catalytic reduction of carbon monoxide by hydrogen. However, the technology is well known and operates in a continuous mode with well characterised catalysts. The feedstocks CO and H_2 are readily obtainable from steam reformation of natural gas (CH_4) over nickel catalysts. The resultant CO/H_2 mix along with some CO_2 is called synthesis gas and in general is used directly as feed for methanol production. Dependent upon pressure some CO_2 may be added to provide a better stoichiometric ratio of $H_2/(2CO+3CO_2)$.

1.4 Previous Investigations.

There have been very few experiments performed on the combustion of alcohols with a view to elucidation of the chemistry of the complex proceses involved. Those that have been performed have mainly considered methanol due to the simpler chemistry associated with the C1 species. The experimental studies have been performed in two groups. The early experiments (Bell and Tipper, 1956, 1957; Bone and Gardiner, 1936; Bonev, 1972; Cullis and Newitt,

1955, 1956, 1957, 1958; Fort and Hinshelwood, 1930; Kane, et al. 1937; Vanpee, 1953) were on the slow oxidations of alcohols under static conditions. These covered the temperature range 300-600K. The slow oxidations in general were followed by pressure change measurements and wet chemical analysis of products at varying times. Various effects were investigated, such as the influence of different surface coatings and added products as well as those due to variation of the initial concentrations of reactants.

The second group in general used more recent techniques and covered temperature regions more in keeping with combustion regimes of 1000-2000K. (Akrich, et al., 1978; Aronowitz, et al., 1977; Aronowitz, et al., 1979; Bowman, 1975; Cathonnet, et al., 1979; Cooke, et al., 1971; Dove and Warnatz, 1983; Gibbs and Calcote, 1959; Gulder, 1982; Metgalchi and Keck, 1982; Tsuboi and Hashimoto, 1981; Vandooren and Van Tiggelen, 1981; Westbrook and Dryer, 1979, 1980; de Wilde, et al., 1968, Wiser and Hill, 1955)

Two main techniques have been used, flame studies and shock tube experiments. Simple pyrolysis has also been used as a way of examining the processes which are important to combustion but without the complications of oxygenated species present. Burning velocities of flames have been investigated largely by engineers to aid in design of combustion chambers as well as the simple macroscopic characterisation of flames. Finally, kinetic modelling to both reproduce the observed results and to obtain rate constants previously unknown or uncertain has been used quite extensively in many studies.

1.5 Methanol

1.5.1 Slow Oxidations.

The major products of the oxidation of methanol were CO, H_2O and lesser amounts of $CO_2$and H_2 (Bell and Tipper, 1956). CH_2O and H_2O_2 were identified as intermediate stable products. The results of this study were qualitatively explained by a seven reaction mechanism involving chain propagation by the hydroperoxy radical, HO_2.

$$CH_3OH + O_2 \text{ -----> } CH_2OH + HO_2 \quad 1.1$$

$$CH_3OH + HO_2 \text{ -----> } CH_2OH + H_2O_2 \quad 1.2$$

$$CH_2OH + O_2 \text{ -----> } CH_2O + HO_2 \quad 1.3$$

$$CH_2O + O_2 \text{ -----> } CHO + HO_2 \quad 1.4$$

$$CHO + O_2 \text{ -----> } CO + HO_2 \quad 1.5$$

$$CH_2O + HO_2 \text{ -----> } CHO + H_2O_2 \quad 1.6$$

$$HO_2 + O_2 \text{ -----> inert products.} \quad 1.7$$

The small amounts of H_2 found were probably formed from decomposition of the hydroxymethyl radical (CH_2OH), HO_2 or CHO with subsequent reaction by hydrogen abstraction on any of the hydrogen containing species.

Other studies produced similar results.(Bone et .al, 1936; Bonev, 1972; Fort et al., 1930; Kane et al., 1937; Vanpee, 1953) Notably though, there is no route for the inclusion of the methoxy radical (CH_3O) which has recently been shown to be important at

higher temperatures and certainly would have a significant role at lower temperatures.

1.5.2 High Temperature Studies.

1.5.2.1 Burning Velocities.

In general, the measurement of burning velocities does not provide useful kinetic data but is obviously of significance in the design of combustion chambers and the characterisation of the combustion of fuel-air mixtures.

However, kinetic models coupled with transport equations are capable of predicting burning velocities and this has beem done by Dove and Warnatz (1983) and Westbrook and Dryer (1980). Both these groups have modelled the work of various groups who have measured burning velocities. (Wiser and Hill; Gulder; Gibbs and Calcote; Metgalchi and Keck)

The model used by Westbrook and Dryer (1980) was taken directly from the one used by them to model combustion of methanol in systems other than flames. (Westbrook and Dryer, 1979.) The reason for this is that a model which is comprehensive enough should be capable of modelling all of the phenomena associated with the particular system under investigation.

Neither group has distinguished between the primary radicals formed, CH_3O and CH_2OH, in their models and further work on the reactions of these radicals and also HCO has been recommended (Dove and Warnatz.)

1.5.2.2 Oxidation.

Methanol oxidation has been studied almost exclusively using two general techniques, shock tubes and flames.

Early shock tube work by Cooke, et al. (1971) covered the range 1570K to 1870K and pressures from 200 to 300 torr. The formation of $^2\Sigma^+OH$ and CO_2 was followed by emission spectroscopy at 306.7 nm. and 4.3 μm respectively. Emission from $^2\Delta CH$ was looked for at 413.5 nm but not observed.

Comparisons were made between ignition delays for methane, methanol, ethanol, and ethane which roughly followed changes in bond dissociation energies. The low CH^* yield was assumed to be because of the low level of C_2 molecules.

$$C_2 + OH \text{ ---> } CH^* + CO \qquad 1.8$$

Very high levels of OH^* were observed and also a severe temperature dependence for the appearance of OH with an apparent activation energy of 348 $kJmol^{-1}$. This could not be explained by

$$CH + O_2 \text{ ---> } CO + OH^* \qquad 1.9$$

but is more likely to be the result of direct CH_3OH dissociation.

$$CH_3OH \text{ ---> } CH_3 + OH \quad \Delta H = 382 \text{ kJmol}^{-1} \qquad 1.10$$

Bowman (1975) has performed a much more extensive shock tube study following OH by resonance absorption at 308 nm., O by chemiluminescent emission on reaction with CO at 370 nm., CO and H_2O by infrared emission at 4.8 and 6.3 μm respectively. The temperature range covered was 1545 to 2180K.

Induction periods were related to the initial oxygen and methanol concentrations and were modelled with a 28 reaction

mechanism. Sensitivity analysis eliminated 9 reactions and indicated that the concentration and temperature profiles were most sensitive to the following five reactions.

$$CH_3OH \text{ ---> } CH_3 + OH \qquad 1.10$$

$$O + CH_3OH \text{ ---> } CH_2OH + OH \qquad 1.11$$

$$H + CH_3OH \text{ ---> } CH_2OH + H_2 \qquad 1.12$$

$$OH + CH_3OH \text{ ---> } CH_2OH + H_2O \qquad 1.13a$$

$$CH_2OH \text{ ---> } CH_2O + H \qquad 1.14$$

At the time of this study these reactions were poorly characterized and the rate constants were uncertain. CH_3O radicals were not included in this mechanism although they were considered possible but not necessarily distinguishable from the other radicals CH_3 or CH_2OH. The decomposition of CH_2OH and CH_3O radicals was considered to be important in the production of CH_2O.

Further shock tube work has been done by Tsuboi and Hashimoto (1981). They have monitored emission profiles of excited CH_3OH, H_2O, CO_2, CO, and CH_2O in the infrared over a temperature range of 1200 to 1800K. A 57 reaction model has been proposed to explain the observed profiles. The reactions of importance were reactions 1.12 to 1.14 and 1.10 with the following additional reactions.

$$CH_3 + CH_3OH \text{ ---> } CH_2OH + CH_4 \qquad 1.15$$

$$CH_2O \text{ ---> } HCO + H \qquad 1.16$$

CH_3O radicals were not considered to be intermediate products.

The unimolecular decomposition of CH_3OH and CH_2OH were found to be pressure dependant. An apparent activation energy of 201 $kJmol^{-1}$ was found for the induction period and since this is due primarily to decomposition of methanol via 1.10 then the reaction would appear

to be significantly in the falloff regime at these temperatures and pressures.

The remaining studies were two flame studies and a turbulent flow reactor study. Akrich, et al. used a quartz microprobe to withdraw samples from the flame for chromatographic analysis of the stable species. The temperature and concentration profiles were modelled with a 21 reaction scheme which once again omitted any contribution from CH_3O radicals. However, their modelling results are self consistent and provide reasonable agreement with their own experiments.

Vandooren and Van Tiggelen (1981) used molecular beam sampling with mass spectrometric detection of both stable species and radical intermediates to determine concentration profiles in methanol flames. Both CH_2OH and CH_3O production was considered but the 24 reaction mechanism developed includes only CH_2OH production and loss (even though ΔH values for reactions involving CH_3O radicals are included.) This is probably due to the paucity of data available for CH_3O reactions.

The most important conclusion of Vandooren and Van Tiggelen was that 60 to 80% of methanol consumption in lean flames was due to reaction with OH and not from decomposition processes. Also there is significantly lower production of CH_3 and thus CH_2 and CH radicals in methanol flames compared with hydrocarbon flames. Consequently the decomposition pathway is mainly via CH_2OH/CH_3O and CH_2O.

The work by Aronowitz et al. (1979) covered a lower temperature range of 950 to 1030K but a considerably wider range of CH_3OH/O_2 ratios. Concentration profiles of the stable species were obtained

by sampling with a stainless steel probe and analysing via gas chromatography. A 28 reaction mechanism was proposed to describe their results which are post induction. As a result of this, radical reactions will dominate as is confirmed from the estimates of the [OH] of 10^{12} to 10^{13} cm^{-3}. The result is abstraction of H by OH is approximately 1000 times faster than CH_3OH decomposition to CH_3 and OH radicals. The low level of CH_3 obtained thus is commensurate with the observations of Vandooren and Van Tiggelen.

HO_2 radicals were also considered important in this system and were emphasized as a radical whose omission from a mechanism could seriously limit the validity of results from other systems.

The 84 reaction scheme of Westbrook and Dryer is reproduced here as the model for future mechanisms giving improved simulation of the properties of methanol combustion.

1.6 Ethanol

1.6.1 Slow Oxidation.

Significantly less work has been done with respect to ethanol. Cullis and Newitt (1956, 1957) performed static work in pyrex vessels analysing pressure changes and determining products by wet chemical means. The products were identified as CH_3CHO, CH_3OH, CH_2O and CO. Under favourable conditions, H_2O_2 was observed

Table 1.1 84 Reaction Mechanism From Westbrook and Dryer.

CH_3OH	+	OH	----->	CH_2OH	+	H_2O	
CH_3OH	+	O	----->	CH_2OH	+	HO	
CH_3OH	+	H	----->	CH_2OH	+	H_2	
CH_3OH	+	H	----->	CH_3	+	H_2O	
CH_3OH	+	HO_2	----->	CH_2OH	+	H_2O_2	
CH_3OH	+	CH_3	----->	CH_2OH	+	CH_4	
CH_3OH	+	O_2	----->	CH_2OH	+	HO_2	
CH_3OH	+	M	----->	CH_3 + OH + M			
CH_2OH	+	O_2	----->	CH_2O	+	HO_2	
CH_2OH	+	M	---->	CH_2O + H + M			
CH_3O	+	O_2	----->	CH_2O	+	HO_2	
CH_3O	+	M	----->	CH_2O + H + M			
CH_2O	+	O	----->	CHO	+	HO	
CH_2O	+	HO_2	----->	CHO	+	H_2O_2	
CH_2O	+	OH	----->	CHO	+	H_2O	
CH_2O	+	H	----->	CHO	+	H_2	
CH_2O	+	M	----->	CHO + H + M			
CH_2O	+	CH_3	----->	CHO	+	CH_4	
CH_4	+	O	----->	CH_3	+	OH	
CH_4	+	M	----->	CH_3	+	H + M	
CH_4	+	H	----->	CH_3	+	H_2	
CH_4	+	HO_2	----->	CH_3	+	H_2O_2	
CH_4	+	OH	----->	CH_3	+	H_2O	
CH_3	+	HCO	----->	CH_4	+	CO	
CH_3	+	OH	----->	CH_2	+	H_2O	
CH_3	+	O	----->	CH_2O	+	H	
CH_3	+	HO_2	----->	CH_3O	+	OH	
CH_3	+	HO_2	----->	CH_4	+	O_2	
CH_3	+	O_2	----->	CH_3O	+	O	
HCO	+	O_2	----->	CO	+	HO_2	
HCO	+	M	----->	CO	+	H + M	
HCO	+	OH	----->	CO	+	H_2O	
HCO	+	O	----->	CO	+	OH	
HCO	+	H	----->	CO	+	H_2	

$HCO + HO_2 \longrightarrow H_2CO + O_2$

$CO + OH \longrightarrow CO_2 + H$

$CO + O + M \longrightarrow CO_2 + M$

$CO + HO_2 \longrightarrow CO_2 + OH$

$CO_2 + O \longrightarrow CO + O_2$

$H_2O + O \longrightarrow OH + OH$

$H_2O + M \longrightarrow H + OH + M$

$H_2O + H \longrightarrow H_2 + OH$

$H_2O_2 + O_2 \longrightarrow HO_2 + HO_2$

$H_2O_2 + OH \longrightarrow HO_2 + H_2O$

$H_2O_2 + H \longrightarrow HO_2 + H_2$

$H_2O_2 + M \longrightarrow OH + OH + M$

$H_2 + M \longrightarrow H + H + M$

$H_2 + O \longrightarrow OH + H$

$O_2 + M \longrightarrow O + O + M$

$O_2 + H \longrightarrow OH + O$

$O_2 + H + M \longrightarrow HO_2 + M$

$HO_2 + O \longrightarrow O_2 + OH$

$HO_2 + H \longrightarrow O_2 + H_2$

$HO_2 + H \longrightarrow OH + OH$

$HO_2 + OH \longrightarrow O_2 + H_2O$

$O + H + M \longrightarrow OH + M$

$C_2H_6 + CH_3 \longrightarrow C_2H_5 + CH_4$

$C_2H_6 + H \longrightarrow C_2H_5 + H_2$

$C_2H_6 + OH \longrightarrow C_2H_5 + H_2O$

$C_2H_6 + O \longrightarrow C_2H_5 + OH$

$C_2H_6 + M \longrightarrow CH_3 + CH_3 + M$

$C_2H_5 + C_2H_3 \longrightarrow C_2H_4 + C_2H_4$

$C_2H_5 + O_2 \longrightarrow C_2H_4 + HO_2$

$C_2H_5 + M \longrightarrow C_2H_4 + H + M$

$C_2H_4 + M \longrightarrow C_2H_3 + H + M$

$C_2H_4 + H \longrightarrow C_2H_3 + H_2$

$C_2H_4 + OH \longrightarrow C_2H_3 + H_2O$

$C_2H_4 + O \longrightarrow C_2H_3 + OH$

$C_2H_4 + O \longrightarrow HCO + CH_3$

$C_2H_3 + M \longrightarrow C_2H_2 + H + M$

$C_2H_2 + M \longrightarrow C_2H + H + M$

$C_2H_2 + H \longrightarrow C_2H + H_2$

$C_2H_2 + OH \longrightarrow C_2H + H_2O$

$C_2H_2 + O \longrightarrow C_2H + OH$

$C_2H_2 + O \longrightarrow CO + CH_2$

$C_2H_2 + O_2 \longrightarrow HCO + HCO$

$C_2H + O \longrightarrow CO + CH$

$C_2H + O_2 \longrightarrow CO + HCO$

$CH_2 + O \longrightarrow CH + OH$

$CH_2 + H \longrightarrow CH + H_2$

$CH_2 + OH \longrightarrow CH + H_2O$

$CH_2 + O_2 \longrightarrow HCO + OH$

$CH + O_2 \longrightarrow CO + OH$

$CH + O_2 \longrightarrow HCO + O$

leading to the conclusion that the HO_2 radical is, as in methanol oxidation, the major chain carrier.

Evidence supporting hydrogen abstraction from the α-carbon was found in the slow formation of CH_2O, present only at the end of the induction period. This would come from decomposition of the ethoxy (CH_3CH_2O) radical :-

$$CH_3CH_2O \longrightarrow CH_3 + CH_2O \qquad 1.17$$

$$CH_3CH_2O \longrightarrow CH_3CHO + H \qquad 1.18$$

Reactions 1.17 and 1.18 have similar activation energies and as such should occur at similar rates. (Cullis and Newitt.) The lack of CH_2O indicates then that CH_3CH_2O is not being formed to any great extent. The more likely route is thus

$$CH_3CH_2OH + X \longrightarrow CH_3CHOH + XH \qquad 1.19$$

where X is any atom or radical. The hydroxyethyl (CH_3CHOH) radical then decomposes by H abstraction or O-H bond fission :-

$$CH_3CHOH + X \longrightarrow CH_3CHO + HX \qquad 1.20$$

$$CH_3CHOH + X \longrightarrow CH_3CHO + H + X \qquad 1.21$$

There does not appear to have been any consideration of the possibility of alternative bimolecular routes such as reaction with O_2 for the removal of the CH_3CH_2O radical which would not produce CH_2O. This would be expected to produce CH_3CHO in the same way as reaction 1.20 and would be faster than the unimolecular decomposition. (Reaction 1.18)

Experimental work on the later stages of the oxidation (Cullis and Newitt, 1957) attempted to identify and explain the distribution

of the C1 products CH_3OH, CH_2O, and CO. These appear to result from oxidation of CH_3CHO by O_2 or by other radicals present. The result is chain branching initiated by CH_3 and peroxide radicals to give the stable products. With an increase in temperature chain branching was expected to decrease as reactions such as :-

$$CH_3 + O_2 \text{ -----> } (CH_3O_2)^* \text{ -----> } CH_2O + OH \quad 1.22$$

become more important giving a more direct route to the final products.

1.6.2 High Temperature Studies.

The only study available was performed by Cooke, et al. (1971), in a shock tube experiment. They found that ignition delay times for CH_3CH_2OH were shorter than CH_3OH which compares favourably with the bond dissociation energies of the predicted initiation reaction;

$$CH_3CH_2OH \text{ ------> } CH_3 + CH_2OH \quad 1.23$$

Following this reaction, radical attack on CH_3CH_2OH would occur, (R1.19), and being faster than their CH_3OH counterparts, further exacerbate the ignition delay differences.

1.7 Other Alcohols.

1.7.1 Slow Oxidation.

The higher alcohols have been sparsely studied (Cullis and Newitt, 1960, 1961; Kane et al., 1937) due to their greater

complexity and also possibly because they have less recognised use as fuels when compared with methanol and ethanol.

Many of the features of these oxidations parallel that of ethanol. The product/time distribution indicated preferential attack on the α C-H groups where these were present. The chain propagators are initially HO_2 and later the organic peroxides formed in oxygen reaction with the other radicals. This also leads to significant amounts of chain branching.

1.7.2 High Temperature Studies.

Very few studies have been performed on the other alcohols. In general no work has been done on the oxidation of the higher alcohols. The data available relates mainly to burning velocities (Gulder; Gibbs and Calcote) and flame structure (Andreussi and Petarca) with almost no kinetic information at all.

1.8 Modelling of Chemical Systems.

As has been discussed previously (see section 1.4 and 1.5), modelling of combustion/oxidation processes has been extensively used in conjunction with experiment both to help in the analysis of results and to discover the values of new rate constants for reactions not yet measured. Several good reviews of combustion modelling and modelling in general have been written. (Chapters 1, 2, and 7 in Gardiner, 1984; Warnatz, 1983; Westbrook and Dryer, 1981)

However, the ability to model such processes is severely limited by our knowledge of the elementary rate constants in the region of interest. Generally, it is much more difficult to perform direct determinations of rate constants at higher temperatures, so extrapolation from lower temperature studies has been very common. There are significant pitfalls associated with this procedure due to uncertainties as a result of unknown or unappreciated temperature dependences or even alternative mechanisms not significant at lower temperatures. Curvature of Arrhenius plots is one manifestation of this phenomenon.

Methanol oxidation is a typical case in point. Prior to 1976 there were no determinations of the rate of OH attack on methanol. This reaction has been shown to be important in methanol oxidation under most combustion conditions. (Aronowitz, et al., 1979; Bowman, 1975; Vandooren et al.; Westbrook and Dryer, 1979) However, consensus as to the appropriate rate coefficient for this reaction at high temperature has not been reached.

Recent work in the temperature range 250 to 1000K (Greenhill and O'Grady; Meier, et al.; Hagele, et al.) has shown good agreement for this reaction.

$$CH_3OH + OH \text{ -------> } CH_3O/CH_2OH + H_2O \qquad 1.13a/b$$

As well as this the work by Meier, et al. and Hagele, et al. has shown that the reaction is branched. This branching is expected to be significant at combustion temperatures due to its higher activation energy. (Hagele, et al.)

The rate constants measured and predicted for the overall reaction are plotted in figure 1.1. The mechanism which has been

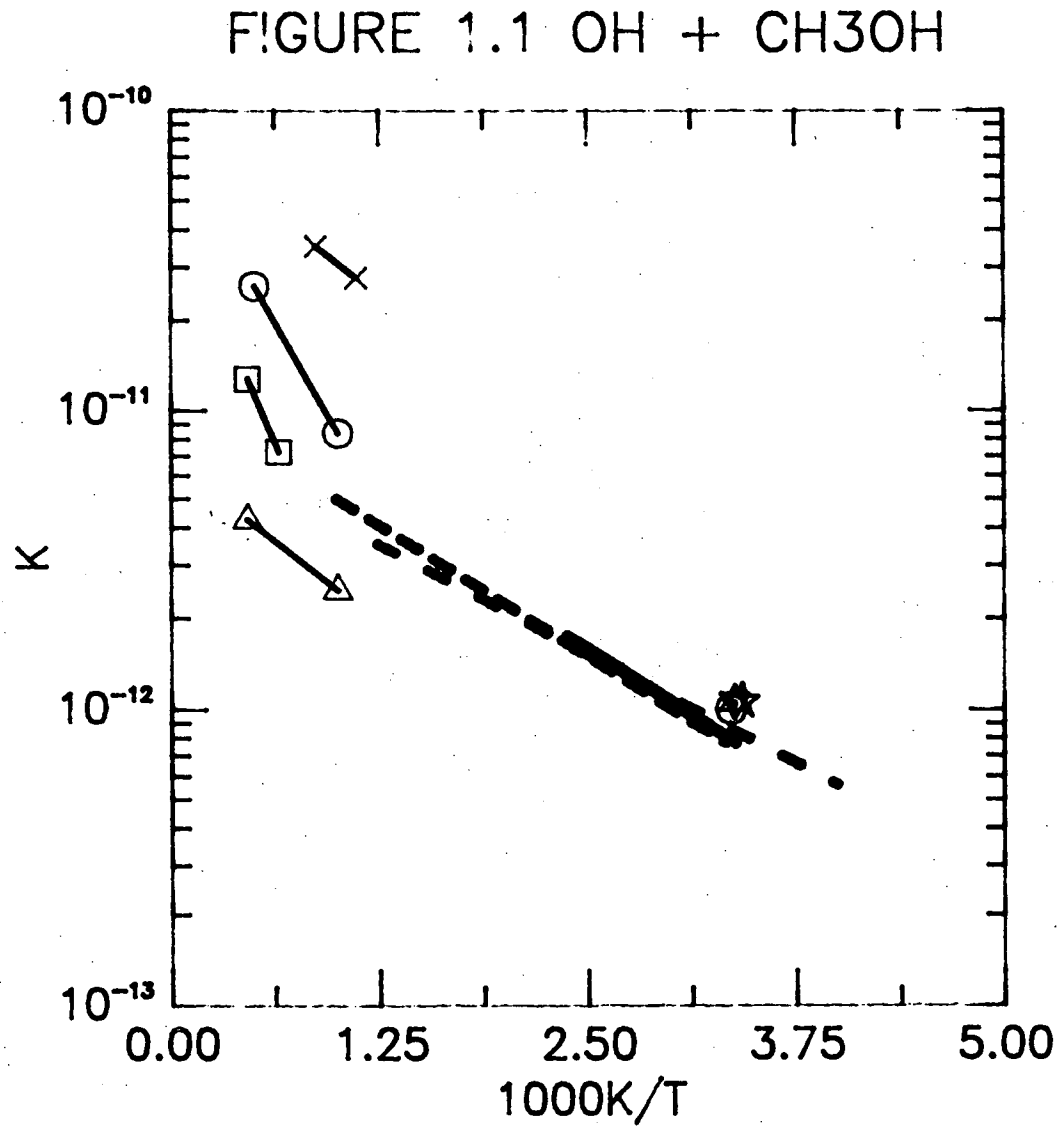

Figure 1.1 Arrhenius plot of OH + Methanol rate data.

- – – – Meier, et al.
- ——— Hagele, et al.
- △ Westbrook, et al.
- □ Bowman.
- × Aronowitz, et al.
- ○ Van Tiggelen, et al.
- — — - This work.

proposed as capable of modelling results from several experimental systems (Westbrook and Dryer) predicts a lower rate constant at combustion temperatures than that from extrapolation of the lower temperature measurements.

This indicates the problems of attempting to gain such data from models. However, such attempts should not be abandoned and hopefully the knowledge of these rate constants at lower temperatures will lead to improved estimates at the higher temperatures. Certainly a lower limit for the rate constant is available which coupled with the knowledge of the branching ratio will provide an improvement of the kinetic models constructed.

1.9 What Next?

It is clear from this limited discussion that there is still considerable work to be done before our understanding of alcohol combustion is adequate. The complexity of the combustion process requires that we carry out several complementary investigations to gain some insight into the combustion phenomenon. These are summarised in figure 1.2.

Experimental studies need to be performed which provide individual rate constants and information on the overall kinetics of a process. Theoretical studies which apply our fundamental understanding of how molecules and radicals react need to be used to obtain those rate constants which are experimentally inaccessible. The individual rate constants are combined to form a mechanism which it is hoped will describe a process of interest. The measure of the

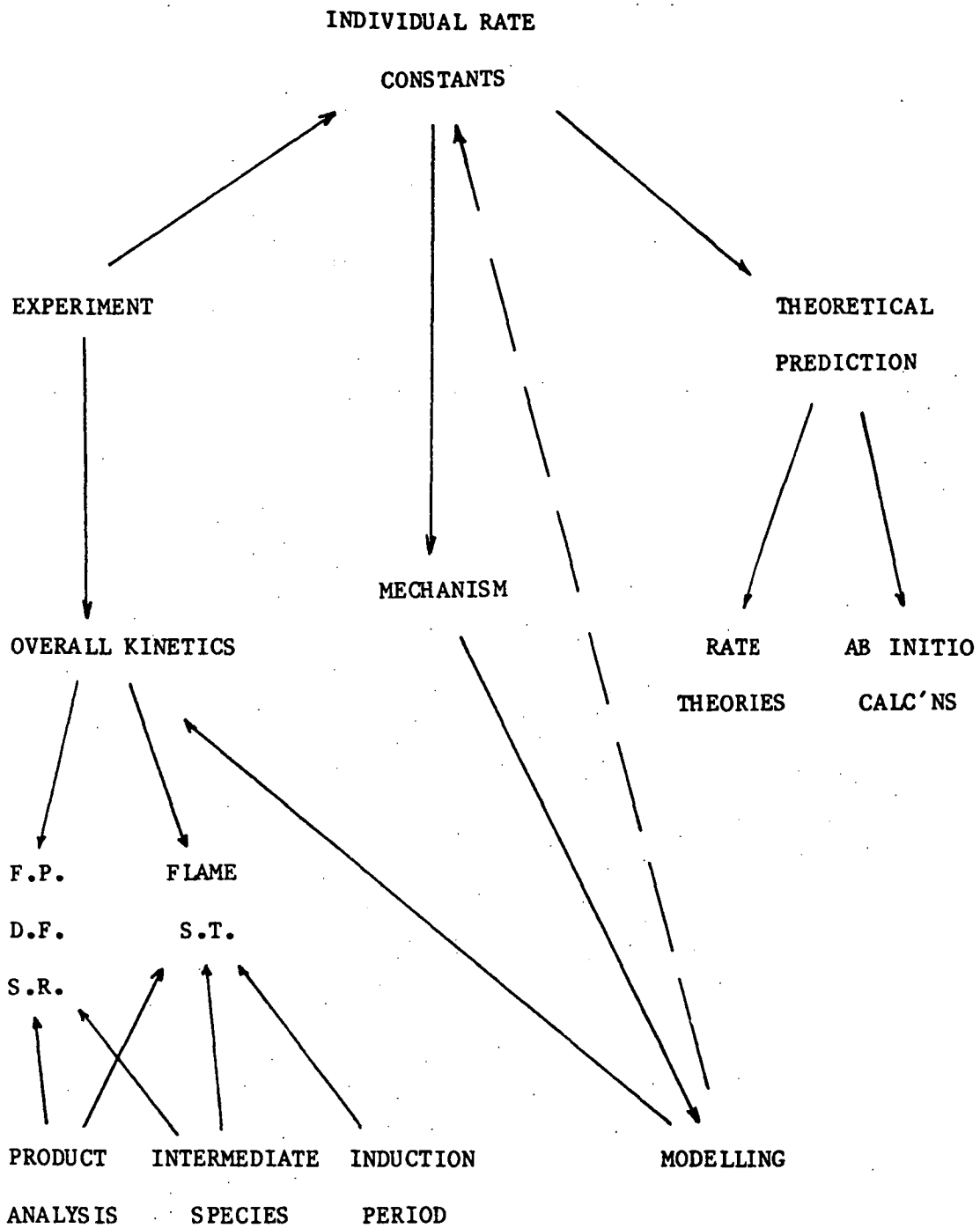
INDIVIDUAL RATE
CONSTANTS
EXPERIMENT
THEORETICAL
PREDICTION
MECHANISM
OVERALL KINETICS
RATE
THEORIES
AB INITIO
CALC'NS
F.P.
D.F.
S.R.
FLAME
S.T.
PRODUCT
ANALYSIS
INTERMEDIATE
SPECIES
INDUCTION
PERIOD
MODELLING

Figure 1.2

mechanism's correctness is its ability to reproduce or model the overall kinetics of the experiments manifested in product and intermediate species profiles, induction periods and temperature and pressure changes.

The modelling thus provides us with a way of refining the mechanism to get an improved understanding of how combustion occurs.

The heirarchical nature of kinetics enables us to apply our knowledge of simpler systems directly to the next most complex situation and thereon up the ladder. Before any significant advances in ethanol combustion are achieved, our knowledge of methanol combustion must be well developed. The reactions of most importance are the radical reactions with methanol, particularly OH;

$$OH + CH_3OH \longrightarrow CH_2OH + H_2O \qquad 1.13a$$

$$\longrightarrow CH_3O + H_2O \qquad 1.13b$$

The unimolecular reactions of the secondary species CH_3O and CH_2OH radicals,

$$CH_2OH \longrightarrow CH_2O + H \qquad 1.14$$

$$CH_3O \longrightarrow CH_2O + H \qquad 1.24$$

$$CH_2OH + H \longrightarrow CH_3OH \qquad 1.25$$

$$\longrightarrow CH_3 + OH \qquad 1.26$$

$$CH_3O + H \longrightarrow CH_3OH \qquad 1.27$$

$$\longrightarrow CH_3 + OH \qquad 1.28$$

and also the abstraction reactions involving CH_3O and CH_2OH radicals.

$$CH_3O/CH_2OH + H \longrightarrow CH_2O + H_2 \qquad 1.29$$

$$CH_3O/CH_2OH + OH \longrightarrow CH_2O + H_2O \qquad 1.30$$

$$CH_3O/CH_2OH + O \longrightarrow CH_2O + OH \qquad 1.31$$

$$CH_3O/CH_2OH + O_2 \text{ ---> } CH_2O + HO_2 \qquad 1.32$$

The work presented in this thesis is the result of research directed at improving our knowledge of the rate coefficients of some of these reactions, particularly reactions 1.13-1.14, 1.24-1.25, and 1.27.

Both experimental and theoretical studies have been performed and a new technique has been developed which is applicable to recombination reactions without energy barriers.

1.10 References.

Akrich, R., Vovelle, C., and Delbourgo, R., Comb. and Flame, 1978, **32**, 171.

Andreussi, P., and Petarca, L., 18th Symp. (Intl.) Comb., 1981, 1861.

Aronowitz, D., Naegeli, D.W., and Glassman, I., J. Phys. Chem., 1977, **81**, 2555.

Aronowitz, D., Santoro, R.J., Dryer, F.L., and Glassman, I., 17th Symp. (Intl.) Comb., 1979, 633.

Bell, K.M., and Tipper, C.F.H., Proc. Royal Soc. (Lon), 1956, **A238**, 256.

Bell, K.M., and Tipper, C.F.H., Trans. Faraday Soc., 1957, **53**, 982.

Bone, W.A., and Gardiner, J.B., Proc. Royal Soc. (Lon),1936, **A154**, 297.

Bonev, V.A., Fiz. Goren. Vzryva., 1972, **8**, 279.

Bowman, C.T., Comb. and Flame, 1975, **25**, 343.

Cathonnet, M., Boettner, J.C., and James, H., J. Chimie Physiq., 1979, **76**, 183.

Cooke, D.F., Dobson, M.G., and Williams, A., Comb. and Flame, 1971, **16**, 233.

Cullis, C.F., and Newitt, E.J., Proc. Royal Soc. (Lon.),1956, **A237**, 530.

Cullis, C.F., and Newitt, E.J., ibid.,1957, **A242**, 516.

Cullis, C.F., and Newitt, E.J., ibid.,1960, **A257**, 402.

Cullis, C.F., and Newitt, E.J., ibid.,1961, **A264**, 392.

Dove, J.E., and Warnatz, J., Ber. Bunsenges. Phys. Chem., 1983, **87**, 1040.

Eden, R.Q.E., in "Technology of Gasoline", Hancock, E.G., Ed., C1985, Blackwell Scientific Publications, Oxford., Chap. 4, pp. 93.

Fort, R., and Hinshelwood, C.N., Proc. Royal Soc. (Lon), 1930, **A129**, 284.

Gardiner, W.C.Jr., "Combustion Chemistry", Springer- Verlag, New York, 1984.

Gibbs, C.J., and Calcote, H.C., J. Chem. Eng. Data, 1959, **4**, 226.

Gulder, O.L., 19th Symp. (Intl.) Comb., 1982, 275.

"Technology of Gasoline", Hancock, E.G., Ed.

Greenhill, P.G., and O'Grady, B.V., Aust. J. Chem., 1986, **39**, 1775.

Hagele, J., Lorenz, K., Rhasa, D., and Zellner, R., Ber. Bunsenges. Phys. Chem., 1983, **87**, 1023.

Kane, G.P., Chamberlain, E.A.C., and Townend, D.T.A., J. Chem. Soc., 1937, 436.

Meier, U., Grotheer, H.H., and Just, Th., Chem. Phys. Letts., 1984, **106**, 97.

Metghalchi, M., and Keck, J.C., Combust. Flame, 1982, **48**, 191.

Ricardo, H.R., "The influence of various fuels on the performance of IC engines.", Report of the Empire Motor Fuels Committee., Institute of Petroleum Technologists, 1924.

Tsuboi, T., and Hashimoto, K., Combust. Flame, 1981, **42**, 61.

Vandooren, J., and Van Tiggelen, P.J., 18th Symp. (Intl.) Comb., 1981, 473.

Vanpee, M., Bull. Soc. Chim. Belge., 1953, **62**, 458.

Warnatz, J., Ber. Bunsenges. Phys. Chem., 1983, **87**, 1008.

Westbrook, C.K., and Dryer, F.L., Comb. Sci. Tech., 1979, **20**, 125.

Westbrook, C.K., and Dryer, F.L., Combust. Flame, 1980, **37**, 171.

Westbrook, C.K., and Dryer, F.L., 18th Symp. (Intl.) Comb., 1981, 749.

de Wilde, E., and van Tiggelen, A., Bull. Soc. Chim. Belg., 1968, **77**, 67.

Wiser, W.H., and Hill, G.R., 5th Symp. (Intl.) Comb., 1955, 553.

Chapter 2

OH And Other Reactions Of Importance In Combustion.

2.1 Introduction.

When we consider a mechanism for combustion such as that proposed by Westbrook & Dryer (1979) for methanol it is instructive to determine the species which participate most frequently. Of the eighty four reactions cited, OH and H are involved in 33 and 30 reactions respectively, with O, O_2 and HO_2 involved in 22, 21 and 20 respectively. Even from this superficial point of view it is obvious that OH and H chemistry are critically important to the combustion of hydrocarbons. When we consider that OH reactions can be anything up to 10 times as fast as the reactions of other radicals, then this emphasises the importance of the OH radical in combustion.

In this chapter the most recent literature of importance in OH chemistry related to combustion will be reviewed. In addition the techniques used to study OH reactions will be summarised. The reactions of the primary radicals CH_2OH and CH_3O will also be discussed where measurements have been made.

2.2 OH Reactions - The Experimental Techniques

2.2.1 Reactors

At temperatures below 1000K two types of reactor have been most extensively used. These are static reactors and linear flow reactors.

In general, static reactors are filled with the reactant gas mixture and the reaction initiated by photolytic techniques. The reaction zone is defined by the intersection of the photolysed region with the detection region. Two assumptions about these reactors are made; a) they are wall-less and b) diffusion of the observed species out of the detector zone is negligible in the time period of the reaction. A wide pressure range can be covered as well which makes this technique useful when third body effects are important.

The volume of the reactor is generally dictated by the requirements of the detection technique. Fluorescent detection techniques require smaller volumes than absorption experiments where long path lengths are required. 'Slow Flow' reactors are included in this category because over the time scale of an experiment the mixture is essentially static. Slow flow reactors were developed to take advantage of improved photolysis capabilities such as higher repetition rates for conventional flash lamps and the advent of pulsed lasers and to ensure that there is no build up of products.

Linear flow reactors as the name implies flow reaction mixtures at high velocities down a tube of appropriate material. Reaction time is proportional to the distance travelled between mixing and detection down the reactor. The reactive species is usually generated by dissociation of a precursor or dissociation followed by a fast secondary reaction to produce the species of interest. e.g.

$$H_2 \text{ - ----> } 2H$$

$$H + NO_2 \text{ -----> } NO + OH$$

Normally the precursor to be dissociated is flowed through a microwave discharge and the reactant is introduced with a moveable probe.

This reactor design has the advantage that many more diverse techniques can be used as detectors than for static reactors. However, it has the disadvantages that wall reactions must be considered, flow characteristics are important, and the measurement of reactant concentrations is not straightforward.

Other techniques have been employed such as stirred flow, and relative rate measurements which generally follow the disappearance of the major reactants by a suitable analytical technique. Rate constants are obtained by comparing the disappearance of the reference compound in the absence and presence of the reactant of interest.

At temperatures above 1000K direct measurements of rate constants can in general only be obtained from shock tube experiments coupled with in situ monitoring of radical species.

Other techniques such as flame studies and turbulent flow reactors must be coupled with theoretical modelling to reproduce observed concentration profiles.

2.2.2 Detection

The two most common detection techniques in use are resonance absorption and resonance fluorescence. Either technique can be used in static or flow systems but the fluorescence technique has three advantages over absorption. Firstly it does not require a large reaction vessel as the observed signal is viewed at right angles to the incident radiation. Secondly the observed signal is directly proportional to the concentration of the emitting species whereas absorption is related to concentration via the Beer-Lambert law.

$$\ln(I_o/I) = \varepsilon c l \qquad 2.1$$

Thirdly and most importantly the sensitivity of fluorescence is 1-2 orders of magnitude greater than absorption and thus more amenable to signal averaging.

Recently lasers have been used as the monitoring light sources but for the simple radicals and atoms resonance lamps are still the preferred source because they are cheap and reliable and, most importantly, they require no tuning as they only emit the appropriate wavelengths for absorption or fluorescence detection.

Electron spin resonance has been used in some cases but it is less useful than other spectroscopic techniques. Mass spectrometric

sampling has been used quite extensively and has the advantage that intermediate species may also be monitored along with the reactive species of interest. These two techniques are usually only used in flow discharge experiments as the time resolution required for static experiments is in general not available without sophisticated additions.

Laser magnetic resonance has proved to be useful for paramagnetic species as it is more sensitive than fluorescence. However, the experimental arrangement is complex when compared to the other techniques.

2.2.3 OH Generation

The method used to generate OH depends upon the experimental system chosen. Photolytic experiments in general use precursors which contain OH moieties. The most common are water and nitric acid. Hydrogen peroxide is used sometimes but it is more reactive than either of the other two precursors and it does not have the thermal stability required for any extended temperature range work.

In some cases OH may be produced by the photolysis of an O containing species e.g. O_2, O_3 or N_2O and subsequent reaction with an H containing moiety will produce OH, e.g. H_2O, H_2, NH_3. The requirement is that this reaction be very fast with respect to the time scale of the reaction under study.

Generation of OH in a discharge flow system has a different requirement as it must be possible to produce a continuous flow of

the radical species. Usually OH is produced by reaction of H atoms with an O containing molecule. Precautions to reduce the loss of OH in wall processes need to be taken, such as coating the walls with halocarbon waxes or teflon or deactivating with concentrated acids.

2.3 OH Reactions since 1982

The two most recent compilations of data on the C/H/O system and high temperature region covered the periods up to December 1980 (Cohen and Westberg, 1983) and till early 1982 (Warnatz, 1984). Of the 27 reactions reviewed by Cohen and Westberg 16 are reactions of OH indicating their importance.

Several other compilations appeared prior to these two and still constitute good sources of data even though some of the reactions may have since been revised by more recent experiments. Westley (1980) has documented, in a standard format, reactions discussed in eleven previous publications by Baulch, et al. (1972, 1973, 1976), Benson, et al. (1975), Benson and O'Neal (1970), Engleman (1976), Herron and Huie (1973), Kerr and Parsonage (1972, 1976), Kondratiev (1972) and Lloyd (1974).

As well as these there are reports related to atmospheric chemistry which provide reviews of lower temperature regions. (Baulch, et al. 1982, 1980; Atkinson, et al. 1979.)

There is no need to discuss these reports as they are readily available. Work on OH reactions since 1982 will be tabulated and compared with the previous recommendation (if any). Alkanes will be

discussed first followed by alkenes, alkynes, CO, oxygen containing neutral molecules and finally radicals.

2.3.1. $OH + CH_4$

Two studies of this reaction have appeared since 1982. The first was a relative rate study analysed by GC using OH and CO as the competitive reaction (Baulch et al (1983)). The second was as a test of a new experimental technique for high temperature (Smith, et al., 1985). The results obtained are in good agreement with the recommendation of Cohen and Westberg (1983) of

$$k(T) = 3.2 \times 10^{-19} T^{2.4} \exp(-1060/T) \ cm^3 s^{-1} \qquad 2.1$$

2.3.2 $OH + C_2H_6$

Six studies of this reaction have been performed since 1982. (Lee, et al. 1982; Baulch, et al. 1983,1985; Tully, et al. 1983, 1986; Jeong, et al. 1984). These are plotted in figure 2.1. The temperature range for all these experiments is less than 800K but they compare well with the expression of Cohen and Westberg.

$$k(T) = 3.6 \times 10^{-17} T^{1.9} \exp(-570/T) \ cm^3 s^{-1} \qquad 2.2$$

The only discrepancy appears to be the work of Jeong, et al. (1984) who obtains a weaker temperature dependence and higher values of k(T) at temperatures below 350K.

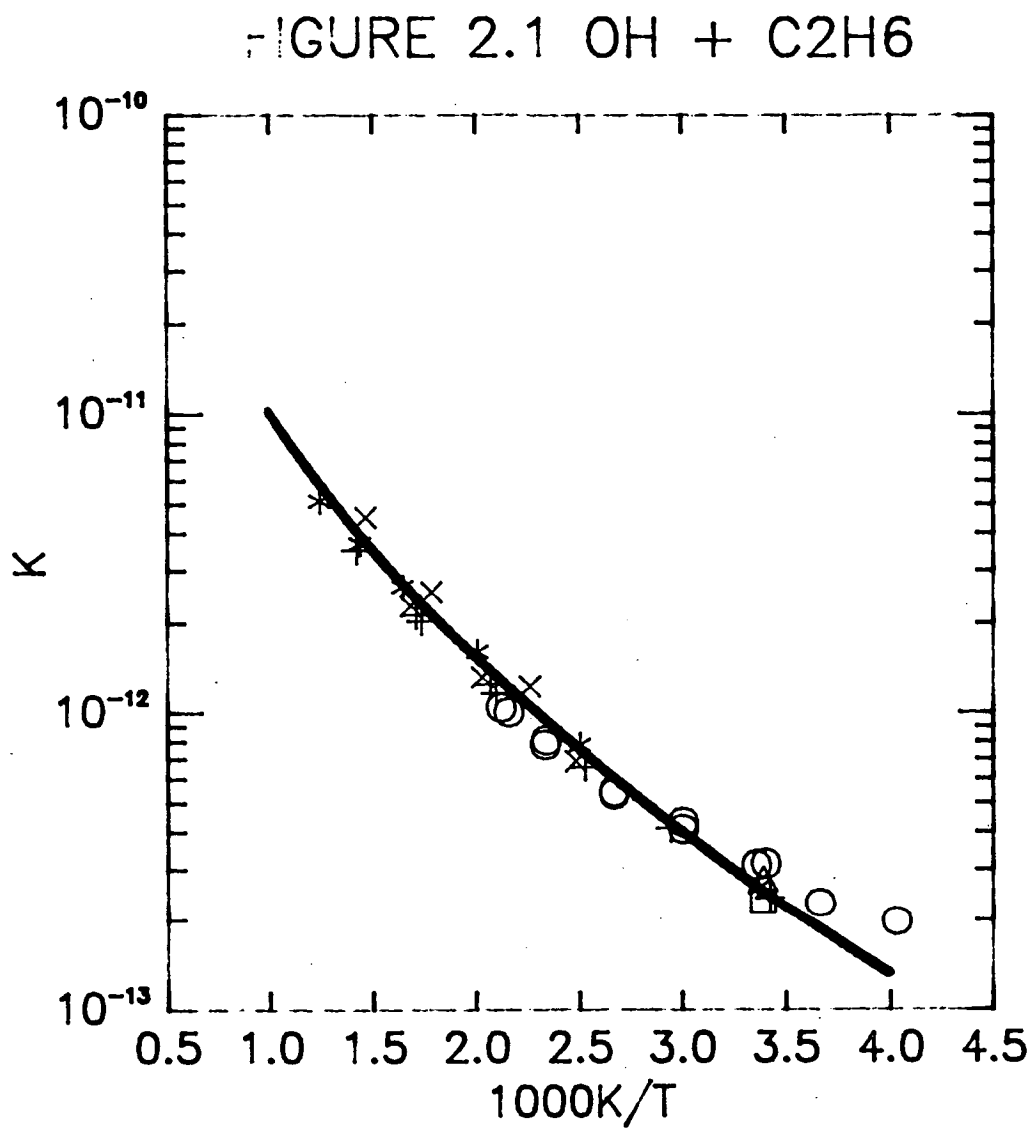

Figure 2.1 Arrhenius Plot
OH + Ethane.

- Cohen, et al. 1983
- Lee, et al. 1982
- Baulch, et al. 1983
- Baulch, et al. 1985
- Jeong, et al. 1984
- Tully, 1983
- Tully, et al. 1986

2.3.3 OH and C_3H_8

Six studies of this reaction have been performed recently (Baulch, et al. 1983, 1985; Atkinson, 1984; Bott and Cohen, 1984, Smith, et al. 1985, and Tully, et al. 1983) but only two of these (Bott and Cohen, 1984 and Smith, et al. 1985) have been at temperatures over 1000K. There is still a significant dearth of data at temperatures in the 1000-2000K range of combustion. In general, all these results are in good agreement with the recommended value from Cohen and Westberg, but the three parameter fit of Tulley, et al. (1983) is distinctly different from that of Cohen and Westberg

$$k(T) = 4.27 \times 10^{-20} T^{2.8} \exp(310/T) \quad cm^{-3}s^{-1} \text{ (Cohen)} \qquad 2.3$$

$$k(T) = 1.59 \times 10^{-15} T^{1.40} \exp(-428/T) \quad cm^{3}s^{-1} \text{ (Tully)} \qquad 2.4$$

From the Arrhenius plot for this reaction (figure 2.2) it is apparent that the Tully results have a slightly lesser T dependence and in general the rate coefficients are slightly higher. The accuracy of the results is not sufficient however, to differentiate between the two fits but consideration of more recent results of Smith, et al. (1985), Bott and Cohen, (1984) and Baulch, et al. (1983) indicate that the Cohen expression is more appropriate.

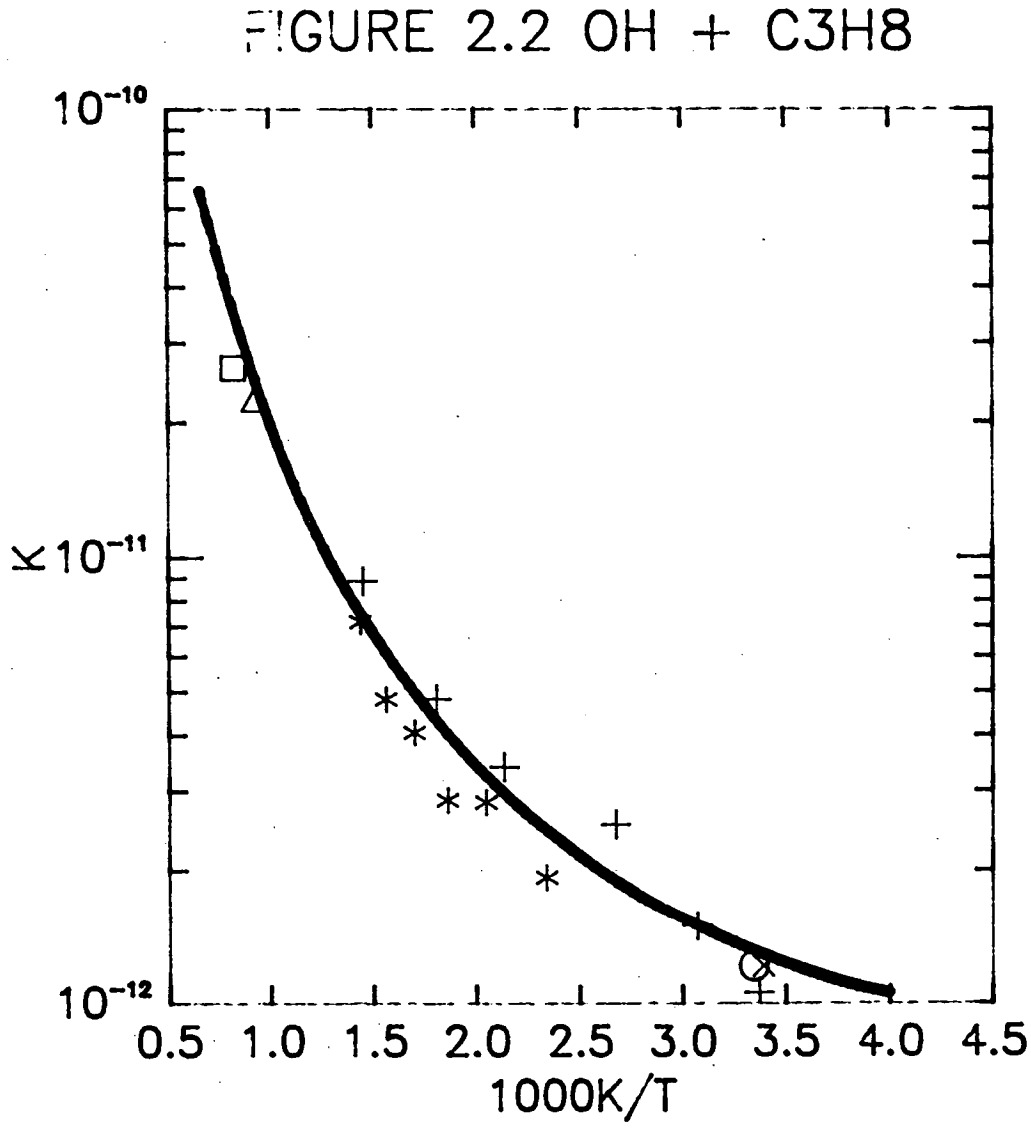

Figure 2.2 Arrhenius Plot
OH + Propane.

- + Tully, et al. 1983
- ○ Atkinson, 1984
- ✳ Baulch, et al. 1983
- × Baulch, et al. 1985
- □ Bott, et al. 1983
- —— Cohen, et al. 1983
- △ Smith, et al. 1985

2.3.4 OH and C_nH_{2n+2}

The reactions of OH with the higher alkanes will not be discussed here as they do not have a direct bearng on the work performed in this thesis.

However three papers have appeared by Atkinson, et al. (1982) on the n-alkanes, Atkinson, et al. (1984) on the branched alkanes and by Bolland, et al. (1984) on iso-butane all at room temperatures.

2.3.5 OH + C_2H_4

There is a severe lack of data over any extensive temperature range for this reaction. The four studies since 1982 have been in the temperature region 290-600K (Bartels, et al. 1982, Tully, 1983, Zellner and Lorenz, 1984, Klein, et al. 1984). They have provided further evidence that the low temperature pathway is an addition to the double bond in a pressure dependent process. Zellner's result is;

$$k\ (T) = 3.32 \times 10^{-12} \exp[(320 \pm 150)K/T]\ cm^3 s^{-1} \quad 2.5$$

There is still significant scatter over all pressures and temperatures but the results of Klein, et al. (1984) are probably the best at room temperature.

2.3.6 OH + C_3H_6

Studies of this reaction have been done by Ohta, (1983, 1984), Smith, (1983), Zellner and Lorenz, (1984), Klein, et al. (1984), Smith, et al. (1985) and Tully and Goldsmith, (1985).

The latest study by Tully and Goldsmith covers the most extensive temperature range 293-896K and the widest range of pressure conditions. High pressure behaviour was observed over 2000 torr and two distinct mechanisms operate; below 500K addition and above 700K abstraction. The intermediate region is difficult to characterise as there is a combination of addition and abstraction process occurring. Figure 2.3 is a plot of the work of Tully, et al. with some of the other recent work as well.

The high pressure rate coefficients for the two regions are;

293-481K

$$k(T) = 4.58 \pm 0.46 \times 10^{-12} \exp[524 \pm 38/T] \text{ cm}^{-3}\text{s}^{-1} \qquad 2.6$$

700-896K

$$k(T) = 3.31 \pm 0.76 \times 10^{-11} \exp[-(1541 \pm 178)/T] \text{cm}^{-3}\text{s}^{-1} \qquad 2.7$$

Further work is required to characterise the fall off behaviour of this reaction.

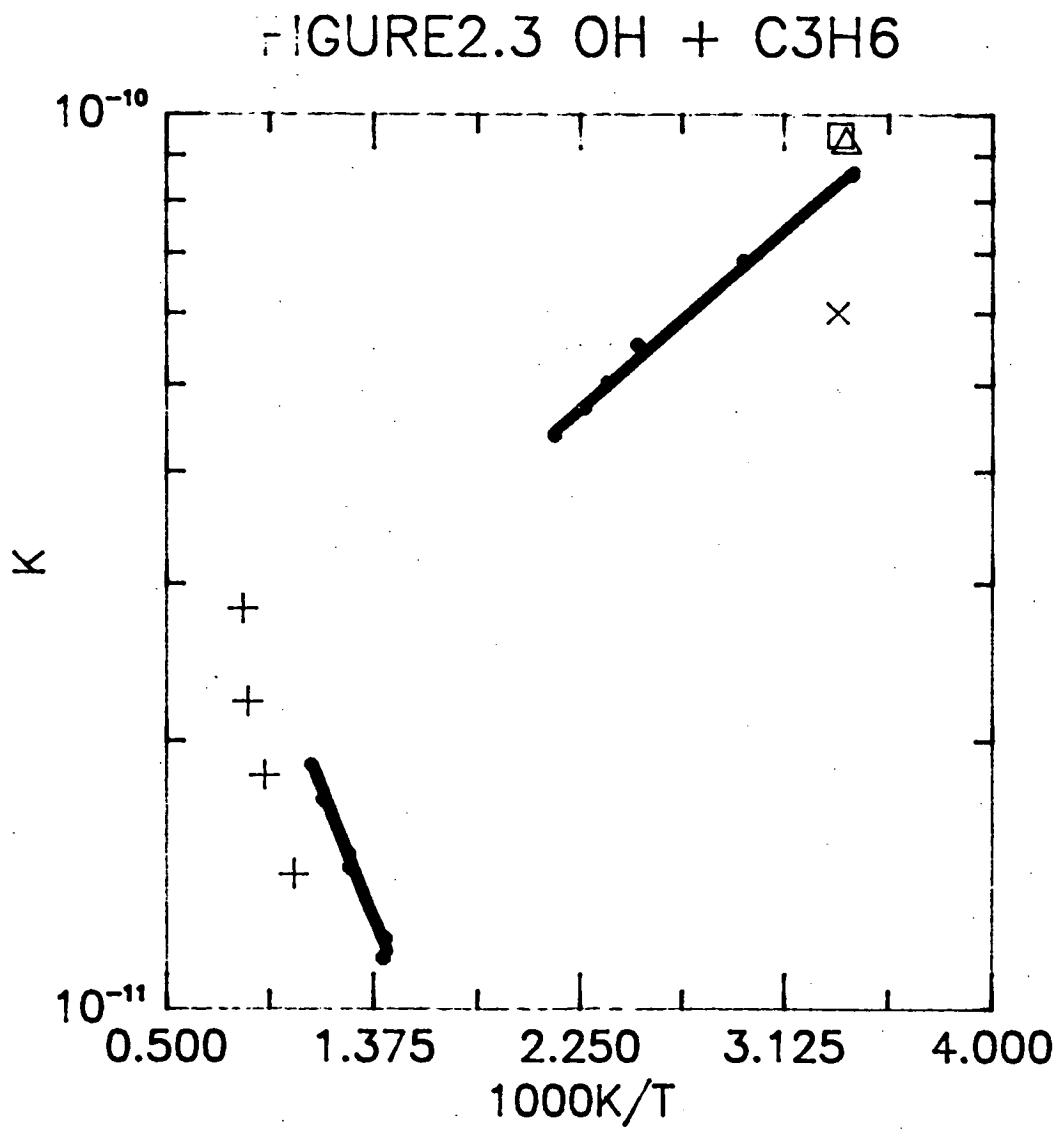

Figure 2.3 Arrhenius Plot
OH + Propene.

- △ Klein, et al. 1984
- × Smith, 1983
- \+ Smith, et al. 1984
- —— Tully, et al. 1985
- □ Zellner, et al. 1984

2.3.7 $OH + C_2H_2$

Several papers have appeared on this reaction in the last four years. (Perry, et al. 1982, Atkinson, et al. 1984, Smith, et al. 1984, Schmidt, et al. 1985, Wahner, et al. 1985, Hatakeyama, 1986).

The fall off behaviour appears to be well characterised at room temperature (figure 2.4).

Behaviour at high temperature is less well researched and understood. The positive temperature dependence of Smith, et al. at 1100-1300K and pressure independence over the 10-140 torr range indicate a direct abstraction process is occurring.

The coefficients are plotted in figure 2.5.

2.3.8 OH + CO

Two papers have appeared on the temperature dependence of this reaction (Ravishankara and Thompson, 1983, Beno, et al. 1985) at two pressures of Argon, 100 and 760 torr respectively. These results are plotted in figure 2.6 along with the recommended result of Warnatz, (1984) and several other results.

It is interesting to note that the work of Beno, et al. (1985) is in distinct disagreement with other work reported from the same laboratory (Jonah, et al. 1984).

Table 2.2 summarises the rate coefficient expressions used to construct figure 2.6.

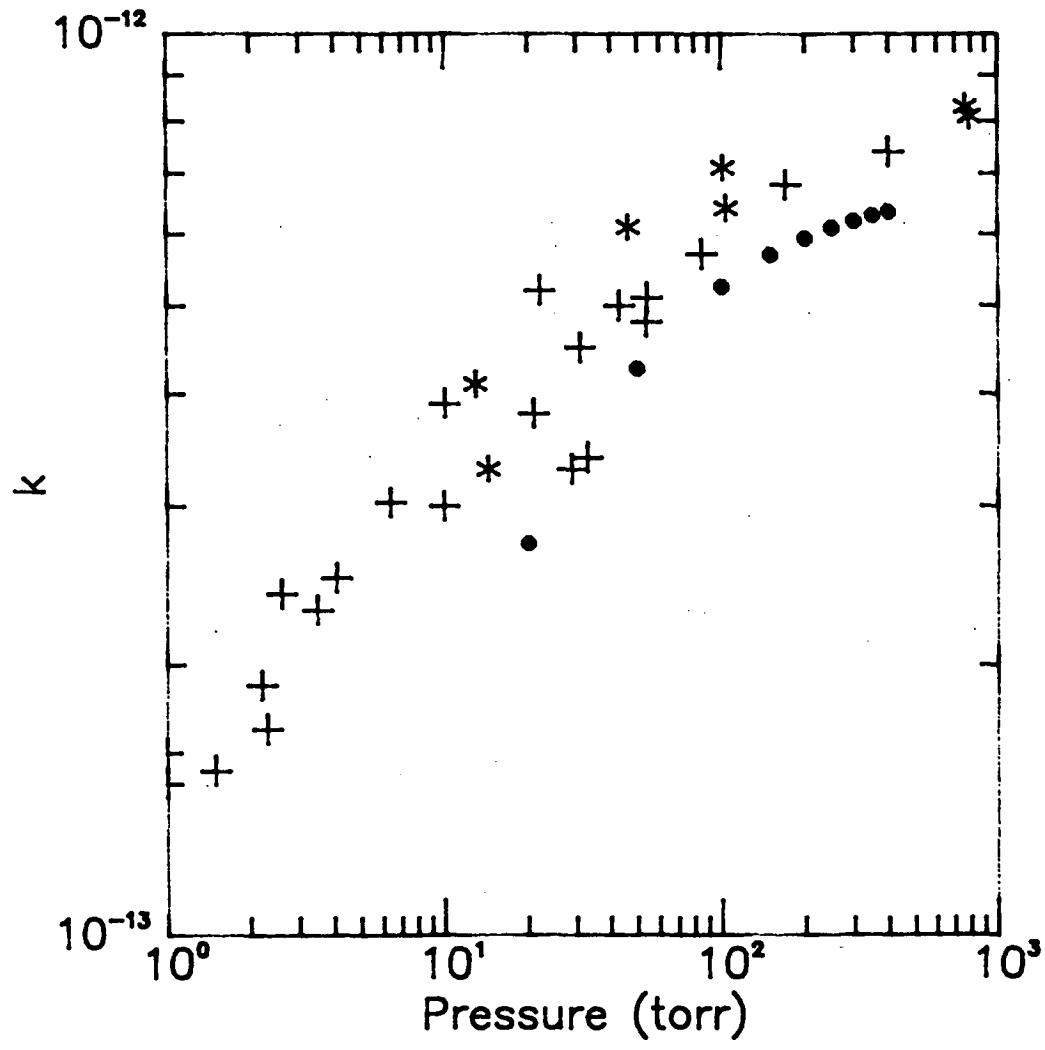

Figure 2.4 Fall Off Curve
OH + Acetylene, 298K

- ● Perry, et al. 1982
- \+ Schmidt, et al. 1985
- ✱ Wahner, et al. 1985

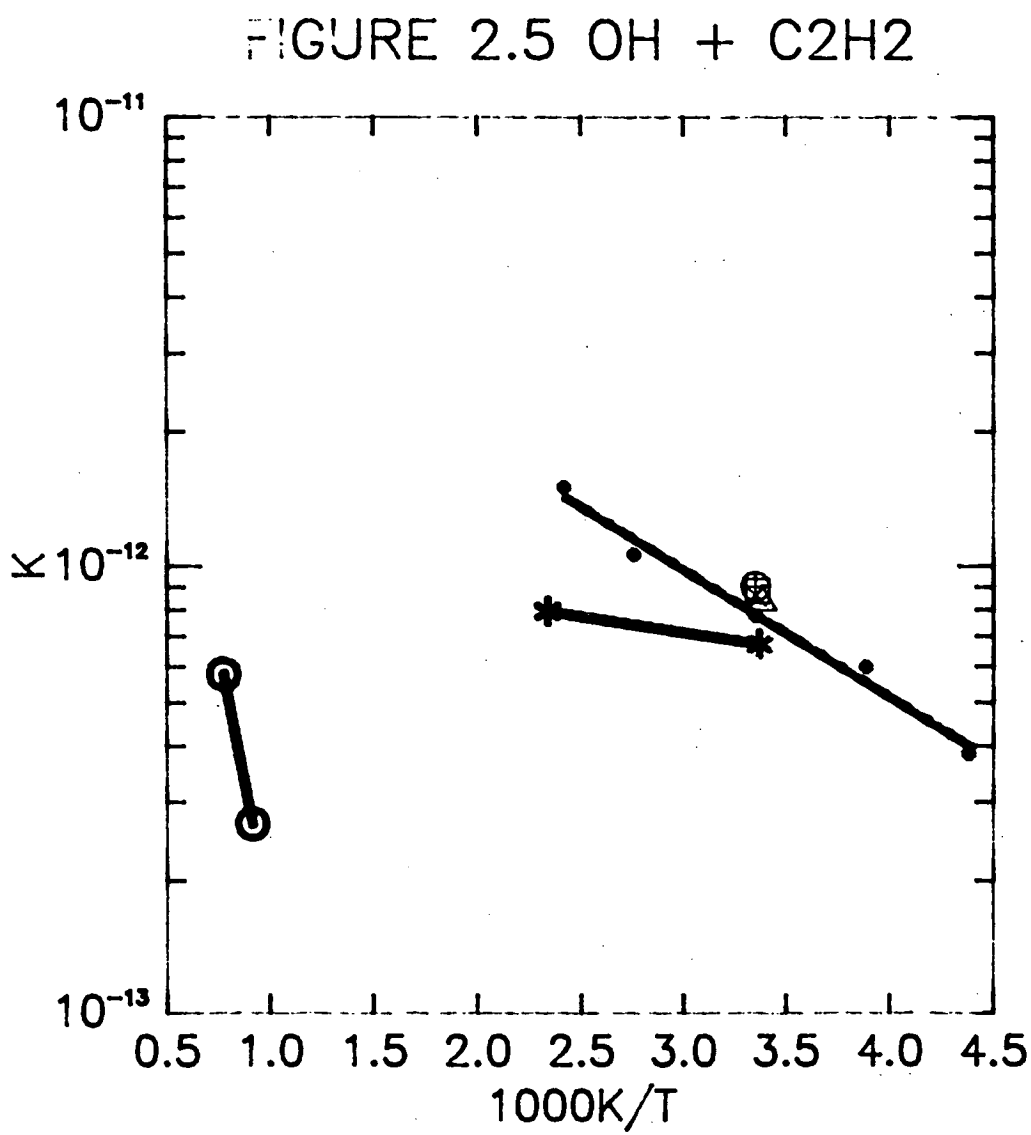

Figure 2.5 High Pressure Arrhenius Plot $k^{\infty}(T)$ OH + Acetylene.

- × Atkinson, et al. 1984
- □ Hatakeyama, 1986
- ✱ Perry, et al. 1982
- △ Schmidt, et al. 1985
- ○ Smith, et al. 1984
- + Wahner, et al. 1985

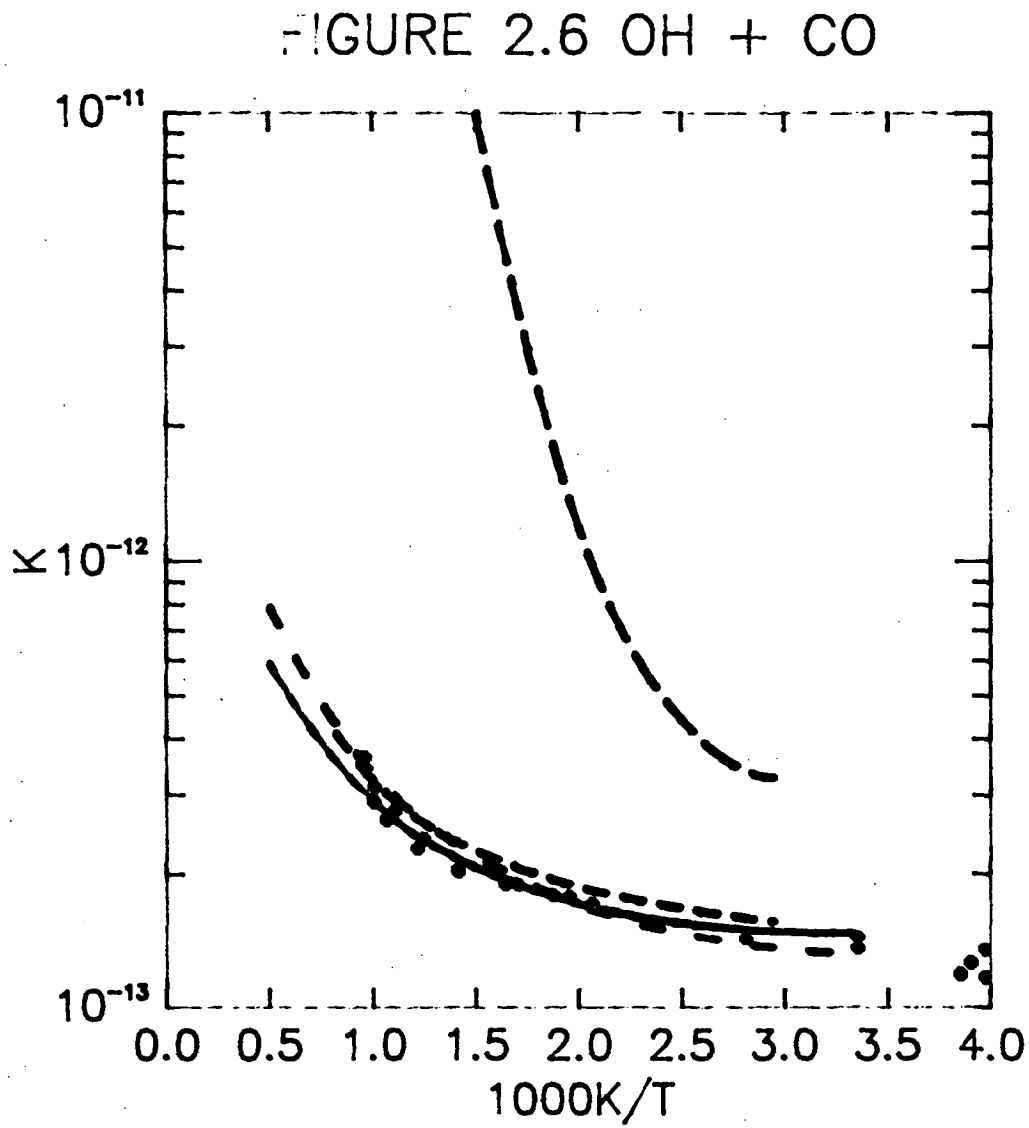

Figure 2.6 Arrhenius Plot
OH + CO.

——— Baulch, et al. 1976
– – Beno, et al. 1985
——— Jonah, et al. 1984
● Ravishankara, et al. 1983
---- Warnatz, 1984

Both results of Beno and Ravishankara are also consistent with the result of Warnatz, and Baulch up to 2000K. The result of Warnatz is still to be recommended in this region.

Table 2.1 OH + CO Rate Coefficients.

References	k (cm^3s^{-1})
Baulch, et al. 1976	$k=2.49x10^{-17}T^{1.3}exp(385/T)$
Ravishankara, et al. 1983	$k=exp(-30.03 + 1.22x10^{-3}T)$
Warnatz, 1984	$k=7.31x10^{-18}T^{1.5}exp(373/T)$
Jonah, et al. 1984	$k=4.05x10^{-14}exp(667/T) + 3.04x10^{-9}exp(-3801/T)$
Beno, et al. 1985	$k=exp(-29.84 + 1.08x10^{-3}T)$

This reaction is also pressure dependent at room temperature and several papers have appeared which study this aspect (Hofzumahaus and Stuhl, 1984, Paraskevopoulos and Irwin, 1984, De More, 1984, Smith and Williams, 1985). In general the results are consistent with a rate coefficient of $1.5x10^{-13}cm^3s^{-1}$ at pressures less than 100 torr, to $2.8x10^{-13}cm^3s^{-1}$ at pressures around one atmosphere. The effect of bath gases vary and the concentration of H_2O has been shown to be important to the determinations (Beno, et al, 1985). The effect of water concentration may explain why the temperature dependence studies give rate constants at room temperature which are characteristic of the results from studies at

lower pressures, rather than results which are indicative of the higher pressures at which the experiments were performed.

2.3.9 $OH + CH_2O$

Three studies of this reaction have been performed since 1984 by Temps and Wagner, (1984), Niki, et al. (1984) and Horowitz, (1984). The results vary by a factor of two but bracket the recommended value of Warnatz, (1984) at 298K. This expression is still to be recommended since there has been no conclusive work presented yet.

$$k(298) = 6.6 \times 10^{-12} cm^3 s^{-1} \qquad 2.8$$

2.3.10 $OH + CH_3CHO$

Michael, et al. (1985) have studied this reaction in the temperature range 244-528K and established that it has a negative T dependence as observed by Atkinson and Pitts, (1978). There are still no high temperature data available. Michael, et al.'s result is

$$k(T) = (5.52 \pm 0.8) \times 10^{-12} \exp(307 \pm 52/T) cm^3 s^{-1} \qquad 2.9$$

2.3.11 OH + HCO

This reaction of importance to combustion has had no direct measurements made up till the work by Temps and Wagner, (1984). They obtained a value of $(1.8\pm0.7)\times10^{-10}cm^3s^{-1}$ at room temperature. This is a factor of two higher than the recommended value of Warnatz, (1984) based on high temperature models.

2.3.12 OH + H_2

This reaction has been extensively studied up to 1980 (Warnatz, 1984). Frank and Just, (1985) have studied it in the range 1700-2500K and found that it could be described with the Arrhenius expression

$$k(T) = (7.42\pm1.08)\times10^{-11}\exp[-(3070\pm260)/T]\,cm^3s^{-1}$$

$$1700 < T < 2500 \qquad 2.10$$

They have placed a $\pm40\%$ scatter on their results which overlaps the recommendation of Warnatz, (1984)and since it covers a much larger temperature range is probably the best until more precise work is undertaken.

2.3.13 $OH + H_2O_2$

Lamb, et al. (1983) have studied this reaction over the temperature range 241-413K. Their results show curvature in this range and are well represented by the three parameter fit

$$k(T) = 7.0 \times 10^{-20}\ T^{2.5}\ \exp(838/T)\ cm^3 s^{-1} \qquad 2.11$$

This is in agreement with previous results above 300K but about 25% higher at 250K. Further work is necessary before this discrepancy is resolved. The reaction is not very important at combustion temperatures as H_2O_2 is formed very slowly (Warnatz, 1984).

2.3.14 $OH + O$

This reaction inhibits combustion as it is the reverse of the $H+O_2$ reaction. Rate coefficients are available only below 425K. Keyser, (1983) and Brune, et al. (1983) reported values of $3.6 \pm 0.4 \times 10^{-11}$ and $3.1 \pm 0.5 \times 10^{-11} cm^3 s^{-1}$ respectively at room temperature which agree well with the recommended value of Warnatz, (1984) of $3.0 \times 10^{-11} cm^3 s^{-1}$.

2.3.15 OH + OH

This reaction has been re-examined by Zellner and Wagner, (1981) and coupled with their earlier work (Ernst, et al. 1978) gives the following expression for k(T)

$$k(T) = \exp(-27.73 \pm 1.49 \times 10^{-3} T)\, cm^3 s^{-1} \qquad 2.12$$

This is to be recommended over the review of Warnatz, (1984).

2.3.16 OH + HO_2

This reaction is of importance because of its chain terminating characteristics. The most recent studies at room temperature by Rozenshtein, et al. (1984) and Braun, et al. (1982) disagree giving $(0.52 \pm 0.12) \times 10^{-10}$ and $1.1 \times 10^{-10} cm^3 s^{-1}$ respectively. While agreement has not been reached yet, consensus of all previous results indicates that the true rate constant is probably within the above range. The recommendation of Warnatz, (1984) is thus too low.

2.4 Reactions of CH_3O/CH_2OH

The reactions of CH_3O and CH_2OH which are important to combustion are the reactions with the radicals O, H, OH, HO_2 and with molecular oxygen. The first four have been rarely studied due to the experimental difficulties associated with production and

reaction of two radicals. The reaction with O_2 has been more extensively studied but only at room temperature.

Additionally, the self and cross reactions of these two radicals will be of importance in any experimental study involving methanol.

2.4.1 CH_3O

No experimental work has been performed on the reactions of CH_3O with O or OH.

Hoyermann, et al. (1981a,b) have studied the reaction

$$CH_3O + H \quad \text{-----} > \quad \text{products}$$

and found a rate constant of $3.3 \times 10^{-11} cm^3 s^{-1}$ at temperatures less than 298K.

The decomposition of the methoxy radical;

$$CH_3O + M \text{ -----} > CH_2O + H + M$$

has only been investigated by Batt, (1979) giving a result of

$$k_{UNI} = 1.6 \times 10^{14} \exp(-13840/T) s^{-1} \qquad 2.13$$

for the temperature range 393-473K.

Lorenz, et al. (1985) have investigated the reaction of CH_3O with O_2 over the range 298-450K.

$$k(T) = 5.5 \pm 2.0 \times 10^{-14} \exp(-1000/T) cm^3 s^{-1} \qquad 2.14$$

When this is combined with the results of Gutman, et al. (1982) over the range 413-628K curvature of the Arrhenius plot is apparent in keeping with the low A factor (figure 2.7).

The self reaction

$$CH_3O + CH_3O \ (+M) \quad \text{-----} > \quad \text{products}$$

has also been investigated at room temperature and found to be very fast $k = 1.1 \times 10^{-11} cm^3 s^{-1}$ (Meier, et al, 1985).

2.4.2 CH_2OH

There is little more data available for reactions of CH_2OH.

The rate constant for the reaction with O atoms has been calculated to be $2 \times 10^{-12} cm^3 s^{-1}$ and that with OH to be $6 \times 10^{-11} cm^3 s^{-1}$ (Grotheer and Just, 1981). The uncertainty factors on these reactions were estimated to be 3 and 10 respectively.

The reaction with H has been investigated by Hoyermann, et al. (1981a,b) and a rate constant of $k = 5 \times 10^{-11} cm^2 s^{-1}$ was obtained. The unimolecular decomposition has not been investigated and the only results available are from models used at high temperatures (Warnatz, 1984).

Three room temperature determinations have been done on the reaction

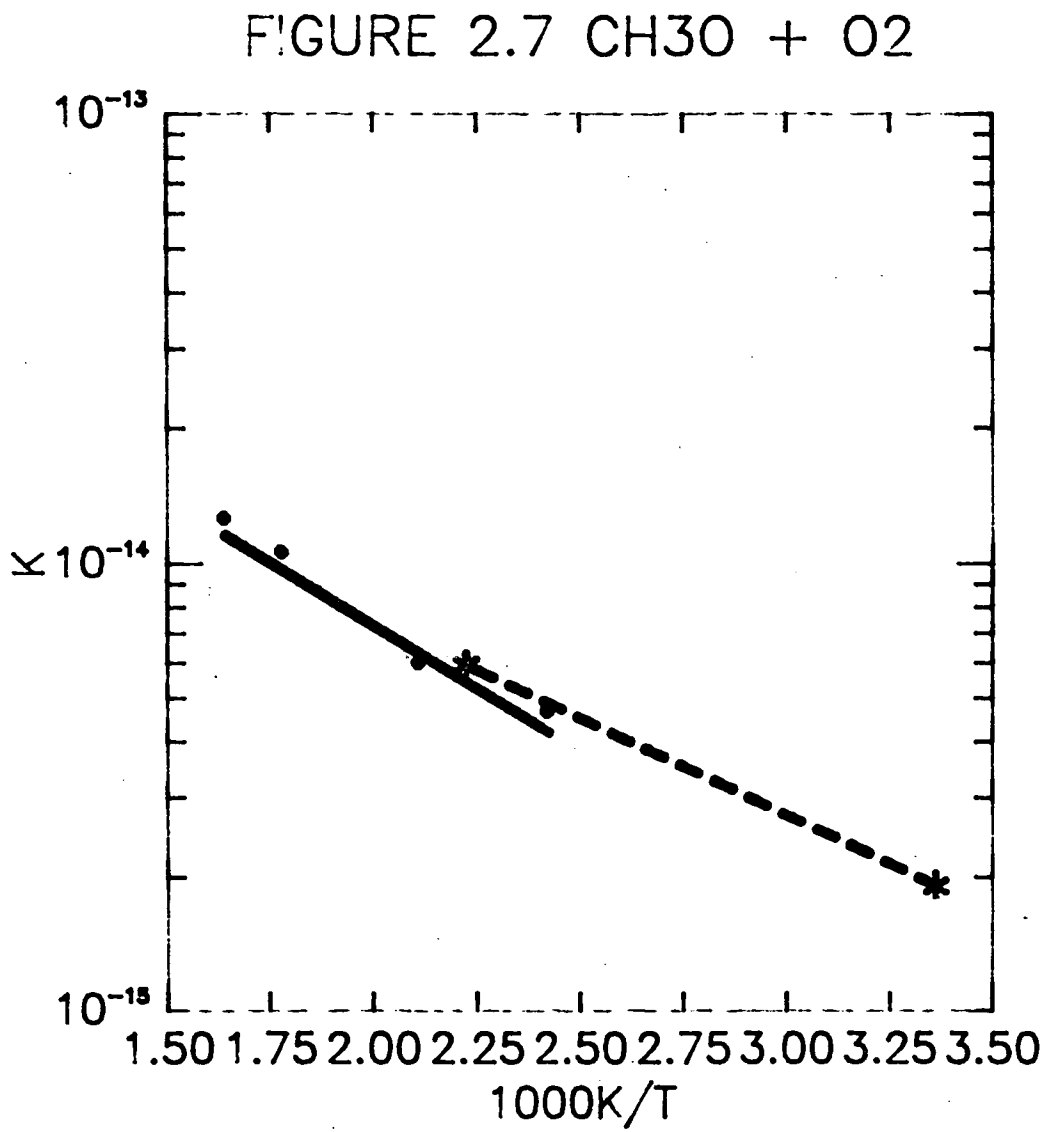

Figure 2.7 Arrhenius Plot
Methoxy + Oxygen.

- ● Gutman, et al. 1982
- ✱ Lorenz, et al. 1985

$$CH_2OH + O_2 \quad \text{-----} > \quad CH_2O + HO_2.$$

Wang, et al. (1984) obtained $1.4\pm0.4 \times 10^{-12} cm^3 s^{-1}$, Grotheer, et al. (1985), $(9.5\pm2.5) \times 10^{-12} cm^3 s^{-1}$ and Radford (1980) $2 \times 10^{-12} cm^3 s^{-1}$. Further work is essential to establish the correct result.

The self reaction of CH_2OH has been determined to be 40% faster than the corresponding reaction of CH_3O. (Meier, et al. 1985)

$$k = 1.5 \times 10^{-11} cm^3 s^{-1} . \qquad 2.15$$

2.4.3 H + CH_3O/CH_2OH stabilization

The work of Hoyermann on $H+CH_3O/CH_2OH$ included extensive isotopic experimentation and product analysis. The relative importance of each channel has been assessed and it has shown that approximately 25% of the reaction proceeds via complex formation to two other channels.

$$H + CH_3O/CH_2OH \quad \text{-----} > \quad CH_2O + H_2 \quad \sim 75\% \qquad (I)$$

$$\text{-----} > \quad CH_3OH^* \quad \sim 25\%$$

$$CH_3OH^* \quad \text{-}\underline{[M]}\text{-} > \quad CH_3OH \qquad (II)$$

$$\text{-----} > \quad CH_3 + OH \qquad (III)$$

At the pressures (0.1-2 torr) of the Hoyermann, et al. (1981a) study the ratio k_{II}/k_{III} - 1/4. 5% of the total reaction results in reformation. Another Hoyermann, et al. (1981b) study at temperatures of 500-680K and pressures of 1.5-6 torr found 10-15% reformation of methanol and predictions for 1000K and 760 torr were for 20% reformation of CH_3OH by II and k_{II}/k_{III} - 4/1 (Abstraction still accounts for ~ 75%).

This has particular consequences for any study of methanol reactions in the presence of H atoms, for example, such as the reaction with OH when H_2O is photolysed as the OH source.

2.5.1 Non Arrhenius Behaviour

The extension of experimental data to wider temperature regimes has resulted in changes to the way the rate coefficients have been parameterized. Arrhenius type behaviour can no longer be assumed to be followed in all cases except over small temperature regions (100-200K). (see section 2.3). The usual parameterisation can be expressed as in 2.14.

$$k = AT^n e^{(-Ea/RT)} \qquad 2.16$$

The parameters A, n, and Ea are determined from a non-linear least squares minimization routine.

This type of behaviour has provided data for the application of predictive theories for rate coefficients to systems exhibiting

curvature in their Arrhenius plots (Mozurkewich, et al, 1984a, 1984b; Lamb, et al, 1984; Wagner, et al, 1981; Smith, et al, 1973; Golden, 1979; Schott, et al, 1974; Walch, et al, 1980). The predictive theories in question are usually forms of collision theory (Light, 1978) or transition state theory (Schott, et al, 1974; Walch, et al, 1980). There are two ways in which we can examine the curvature of an Arrhenius plot. The underlying reasons for the curvature can be examined, or we can attempt to explain the temperature dependence by use of a rate theory. The second approach is made much easier if we have some perception of the underlying causes since a theory appropriate to the cause of the curvature can then be chosen.

2.5.2 Causes of Curvature in Arrhenius Plots

There are four identifiable reasons why such plots may display curvature. These are the presence of an indirect reaction pathway, tunnelling, state specificity, and non-equilibrium effects. An indirect pathway implies that there is more than one barrier to reaction as in the case of,

$$OH + CO \quad \text{----->} \quad H + CO_2$$

This has a well established curvature as described in section 2.3.8 with a rate constant of

$$k = 7.3\times10^{-18}\ T^{1.5}\ \exp(373/T)\ cm^3s^{-1} \qquad 2.17$$

The curvature along with observation of a pressure dependence at room temperature (De More, 1984; Smith, et al, 1985, Paraskevopoulos, et al, 1984) indicates that there are two barriers to reaction separated by a stable intermediate HOCO as shown in figure 2.8. This reaction has been discussed by Mozurkewich, et al. (1984b), and also by Zellner, (1984).

Agreement between theory and experiment is reasonable within the error limits placed on the experimental data but further work is required.

Tunnelling is the phenomenon associated with an apparent increase in the rate constant which is not consistent with the barrier height of the reaction. This can, in general, only be treated by quantum mechanical arguments and requires a quite sophisticated model. The reaction

$$OH + H_2 \quad \text{-----}> \quad H_2O + H$$

has been treated by assuming that tunnelling occurs (Zellner, 1984; Schatz and Walch, 1980). As well as this approach, Zellner, et al. (1981), have tried a state specific collision theory and did not obtain agreement with experiment. They assumed that room temperature reaction occurred via the ground vibrational state only and consequently they underestimated the barrier because no account was taken of a tunnelling contribution.

FIGURE 2.8 OH + CO POTENTIAL

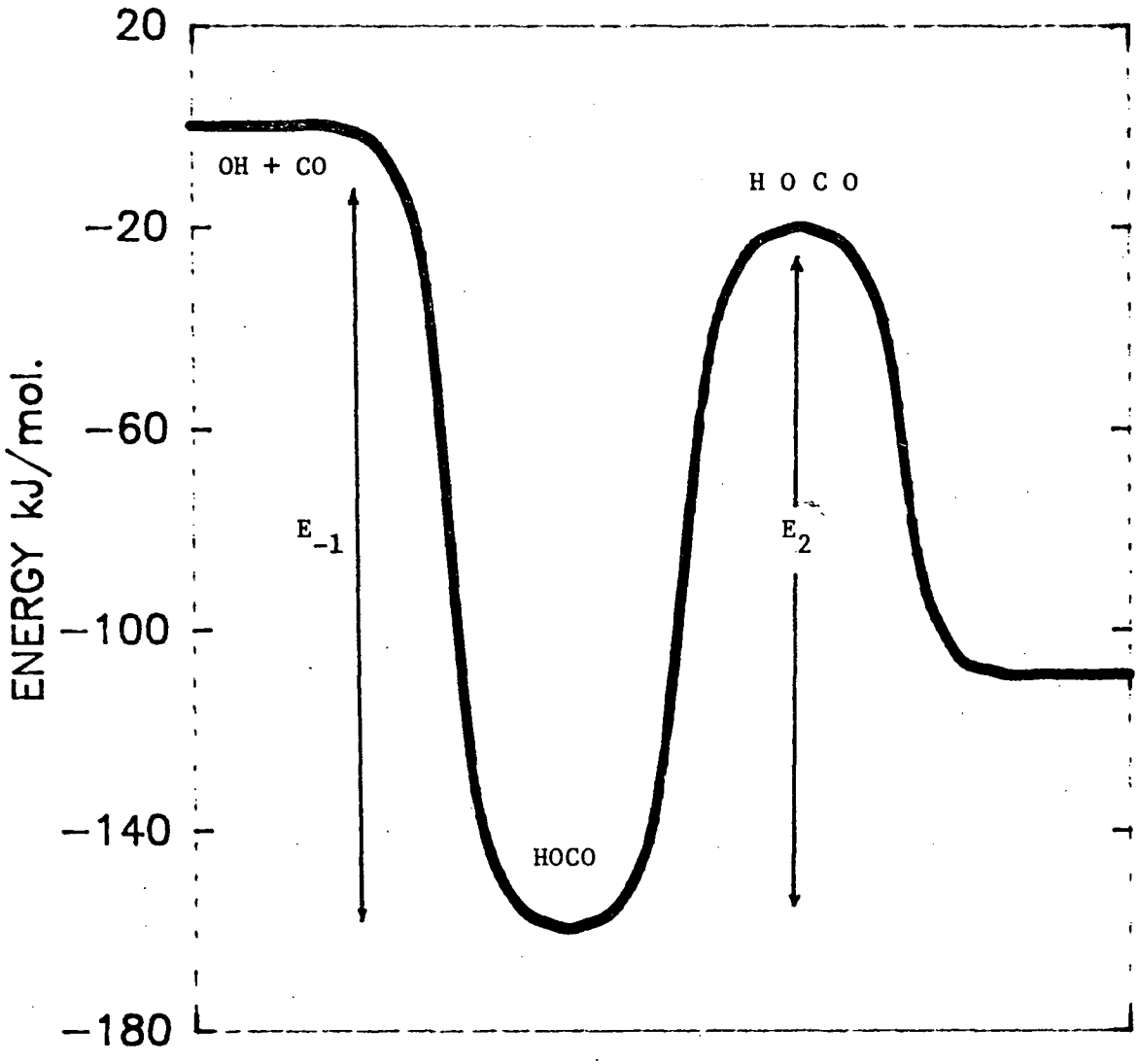

Figure 2.8 Potential Surface
For OH + CO --> CO_2 + H
From Zellner, 1984

The state specificity of a reaction is due to enhanced (or reduced) reactivity from different excited states of the molecule. This concept is generally applied to vibrational states as rotational and translation states relax very quickly under the usual conditions for kinetic experiments. The curvature of the thermal rate coefficient is shown in figure 2.9 along with the $k_{v=0,1}$ state specific rate coefficients (Zellner, 1984). This indicates that only above 1500K is there significant curvature.

The final influence which may cause curvature are non-equilibrium effects in which perturbation of the equilibrium distribution of states is caused by reaction, and energy transfer via inelastic collisions is insufficient to maintain the equilibrium. These effects only become important if a significant portion of reaction goes via an excited state and if vibrational relaxation is slow (Zellner, 1984).

2.5.3 Theories

There are two general forms of theory in use apart from ab initio calculations. These are collision theory and transition state theory. The applications of these theories have been dealt with quite extensively by Zellner, (1984) and only some salient points will be indicated here.

The collision theory rate coefficient expression is;

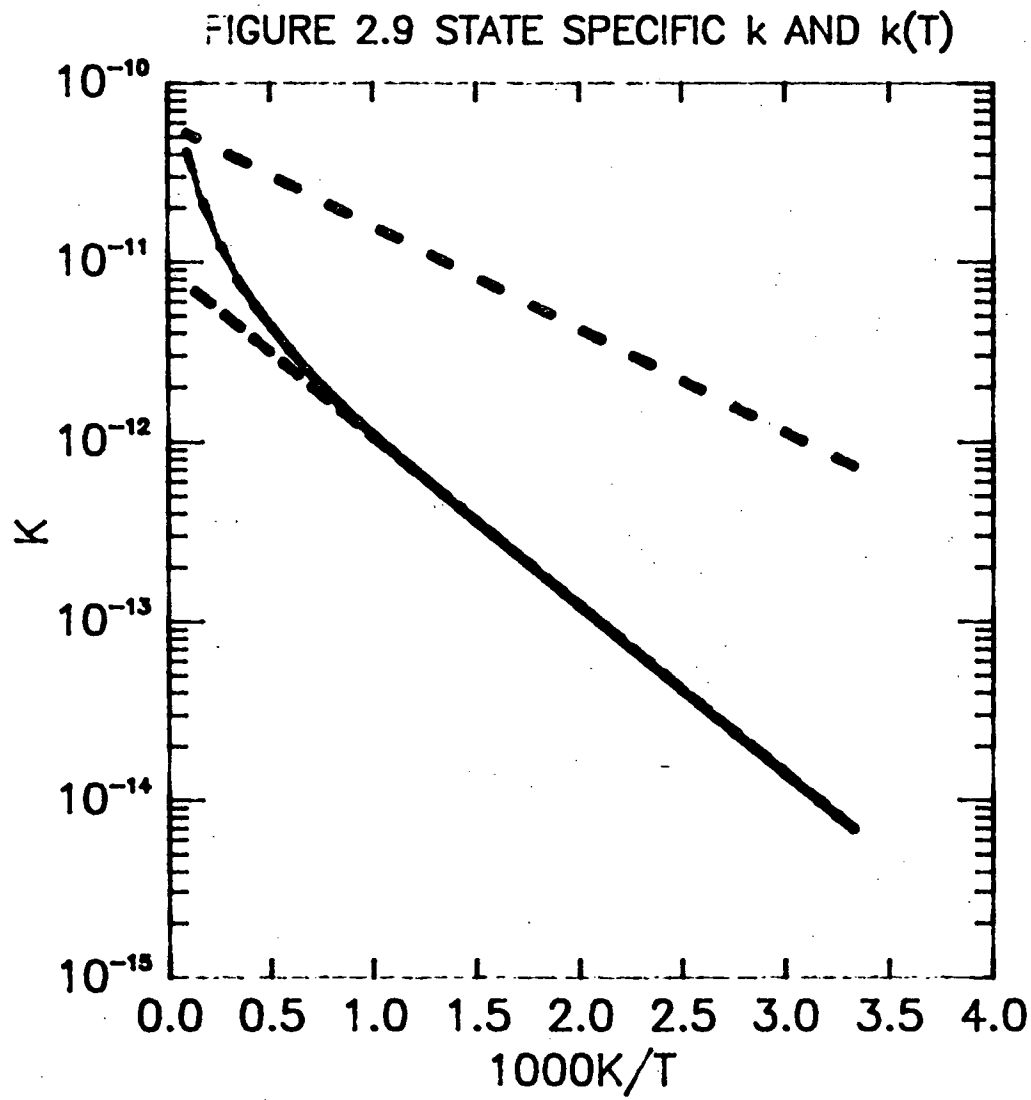

Figure 2.9 The Effect of State Specificity on $OH + H_2 \rightarrow H_2O + H$

- - - - - $k_{v=0}$
- - - $k_{v=1}$
——— k(T)

Zellner, 1984

$$k = (8k_BT/\pi\mu)^{1/2}(k_BT)^{-2}\int_{E^0}^{\infty} E\sigma(E)e^{-E/k_BT}dE \qquad 2.18$$

The temperature dependence of this expression is nominally $T^{-3/2}$ times the T dependence associated with the integral of the reactive cross section, $\int \sigma(E).dE$. Here E^o is the threshold energy not the activation energy E_A. The threshold energy is that energy below which $\sigma(E)$ is zero. The relationships between E_A and E_o were initially derived by Tolman (1927) and additionally predict that E_A increases with temperature and also that $E_A \rightarrow E^o$ as $T \rightarrow 0$.

The form of $\sigma(E)$ will dictate the temperature dependence of eqn. 2.18 and this may be illustrated with examples of hard sphere cross section and an energy dependent cross section.

The hard sphere cross section is

$$\sigma(E) = 0 \quad E \leq E^o$$
$$= \pi d^2 \quad E > E^o \qquad 2.19$$

where $d = R_A + R_B$ and is the reactive collision diameter for A+B.

If we substitute 2.19 into 2.18 we get

$$k = (8\pi kT/\mu)^{1/2} d^2(1 + E^o/kT)e^{-E^o/kT} \qquad 2.20$$

Note that as T increases the temperature dependence of k will tend to $T^{1/2}$ as the term $(1 + E^{o}/kT)$ will tend to one.

Consider now an energy dependent cross section (line of centres)

$$\sigma(E) = 0 \quad E \leq E^{o}$$

$$= \pi d^{2} E^{-1}(E-E^{o}) \quad E > E^{o} \qquad 2.21$$

Substituting 2.21 into 2.18 gives

$$k = (8\pi kT/\mu)^{1/2} d^{2} e^{-E^{o}/kT} \qquad 2.22$$

which is the high energy limiting case of 2.20.

This function also predicts that the activation energy will increase with temperature

$$E_{A} = (E^{o} + kT/2)\,6.023\times10^{23} \quad \text{(mole units)} \qquad 2.23$$

as indicated by Tolman (1927).

In general, an energy dependent $\sigma(E)$ will lead to an E dependent activation energy and excitation functions (reactive cross sections) of the form

$$\sigma(E) = 0 \qquad E \leq E^{o}$$

$$\propto E^{-1}(E-E^{o})^{n+1/2} \qquad E > E^{o} \qquad 2.24$$

give rate coefficients of the form

$$k \propto T^{n} e^{-E^{o}/kT} \qquad 2.25$$

There are other forms of collision theory which relate to state specificity and vibrational enhancement which provide varying type of results. The most important result of this discussion is that a knowledge of the reactive cross section, whether it be a collision cross section or state specific, is critical to the formulation of the theory, its resultant temperature dependence, and its application to explain experimental results.

Transition state theory differs from collision theory by virtue of the fact that the parameters required for the calculation are in principle obtainable from molecular properties

$$k = (kT/h)(Q_{AB}/Q_{A}Q_{B})e^{-\Delta\epsilon_{z}/kT} \qquad 2.26$$

When we take account of the translational and rotational partition functions and their temperature dependence then eqn. 2.26 may be expressed as

$$k = \text{constant.}\ T^{-(n+1)/2}[Q_{vib}/(Q_{vibA}Q_{vibB})]e^{-\Delta\varepsilon_z/kT} \qquad 2.27$$

Here the value of n is the number of rotational degrees of freedom lost in the formation of the activated complex.

The alternative thermodynamic formulation of transition state theory results in the following expression

$$k = (kT/h)R'T\ e^{(\Delta S^+/R - \Delta H^+/RT)} \qquad 2.28$$

where $R' = 82.06\ cm^3 atm\ K^{-1} mol^{-1}$.

The A factor can be identified with the term

$$A = e^2(kT/h)R'T\ e^{\Delta S^+/R}\ cm^3 mol^{-1} \qquad 2.29$$

since

$$E_A = \Delta H^+ + 2RT \qquad 2.30$$

Assuming that ΔS^+ is temperature independent then this form of transition state theory gives $k \propto T^2$.

In general ΔS^+ and ΔH^+ are temperature dependent but the effects can be quite small as the average heat capacity of activation $\langle \Delta Cp^+ \rangle$ is usually small.

2.5.4 Theoretical Vs Empirical

While the accuracy of experimental results has improved sufficiently to unequivocably indicate curvature of Arrhenius plots it has not the accuracy to indicate the form of the temperature dependence from statistical fits.

In view of this, the values of n which are non-integral or not multiples of 0.5 found by empirical fits to equation 2.16 should not be regarded as having a theoretical basis. It would be better to use knowledge of the reaction to predict the possible reasons for the curvature and use an appropriate theory with a predefined T dependence to parameterise the rate coefficient. This should include the temperature dependence of the activation energy, which probably accounts for that portion of the empirical temperature dependence which is not explicitly accounted for by the pre-exponential factor in the theoretical treatments.

2.5.5 Multiple Pathways

There is one further cause of non-Arrhenius behaviour which is not related to any of the fundamental effects of temperature indicated in the previous sections. This is unaccounted alternative pathways with different activation energies. These can make significant contributions particularly at higher temperatures. The reaction of OH with CH_3OH is a good example of this phenomenon with the reaction proceeding via two pathways

FIGURE 2.10 OH + CH3OH

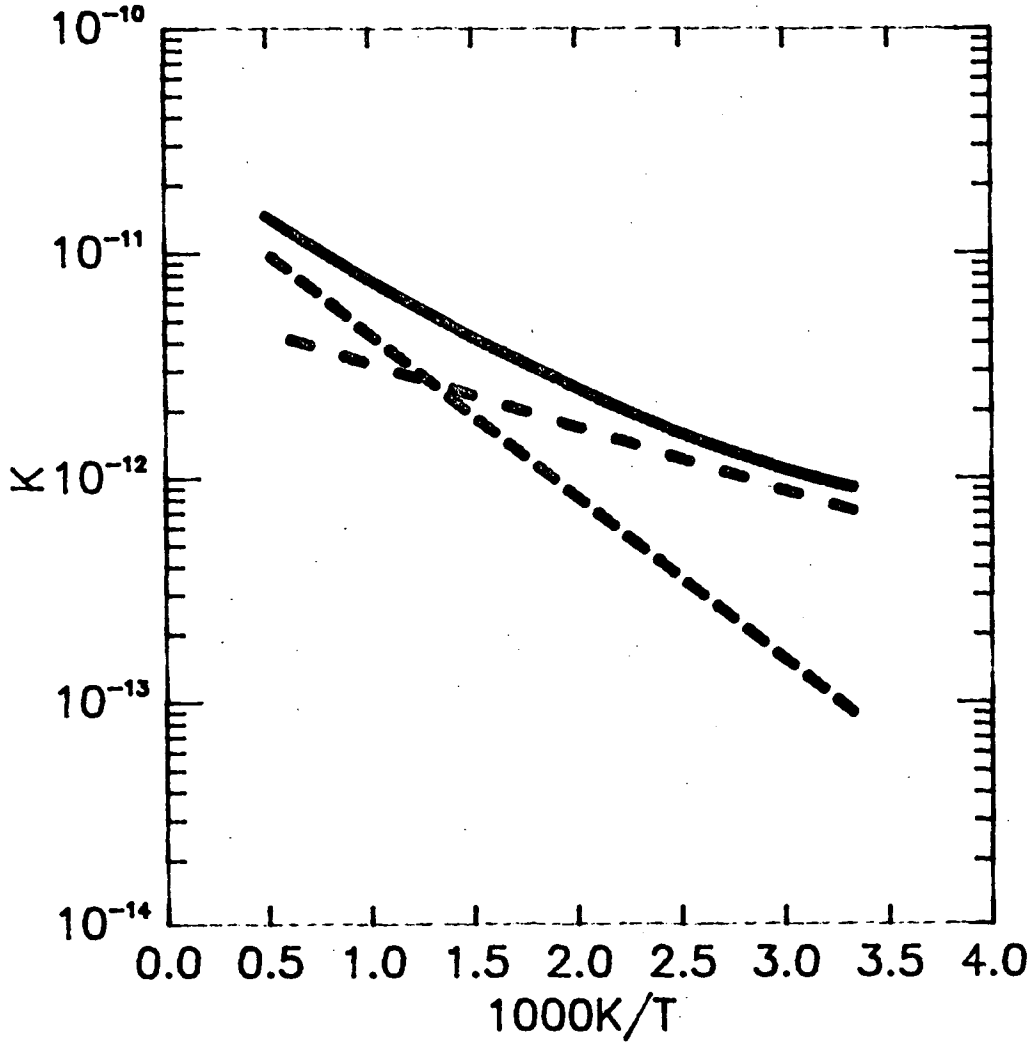

Figure 2.10 Arrhenius Plot of The Two Channel Reaction of OH With Methanol.

— — OH + CH_3OH --> CH_2OH + H_2O

– – – OH + CH_3OH --> CH_3O + H_2O

——— $k(T)_{combined}$

$$OH + CH_3OH \quad \text{-----} > \quad CH_2OH + H_2O \qquad R2.1$$

$$\text{-----} > \quad CH_3O + H_2O \qquad R2.2$$

Hagele, et al. (1984) have predicted that R2.1 will provide the observed temperature dependence at temperatures below 1000K but above 1000K the reaction will proceed predominantly via R2.2. This is shown in figure 2.10.

The possibility of this type of effect though is easily predicted from the structure of the reactants. However, the importance of the secondary reaction is not easily determined as activation energies are not simply predictable.

2.6 Conclusions.

The importance of the OH radical in combustion cannot be under-estimated. While much work has been done on many reactions, more research needs to be carried out to resolve those questions that have arisen from the current work and to extend the investigations to other reactions of OH over an extended temperature range.

2.7 References

Atkinson, R., Pitts, J.N. Jr., J. Chem. Phys., 1978, 68, 3581.

Atkinson, R., Darnall, K.R., Lloyd, A.C., Winer, A.M., Pitts, J.N., Jr., Adv. Photochem.,1979, 11, 375.

Atkinson, R., Aschmann, S.M., Carter, W.P.L., Winer, A.M., Pitts, J.N. Jr., Int. J. Chem. Kinet., 1982, 14, 781.

Atkinson, R., Carter, W.P.L., Aschmann, S.M., Winer, A.M., Pitts, J.N. Jr., Int. J. Chem. Kinet., 1984, 16, 469.

Atkinson, R., Aschmann, S.M., Int. J. Chem. Kinet., 1984, 16, 259.

Baulch, D.L., Drysdale, D.D., Horne, D.G., Lloyd, A.C., "Evaluated Kinetic Data for High Temperature Reactions, Vol 1: Homogeneous Gas Phase Reactions of the H_2-O_2 System," Butterworths, London, 1972.

Baulch, D.L., Drysdale, D.D., Horne, D.G., "Evaluated Kinetic Data for High Temperature Reactions, Vol 2: Homogeneous Gas Phase Reactions of the H_2-N_2-O_2 System," Butterworths, London, 1973.

Baulch, D.L., Drysdale, D.D., Duxbury, J., Grant, S.J., "Evaluated Kinetic Data for High Temperature Reactions, Vol 3: Homogeneous Gas Phase Reactions of the O_2-O_3 System, the CO-O_2-H_2 System, and of Sulphur Containing Species," Butterworths, London, 1976.

Baulch, D.L., Craven, R.J.B., Din, M., Drysdale, D.D., Grant, S., Richardson, D.J., Walke, A., Watling, G., J. Chem. Soc. Faraday Trans. I, 1983, 79, 689.

Baulch, D.L., Campbell, I.M., Saunders, S.M., J. Chem. Soc. Faraday Trans. I, 1985, 81, 259.

Baulch, D.L., et al., J. Phys. Chem. Ref. Data, 1980, 9, 295; 1982, 11, 327.

Beno, M.F., Jonah, C.D., Mulac, W.A., Int. J. Chem. Kinet., 1985, 17, 1091.

Benson, S.W., Golden, D.M., Lawrence, R.W., Shaw, R., Woolfolk, R.W., "Estimating the Kinetics of Combustion Including Reactions Involving Oxides of Nitrogen and Sulfur," Environmental Protection Agency Report No. EPA-600/2-75-019, August 1975.

Benson, S.W., O'Neal, H.E., "Kinetic Data on Gas Phase Unimolecular Reactions," NBS-NSRDS-21, 1971.

Bohland, T., Temps, F., Wagner, H.Gg., Z. Phys. Chem. Neue Folge, 1984, 142, 129.

Bartels, M., Hoyermann, K., Sievert, R., 19th Symp. (Intl.) Ckmb., 1982, 61.

Bott, J.F., Cohen, N., Int. J. Chem. Kinet., 1984, 16, 1557.

Braun, M., Hofzumahaus, A., Stuhl, F., Ber. Bunsenges. Phys. Chem., 1982, 86, 597.

Brune, Wm.H., Schwab, J.J., Anderson, J.G., J. Phys. Chem., 1983, 87, 4503.

Cohen, N., Westberg, K.R., J. Phys. Chem. Ref. Data, 1983, 12, 531.

Cox, R.A., Derwent, R.G., Kearsey, S.V., Batt, L., Patrick, K.G., J. Photochem., 1980, 13, 149.

De More, W.B., Int. J. Chem. Kinet., 1984, 16, 1187.

Engleman, V.S., "Survey and Evaluation of Kinetic Data on Reactions in Methane/Air Combustion," Environmental Protection Agency Report No. EPA-600/2-76-003, January 1976.

Frank, P., Just, Th., Ber. Bunsenges. Phys. Chem., 1985, 89, 181.

Golden, D.M., J. Phys. Chem., 1979, 83, 108.

Grotheer, H.H., Riekert, G., Meier, V., Just, Th., Ber. Bunsenges. Phys. Chem., 1985, 89, 187.

Grotheer, H.H., Just, Th., Chem. Phys. Letts., 1981, 78, 71.

Gutman, D., Sanders, N., Butler, J.E., J. Phys. Chem., 1982, 86, 66.

Hatakeyama, S., Washida, N., Akimoto, H., J. Phys. Chem., 1986, 90, 173.

Herron, J.T., Huie, R.E., J. Phys. Chem. Ref. Data, 1973, 2, 467.

Hofzumahaus, A., Stuhl, F., Ber. Bunsenges. Phys. Chem., 1984, 88, 557.

Horowitz, A., J. Phys. Chem., 1984, 88, 1588.

Hoyermann, K., Lohtfield, N.S., Sievert, R., Wagner, H.Gg., 18th Symp. (Intl.) Comb., 1981a, 831.

Hoyermann, K., Sievert, R., Wagner, H.Gg., Ber. Bunsenges. Phys. Chem., 1981b, 85, 149.

Jeong, K.-M., Hsu, K.-J., Jeffries, J.B., Kaufman, F., J. Phys. Chem., 1984, 88, 1222.

Keyser, L.F., J. Phys. Chem., 1983, 87, 837.

Kerr, J.A., Parsonage, M.J., "Evaluated Kinetic Data on Gas Phase Addition Reactions: Reactions of Atoms and Radicals with Alkenes, Alkynes and Aromatic Compounds," Butterworths, London, 1972.

Kerr, J.A., Parsonage, M.J., "Evaluated Kinetic Data on Gas Phase Hydrogen Transfer Reactions of Methyl Radicals," Butterworths, London, 1976.

Klein, Th., Barnes, I., Becker, K.M., Fink, E.H., Zabel, F., J. Phys. Chem., 1984, 88, 5020.

Kondratiev, V.N., "Konstanty Skorosti Gazofaznykh Reaktsij Spravochnik," (Izdatelstvo "Nauka", Moskva, 1970) ("Rate Constants of Gas Phase Reactions, Reference Book," R.M. Fristrom, Ed., Com-72-10014, NBS 1972.)

Lamb, J.J., Molina, L.T., Smith, C.A., Molina, M.J., J. Phys. Chem., 1983, 87, 4467.

Lamb, J.J., Mozurkewich, M., Benson, S.W., J. Phys. Chem., 1984, 88, 6441.

Lee, J.H., Tang, I.N., J. Chem. Phys., 1982, 77, 4459.

Lloyd, A.C., Int. J. Chem. Kinet., 1974, 6, 169.

Lorenz, K., Rhasa, D., Zellner, R., Fritz, B., Ber. Bunsenges. Phys. Chem., 1985, 89, 341.

Meier, U., Grotheer, H., Riekert, G., Just, Th., Ber. Bunsenges. Phys. Chem., 1985, 89, 325.

Michael, J.V., Keil, D.G., Kelmn, R.B., J. Chem. Phys., 1985, 83, 1630.

Mozurkewich, M., Benson, S.W., J. Phys. Chem., 1984a, 88, 6429.

Mozurkewich, M., Lamb, J.J., Benson, S.W., J. Phys. Chem., 1984b, 88, 6435.

Niki, H., Maker, P.D., Savage, C.M., Breitenbach, L.P., J. Phys. Chem., 1984, 88, 5342.

Ohta, T., J. Phys. Chem., 1983, 87, 1209.

Ohta, T., Int. J. Chem. Kinet., 1984, 16, 879.

Paraskevopoulos, G., Irwin, R.S., Chem. Phys. Letts., 1982, 93, 138.

Paraskevopoulos, G., Irwin, R.S., J. Chem. Phys., 1984, 80, 259.

Perry, R.A., Williamson, D., Chem. Phys. Letts., 1982, 93, 331.

Quick, C.R.Jr., Tiee, J.J., Chem. Phys. Letts., 1983, 100, 223.

Ravishankara, A.R., Thompson, R.L., Chem. Phys. Letts., 1983, 99, 377.

Rohzenshtein, V.B., Gershenzon, Yu. M., Il'in, S.D., Kiskovitch, O.P., Chem. Phys. Letts., 1984, 112, 473.

Schmidt, V., Zhu, G.Y., Becker, K.H., Fink, E.H., Ber. Bunsenges. Phys. Chem., 1985, 89, 321.

Smith, R.H., J. Phys. Chem., 1983, 87, 1596.

Smith, G.P., Fairchild, P.W., Crosley, D.R., J. Chem. Phys., 1984, 81, 2667.

Smith, G.P., Fairchild, P.W., Jeffries, J.B., Crosley, D.R., J. Phys. Chem., 1985, 89, 1269.

Smith, I.W.M., Zellner, R., J. Chem. Soc. Faraday II, 1973, 69, 1617.

Smith, I.W.M., Williams, M.D., Ber. Bunsenges. Phys. Chem., 1985, 89, 319.

Schatz, G.C., Walch, S.P., J. Chem. Phys., 1980, 72, 776; 1976, 65, 4642, 4648.

Schott, G.L., Getzinger, R.W., Seitz, W.A., Int. J. Chem. Kinet., 1974, 6, 921.

Temps, F., Wagner, H.Gg., Ber. Bunsenges. Phys. Chem., 1984, 88, 415.

Tolman, R.C., "Statistical Mechanics with Applications to Physics and Chemistry", Chemical Catalogue Company, New York, 1927.

Tully, F.P., Ravishankara, A.R., J. Phys. Chem., 1980, 84, 3126.

Tully, F.P., Chem. Phys. Letts., 1983, 96, 148.

Tully, F.P., Ravishankara, A.R., Carr, K., Int. J. Chem. Kinet., 1983, 15, 1111.

Tully, F.P., Goldsmith, J.E.M., Chem. Phys. Letts., 1985, 116, 345.

Tully, F.P., Droege, A.T., Koszykowski, M.L., Melius, C.F., J. Phys. Chem., 1986, 90, 691.

Wagner, G., Zellner, R., Ber. Bunsenges. Phys. Chem., 1981, 85, 1122.

Wahner, A., Zetzsch, C., Ber. Bunsenges. Phys. Chem., 1985, 89, 323.

Walch, S.P. et. al., J. Chem. Phys., 1980, 72, 2894.

Wang, W.C., Suto, M., Lee, L.C., J. Chem. Phys., 1984, 81, 3122.

Warnatz, J., In "Combustion Chemistry", Ed. W.C. Gardiner, Jr., Springer-Verlag, New York, 1984, pp 197-360.

Westley, F., "Table of Recommended Rate Constants for Chemical Reactions Occurring in Combustion.", NBS-NSRDS-67, April 1980.

Zellner, R., Steinert, W., Chem. Phys. Letts., 1981, 81, 568.

Zellner, R., Lorenz, K., J. Phys. Chem., 1984, 88, 984.

Zellner, R., In "Combustion Chemistry", Ed. W.C. Gardiner, Jr., Springer-Verlag, New York, 1984, pp 163, 167.

Chapter 3

The Reaction Of OH With Methanol and Ethanol.

3.1 Previous Studies

The reactions of hydroxyl radicals have been shown to be key reactions in the oxidation of hydrocarbons and other fuels and in the chemistry of the lower atmosphere. (Atkinson,et al. 1979; Baulch, et al. 1981; Westbrook, et al. 1979). The reactions are fast (Atkinson) and have low activation energies. However, despite their importance few measurements have been made until recently of the rate constants over an extended temperature range.

3.1.1 Methanol

Recent investigations of the reaction of OH with methanol (Campbell, et al. 1976; Hagele, et al. 1983; Meier, et al. 1984; Overend, et al. 1978; Ravishankara, et al. 1978),

$$OH + CH_3OH \longrightarrow CH_2OH + H_2O \qquad R1a$$

$$\longrightarrow CH_3O + H_2O \qquad R1b$$

have shown that the reaction has an activation energy lower than that predicted by the modelling of high temperature flame (Vandooreen, et al. 1980), flow reactor (Aronowitz, et al. 1979) and shock tube (Bowman, 1975) studies which highlights the problems inherent in attempting to derive rate constants from computer modelling of complex reaction mechanisms.

The techniques suitable for studying these reactions at temperatures between 300 and 1000K are direct unlike the techniques necessary at combustion temperatures and as such should be much more reliable. Two different experimental techniques have been used covering the ranges 300-1000K and 300-450K respectively. Discharge flow coupled with laser induced fluorescence and time of flight mass spectrometry was used for experiments up to 1000K (Meier, et al. 1984), and laser flash photolysis coupled with resonance fluorescence and laser induced fluorescence for the lower range. (Hagele, et al. 1983).

3.1.2 Ethanol

The corresponding reaction of OH with ethanol has been investigated to an even lesser degree.

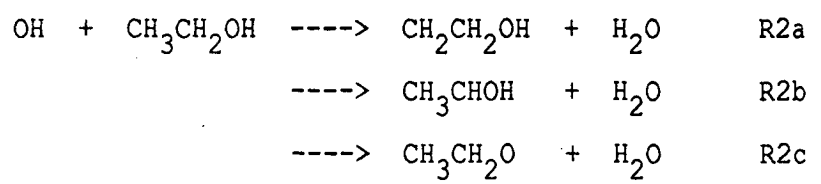

Three direct studies using flash photolysis/resonance absorption (Overend, et al. 1978), flash photolysis/resonance fluorescence (Ravishankara, et al. 1978) and discharge flow/laser induced fluorescence (Meier, et al. 1985) respectively and one relative rate study (Campbell, et al. 1976) have yielded rate constants at room temperature which range from 1.76 to 3.65 x 10^{-12} cm^3s^{-1}. Only the study of Meier has addressed the temperature dependence of the reaction.

3.1.3 (D_3)Methanol

To the best of our knowledge the rate constant for the reaction of OH with (D_3)methanol has not been measured previously.

$$OH + CD_3OH \longrightarrow CD_2OH + HOD \qquad R3a$$

$$\longrightarrow CD_3O + H_2O \qquad R3b$$

Both Hagele, et al. (1983) and Meier, et al. (1984) have reported the branching ratio of reaction R1 and conclude that R1a is the dominant process at room temperature. A study of reactions R3a and R3b would provide evidence of the validity of this result. The presence of an isotope effect would confirm that the reaction is branched.

3.2 Experimental

3.2.1 Reaction Vessel.

All experiments were performed using the flash photolysis/resonance absorption technique. Two considerations were important with respect to the reaction vessel design. It was important that the reaction volume was fully contained both within the photolysed region and also within the heated region of the furnace. The design was also constrained by the necessity to seal the flash lamp electrodes into the reaction vessel without exceeding

the the thermal capabilities of the sealant. These constraints were met in the following way.

The reaction vessel consisted of suprasil tubing of 30mm diameter and approximately 1m length surrounded by a coaxial pyrex tube 40mm in diameter. The annular space formed was enclosed by sealing in two circular stainless steel electrodes each with a small hole bored in it for the admission of the fill gas. The annular lamp design provided the best illumination for the photolysis region and effectively eliminated concentration gradients due to uneven illumination. The length of the reaction vessel was such that the electrodes protruded from the ends of the furnace enabling the use of a common silicon based rubber (Dow Corning Silicone) as the sealant.

A reaction zone 43 cm long was defined by internal windows fused into the reaction vessel approximately 25 cm from each end. This arrangement allowed the total reaction volume to be heated using the electric furnace. Figure 3.1 is a diagram of the reaction vessel and furnace arrangement.The temperature of the furnace could be maintained to $\pm$5K and the temperature of the reactant gas mixture was measured by a chromel-alumel thermocouple. The photolysis flash was generated in a flowing stream of nitrogen at ~5 torr pressure with an Applied Photophysics capacitor bank Model 150-03. Typical flash energies were in the range 300-400 J with an effective flash duration (time elapsed until the flash had decayed to a level low

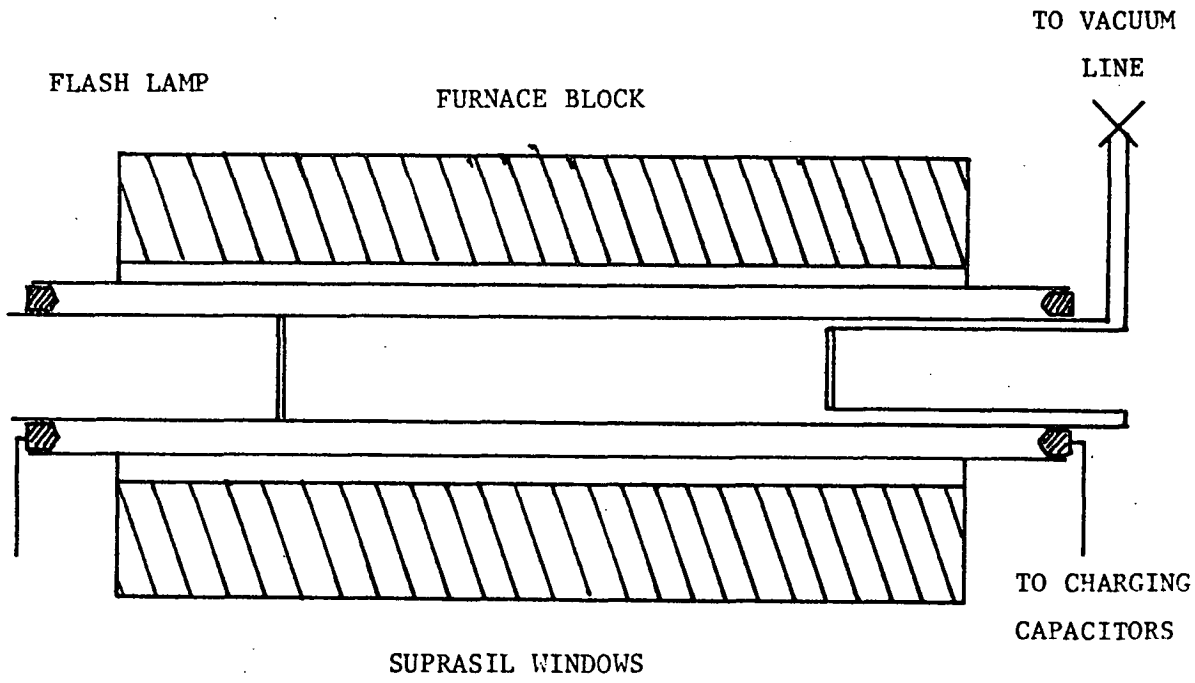

Figure 3.1 Furnace And Reaction Vessel Detail.

enough not to interfere with recording of the OH decay profile) under the conditions of the experiment of 70-80μs.

Experiments at temperatures below 298K were performed in a similar reaction vessel to the one described except that the furnace was replaced with a cooling jacket through which was circulated a refrigerated ethylene glycol/H_2O mixture.

OH radicals were generated by the photolysis of water vapour in most experiments. The effect of using a different OH radical precurser was tested by using nitric acid for one of the room temperature determinations. OH was also generated in some earlier work by photolysis of ozone and reaction of O atoms with H_2O. (Greenhill, 1981)

3.2.2 Resonance Lamp and Detection System.

Figure 3.2 is a diagram of the complete experimental system. The hydroxyl radicals were detected by absorption of lines of the (0,0) band of the $A^2\Sigma - X^2\pi$ transition from a microwave discharge through a 5% H_2O/Argon mixture at 1 torr pressure. The lamp consisted of a quartz tube 1 cm. in diameter with a 1 cm quartz window fused at one end tapered at the other to accommodate connection to the flow system. A side arm admitted the H_2O/Ar mixture from a bubbler to the lamp. The tube was contained within the cavity of an Electro Medical Supplies 2.54GHz microwave generator.

The radiation emitted by the lamp was roughly collimated with a single plano-convex lens, passed through the reaction vessel and

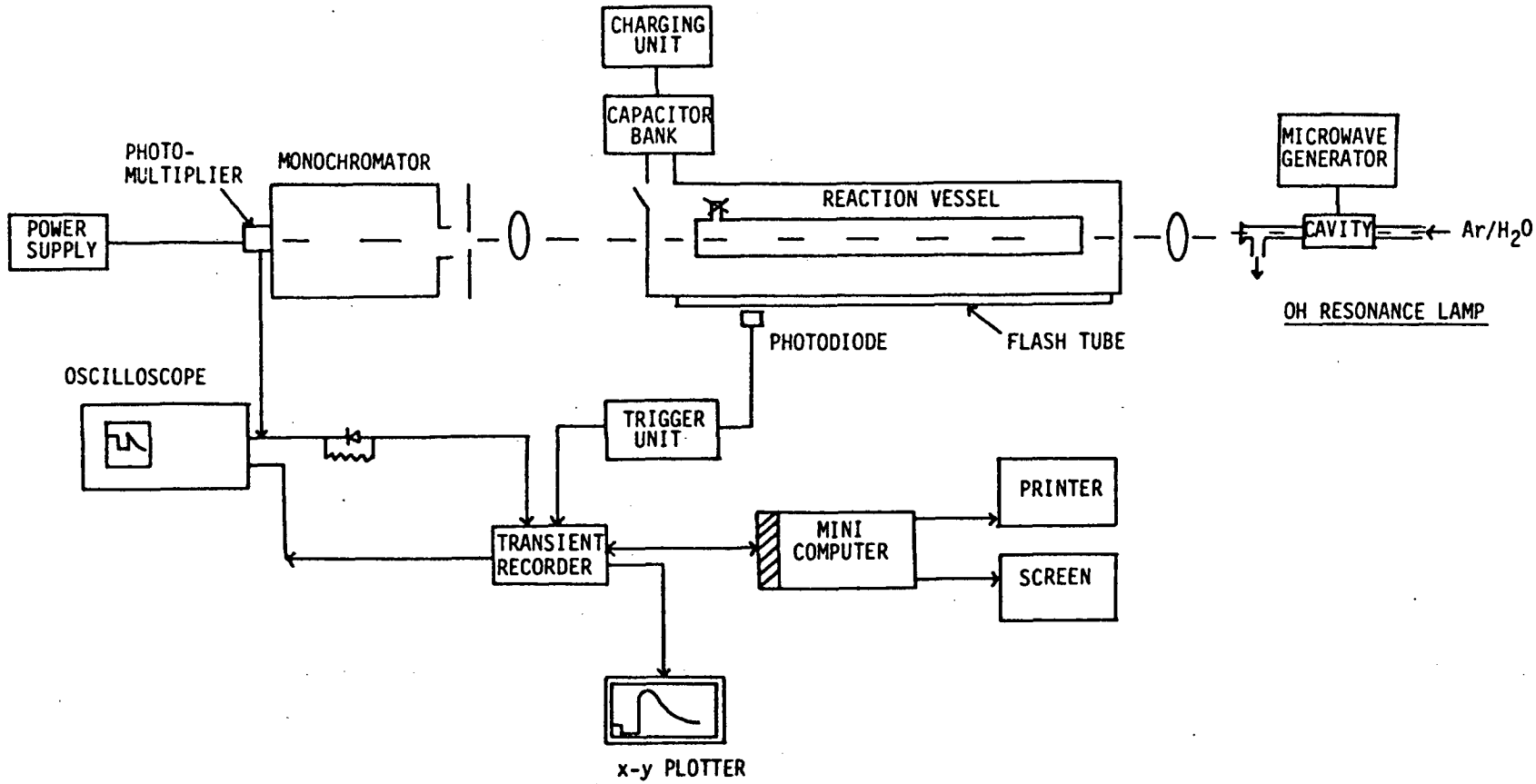

Figure 3.2 FLASH PHOTOLYSIS SYSTEM

focused with a simple collimater and a second plano-convex lens onto the entrance slit of a Unicam SP500 quartz prism monochromator. After passage through the monochromator the radiation was incident on a Hamatsu photomultiplier (R212UH) wired for fast response. A diagram of the circuit for the photomultiplier is given in figure 3.3.

The monochromator was centred on the emmission maximum at about 308.1 nm. This resulted in acceptance of the $Q_1 3$ line as well as the $Q_1 2$ (308.00 nm), $Q_1 4$ (308.33 nm) and the $P_1 1$ (308.17 nm) lines with a slit width of 0.1 mm and a bandpasss of 0.4nm. The spectrum for this transition is shown in figure 3.4 along with the spectrum observed under these experimental conditions.

The signal from the photomultiplier, following photolysis of the reaction mixture was captured by a Datalab DL 905 transient recorder (1024 x 8 bit words) and then transferred to a microcomputer system for storage. The I_o value was determined by running the transient recorder in either the pre-trigger mode and recording the unattenuated resonance lamp signal for 100 ms before the flash or in the A/B mode, which enabled the sweep time B near the end of the reaction time to be increased over the sweep time A used during the reaction, and recording the signal at long times after the reaction was complete, that is, when [OH] = 0.

Early in the work it was found that the transient recorder was susceptible to overloading from the scattered light signal generated by the photolysis flash resulting in slow response times. To prevent this large signal affecting the transient recorder a 6.5V cut off

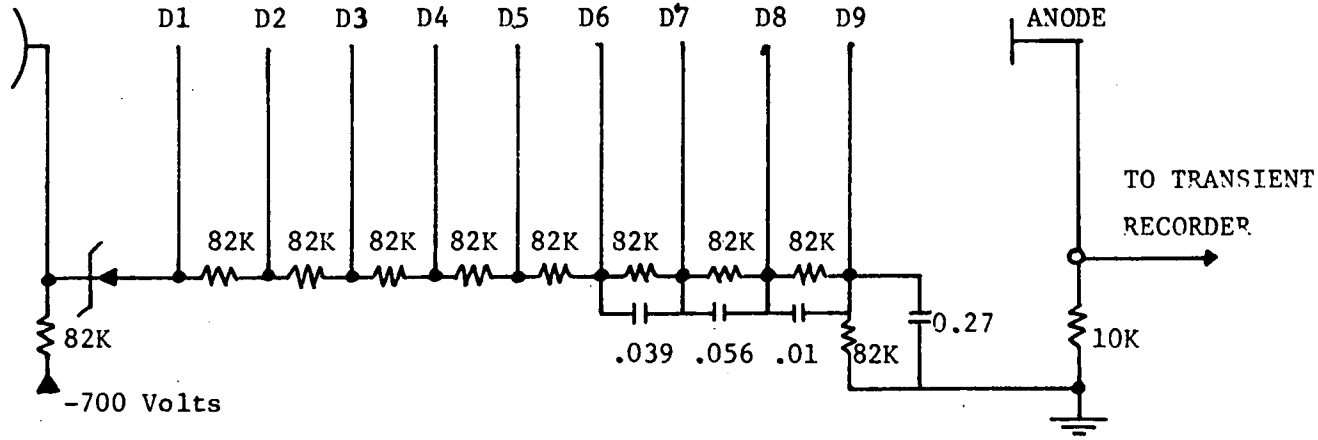

Figure 3.3 Dynode Circuit Of 1P28 Photomultiplier.

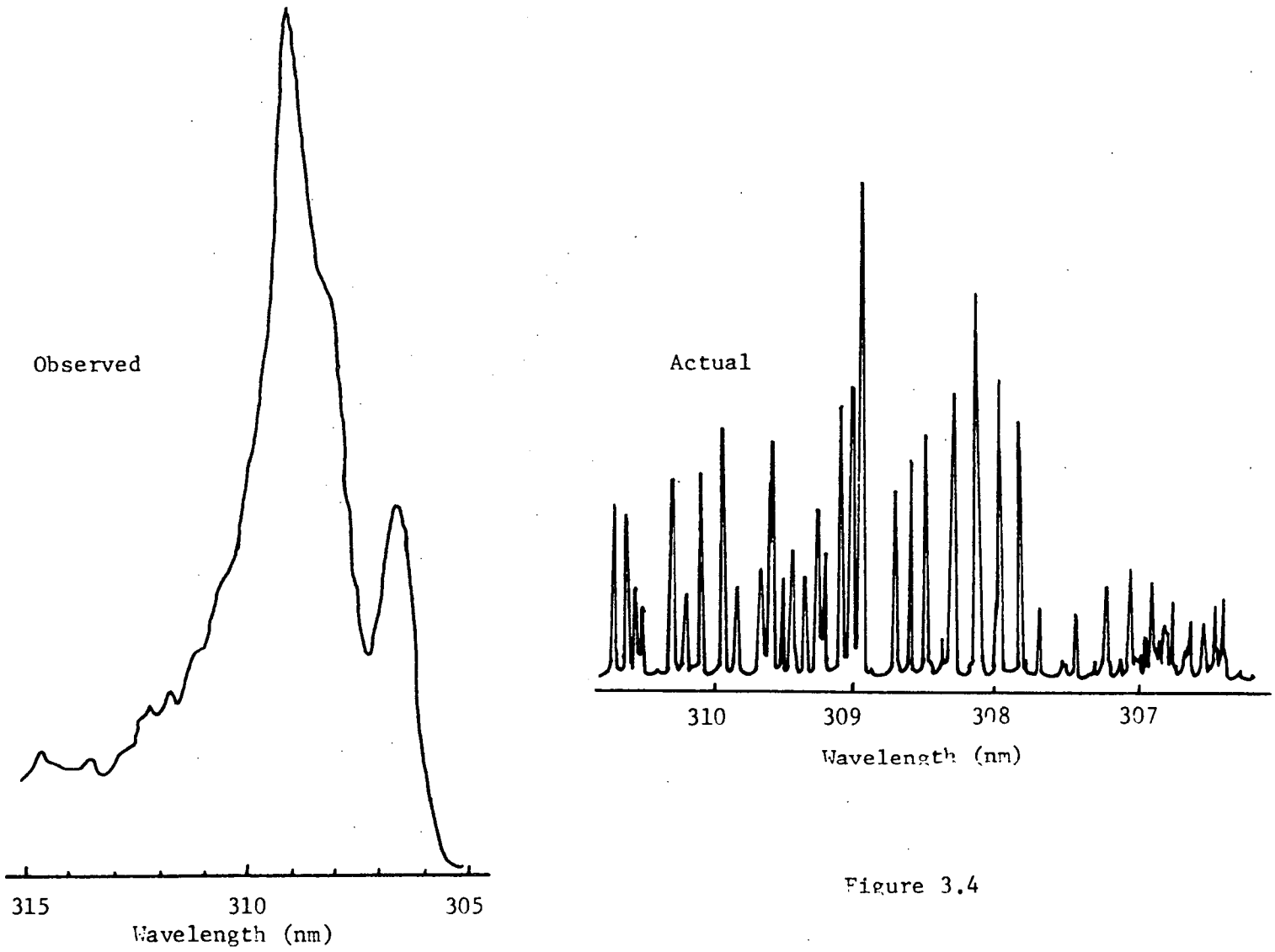
Observed
315
310
305
Wavelength (nm)
Actual
310
309
308
307
Wavelength (nm)

Figure 3.4

diode was placed between the photomultiplier and the transient recorder.

The data transfer from the transient recorder was accomplished via the inbuilt parallel interface of the transient recorder. A parallel interface board was designed to obey the S100 protocol used by the expansion interface of the microcomputer. Data captured by the transient recorder was displayed on an oscilloscope and could be rejected at this stage if neccessary. Signals accepted for processing were output to an X-Y plotter so a hardcopy was available. In general a day's experimental work was processed overnight from the raw data stored on magnetic disk.

3.2.3 Signal Conditioning and Processing.

The conversion of the observed I values (where I is the intensity of the transmitted 308.1 nm radiation) to relative hydroxyl radical concentrations was made using Beer's Law in its usual form;

$$\log(I_o/I) = \varepsilon_{OH}\ [OH]\ l$$

$$\text{or} \quad [OH]_{relative} = \text{constant}\ (\log(I_o/I))$$

The observed I versus time curve was truncated to remove points which may be affected by the tail of the flash, typically 50-60μs after the flash peak, and points when the noise on the signal overlapped the I_o value (when the reduction in absorption due to OH loss increased the transmitted intensity to close to I_o). The signal to noise ratio was typically 10-15 to 1. A typical absorption profile is shown in figure 3.5.

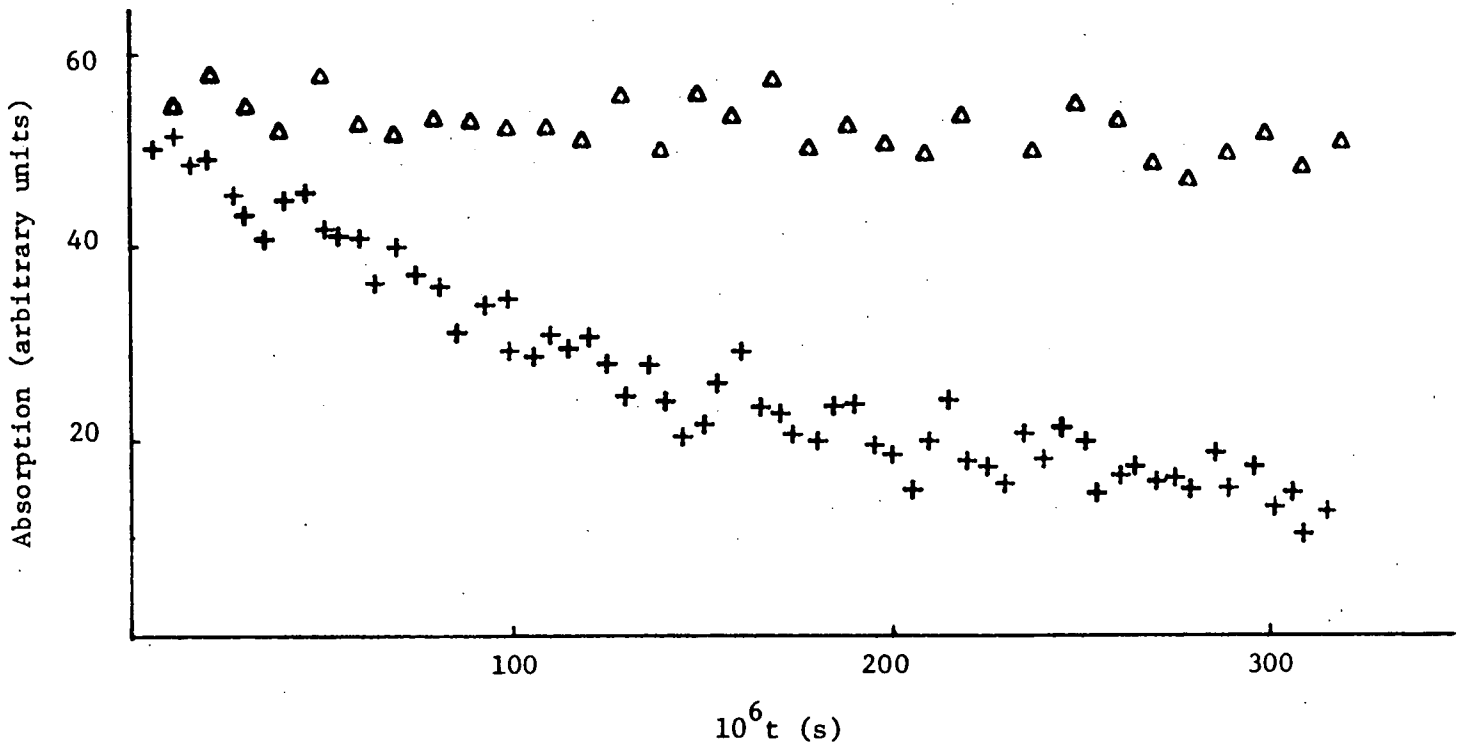

Figure 3.5 OH Absorption Profile [EtOH] = 1.71×10^{15} cm^{-3} (+)
[EtOH] = 0 cm^{-3} (Δ)

The initial OH concentration was estimated from the initial absorption of the resonance radiation and the oscillator strength of the $A^2\Sigma - X^2\pi$ transition in the same manner as other workers. (Overend, et al. 1975, 1978). For absorptions observed in this work and a pathlength of 43 cm, we estimate typical initial OH concentrations in the range $1 - 3 \times 10^{13} cm^{-3}$.

Other workers have suggested that Beer's Law should be used in the form

$$\log(I_o/I) = (\varepsilon_{OH} [OH] l)^{\gamma}$$

where γ is a constant. In the present work, γ was found to be 1 ± 0.1 for $I > 70\% I_o$

This is consistent with the results obtained in experiments where [OH] was measured by absorption. (Overend, et al. 1975,1978; Smith, et al. 1973a,b; Wagner, et al. 1981; Hofzumahaus, et al. 1984; Braun, et al. 1982). In general, a small bandpass (< 1nm) encompassing only a few lines coupled with absorptions less than 30% allow Beer's Law to be used in a conventional form. The assumption of Doppler line shapes for the rotational lines of the OH spectrum has shown (Wagner, et al. 1981) that absorption of these lines is linear as a function of [OH] up to $[OH]=1 \times 10^{14} cm^{-3}$.

However, when the concentration of hydroxyl radical is large (Gordon, et al. 1975) or the bandpass is large (Bott, et al. 1984; Ernst, et al. 1978; Spindler, et al. 1982) then the modified form must be used.

It was not possible in this work to obtain any conclusive experimental evidence of the effect of varying OH concentrations. With the single shot methodology employed, any significant reduction

in $[OH]_o$ would have reduced the absorption to a level where the observation and analysis of decays would be extremely unreliable. Any increase in $[OH]_o$ would have resulted in the absorption not obeying Beer's law.

3.2.4 Reagents.

Alcohols were Aldrich Chemicals spectrophotometric grade (99.9%+). Methanol and ethanol were redistilled and stored over molecular sieve. Prior to making reaction mixtures, the alcohols were further vacuum distilled trap to trap and the middle portion used for the preparation of mixtures.

High Purity Argon (99.99% min.) from C.I.G. was used without further purification. Water was distilled and degassed by successive freeze, pump, thaw cycles before use.

Nitric acid was prepared by vacuum distillation from a 1:2 mixture of concentrated nitric and sulphuric acids and condensed in a liquid nitrogen trap.

The reactant gas mixtures were prepared manometrically from distilled water, absolute alcohol and High Purity Argon in two stages. Initially a mixture containing a known percentage (~4-5%) of alcohol in Argon was prepared and stored in a 10 l glass bulb. This was used as the source of reactant which was mixed with water vapour and further diluted with Argon to give the required reactant concentrations. These mixtures were stored and were allowed to mix for 48 hours before use. Typical mixtures contained 0.5-1% H_2O and 5 - 200 x $10^{14}cm^{-3}$ CH_3OH or 1.4 - 35 x $10^{14}cm^{-3}$ C_2H_5OH in 100 torr of

argon. Nitric acid was used as the OH precursor (replacing the water) in one 300K determination of reaction R1.

3.3 Results

In an excess of alcohol the rate law for the reaction between OH and an alcohol can be written as

$$d[OH]/dt = -k_{1st}[OH]$$

where k_{1st} is a pseudo first order rate constant given by $k_{bim}[ROH] + k_s$. The constant k_s includes all losses of OH by secondary processes. As the alcohols have hydrogen atoms in different environments, k_{bim} will represent the sum of the rate constants for the different reaction channels. A plot of ln[OH] versus time yields k_{1st} for a particular alcohol concentration and a second plot of k_{1st} versus alcohol concentration will give k_{bim}.

Values of the pseudo first order rate constant and its variance were calculated using linear least squares techniques (Cvetanovic, et al. 1975) applied to the variation of $\ln[OH]_{rel}$ with time. The bimolecular rate constant was determined from weighted linear least squares analysis of k_{1st} as a function of alcohol concentration.

Much of the criticism of the photolysis technique used here stems from the non-selectivity of the photolysis flash, i.e. the wide wavelength range of radiation emitted by the flash lamp. It is important to know whether the reactant is photolysed and if so what products and quantities of products are formed. We performed experiments involving photolysis of an alcohol/argon mixture in the absence of water vapour to determine if a) there was any production

of OH by direct photolysis of the alcohol, and b) if there were any other products formed during the photolysis which may interfere with the reactions under study.

No absorption of the OH resonance radiation was observed indicating that OH was not formed from photolysis of the alcohols. Samples of the post photolysis mixture were taken for analysis by gas chromatography/mass spectrometry. After five photolysis flashes on the same mixture, products produced constituted less than 0.5% of the total reactant concentration. This level of impurity is too low to affect the observed rate constants. The m/e values for these minute levels of impurities were consistent with them being aldehydes.

A more extensive study of the photolysis of alcohols by the N_2 flash lamp used in this study has been undertaken and the results obtained have been documented in chapter 4.

3.3.1 Methanol

Typical plots of $\ln[OH]_{rel}$ vs. time, k_{1st} vs. [MeOH], and k_{bim} vs. 1/T are given in figures 3.6, 3.7, and 3.8 respectively.

Over the temperature range 260 to 803K the rate coefficient $k_{R1}(T)$ $(=k_{R1a}+ k_{R1b})$ is well represented by

$$k_{R1}(T) = (8.04 \pm 1.96) \times 10^{-12} \exp[-(664 \pm 88)K/T] \text{ cm}^3\text{s}^{-1}. \quad (1)$$

The error limits are one standard deviation.

This gives a value at 298K of 0.87×10^{-12} cm^3s^{-1}. The temperatures and corresponding rate coefficients are given in table 3.1 for all the studied temperatures.

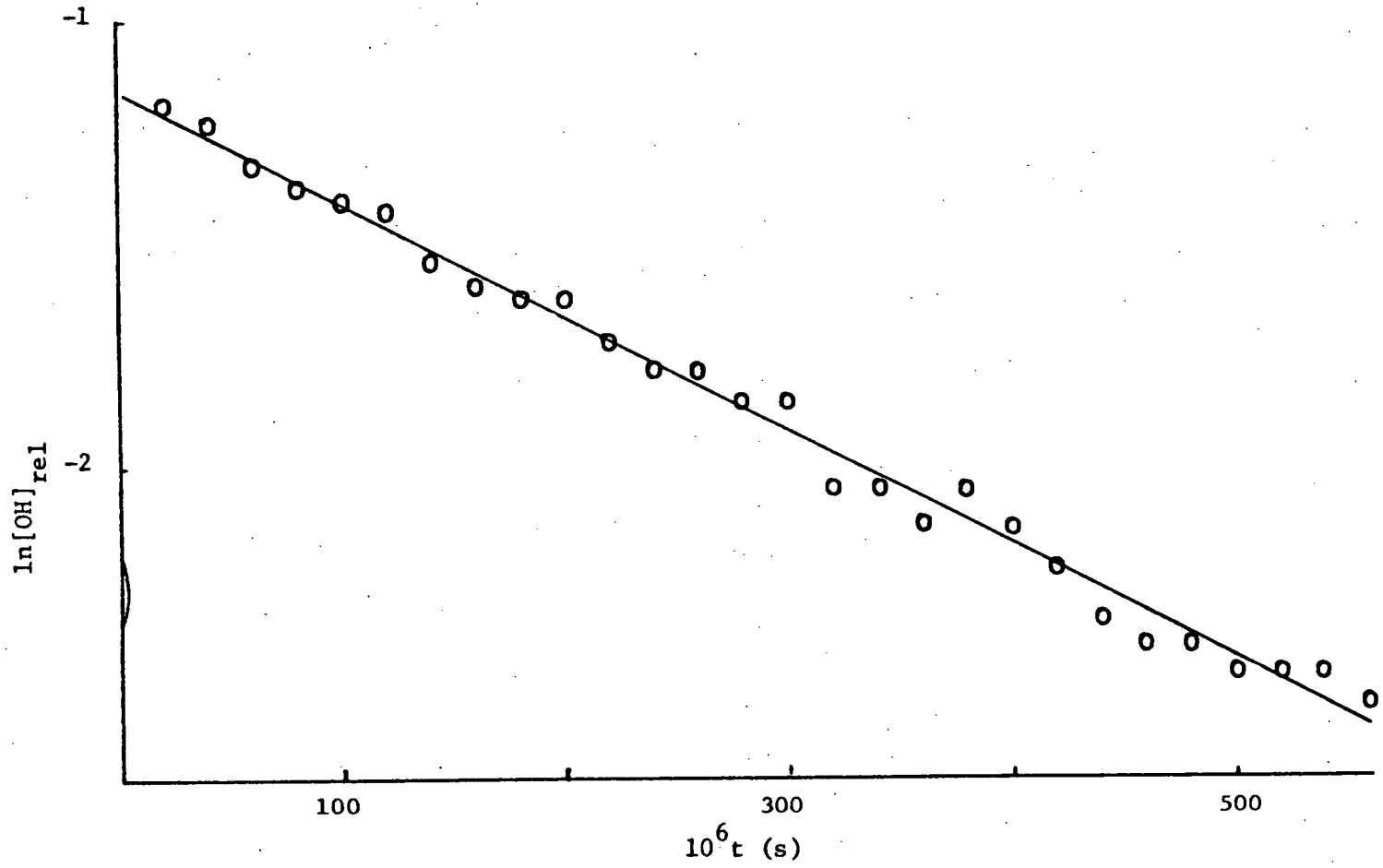

Figure 3.6 ln[OH] vs. time [MeOH] = 2.0 x 10^{15} cm^{-3}

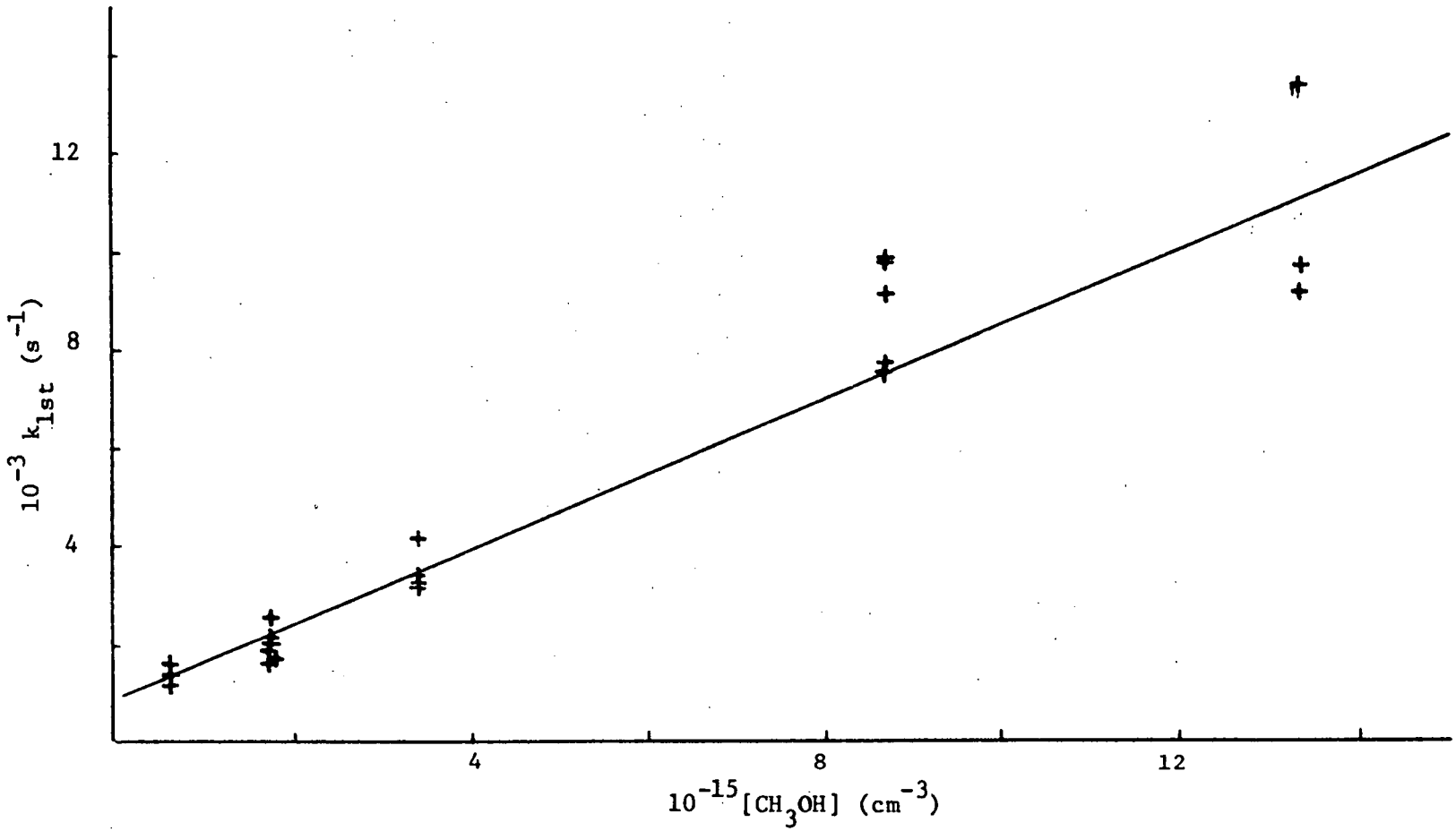

Figure 3.7 Pseudo-first Order Rate Constant as a Function of [MeOH] T=292K

FIGURE 3.8 OH + CH3OH

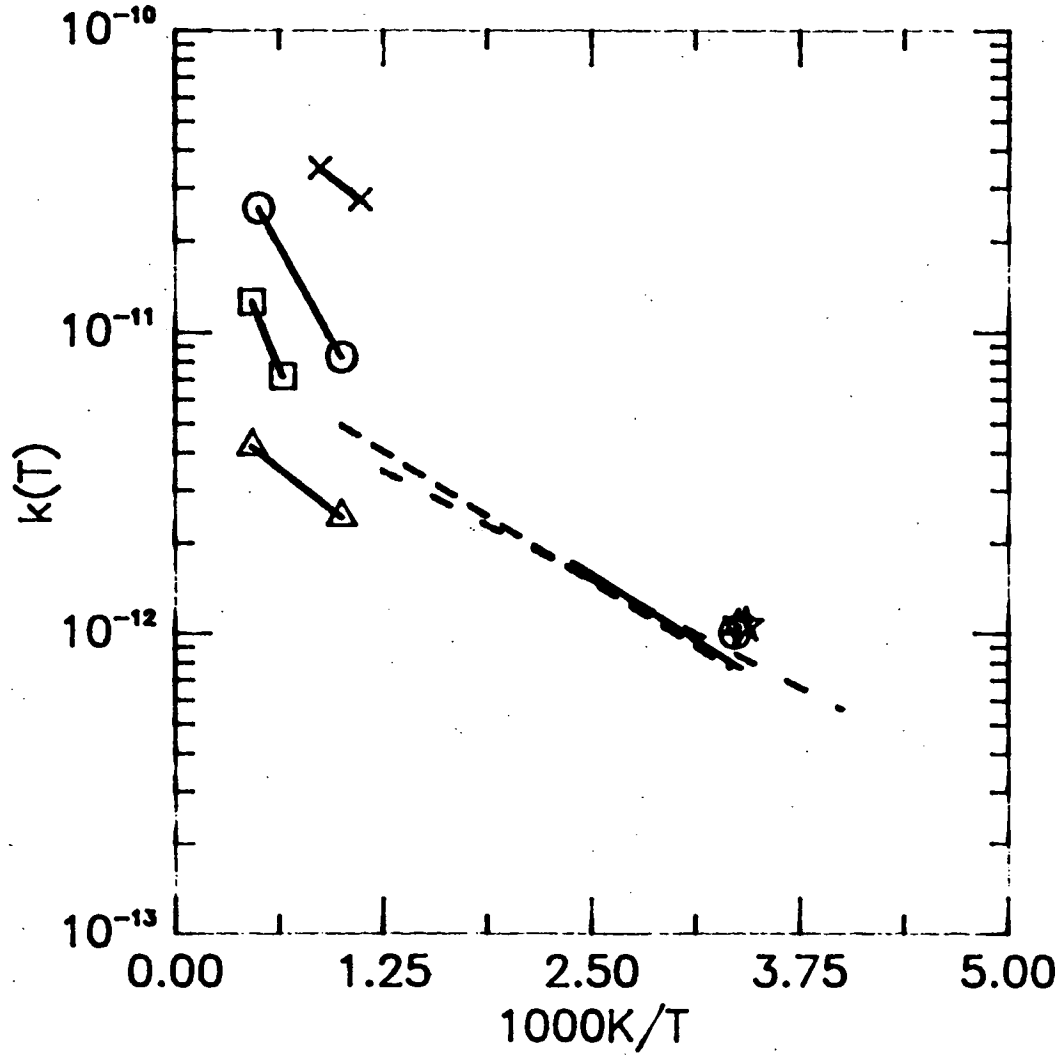

Figure 3.8 Arrhenius Plot of All Experimental Data on OH + CH_3OH.

- × Aronowitz, et al. 1979
- □ Bowman, 1975
- Campbell, et al. 1976
- —— Hagele, et al. 1983
- - - - Meier, et al. 1984
- Overend, et al. 1978
- Ravishankara, et al. 1978
- ○ Vandooren, et al. 1980
- △ Westbrook, et al. 1979
- — — This Work

Table 3.1. Experimental Values Of k_{bim} For

$OH + CH_3OH$ ---> products.

T K	$10^{12}k_{bim}$ cm^3s^{-1}	$10^{12}\sigma(k)$[a] cm^3s^{-1}	Number of Expts.
260	0.54	0.04	28
292	0.76	0.04	21
300	0.75	0.08	21
331	1.13	0.05	22
362	1.44	0.06	26
453	1.44	0.09	20
465	1.35	0.08	20
570	2.06	0.17	20
597.5	2.67	0.24	20
669	2.79	0.25	19
803	5.76	0.59	18

[a]One standard deviation.

All the first order rate constants obtained in this work are tabulated in appendix A along with the temperatures, concentrations and pressures for each experiment.

3.3.2 (D_3)Methanol.

At 293K the rate constant ($k_{R3}=k_{R3a}+k_{R3b}$) for reaction of OH with CD_3OH was found to be:

$$k(293) = 5.0 \pm 0.2 \times 10^{-13} cm^3 s^{-1}. \qquad (3)$$

This gave on overall isotope effect at 293K of $k_H/k_D = 1.65$. Figure 3.9 is a plot of k_{1st} as a function of $[CD_3OH]$. Appendix A contains the experimental first order rate constants for this reaction.

Based on the branching ratios determined by Hagele, et al. (1983) and Meier, et al. (1984), we can calculate a true isotope effect for abstraction from the carbon. We have taken the average of the three branching ratios quoted in these reports which gives $k_{R1b}/(k_{R1a}+k_{R1b}) = 0.18$. The corrected isotope effect for H/D abstraction from carbon in methanol is thus 2.1±0.2.

3.3.3 Ethanol

Typical plots of $\ln[OH]_{rel}$ vs. t, k_{1st} vs $[C_2H_5OH]$ and $\ln k_{bim}$ vs 1/T are shown in figures 3.10, 3.11 and 3.12 respectively.

Over the temperature range covered in this study the rate coefficient $k_{R2}(T)$ $(=k_{R2a}+k_{R2b}+k_{R2c})$ is well represented by

$$k_{R2}(T) = (1.25 \pm 0.24) \times 10^{-11} \exp[-(360 \pm 52)K/T] \ (cm^3 s^{-1}) \qquad (2)$$

which gives a value at 298K of 0.38×10^{-11} $cm^3 s^{-1}$. Table 3.2 lists the experimental rate coefficients and the corresponding

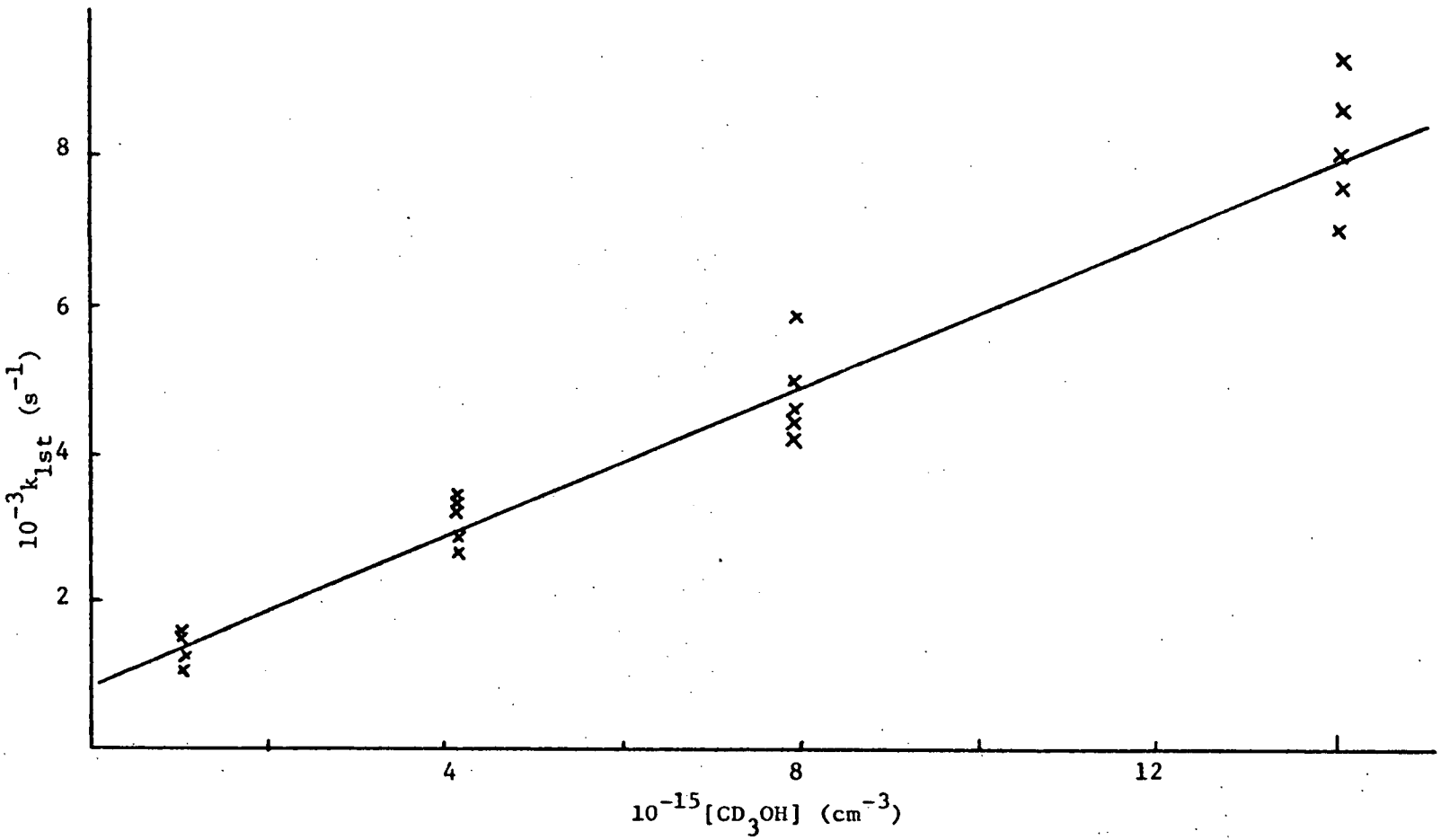

Figure 3.9 Pseudo-first Order Rate Constant as a Function of $[CD_3OH]$ T=293K

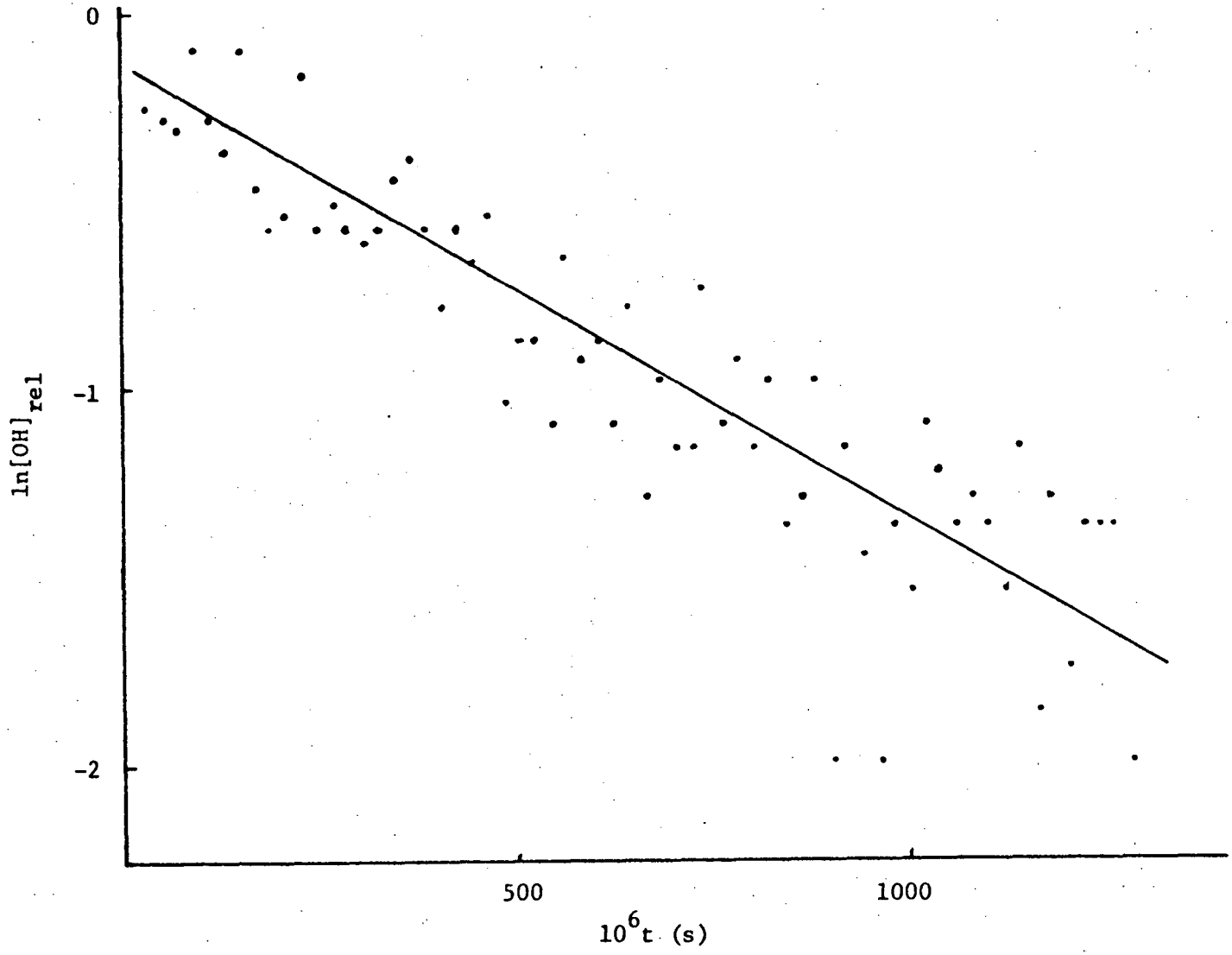

Figure 3.10 $\ln[OH]_{rel}$ vs. time [EtOH] = 1.37 x 10^{14} cm^{-3}

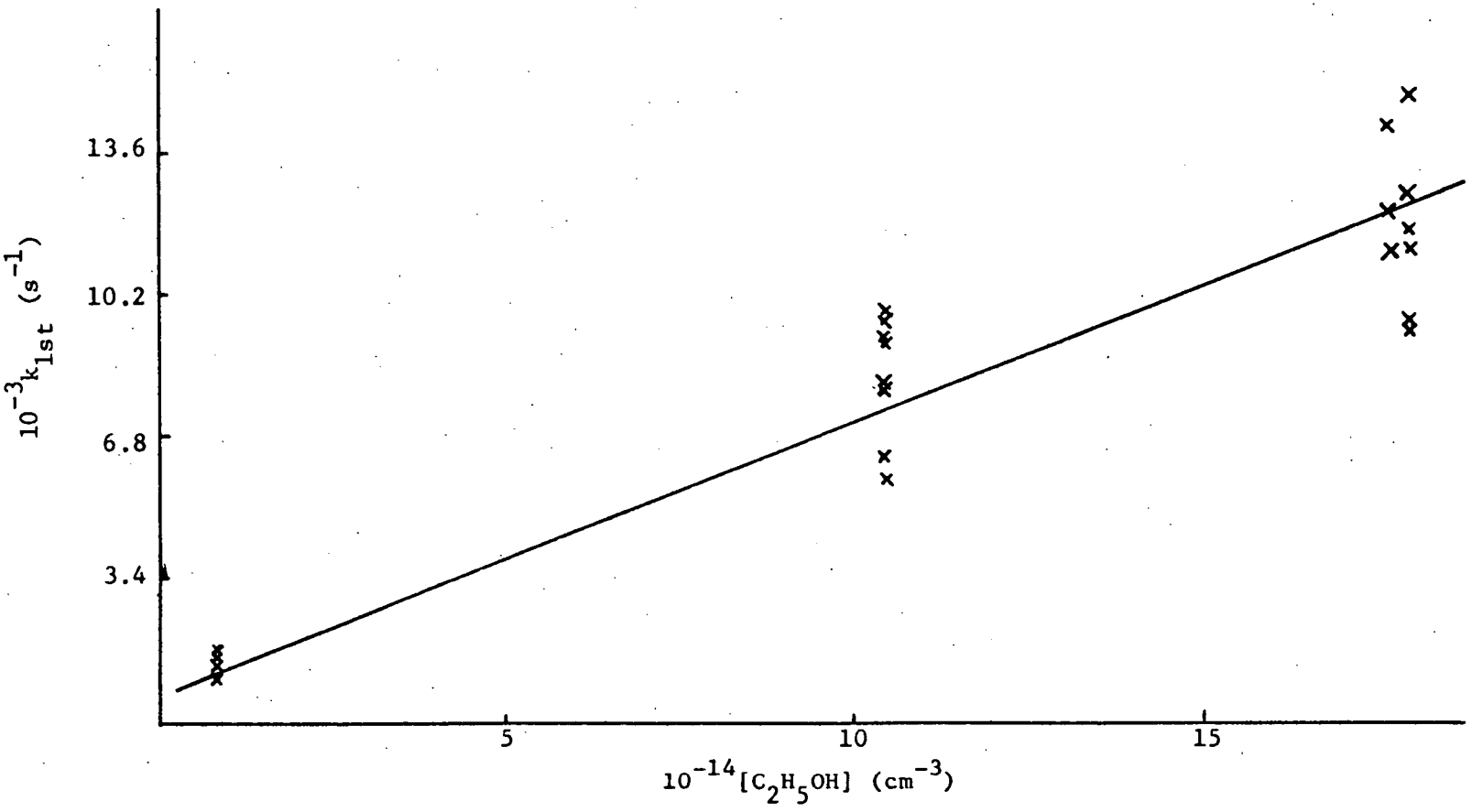

Figure 3.11 Pseudo-first Order Rate Constant as a Function of [EtOH] T=459K

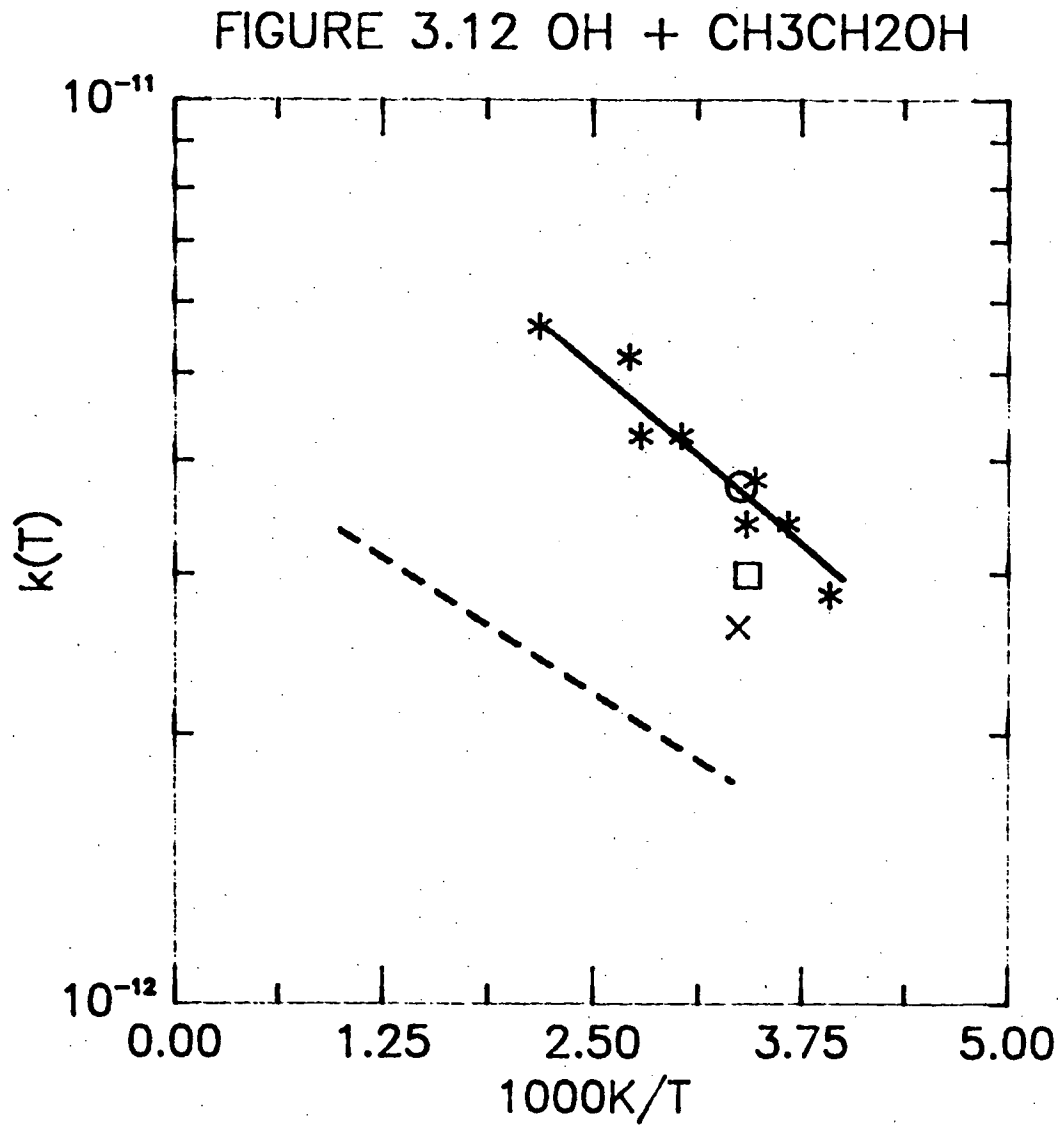

Figure 3.12 Arrhenius Plot of All Experimental Data on OH + CH_3CH_2OH

- Campbell, et al. 1976
- Meier, et al. 1984
- Overend, et al. 1978
- Ravishankara, et al. 1978
- This Work

temperatures. Appendix A contains a compilation of the experimental first order rate constants for this reaction.

Table 3.2. Experimental Values Of k_{bim} For

$OH + C_2H_5OH$ ---> products.

T K	$10^{12}k_{bim}$ cm^3s^{-1}	$10^{12}\sigma(k)^a$ cm^3s^{-1}	Number of Expts.
255	2.84	0.15	25
273	3.40	0.14	19
289	3.80	0.24	30
293	3.40	0.17	26
331	4.26	0.19	23
360	4.26	0.18	24
369	5.21	0.36	30
459	5.63	0.48	28

[a]One standard deviation.

3.4 Discussion

3.4.1 Methanol.

The rate constants determined in this work are tabulated along with the results from the literature in table 3.3 and plotted in figure 3.8.

The results obtained for the overall rate constant for the reaction of OH with methanol are in excellent agreement with two

recent studies of the temperature dependence of this reaction by Hagele and Meier. The agreement obtained between this work and the

Table 3.3. Comparison Of Rate Coefficients Of

$OH + CH_3OH$ ---> products

$10^{12}k_2$ cm^3s^{-1}	$10^{12}A$ cm^3s^{-1}	E_a/R K	T K	Ref.
0.81[a]	12 ± 3	810±50	295-420	Hagele, (1983)
1.06±0.10			296	Overend, (1978)
1.00±0.10			298	Ravishankara, (1978)
0.77[a]	11 ± 3	798±45	300-1000	Meier, (1984)
0.95±0.10			292	Campbell, (1976)
0.87[a]	8.0 ±1.9	664±88	250-803	this work

[a] 300K

published results indicates that the technique that has been employed is suitable and provides satisfactory results for systems involving the reactions of hydroxyl radicals. This is particularly encouraging as very few studies using this technique have been performed at temperatures above 500K. This has been largely due to the difficulties associated with heating the reaction vessel while retaining the integrity of seals and joints.

It is reasonable to suppose that the same technique can provide satisfactory results for the OH + ethanol system.

3.4.2 (D_3)Methanol

This is the first reported result for reaction R3a+R3b. The presence of an isotope effect is evidence that the predominant process in hydroxyl radical attack on methanol is reaction R1a (R3a). This result is in agreement with the branched mechanism reported by Hagele and Meier.

Very little work has been done on isotope effects in hydroxyl radical reactions. Systems studied are H_2-D_2 (Smith, et al. 1973), HCl-DCl (Smith, et al. 1973; Husain, et al. 1984), CH_4-CD_4 (Gordon, et al. 1975) and C_6H_6- C_6D_6 (Lorenz, et al. 1983). The isotope effect varied from 1.4 for the benzene system at 453K to 11 for the methane system at 416K. For hydrogen and HCl at room temperature the effects were 3.2 and 2.0 respectively and these would decrease as the temperature increased due to the higher activation energy of the D abstraction. This result of 2.1 appears to be in agreement with most of the values observed for this effect. The high result obtained by Gordon, et al. appears to be inconsistent with the available results.

3.4.3 Ethanol.

Comparison with the results of other workers in table 3.4 and figure 3.12 shows a marked difference in the rate coefficients quoted. The result obtained here is in good agreement with the highest result in the group of room temperature results, but a factor of 2 higher than the results of Meier et al. The initial OH

concentration is somewhat higher in the present work than that used by Meier and this may lead to a greater contribution by secondary reactions to the OH decay.

Table 3.4. Comparison Of Rate Coefficients Of

$OH + C_2H_5OH$ ---> products

$10^{12}k_2$ cm^3s^{-1}	$10^{12}A$ cm^3s^{-1}	E_a/R K	T K	Ref.
3.74±0.37			296	Overend, 1978
2.62±0.36			298	Ravishankara, 1978
1.77[a]	4.4±1.0	274±90	300-1000	Meier, 1984
2.99±0.33			292	Campbell, 1976
3.8[a]	12.5±2.4	360±52	250-459	this work

[a] 300K

The effect of the [OH] can be assessed by modelling the system with a suitable set of elementary reactions.

Table 3.5 specifies the reaction scheme used in this study and the rate coefficients used. Some features of this mechanism are as follows. The scheme includes two reactions which will be of importance in a system such as the experimental arrangement employed here that contains significant levels of hydrogen atoms. The rates of reactions R15 and R16 were taken from a theoretical prediction of the rate coefficients of the corresponding methanol species calculated by application of RRKM theory with a Gorin model.

(Greenhill, et al. 1986). It is assumed that the recombinations are slower than those calculated for the methanol reactions. The values

Table 3.5. Reaction Mechanism and Rate Coefficients.

	Reaction	A $cm^3 s^{-1}$	E_a kJ $mole^{-1}$	Ref.
1	$CH_3CH_2OH + OH \rightarrow CH_3CHOH + H_2O$	3.73×10^{-12}	0.0[a]	this work
2	$CH_3CH_2OH + OH \rightarrow CH_3CH_2O + H_2O$	4.63×10^{-13}	0.0[a]	this work
3	$CH_3CH_2OH + H \rightarrow CH_3CH_2 + H_2O$			
4	$CH_3CH_2OH + H \rightarrow CH_3CHOH + H_2$	2.0×10^{-11}	33.8[A]	
5	$CH_3CH_2OH + H \rightarrow CH_3CH_2O + H_2$			
6	$2\ CH_3CHOH \rightarrow$ products	1.0×10^{-11}	0.0	Meier
7	$2\ CH_3CH_2O \rightarrow$ products	1.0×10^{-11}	0.0	Meier
8	$CH_3CHOH + CH_3CH_2O \rightarrow$ products	1.0×10^{-10}	0.0	Meier
9	$CH_3CH_2O + OH \rightarrow CH_3CHO + H_2O$	3.0×10^{-10}	0.0	Meier
10	$CH_3CHOH + OH \rightarrow CH_3CHO + H_2O$	3.0×10^{-10}	0.0	Meier
11	$CH_3CH_2O + H \rightarrow CH_3CHO + H_2$	1.0×10^{-10}	0.0	-[b]
12	$CH_3CHOH + H \rightarrow CH_3CHO + H_2$	1.0×10^{-10}	0.0	-[b]
13	$CH_3CH_2O \rightarrow CH_3CHO + H$	1.47×10^{-9}[c]	-	GOGG
14	$CH_3CHOH \rightarrow CH_3CHO + H$	1.13×10^{-6}[c]	-	GOGG
15	$CH_3CHOH + H \rightarrow CH_3CH_2OH$	1.16×10^{-11}	-0.39	GOGG[d,e]
16	$CH_3CH_2O + H \rightarrow CH_3CH_2OH$	4.73×10^{-12}	-0.06	GOGG[d,e]
17	$CH_3CHO + OH \rightarrow$ products	6.9×10^{-12}	-2.16[B]	
18	$CH_3CHO + H \rightarrow$ products	2.24×10^{-11}	13.8[C]	
19	$2\ OH \rightarrow H_2O + O$	1.83×10^{-12}	0.0[B]	
20	$2\ OH \rightarrow H_2O_2$	2.13×10^{-12}	0.0[B,d]	
21	$H + OH \rightarrow H_2O$	7.72×10^{-15}	-3.64[B,d]	

[A] 'Handbook Of Bimolecular And Termolecular Gas Reactions.', Vol. 1., Kerr, J.A., Ed. (CRC Press: 1981)

[B] J. Phys. Chem. Ref. Data., 1982, **11**, 327.

[c]Whytock, D.A., Michael, J.V., Payne, W.A., and Stief, L.J., J. Chem. Phys., 1976, **65**, 4871.

GOGG Greenhill, et al. 1986

Meier Meier, et al. 1985

[a]Activation energies omitted and rate constant expressed as a pre-exponential factor only at 300K.

[b]Estimated

[c] s^{-1} at 300K

[d] Calculated for total pressure = 100torr

[e] Arbitrarily half methanol rate.

for the rates of self reaction (reactions R6 and R7) and cross reaction (reaction R8) were those determined by Meier, et al. (1985) and the unimolecular decomposition of the radicals was assumed to be as slow as those of the corresponding methanol species at these temperatures. The rates of OH reaction with the secondary species were also those obtained by Meier. Only two pathways for OH attack on ethanol have been included, one on the hydroxy group and one on the C_1 carbon. Attack on the C_2 carbon is a minor pathway (Meier, et al. 1985) when compared with the alternatives and in this study we have included it within the rate coefficients of the other pathways.

The majority of the secondary reactions (for example reactions involving species produced from the initial products) have no influence on the model as they are of such low concentration. They have been included for completeness. In most of the modelling performed in this work, the secondary reactions with unknown rate parameters have been given rate coefficients which are the order of the collision frequencies. This should have the effect of maximising

any contribution of the secondary reactions to the modelled profiles and in effect be a 'worst possible case'.

The program used was modified from one used by Ellis and Gilbert (1977) to model sound propogation in reacting systems. It uses the Gear algorithm (Gear, 1971) to solve the stiffly coupled differential equations representing the reactions occuring after identifying the independent species and thus the independent equations. Initial conditions for reactant species were selected assuming that photolysis produced effectively instantaneous concentrations of the radicals and did not disturb the thermal or temperature equilibrium of the system.

To test the effect of the initial concentration of OH, that is, the necessity for pseudo first order conditions, the initial OH concentrations were varied up to a level where they were comparable to the lowest reactant concentrations used. In this situation there is a significant loss of ethanol and it is no longer valid to assume pseudo first order conditions. This results in plots of ln[OH] vs. t which are curved, the degree of curvature being dictated by the change in ethanol concentration.

Calculation of k_{1st} at varying alcohol concentrations with such high $[OH]_o$ results in plots of k_{1st} as a function of [ROH] which have two quite distinct regions. At low [ROH], where [ROH]/[OH] ≈ 1, there is high curvature as the plot moves towards the origin. Analysis to obtain the bimolecular rate constant would produce results which were much too high. However, when [ROH]/[OH] >> 1 the plots are almost linear with an intercept that is dictated by the

$[OH]_o$ and results which are close to the true rate coefficients. Such intercepts were observed in this work.

The results of the computation indicate that even under conditions when $[OH]_o = 0.5[C_2H_5OH]_{min}$ it would be difficult to detect curvature in the experimental ln[OH] vs. t plots. However, attempts to fit the observed decays with functions other than a linear one produced cumulative errors which were greater than for a linear fit. This tends to indicate that the initial OH concentration in the experimental work is in fact lower than that used in these modelling studies.

It is important to note that the modelled results indicate only a slight curvature of the ln[OH] vs. t plot under conditions which could never be regarded as pseudo-first order. More importantly, they reproduce the observed first order decay of OH very closely. The number of half lives over which the reaction is observed is also important. In general the reactions were followed for two to three half lives in these experiments. This highlights the difficulty of distinguishing between first and second order kinetics over so few half lives from typical experimental data. At higher concentrations of ethanol the modelled decays are even more linear and reproduce the observed decays almost exactly.

Results obtained at varying $[OH]_o$ are displayed in figure 3.13. What is particularly important is that these plots are linear within the experimental error for [ROH]/[OH] ratios greater than 10 even at very high $[OH]_o$. Any rate constants obtained without an analysis of the effect of [OH] and secondary reactions would be in error even though k_{1st} varies linearly with alcohol concentration.

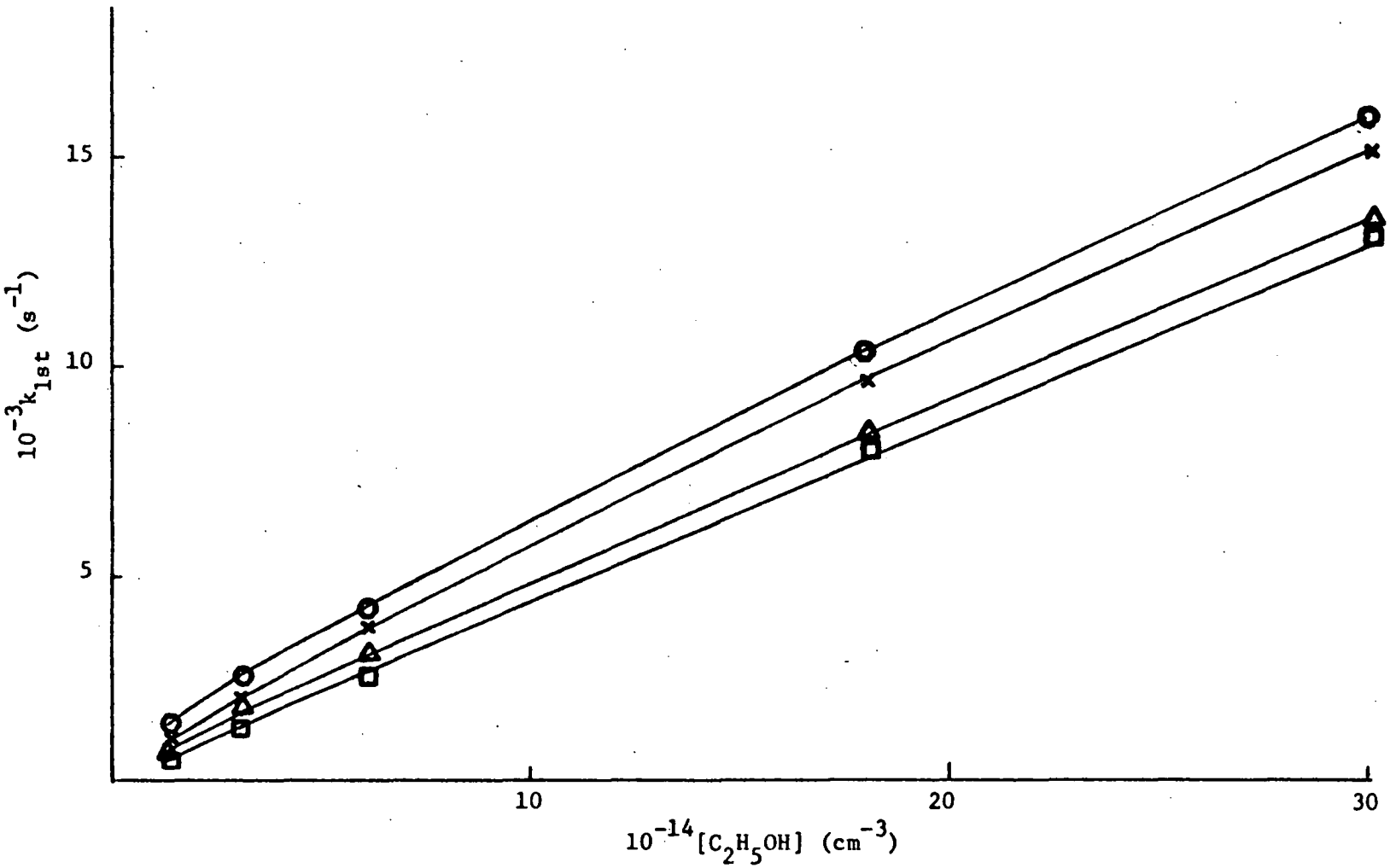

Figure 3.13 Effect of $[OH]_o$ on Pseudo-first Order Rate Constant $10^{-13}[OH]_o cm^{-3}$. (O) 6.0; (×) 2.0; (△) 0.5; (□) 0.2.

The observed k_{bim} increases by up to 20% at an initial OH concentration of $6 \times 10^{13} cm^{-3}$ over the true value for the rate constant. At the estimated $[OH]_o$ for this work and across the temperature range of the experiments, we calculated an average downward correction of 14.5% to the observed k_{bim} is required to obtain the true bimolecular rate coefficients.

This analysis indicates that to reproduce the results of Meier, (i.e. k_{bim} a factor of 2 lower than these experiments indicate), then the observed pseudo-first order rate constants at the higher ethanol concentrations would have to be reduced by a factor of 2 also. There is no question of the conditions being not pseudo-first order at these concentrations where the [EtOH]/[OH] ratio was the order of 100.

An attempt has been made to reproduce the results observed in this work using the results obtained by Meier et al. The rate constants determined were put into the model developed for the current work and simulations were run for varying OH radical concentrations and reactant concentrations. Figure 3.14 is a representative plot for ethanol concentrations over the range indicated and an initial OH concentration of $6 \times 10^{14} cm^{-3}$. The first order rate constants observed in this work cannot be reproduced by using the rate coefficients determined by Meier et al. even at very high $[OH]_o$ and very fast secondary reaction rate coefficients. Such a high initial [OH] would naturally result in the observed decays being strongly affected by nearly all reactions other than the one of interest, but such a calculation illustrates the point that the

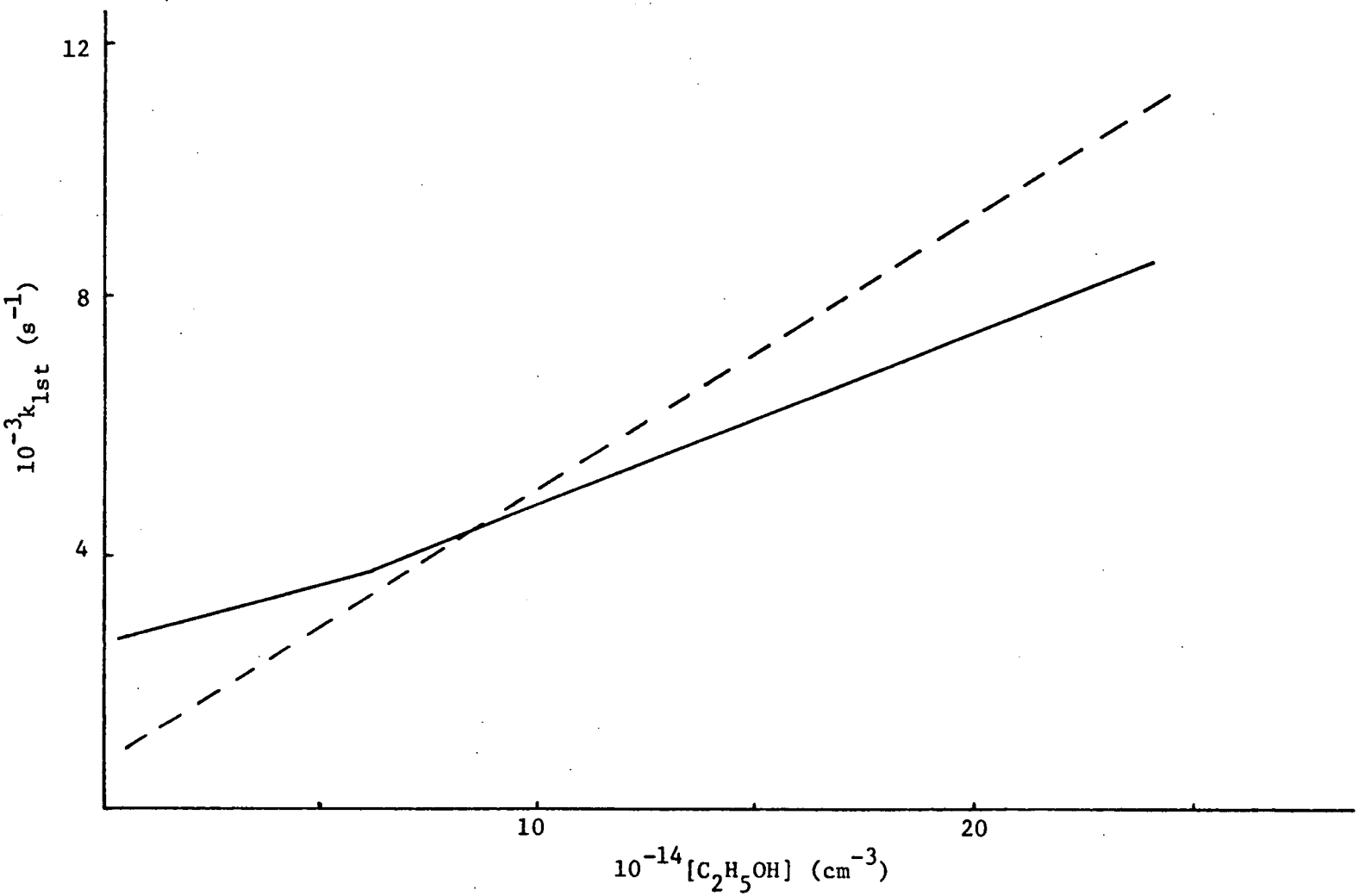

Figure 3.14 Pseudo-first Order Rate Constant as a Function of [EtOH]

(----) Experimental. (——)Modelled $[OH]_o = 6 \times 10^{14} cm^{-3}$

conventional criticism of underestimation of the $[OH]_o$ is not valid in this case.

The reason for the disparity between results obtained in this work and that of Meier et al. is not clear but one further possibility is apparent. The pseudo-first order rate constants obtained in Meier's work were all in the region of 0 to 700 s^{-1} and the majority of the results had values less than 400 s^{-1}. These compare with k_{1st}'s between 1000 and 15000s^{-1} from our work. The relative magnitude of our first order rate constants is of course a result of the relatively high reactant concentrations used but it is highly unlikely that the measured concentrations in this work are significantly in error. Recent work (Ravishankara, et al. 1985) on the reaction of OH with HBr using the discharge flow technique has concluded that the most likely source of error in such experiments was the incorrect determination of the HBr concentration. Discrepancies of up to a factor of two were observed. This was attributed to wall absorption and similar comments may apply here.

3.5 References.

Aronowitz, D., Santoro, R.J., Dryer, F.L., and Glassman, I., 17th Symp. (Intl) On Combustion, 1979, 633.

Atkinson, R., Darnall, K.R., Lloyd, A.C., Winer, A.M., and Pitts, J.N. Jr., Adv. Photochem., 1979, **11**, 375.

Baulch, D.L., and Campbell, I.M., "Gas Kinetics and Energy Transfer", Vol. **4**, Chem. Soc. Specialist Periodical Reports, 1981, p.137.

Bott, J.F., and Cohen, N., Int. J. Chem. Kinet., 1984, **16**, 1557.

Bowman, C.T., Combustion and Flame, 1975, **25**, 343.

Braun, M., Hofzumahaus, A., and Stuhl, F., Ber. Bunsenges. Phys. Chem., 1982, **86**, 597.

Campbell, I.M., McLaughlin, D.F., and Handy, B.J., Chem. Phys. Letts., 1976, **38**, 362.

Cvetanović, R.J., Overend, R.P., and Paraskevopoulos, G., Int. J. Chem. Kinet. Symp. **1**, 1975, 249.

Ellis, R.J., and Gilbert, R.G., J. Acoust. Soc. Am., 1977, **62**, 245.

Ernst, J., Wagner, H.Gg., and Zellner, R., Ber. Bunsenges. Phys. Chem., 1977, **81**, 1270.

Ernst, J., Wagner, H.Gg., and Zellner, R., Ber. Bunsenges. Phys. Chem., 1978, **82**, 409.

Gear, C.W., "Numerical Initial Value Problems in Ordinary Differential Equations.", 1971, Prentice-Hall, New York.

Gordon, S., and Mulac, W.A., Int. J. Chem. Kinet. Symp. **1**, 1975, 289.

Greenhill, P.G., O'Grady, B.V., and Gilbert, R.G., Aus. J. Chem., 1986, 39, 1929.

Hagele, J., Lorenz, K., Rhasa, D., and Zellner, R., Ber. Bunsenge. Phys. Chem., 1983, **87**, 1023.

Hofzumahaus, A., and Stuhl, F., Ber. Bunsenges. Phys. Chem., 1984, **88**, 557.

Husain, D., Plane, J.M.C., and Xiang, C.C., J. Chem. Soc., Faraday Trans. 2, 1984, **80**, 713.

Lorenz, K., and Zellner, R., Ber. Bunsenges. Phys. Chem., 1983, **87**, 629.

Meier, U., Grotheer, H.H., and Just, Th., Chem. Phys. Letts., 1984, **106**, 97.

Meier, U., Grotheer, H.H., Riekert, G., and Just, Th., Chem. Phys. Letts., 1985, **115**, 221.

Overend, R.P., Paraskevopoulos, G., and Cvetanović, R.J., Can. J. Chem., 1975, **53**, 3374.

Overend, R., and Paraskevopoulos, G., J. Phys. Chem., 1978, **82**, 1329.

Ravishankara, A.R., and Davis, D.D., J. Phys. Chem., 1978, **82**, 2852.

Ravishankara, A.R., Wine, P.H., and Wells, J.R., J. Chem. Phys., 1985, **83**, 447.

Smith, I.W.M., and Zellner, R., J. Chem. Soc., Faraday Trans. 2, 1973, **69**, 1617.

Smith, I.W.M., and Zellner, R., J. Chem. Soc., Faraday Trans. 2, 1973, **70**, 1045.

Spindler, K., and Wagner, H.Gg., Ber. Bunsenges. Phys. Chem., 1982, **86**, 2.

Vandooren, J., and Van Tiggelen, P.J., 18^{th} Symp. (Intl) On Combustion, 1980, 473.

Wagner, G., and Zellner, R., Ber. Bunsenges. Phys. Chem., 1981, **85**, 1122.

Westbrook, C.K., and Dryer, F.L., Comb. Sci. Technol., 1979, **20**, 125.

Chapter 4.

The Pulsed Photolysis Of Methanol and Ethanol.

4.1 Introduction.

The reason for looking at the photolysis of methanol and ethanol is simple. Photolysis of the alcohols under the experimental conditions of the flash photolysis-resonance absorption experiments may provide a perturbing influence upon the experimental observations. The study performed here is not intended to be detailed as it is only concerned about the possible effects the photolysis of reactant could have on the observed rate constants.

4.2 U.V. Spectra.

The vacuum ultra-violet absorption spectrum of methanol and ethanol has been measured by Harrison et al. (1959) and is shown in figure 4.1. Methanol and ethanol show weak absorptions with maxima at 184.5 nm. and 181.5 nm. and extinction coefficients of 0.150 and 0.320 $cm^2 mol^{-1}$ respectively.

The transmission of the suprasil quartz reaction vessel effectively cuts off at approximately 160 nm., so only absorption at longer wavelengths need be considered. At the absorption maxima of the alcohols approximately 90-95% of the incident radiation from the flash is transmitted through the walls of the reaction vessel.

The nitrogen flash lamps used successfully produced significant quantities of OH from water photolysis so emission must cover the range 180-160 nm. adequately.

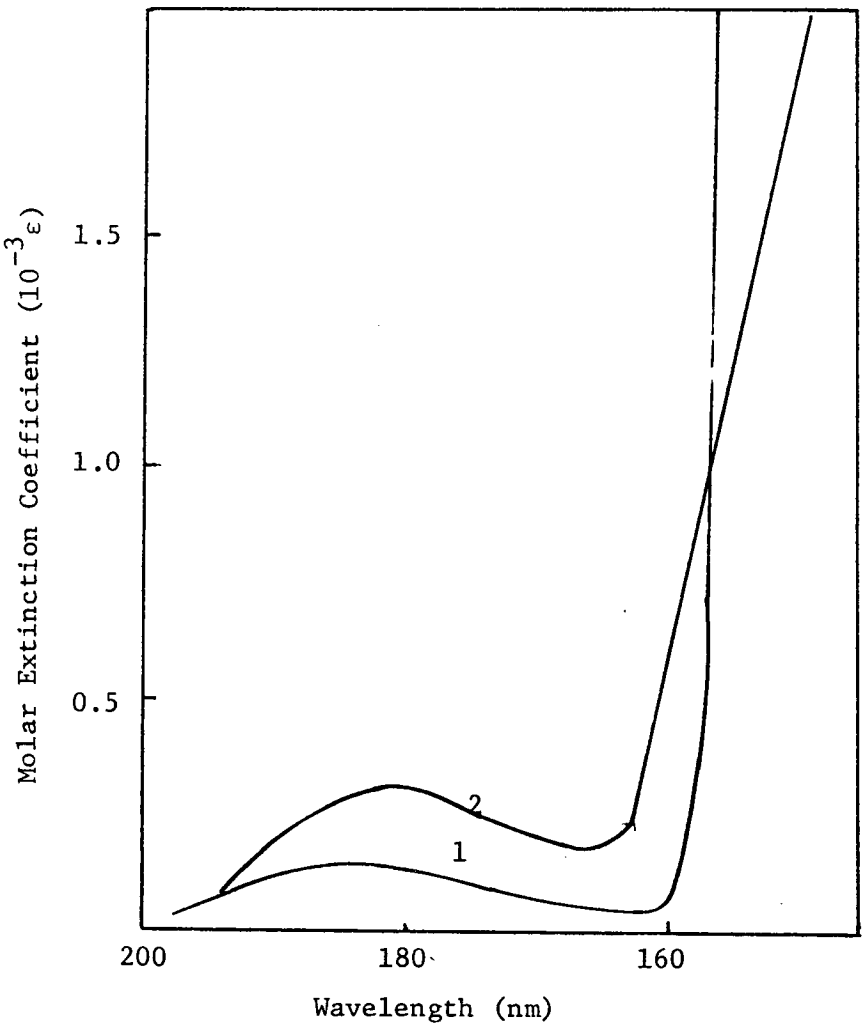

Figure 4.1 Absorption Spectra of Methanol (1) and Ethanol (2). From A.J.Harrison, B.J.Cederholm, and M.A.Terwilliger; J. Chem. Phys., 1959, 30, 355.

4.3 Previous Studies.

The previous studies of the photolysis of methanol and ethanol are limited.

4.3.1 Methanol.

The earliest gas phase studies were performed in the 1930's. Terenin and Neujmin (1935) used wavelengths down to 130nm. to photodissociate and excite the emission of the fragments. Emission at 306.2nm was observed from OH^* only at excitation wavelengths of less than 150nm. This provides sufficient energy to break the C-O bond and also excite the OH to its $A^2\Sigma$ state.

$$CH_3OH \text{ -----> } CH_3 + OH \qquad R4.1$$

Patat and Hoch (1935) determined the primary process to be

$$CH_3OH \text{ -----> } CH_2O + H_2 \qquad R4.2$$

However, it is not clear from this work whether this was a direct process or whether radical intermediates were involved.

Other studies have been on the solid compound (Farkas, et al. 1939) and in aqueous solution. (Fricke and Hart 1936; Farkas and Hirshberg 1937)

Twenty years elapsed before further work by Porter and Noyes (1959), and Harrison and Lake (1959) showed that both R4.1 and R4.2 as well as the following,

$$CH_3OH \text{ -----> } CH_2OH + H \qquad R4.3$$

$$CH_3OH \text{ -----> } CH_3O + H \qquad R4.4$$

were occurring. Stable products CH_4, CH_2O, H_2, CO, and $(CH_2OH)_2$ were identified by Porter and Noyes, the CO being due to decomposition of CH_2O. Subsequent to this, studies by Hagege, Leach, and Vermeil,(1965), and Hagege, et al. (1965) using 184.9nm. radiation determined the approximate ratios of the three processes 4.1:4.2:4.3+4.4 as 5:20:75. This was consistent with their conclusion of excitation to a singlet (^1X) state and subsequent dissociation. (Hagege, et al. 1968).

Herasymowych and Knight (1973) also photolysed at 184.9nm. and discovered that yields of H_2 and CH_4 were reduced by addition of an inert collider, in this case, CO_2. This contradicts the predissociation hypothesis of Hagege et al.

The most recent workers have turned to lasers to study the photolysis processes, particularly by infrared multiphoton dissociation (Ambartzumian, et al. 1975; Bialkowski, et al.,1977,1978; McAlpine, et al. 1980; Schmiedl, et al. 1981). One ultraviolet laser experiment has been performed by Jackson et al. (1978) in which they monitored the fluorescent emission from the excited products formed following photolysis with an ArF laser at 193 nm.

Two theoretical studies using ab initio techniques have been performed in an attempt to reconcile the observed product distribution. (Kassab, et al. 1983; Buenker, et al. 1984) Buenker has also performed liquid phase methanol photolysis to ascertain the products and provide evidence for their theoretical results.

The results are in agreement with those of Hagege, Leach and Vermeil in that the dominant process is loss of a single H atom,

$$CH_3OH \text{ -----> } CH_2OH + H \qquad R4.3$$

$$CH_3OH \text{ -----> } CH_3O + H \qquad R4.4$$

and R4.1 is a minor process at 184.9 nm. However, the photolysis of CH_3OD produced almost no H_2 indicating that the OD (and thus the OH) bond is preferentially cleaved over a CH bond. Thus R4.4 is the dominant process in conditions where collisional deactivation dominates all other processes; that is, in the liquid phase.

This is apparently inconsistent with the results of Porter and Noyes who found relatively large amounts of ethylene glycol after analysis.

The dominance of different pathways is explained by the relative height of barriers to CH and CO bond scission and also to H_2 elimination in the excited state. (Buenker, et al.).

4.3.2 Ethanol.

Ethanol has only been very sparsely investigated. Terenin and Neujmin (1935) reported parallel studies to methanol at wavelengths down to 130 nm. As in the case of methanol they observed OH^* emission at excitation wavelengths less than 150 nm.

Patat and Hoch (1935) observed acetaldehyde and hydrogen as products of the photolysis. Harrison and Lake (1959) also observed in addition to other products, CH_2O and C_2H_4, the latter apparently

as a primary product.These observations suggest that the following primary process occurs;

$$CH_3CH_2OH \text{ -----> } CH_2CH_2 + H_2O \qquad R4.5$$

as well as the expected processes,

$$CH_3CH_2OH \text{ -----> } CH_3CH_2 + HO^* \qquad R4.6$$

$$CH_3CH_2OH \text{ -----> } CH_3CHO + H_2 \qquad R4.7$$

There were no direct indications that R4.8 or R4.9 occurred.

$$CH_3CH_2OH \text{ -----> } CH_3CHOH + H \qquad R4.8$$

$$CH_3CH_2OH \text{ -----> } CH_3CH_2O + H \qquad R4.9$$

However, formaldehyde may well be formed from the photolysis or simple dissociation of the ethoxy radical formed in R4.9.

$$CH_3CH_2O \text{ -----> } CH_3 + CH_2O \qquad R4.10$$

Garibyan et al. (1971) observed ESR signals due to CH_3CHOH after photolysis with a mercury lamp which indicates R4.8 is occurring. Abdel-Hamid (1972) observed similar signals after the photosensitized decomposition of ethanol at 77K as did Shiotani and Chachaty (1974).

As in the case of methanol, Jackson et al. (1978) have observed fluorescence from OH and CH after photolysis of ethanol with an ArF laser and ascribed it to two photon excitation of the $n \rightarrow \sigma^*$ transition.

Both Danen (1979) and Selwyn, et al. (1978) were able to selectively initiate R4.5 using a CO_2 laser on the P(28) line of the 001-020 transition (1039.37 cm^{-1}). At pressures greater than 10 torr the reactions R4.5, R4.7 and R4.10 were found to occur in the ratio 2 : 3 : 1.

Yamabe et al. (1984) have performed a theoretical study of the unimolecular decomposition of ethanol in an attempt to understand the results obtained above using infrared lasers.

4.4 Experimental

4.4.1 Apparatus

Experiments were performed using essentially the same experimental arrangement as described in Chapter 3 so that the experimental conditions were as similar as possible. Modifications were made to enable the reaction mixture to be quantitatively transferred to a stainless steel sample bulb so that analysis could be performed at a site remote to the photolysis. Figure 4.2 is a diagram of the modified experimental system. The resonance absorption system was not required for this portion of the work as OH produced by photolysis was not monitored.

One end window was replaced with a brass fitting consisting of a flange, tubing and a shutoff tap. The tap was connected via a flexible fitting to the sample bulb through a two position selectable valve. In one position this enabled the sample bulb to be

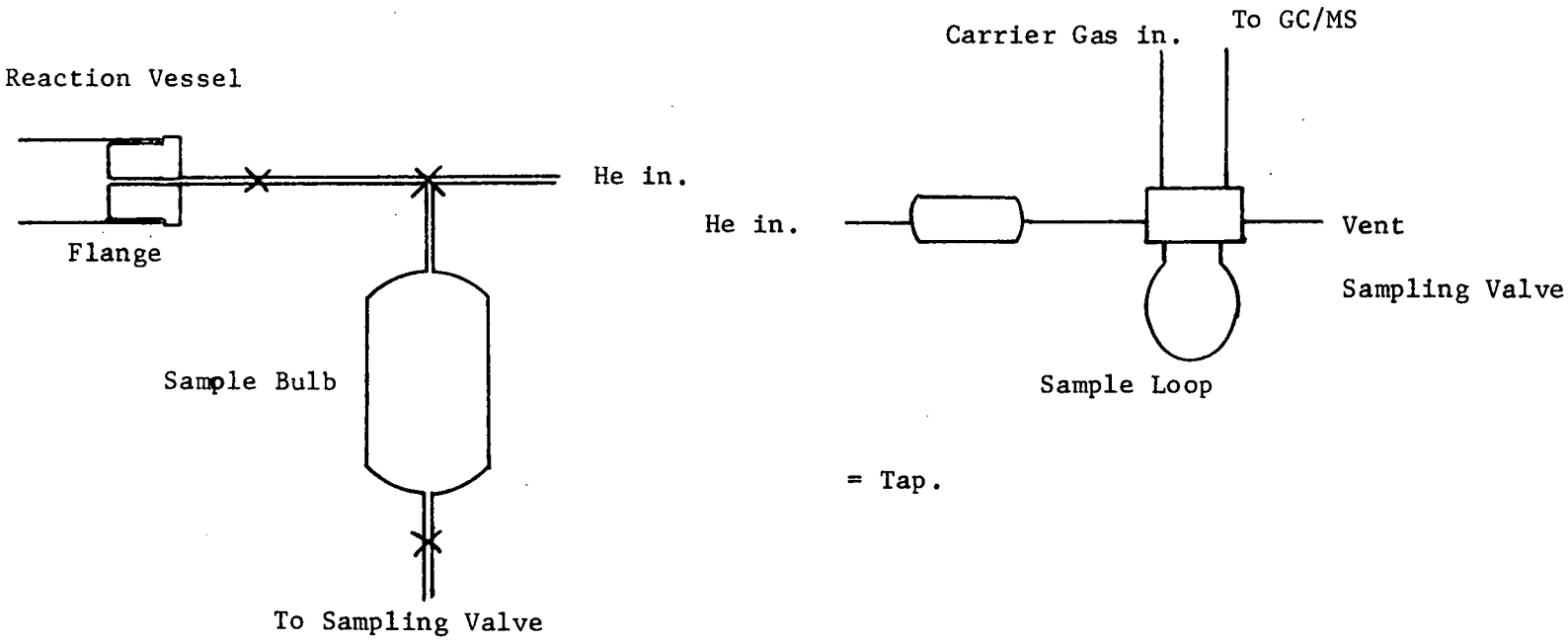

Figure 4.2 Apparatus for Sampling Photolysis Mixtures Via Gas Chromatography-Mass Spectrometry.

evacuated and in the other position for it to be filled with the mixture for analysis. The sample bulb had an internal volume of 150 cm^3 and was sealed at the outlet end with a stainless steel ball valve. This was connected to a gas sampling valve at the inlet of the gas chromatograph injector with stainless steel tubing and graphitized seals.

The analyses were carried out with a Hewlett Packard HP 5890 Gas Chromatograph with a mass selective detector model HP 5970. This instrument is interfaced with a Hewlett Packard model HP200 series computer and provides full instrument control and data analysis capabilities. The mass selective detector is essentially a small quadrupole mass spectrometer. The gas chromatograph is designed to use capillary columns and is fitted with a split injector.

For this work a Chrompack 25m capillary column (4.7 micron diameter) was used. This uses CP Sil 5 Cb liquid phase coating and gave good separation of polar components CH_3OH, H_2O, CH_2O, CH_3CHO and CH_3CH_2OH at 30C. Non polar components were bunched with the Argon diluent gas from the sample.

The sample injector was connected to the column by a split injector which enabled the sample size admitted to the gas chromatograph to be varied. Two sample loops of approximately 0.2 and 2.0 ml were used for all experiments.

4.4.2 Procedure

Methanol and ethanol were photolysed in the presence and absence of water using the nitrogen filled flash lamp constructed for the previous kinetic work.

For the methanol experiments mixtures containing approximately 1 and 10 to 11% methanol were used. This corresponds to a similar amount and to 10 times the amount of methanol used in experiments described in chapter 3. In the ethanol experiments alcohol concentrations were in the range 4-6% which is approximately 100 times that used in the previous experiments. The quantity of water used was about 2% (about 2 times that used previously) and was not varied in experiments with added water, so no effects due to water concentration on the product distribution could be determined.

An appropriate mixture was let into the reaction vessel to a pressure of approximately 100torr and pulse photolysed the predetermined number of times. After photolysis the mixture was allowed to expand into the previously evacuated sample bulb and then flushed through with diluent gas until the final pressure was approximately 760torr. The sample bulb was then transferred to the GC/MSD and a helium line was connected to enable samples to be transferred to the injector loop.

In the early experiments, argon was used as the diluent gas for some of the methanol experiments, however this interfered with the detection of the non-polar and permanent gases as they were eluted coincidently. Helium was substituted for the argon in the later

methanol experiments and all of the ethanol experiments as its m/e value falls outside the mass range detected and thus did not interfere with the analysis of those components normally eluted with the carrier.

Samples were introduced to the gas chromatograph by flushing the sampling vessel with a slow flow of helium (10-20 cm^3min^{-1}) through the the injector loop of the sampling valve and injecting while the flow was continuing. This enabled several samples to be analysed from the same photolysis mixture as a test for reproducibility within a sample.

Data collection was initiated at the injection time and the resultant total ion chromatograph stored for later analysis.

4.5 Results and Discussion.

The results of this work are presented as the total ion chromatograms and mass spectra of the components.

4.5.1 Methanol

The photolysis of methanol produced no detectable products after 1, 5 or 20 photolyses either in the presence or absence of water. Figure 4.3 is the total ion chromatogram after 20 pulses on mixtures containing a) 1% methanol and b) 11% methanol. Figure 4.4 is as for figure 4.3 with 2% water added to each mixture.

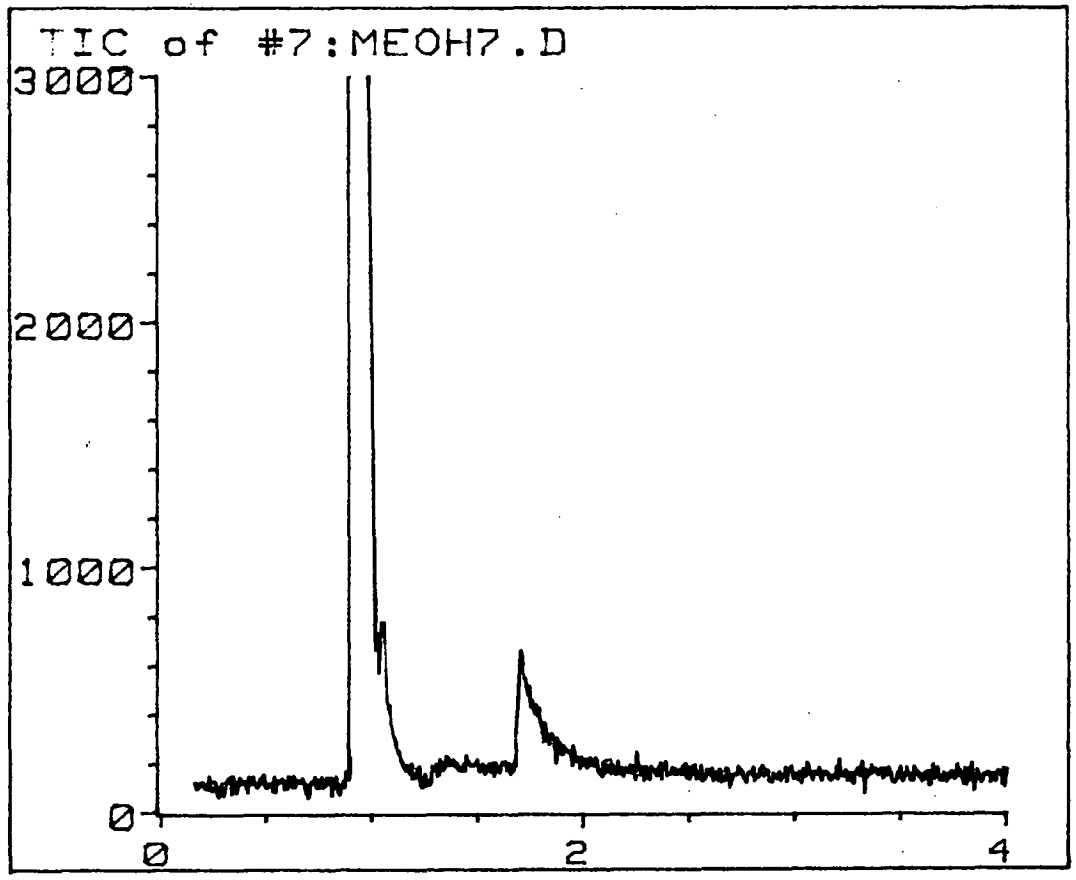

Figure 4.3a TIC of 1% Methanol Mix After 20 Pulses.

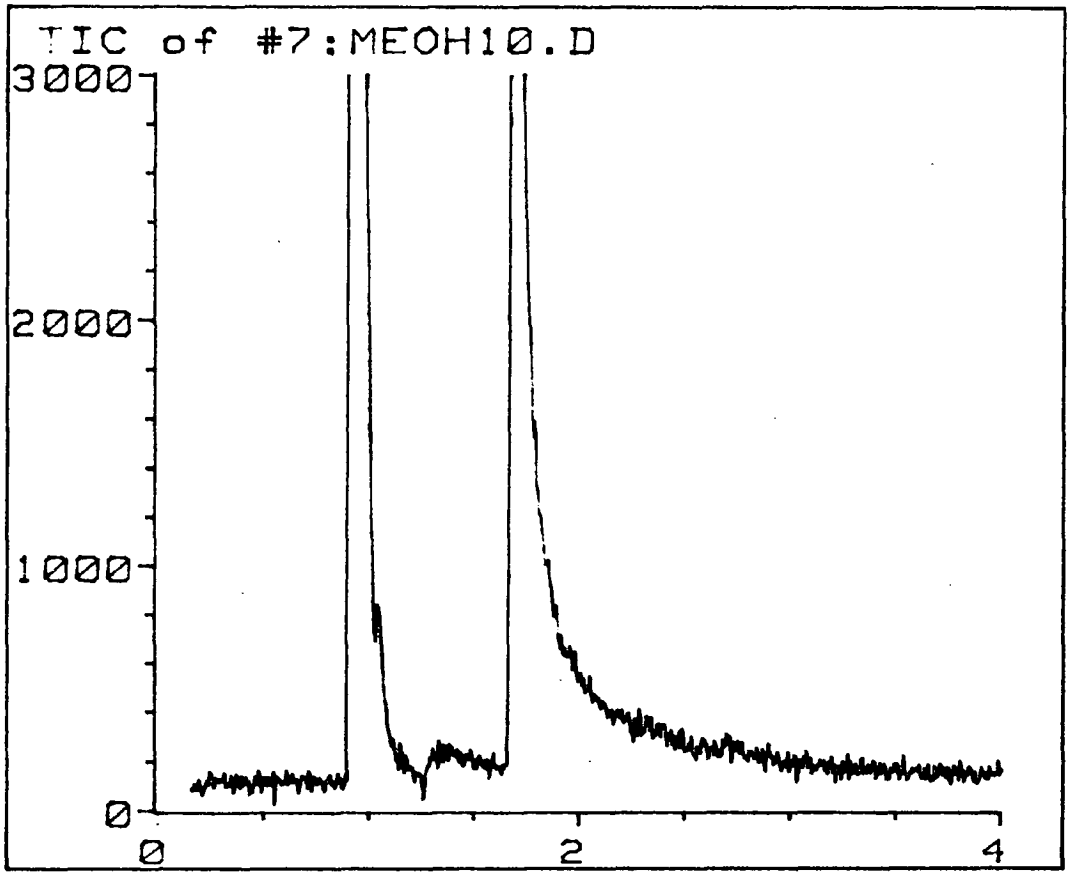

Figure 4.3b TIC of 11% Methanol Mix After 20 Pulses.

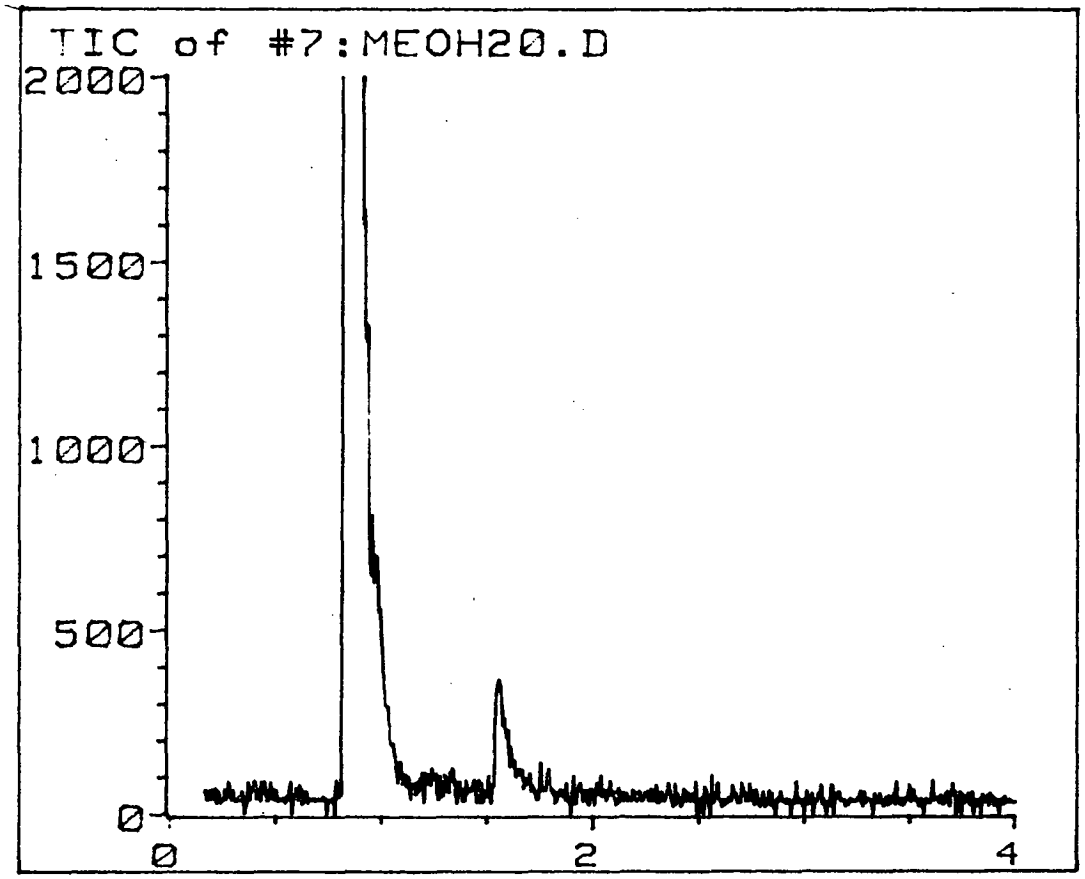

Figure 4.4a TIC of 1% Methanol and 2% Water Mix After 20 Pulses.

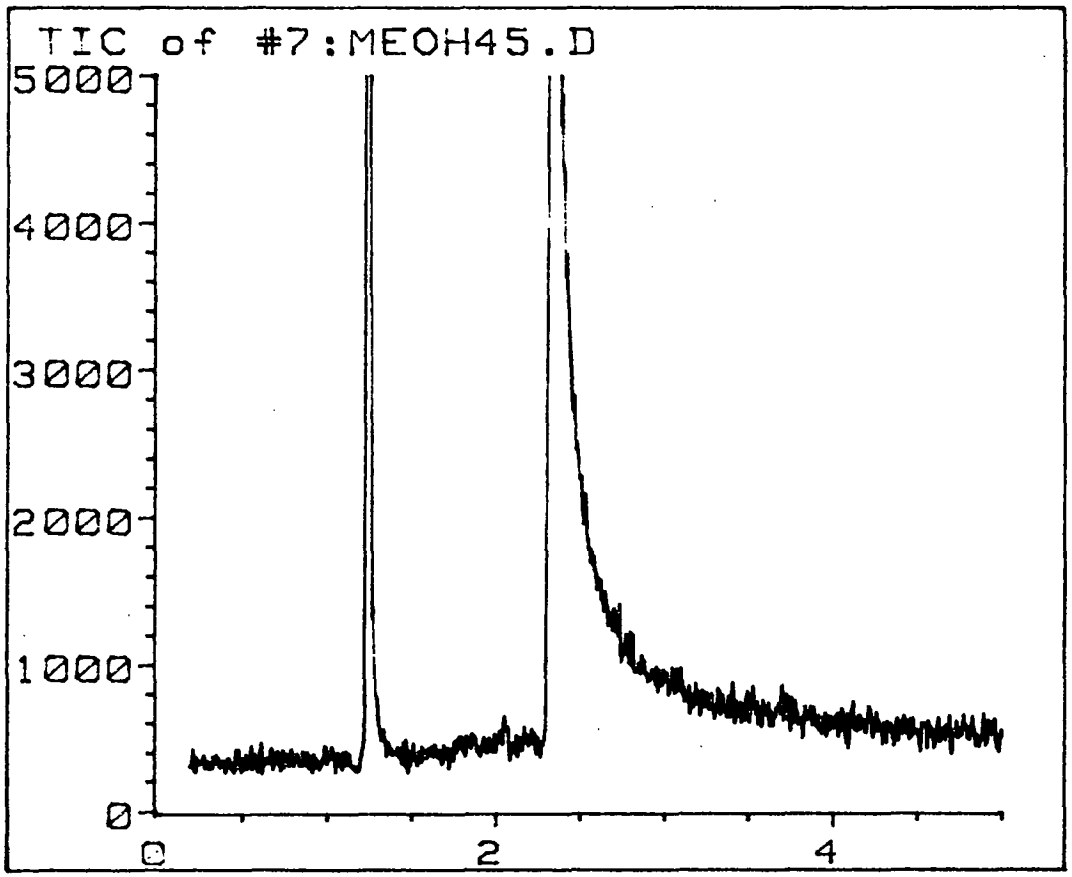

Figure 4.4b TIC of 11% Methanol and 2% Water Mix After 20 Pulses.

Experiments using a 10% methanol mixture with and without approximately 2% water added were performed in which photolysis was done one hundred times. The results are shown in figures 4.5 and 4.6.

In these experiments CH_2O and CH_3OCH_3 were the only identifiable products. The dimethyl ether was identified by comparison with a genuine sample prepared by distillation of a sulphuric acid/methanol mixture (see appendix B). CH_2O was identified from its mass spectrum. The observed mass spectra are shown in figures 4.7 and 4.8 for CH_2O and CH_3OCH_3 respectively, and the spectrum of the genuine sample of CH_3OCH_3 is shown in figure 4.9. Retention times and approximate relative concentrations are given in Table 4.1.

Table 4.1 Retention Times for Methanol Photolysis.

Compound	Retention Time (min)	Relative Concentration (%)
CH_2O	1.49	0.4
CH_3OCH_3	1.96	0.9
CH_3OH	2.23	98.7

The very low levels of products observed indicate that there could be no possible interference from secondary products on the observed OH decays.

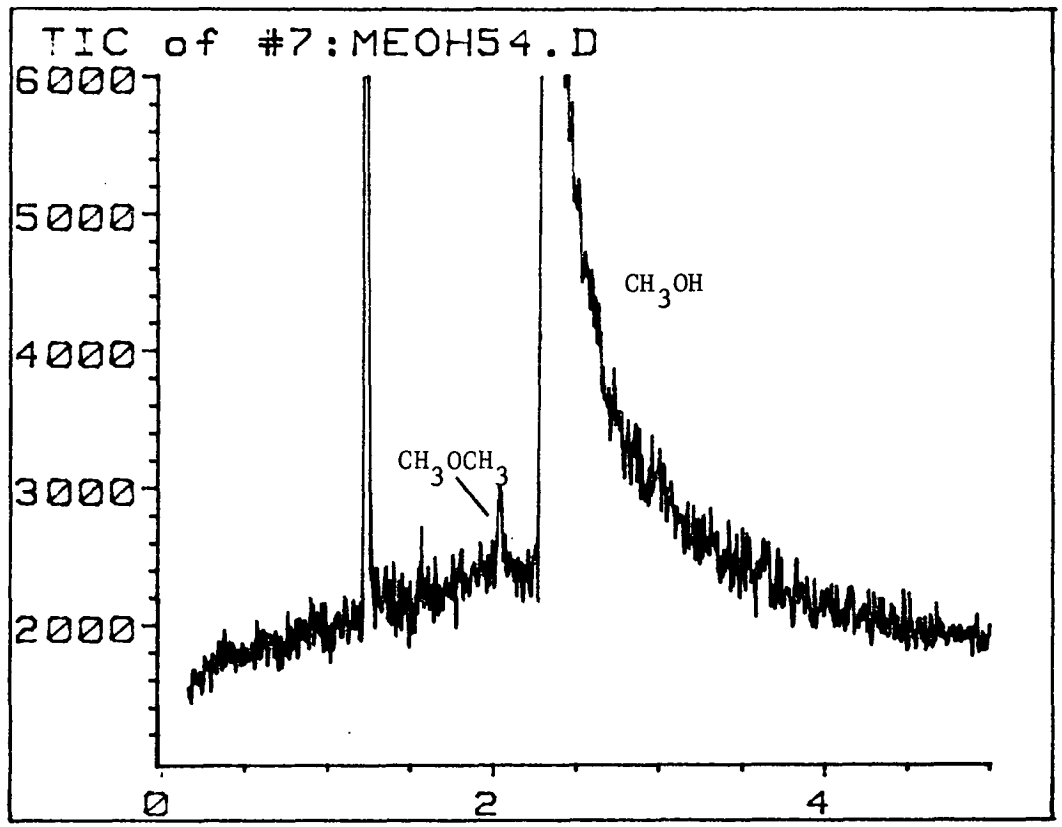

Figure 4.5 TIC of 10% Methanol Mix After 100 Pulses.

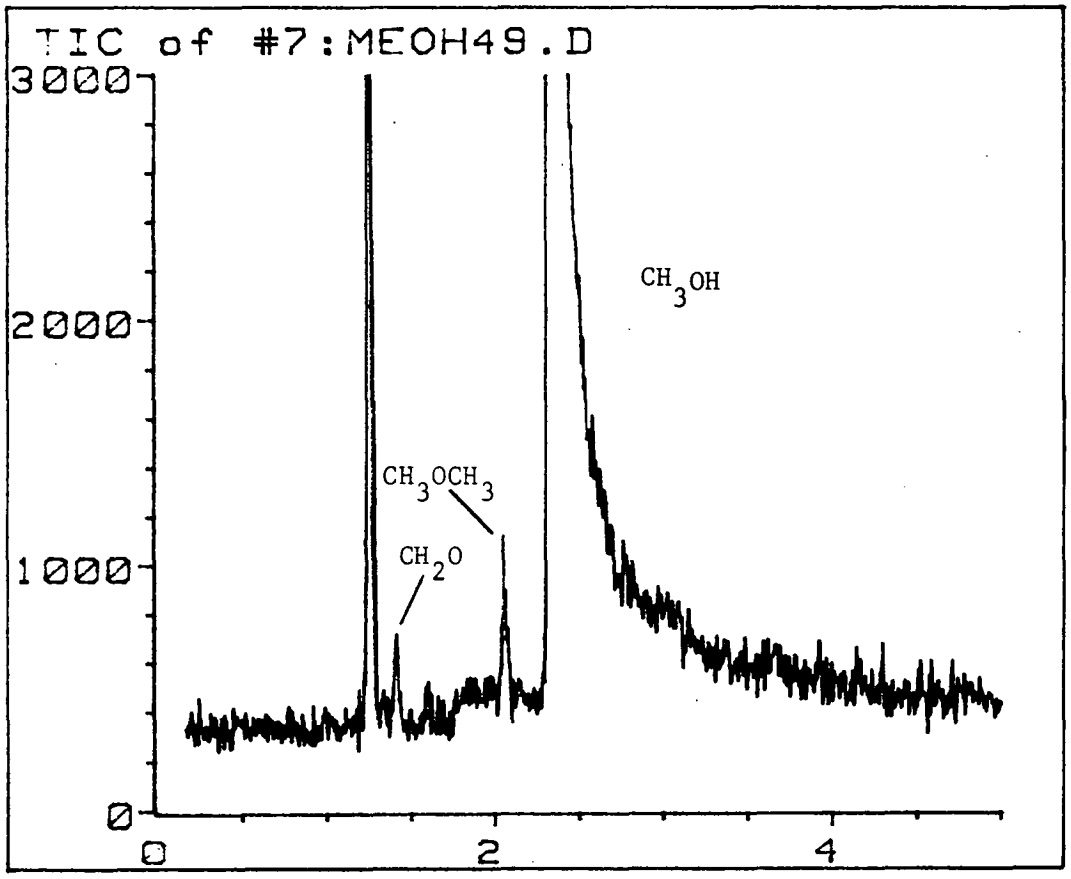

Figure 4.6 TIC of 10% Methanol and 2% Water Mix After 100 Pulses.

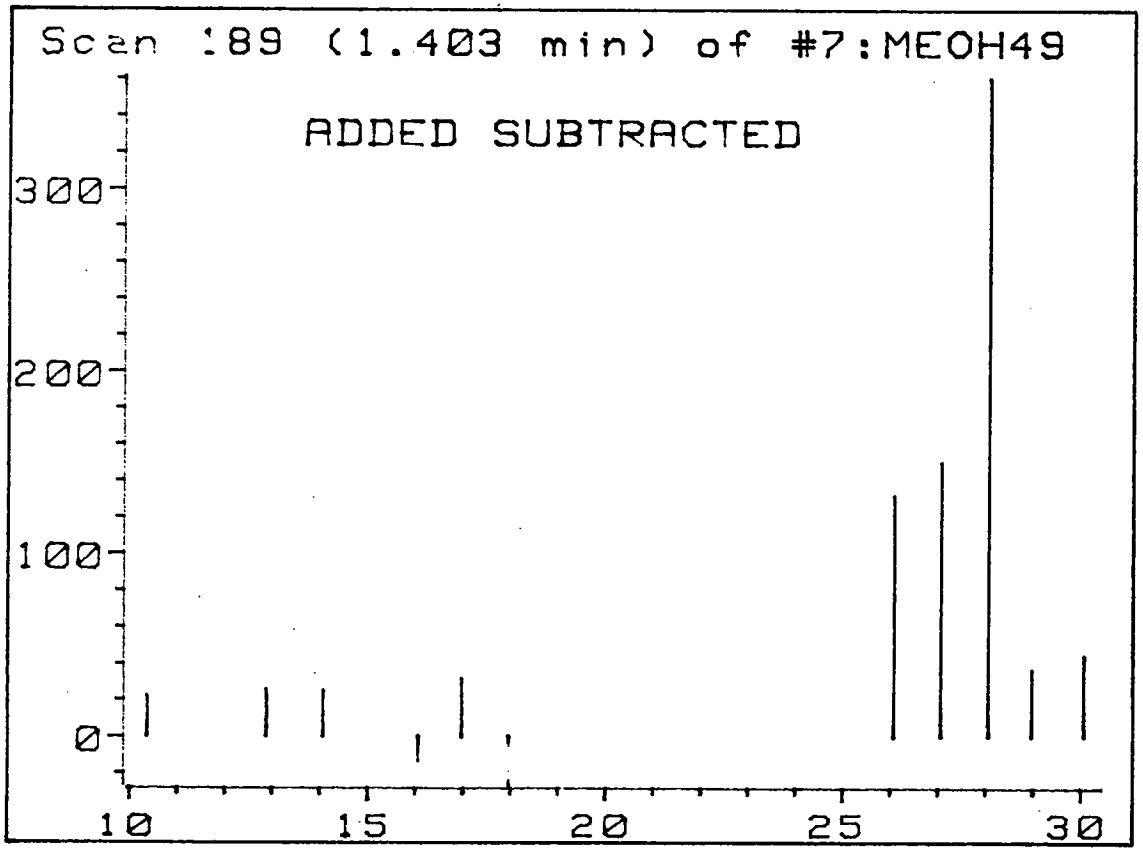

Figure 4.7 Mass Spectrum of CH_2O From Methanol/Water Mix

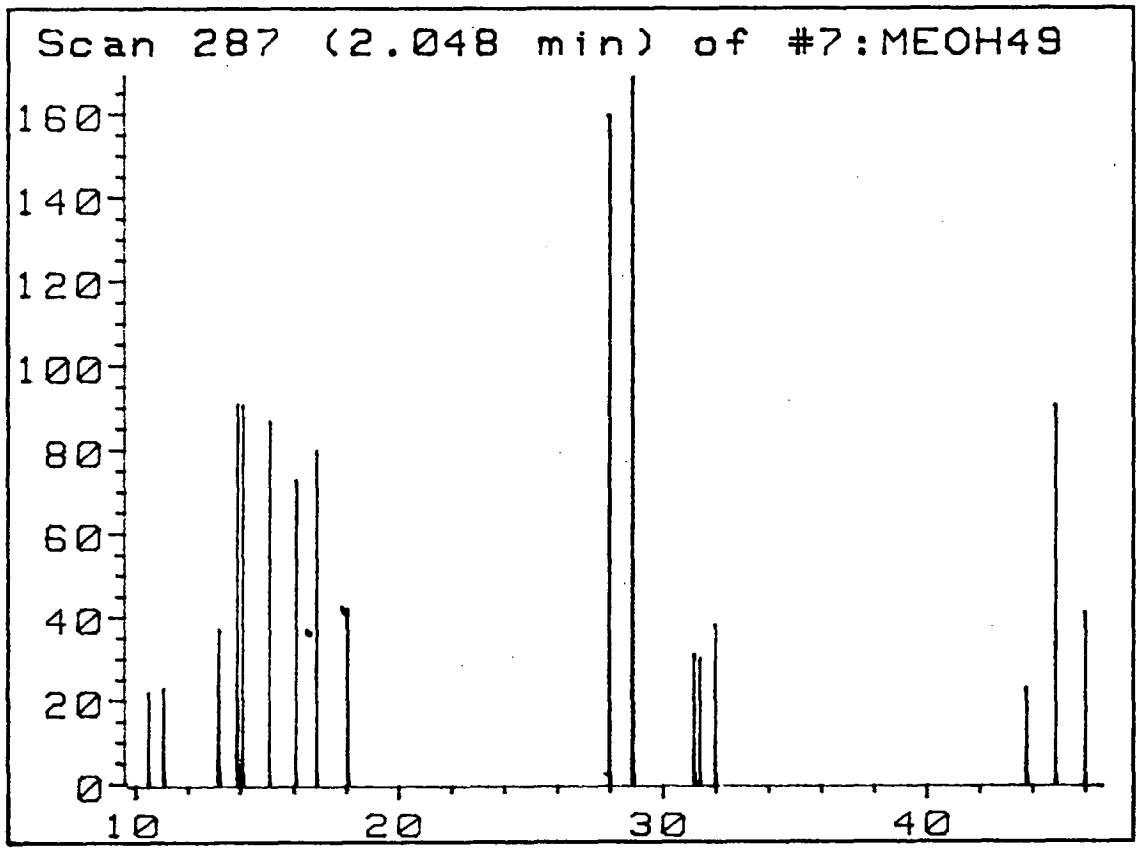

Figure 4.8 Mass Spectrum of CH_3OCH_3 From Methanol/Water Mix.

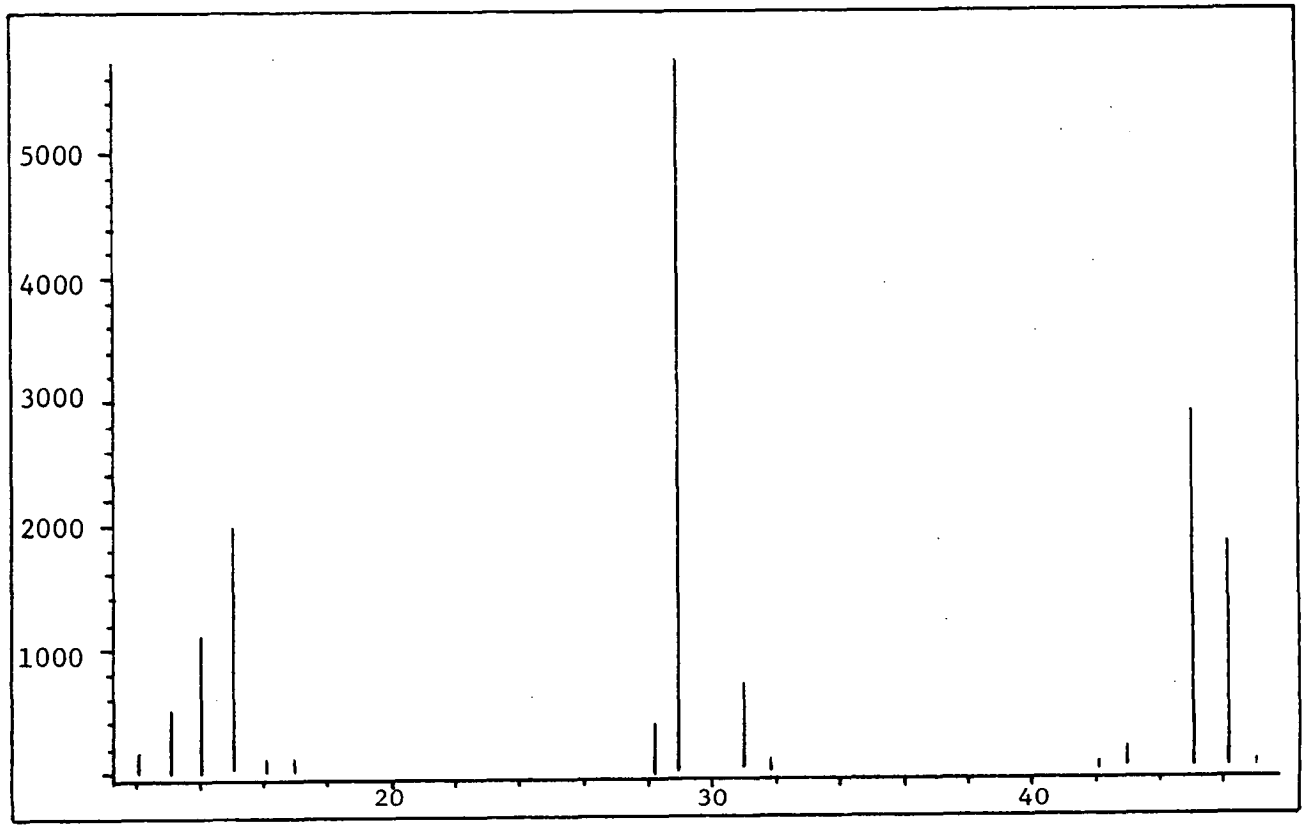

Figure 4..9 Mass Spectrum of Genuine Sample of CH_3OCH_3

The presence of CH_3OCH_3 appears to be a novel observation. Products observed previously from CH_3OH photolysis were CH_4, CH_2O, H_2, CO, and $(CH_2OH)_2$, (see section 4.2.1), and these products could be expected from the current work.

However, the very low total level of products produced in these experiments prevented identification of all but the major products. The level of CO was not distinguishable from the background level due to air contamination. H_2 was not looked for, and $(CH_2OH)_2$ was not detected, nor was CH_4.

The mechanism of production of CH_2O from methanol can be quite readily explained in terms of a series of radical abstraction reactions by OH and H with CH_3OH, CH_3O and CH_2OH and by direct photolysis.

The lack of $(CH_2OH)_2$ is almost certainly due to the different conditions of the two sets of work. In this dilute, gas phase work, collisions between CH_2OH radicals and subsequent stabilization is several orders of magnitude less likely than in the liquid phase.

The novel observation of CH_3OCH_3 is less easily accounted for. The formation of CH_3OCH_3 can only be via insertion or recombination. The insertion reaction of methylene, CH_2, with methanol has been studied by O'Grady, (1966), and by Kerr, et al. (1967)

$$CH_2 + CH_3OH \quad \text{----->} \quad CH_3OCH_3 \qquad \text{R4.11}$$

$$\text{----->} \quad CH_3CH_2OH \qquad \text{R4.12}$$

The rate of insertion into an O-H bond is a factor of 10.9 faster than into a C-H bond so R4.11 could be expected to dominate. However, it is difficult to see how CH_2 could be formed in the current work. Hoyermann, et al. have also found that the reaction of H with CH_3O or CH_2OH produced no CH_2.

The alternative mechanism of recombination is more likely in this system for the reasons discussed below. CH_3O and CH_2OH radicals will be produced in reactions R4.13 and R4.14 with

$$CH_3OH + OH \longrightarrow CH_3O + H_2O \qquad \text{R4.13}$$

$$CH_3OH + OH \longrightarrow CH_2OH + H_2O \qquad \text{R4.14}$$

approximately 10 to 20% of methanol consumed being due to R4.13 (Hagele, et al. 1983; Meier, et al. 1984). The photolysis of methyl acetate (Hassinen, et al. 1979) in the gas phase produced CH_3OCH_3 via the reaction

$$CH_3O + CH_3 \xrightarrow{[M]} CH_3OCH_3 \qquad \text{R4.15}$$

with a rate constant of 5.5×10^{-11} $cm^3 s^{-1}$. Similarly Yee Quee, et al. (1966) have observed CH_3OCH_3formed via R4.15 in the photolysis of dimethyl carbonate, $CH_3OCOOCH_3$. CH_3O is a primary product of reaction R4.13 but CH_3 is not produced in any of the previously discussed reactions except R4.1. This is a minor process at 184.9 nm (see section 4.3.1) and would be expected to be also minor under the conditions of this work.

An alternative explanation in terms of the recombination reactions discussed in chapter 6 is proposed. As found by Hoyermann, et al. (1981), the reactions of H atoms with CH_3O and CH_2OH are fast and lead to a mixture of products via abstraction reactions as well as the following:

$$CH_2OH + H \longrightarrow CH_3OH^* \longrightarrow CH_3OH \qquad R4.16$$

$$\longrightarrow CH_3OH^* \longrightarrow CH_3 + OH \qquad R4.17$$

$$CH_3O + H \longrightarrow CH_3OH^* \longrightarrow CH_3OH \qquad R4.18$$

$$\longrightarrow CH_3OH^* \longrightarrow CH_3 + OH \qquad R4.19$$

At pressures of 0.1-2 torr reactions R4.16 and R4.18 are in the fall off regime as found by application of microcanonical variational transition state theory (Greenhill, et al. 1986; see also chapter 6). Under these conditions collisional stabilisation of CH_3OH^* is less likely and the dissociative processes R4.17 and R4.19 are more important. Approximately 15% of the reaction was found to go via R4.17 and R4.19 (Hoyermann, et al.).

Under the conditions of the current experiments of 100 torr total pressure less of the reaction will proceed via R4.17 and R4.19 than at lower pressures but it will still be a quite significant source of CH_3 radicals. CH_3OCH_3 can then be formed via R4.15.

4.5.2 Ethanol

The pulsed photolysis of ethanol/helium mixtures produced ethanal, (CH_3CHO), in identifiable quantities with as few as five photolyses. After 100 pulses, CO_2, C_2H_4, CH_2O, $CH_3CH_2OCH_3$ and CH_3COCH_3 could also be identified. Yields were enhanced on the addition of water. Chromatograms of mixtures of CH_3CH_2OH/H_2O (4%/2%) and CH_3CH_2OH (6.25%) in He after 100 pulses are shown in figures 4.10 and 4.11 respectively.

Retention times and approximate relative concentrations of the components are given in table 4.2. The production of methyl ethyl ether and acetone appears to be a novel observation with respect to ethanol photolysis.

Table 4.2 Retention Times for Ethanol Photolysis.

Compound	Retention Time (min)	Relative Concentration (%)
CO_2	1.30	0.9
C_2H_4	1.33	0.9
CH_2O	1.38	0.8
CH_3CHO	2.26	7.6
$CH_3CH_2OCH_3$	3.20	0.7
CH_3CH_2OH	3.60	87.9
CH_3COCH_3	4.95	1.2

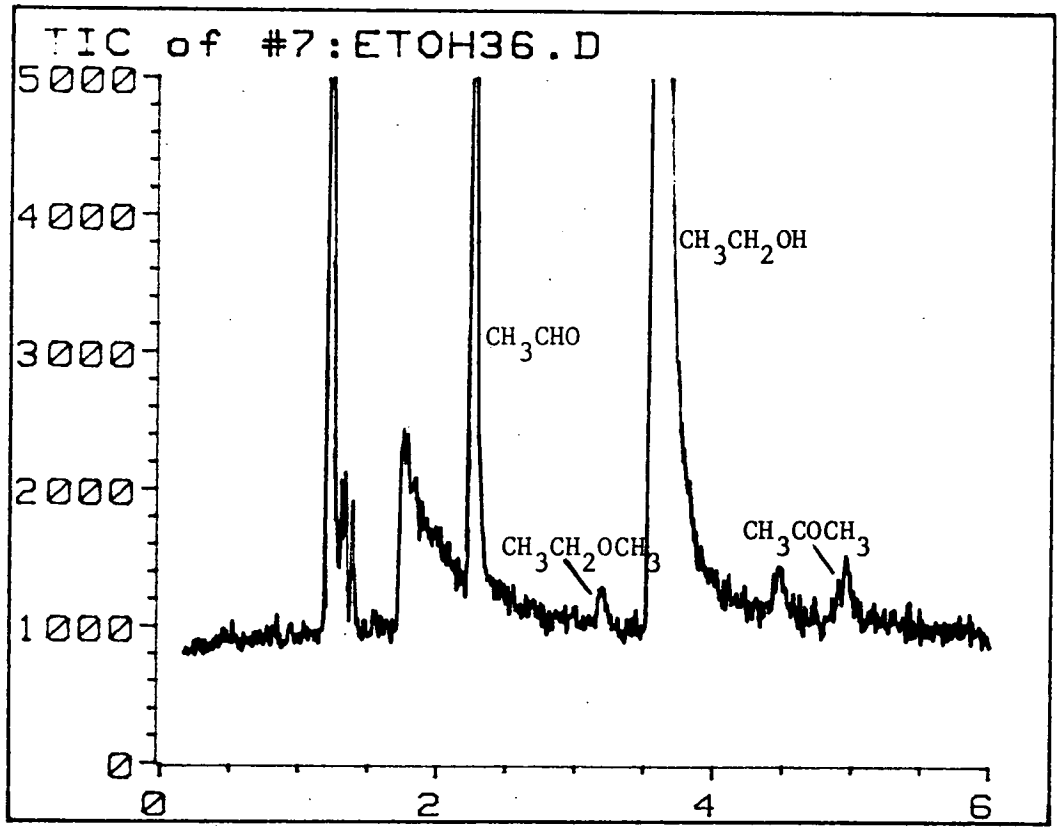

Figure 4.10 TIC of 4% Ethanol 2% Water Mix After 100 Pulses.

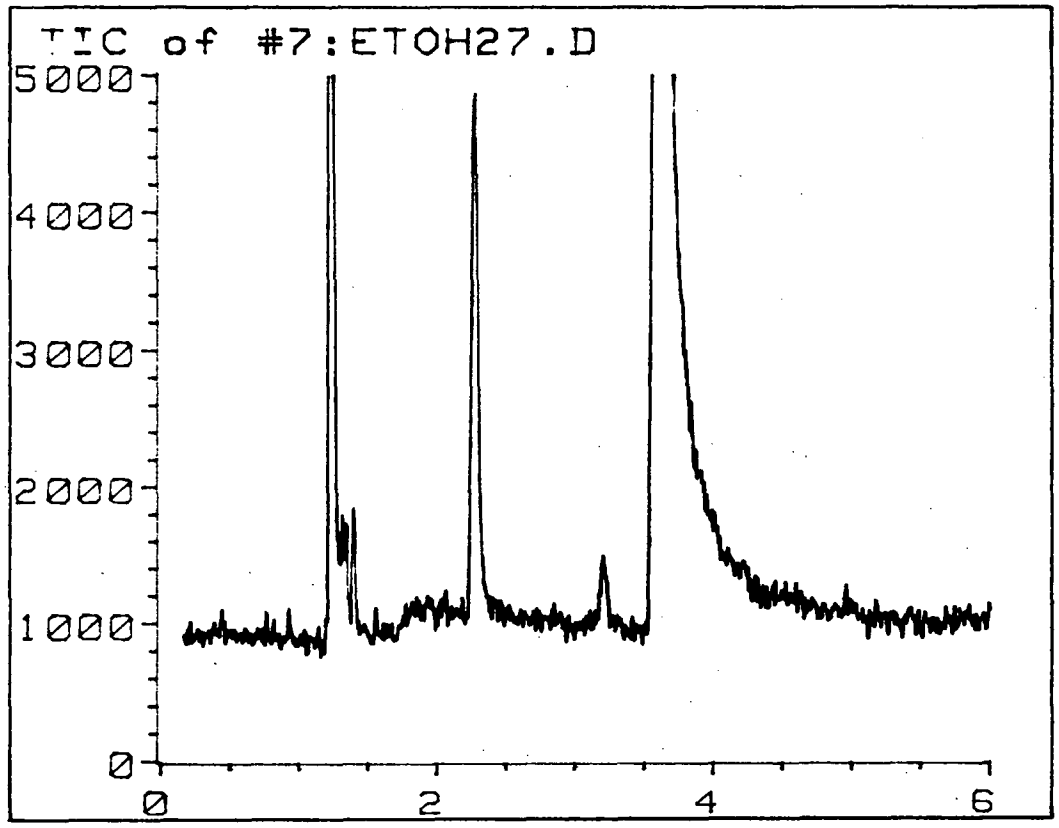

Figure 4.11 TIC of 6% Ethanol Mix After 100 Pulses.

The yields of CH_3CHO increased with the number of times a mixture was photolysed. This is shown graphically in figure 4.12 for the cases both with and without added water.

At low numbers of pulses only CH_3CHO could be identified as a product. This is consistent with the results of Patat and Hoch and reactions R4.7, R4.8 and R4.9 occurring. It is not possible to distinguish between direct production of CH_3CHO via R4.7 and production of CH_3CHOH and CH_3CH_2O via reactions R4.8 and R4.9 followed by radical abstraction or disproportionation.

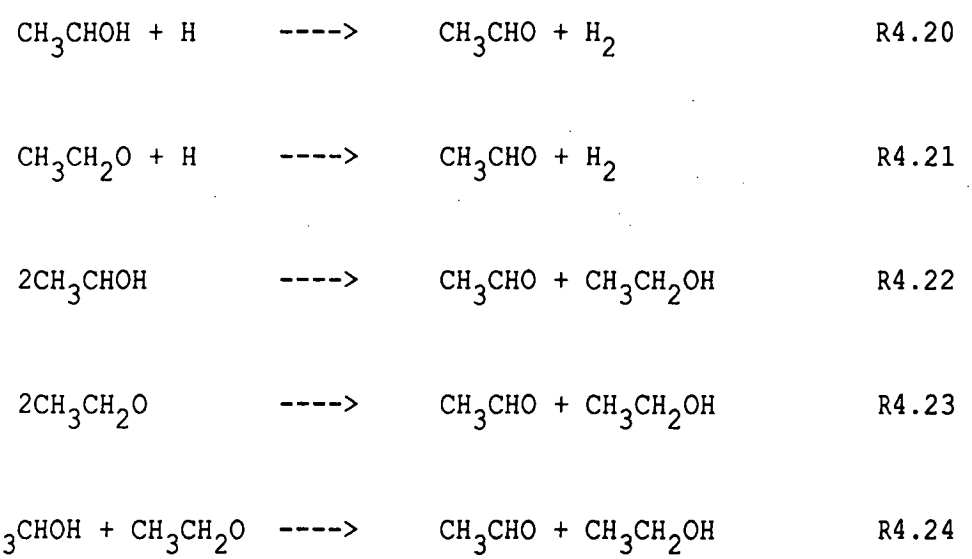

$$CH_3CHOH + H \longrightarrow CH_3CHO + H_2 \qquad R4.20$$

$$CH_3CH_2O + H \longrightarrow CH_3CHO + H_2 \qquad R4.21$$

$$2CH_3CHOH \longrightarrow CH_3CHO + CH_3CH_2OH \qquad R4.22$$

$$2CH_3CH_2O \longrightarrow CH_3CHO + CH_3CH_2OH \qquad R4.23$$

$$CH_3CHOH + CH_3CH_2O \longrightarrow CH_3CHO + CH_3CH_2OH \qquad R4.24$$

Evidence for the radical route is found in the presence of methyl ethyl ether, $CH_3OCH_2CH_3$. This is presumably formed in an analogous fashion to CH_3OCH_3 by recombination of CH_3CH_2O and CH_3.

$$CH_3CH_2O + CH_3 \longrightarrow CH_3CH_2OCH_3 \qquad R4.25$$

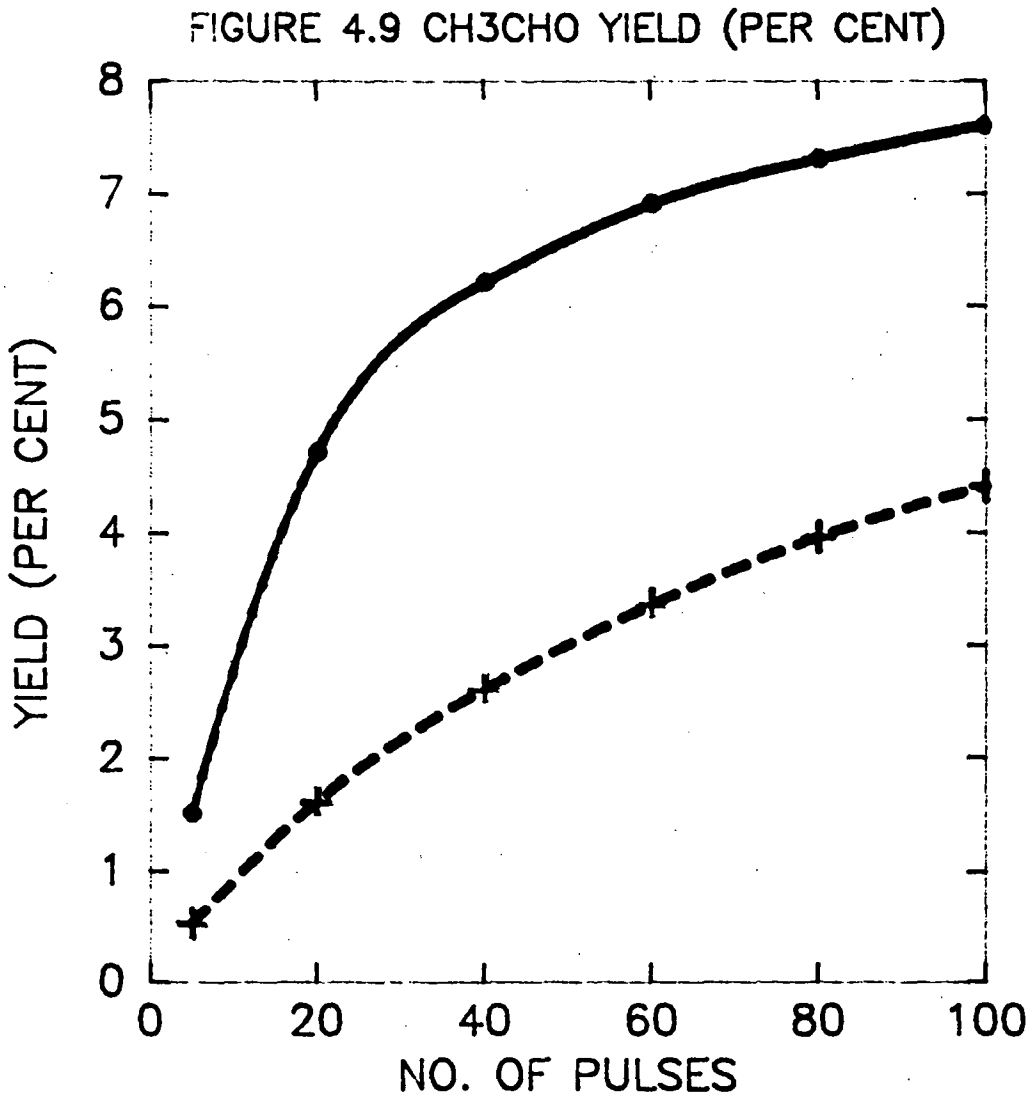

Figure 4.12 Relative Yield of CH_3CHO as a Function of the Number of Photolysis Pulses.

—— With Water

- - - Without Water

The CH_3 in this case almost certainly came from secondary photolysis of CH_3CHO as recombination dissociation of CH_3CH_2O and H would give CH_3CH_2 and OH not CH_3.

$$CH_3CH_2O + H \quad \text{----->} \quad CH_3CH_2OH^* \quad \text{----->} \quad CH_3CH_2 + OH \qquad \text{R4.26}$$

The likelihood of collisional stabilisation is also enhanced over CH_3OH^* as $CH_3CH_2OH^*$ is a larger molecule.

After 100 pulses, 2-propanone, (CH_3COCH_3) was also detected in similar yield to $CH_3CH_2OCH_3$. The mechanism of formation of CH_3COCH_3 is not clear but several possiblities exist.

Firstly CH_3 radical attack on the hydroxyethyl CH_3CHOH or ethoxy CH_3CH_2O may yield CH_3COCH_3 by elimination of H_2.

$$CH_3CHOH + CH_3 \quad \text{----->} \quad CH_3COCH_3 + H_2 \qquad \text{R4.27}$$

$$CH_3CH_2O + CH_3 \quad \text{----->} \quad CH_3COCH_3 + H_2 \qquad \text{R4.28}$$

R4.28 would be unlikely as attack on the carbon atom would be highly hindered. Recombination resulting in $CH_3CH_2OCH_3$ formation is more likely as is H abstraction to give CH_3CHO and CH_4. This H-abstraction pathway will be dominant over other alternatives.

Secondly H abstraction by radicals from CH_3CHO to give CH_3CO radicals and subsequent recombination with CH_3 may occur.

$$CH_3CHO + X \quad \text{----->} \quad CH_3CO + HX \qquad \text{R4.29}$$

$$CH_3CO + CH_3 \quad \text{----->} \quad CH_3COCH_3 \qquad \text{R4.30}$$

This mechanism is more likely due to the increasing amounts of CH_3CHO formed as the number of pulses increases.

The third alternative is elimination of a single H atom from acetaldehyde by CH_3

$$CH_3 + CH_3CHO \quad \text{----->} \quad CH_3COCH_3 + H \qquad \text{R4.31}$$

Thermochemically reactions R4.29 and R4.30 are exothermic by approximately 212 kJ mol^{-1} if X is either H or CH_3 as is likely, wherea R4.31 is 20 kJ mol^{-1} endothermic. The combination of radical abstraction followed by recombination would be expected to be more favourable dependent upon the relative height of the barriers.

Minor products CO_2, C_2H_4 and CH_2O could also be detected after 100 pulses. The presence of C_2H_4 indicates the possibility of R4.5 occurring,

$$CH_3CH_2OH \quad \text{----->} \quad CH_2CH_2 + H_2O \qquad \text{R4.5}$$

as observed by Harrison and Lake (1959). Alternatively decomposition of C_2H_5 formed in R4.26 may occur.

$$CH_3CH_2 \quad \text{----->} \quad CH_2CH_2 + H \qquad \text{R4.32}$$

However, as production of CH_3CH_2 is going to be less likely than collisional stabilisation

$$CH_3CH_2O + H \xrightarrow{} CH_3CH_2OH^* \xrightarrow{[M]} CH_3CH_2OH \qquad R4.33$$

or H abstraction by R4.20 and R4.21, this is unlikely to be a major source of CH_2CH_2.

CH_2O and CO_2 are formed by decomposition and reactions of the higher radicals. CH_2O may also be formed via the competitive reaction

$$HCO + H \xrightarrow{} H_2CO \qquad R4.34$$

$$HCO + H \xrightarrow{} CO + H_2 \qquad R4.35$$

R4.34 is analogous to reaction R4.16 for CH_2OH radicals in that the transition state will be a simple fission one and there will be no barrier to recombination.

The products obtained in the pulsed photolysis of CH_3CH_2OH/H_2O mixtures were the same as those in the absence of H_2O. Yields were enhanced but changes in distribution were not distinguishable in these experiments. In general the mechanism described previously will account for all of the observed products, the increased yields being explained by increased CH_3CHOH and CH_3CH_2O concentrations from the reactions of CH_3CH_2OH with OH.

$$CH_3CH_2OH + OH \quad \text{----->} \quad CH_3CHOH + H_2O \qquad R4.36$$

$$\text{----->} \quad CH_3CH_2O + H_2O \qquad R4.37$$

Most of the OH produced via the photolysis of H_2O will react with CH_3CH_2OH leaving H to be removed by subsequent reaction with CH_3CHOH and CH_3CH_2O as well as the other processes discussed previously.

4.6 Effect of Products on Measured Rate Constants

In the case of methanol there will be no observable effect as the quantities of products are the order of 0.01% or 1/10000th of the reactant concentrations per pulse.

In the case of ethanol, assuming that 1% of CH_3CH_2OH is transformed to CH_3CHO after 5 pulses, then after 1 pulse the quantity will be 0.2%. The rate constant at 298K for OH attack on CH_3CHO is four times that on CH_3CH_2OH so this amount of CH_3CHO will enhance the rate by approximately 0.8%. This is considerably less than the experimental scatter and so the effect on the observed rate constant will be undetectable.

4.7 Further Work

This work has produced some novel results which are still poorly understood. There is scope for considerable further work to be performed on both the CH_3OH and CH_3CH_2OH systems. The reasons for the production of CH_3OCH_3 rather than CH_2O in the photolysis of CH_3OH need to be studied. The effect of pressure and alcohol concentration need to be investigated for both systems as well as the reason for the apparent lack of $(CH_2OH)_2$ in the methanol system.

The effect of wavelength and intensity may also be important as well as the effect of different colliders.

One necessary experiment is to determine if there is a change in the distribution of products due to the addition of water. This will reflect the effect of higher radical concentrations caused by higher OH and H concentrations and will provide further insight to the mechanism of alcohol oxidation.

4.8 References

Abdel-Hamid, A.A., Z. Phys. Chem., Leipzig, 1972, 251, 72.

Ambartzumian, R.V., Chekalin, N.V., Letokhov, V.S., Ryabov, E.A., Chem. Phys. Letts., 1975, 36, 301.

Anderson, D., McAlpine, R.D., Evans, D.K., Adams, H.M., Chem. Phys. Letts., 1981, 79, 337.

Bialkowski, S.E., Guillory, W.A., J. Chem. Phys., 1977, 67, 2061.

Bialkowski, S.E., Guillory, W.A., J. Chem. Phys., 1978, 68, 3339.

Buenker, R.J., Olbrich, G., Schuchmann, H. P., Schurmann, B.L., von Sonntorg, C., J. Am. Chem. Soc., 1984, 106, 4362.

Danen, W.C., J. Am. Chem. Soc., 1979, 101, 1188.

Farkas, L., Hirshberg, Y., J. Am. Chem. Soc., 1937, 59, 2450.

Farkas, L., Hirshberg, Y., Sandler, L., J. Am. Chem. Soc., 1939, 61, 3394.

Fricke, H., Hart, E.J., J. Chem. Phys., 1936, 4, 418.

Garibyan, T. A., Mantashyan, A.A., Nalbandyan, A.B., Saakyan, A.S., Arm. Khim. Zh., 1971, 24, 13.

Greenhill, P.G., Gilbert, R.G., J. Phys. Chem., 1986, 90, 3104.

Hagege, J., Roberge, P.C., Vermeil, C., J. Chem. Soc., Faraday, 64, 3288, (1968); J. Chim. Phys., 1968, 65, 641.

Hagege, J., Leach, S., Vermeil, C., J. Chim. Phys., 1965, 62, 736.

Hagele, J., Lorenz, K., Rhasa, D., Zellner, R., Ber Bunsenge. Phys. Chem., 1983, 87, 1023.

Harrison, A.J., Lake, J.S., J. Phys. Chem., 1959, 63, 1489.

Hassinen, E., Koskikallio, J., Acta. Chem. Scand. A., 1979, 33, 625.

Herasymowyoh, O.S., Knight, A.R., Can. J. Chem., 1973, 51, 147.

Hoyermann, K., Loftfield, N.S., Sievert, R., Wagner, H. Cg., 18th Symp. (Intl.) Comb., 1981, 831.

Jackson, W.M., Halpern, J.B., Lin, C. S., Chem. Phys. Letts., 1978, 55, 254.

Kassab, E., Gleghorn, J.T., Evleth, E.M., J. Am. Chem. Soc., 1983, 105, 1746.

Kerr, J. A., O'Grady, B.V., Trotman-Dickenson, A.F., J. Chem. Soc. A., 1967, 897.

Mashi, M., Hess, P., Chem. Phys. Letts., 1981, 77, 541.

McAlpine, R.D., Evans, D.K., McClusky, F.K., J. Chem. Phys., 1980, 73, 1153.

Meier, U., Grotheer, H.H., Just, Th., Chem. Phys. Letts., 1984, 106, 97.

O'Grady, B.V., Ph.D. Dissertation, University of Wales, 1966.

Patat, F., Hoch, H., Z. Elektrochem., 1935, 41, 494.

Porter, R.P., Noyes, W.A., Jr., J. Am. Chem. Soc., 1959, 81, 2307.

Schmiedl, R., Meier, V., Welge, K.H., Chem. Phys. Letts., 1981, 80, 495.

Selwyn, L., Back, R.A., Willis, C., Chem. Phys., 1978, 36, 323.

Shiotani, M., Chachaty, C., Bull. Chem. Soc. Japan, 1974, 47, 28.

Terenin, A., Neujmin, H., J. Chem. Phys., 1935, 3, 436.

Warnatz, J., In "Combustion Chemistry.", Ed. W.C. Gardiner, Springer-Verlag, New York, 1984.

Yamabe, T., Koizumi, M., Yamashita, K., Tachibana, A., J. Am. Chem. Soc., 1984, 106, 2255.

Yee Quee, M.J., Thynne, J.C.J., J. Chem. Soc. Faraday Trans., 1966, 62,. 3154.

CHAPTER 5

The Theoretical Prediction of CH_3O and CH_2OH Gas Phase Decomposition Rate Coefficients

5.1 Introduction

As has been discussed in earlier chapters, the fate of CH_2OH and CH_3O are important in methanol reactions. In particular, the rate of the unimolecular dissociation of these radicals to CH_2O and H will have quite different significance in different temperature regimes. Experimentally, it is difficult to obtain rate data on the unimolecular reactions of radicals separated from the influence of other reactions which may in themselves be not well understood.

It is thus quite important to have a theory, whether it be ab initio or semi-empirical, capable of predicting these rate coefficients as an alternative to "guesstimating" them. There are two objectives to the work described here. They are: (i) to calculate the rates of the unimolecular decomposition reactions of CH_2OH and CH_3O

$$CH_2OH + M \quad \text{-----} > \quad CH_2O + H + M \qquad \text{R5.1}$$

$$CH_3O + M \quad \text{-----} > \quad CH_2O + H + M \qquad \text{R5.2}$$

and (ii) to set out precisely the method by which these calculations have been made with the ultimate aim of providing a technique for use by experimental kineticists which is relatively easy to use in the prediction of rate parameters for unknown reactions.

5.2 Theoretical Background

The thermal rate coefficient, k_{uni}, for a unimolecular reaction can be calculated from the solution of the integral eigenvalue master equation (Tardy, et al., 1977; Quack, et al., 1977; Holbrook, 1983)

$$-g(E)k_{uni} = w\int_o^\infty [P(E,E')g(E')-P(E',E)g(E)]dE' - k(E)g(E) \qquad 5.1$$

Here w is the collision frequency (Lennard-Jones or gas kinetic hard sphere), P(E,E') is the probability of collisional excitation from a state with internal energy, E' to one with energy E, g(E) is the eigenfunction and is the population of molecules with energy E, and k(E) is the microscopic rate coefficient at energy E.

The solution to equation 5.1 is readily obtainable given the values of k(E) and P(E,E') using a commercially available program (Gilbert, 1983a). The values of k(E) can be found using a reliable ab initio method. RRKM theory (Robinson and Holbrook, 1972) provides the following expression for the k(E)'s:

$$k(E) = \int_{E_o}^\infty \rho(E^+)dE \,/h\rho(E) \qquad 5.2$$

where h is Planck's constant and $\rho(E)$ and $\rho(E^+)$ are the density of states for the reactant and transition state respectively. E_o is the critical energy for the reaction.

The $\rho(E)$'s can be calculated easily using a standard program (Gilbert, 1983a) from molecular parameters of the reactants and transition state. These parameters are the vibrational frequencies, moments of inertia of any free or hindered internal rotors (with a specification of the hindrance in the latter case), the overall moment of inertia and the symmetry number.

The rotational degrees of freedom may also need to be separated into active (along the reaction coordinate) and inactive (Robinson, et al., 1972; Forst, 1973; Troe, 1977).

The required parameters can be obtained from spectroscopic, ab initio, or thermodynamic data. The problem to be treated when applying the theory is to describe the transition state and its parameters. It must be chemically and physically reasonable if the theoretical prediction is to have any credence. The critical energy, E_o, can be estimated from tabulated thermochemical data (Benson, 1976) and for multi-centre activated complexes, reliable semi-empirical estimates for the parameters of the transition state are available (Benson, 1976). If necessary, the same procedures can be applied to the reactants.

For the reactions considered here, the transition states are similar simple fission activated complexes. The procedures for such activated complex calculations are less well defined and a method is described here that is believed to be adequate for such reactions.

A number of techniques for calculating the $k(E)$'s for simple fission activated complexes have been developed and the simplest approach has been chosen . Gorin (1927) placed the activated

complex at the top of a centrifugal (rotational) barrier. Benson (1976) has semi-empiricised this by comparison with a large body of data and thus, while not being entirely suitable for every specific case, the generalisation to many systems should overcome many of the physical and mathematical deficiencies and provide k(E)'s of acceptable acuracy for modelling in the combustion regime (where these reactions will be important).

This model has a theoretical basis which has been proven to be incorrect (Garrett, et al., 1979; Rai, et al., 1983; Bunker, et al., 1968; Hase, 1976; Greenhill, et al., 1986; see also chapter 7). Alternative, rigorous procedures to the Gorin model have been developed based on variational techniques (Greenhill, et al., 1986; Quack, et al., 1974, 1975; Troe, 1981; Cobos, et al., 1985). These techniques place no constraints on the nature of the activated complex except that the dynamical equations are obeyed and the variational criterium must select the activated complex(es). However, these procedures are in general more complex and time consuming to apply than the Gorin model and one of the aims of this work was to produce a readily implemented method for reactions with simple fission transition states. The Gorin model has been chosen for this reason.

5.3 The Gorin Model Assumptions

The assumptions used in the Gorin model to specify k(E) for the two reactions considered here are described below. The critical energy for the dissociation is the sum of the difference in zero-point energies of products and reactants, ΔH^{o}, and any barrier to the reverse reaction; that is, the recombination. The only data available for the recombination reaction is for the isoelectronic system, $H+C_2H_4$. Evidence suggests that this reaction has a barrier to recombination of 8kJ mol^{-1} (Hase,, et al., 1982; Sugawara, et al., 1981). We choose this value plus ΔH^{o} for each reaction giving 121.3kJ mol^{-1} and 100.4kJ mol^{-1} for R5.1 and R5.2 respectively.

The transition state is made up of the two free or hindered rotors (A and B) with vibrational frequencies of the separated moieties A and B. That is, the two portions of the molecule AB are assumed to form a pair of free or hindered rotors depending on their separation. In the case of reactions R5.1 and R5.2, moiety A is CH_2O (whose vibrational frequencies and moments of inertia are well-known), and moiety B is an H atom; the vibrational frequencies and geometries of the reactants (CH_2OH and CH_3O) are available from spectra and from ab initio calculations (see Table 5.1). The vibrational frequencies for the reactants and activated complexes involved in the present systems are listed in Table 5.1.

In addition to the vibrational frequencies, there are some degrees of freedom in the activated complex (corresponding to

deformation modes in the parent AB molecule) which are treated as 2-dimensional hindered rotors. If either A or B is an atom (as is the

Table 5.1 RRKM Parameters For Reactions R6.1 and R6.2

CH_2OH (A) and Transition State (C) (Reaction R5.1)						
Frequencies (cm^{-1}) (A)	Frequencies (cm^{-1}) (C)	Rotations	B values (cm^{-1}) (A)		B values (cm^{-1}) (C)	
3650	2977	ext. inactive	0.944	(2,2)	0.755	(2,2)
2960	2844	ext. active	6.470	(1,1)	2.583	(1,1)
2883	1744	internal			7.093	(2,2)
1459	1280					
1334	1160					
1183	1503					
1048						
569		θ = 88.0 degrees				
420		E_o = 121.3 kJ mol^{-1}				

CH_3O (A) and Transition State (C) (Reaction R5.2)						
Frequencies (cm^{-1}) (A)	Frequencies (cm^{-1}) (C)	Rotations	B values (cm^{-1}) (A)		B values (cm^{-1}) (C)	
3320	2977	ext. inactive	0.876	(1,2)	1.317	(1,2)
3311	2844	ext. active	5.495	(1,1)	0.745	(2,1)
3216	1744	internal			110.0	(2,2)
1657	1280					
1599	1160					
1582	1503					
1159						
1064		θ = 71.1 degrees				
717		E_o = 100.4 kJ mol^{-1}				

case in the systems studied here), one has a single two-dimensional rotor to consider (whose moment of inertia I_r is determined from individual components I_a and I_b as shown below); if both are polyatomic, one has instead two two-dimensional internal rotors with moments of inertia I_a and I_b.

In the Gorin model, the bond broken has in the activated complex, a length r^+ separating the two moieties whose value is taken to be the bond length at the centrifugal barrier to recombination. A number of methods for estimating r^+ are available (Troe, 1977; Benson, 1976; Benson, 1983). We adopt here the recipe of Benson (1983) which (although obtained using dubious arguments) has been chosen to give agreement with extensive data and should thus be adequate for the present purpose. In this model, r^+ is taken to be 2.8 times the normal bond length. It should be noted that the preferred (but more involved) microcanonical variational transition state theory yields an r^+ which is a function of E (or, in the canonical version, a function of temperature); for reasons explained above, we ignore this refinement here.

The moments of inertia of the two-dimensional hindered rotors whose motion corresponds to the AB deformations are found by allowing the separate A and B moieties to bend until the two come into van der Waals contact. One defines (Benson, 1976) the angle as that subtended when these moieties so bend. The equivalent solid angle $\Delta\Omega$ is given by

$$\Delta\Omega/4\pi = (1-\cos\theta)/2 \qquad 5.3$$

This factor which takes the hindrance into account is then used to adjust the moment of inertia of the internal rotor(s) by replacing the moment of inertia of the free rotor (I) by $(\Delta\Omega/4\pi)I$.

If we have a transition state of the form:

A-------B,

then both moieties have three principal moments of inertia I_a, I_b and I_c values associated with them such that the two (I_a and I_b) corresponding to the two-dimensional internal rotation about the symmetry axis are identical (or very similar) and the other (I_c) is different. For the case where one of A or B is an atom (as in the systems studied here), the two-dimensional moment of inertia for the free internal rotation is replaced by the reduced moment, I_r, where

$$I_r = I_A I_B/(I_A+I_B) , \qquad 5.4$$

where (if B is the monatomic species) I_A is the moment of top A about its symmetry axis and I_B is the moment of B about the centre of mass of A. Specific illustrations have been given elsewhere (Benson, 1976). The hindrance [i.e., the angle θ in equation 5.3] can be obtained from the hard-sphere geometries analytically or by using solid models. All moments of inertia were calculated exactly from the experimental or ab initio geometries. They are listed in Table 5.1 (where the factor $\Delta\Omega/4\pi$ is included in all I), along with the values of θ.

Finally, in considering the rotational degrees of freedom, it is important to note in cases such as the present (where there is a large difference in the moments of inertia of parent molecule and activated complex) that one of the external moments of inertia is "active", i.e., that it must be treated as an internal degree of freedom; this is simply because (Troe, 1977) the K quantum number in rotation is not conserved in a non-rigid molecule, but can exchange energy with the vibrational degrees of freedom. I_c, the moment of inertia of the overall rotation (of molecule and of activated complex) corresponding to this quantum number is identified as that one of the three external moments of inertia which is not equal to (or well separated from) the other two.

The values for the various rotational degrees of freedom for the systems under study are listed and explained in Table 5.1. This completes the specification of the k(E).

5.4 Collisional Energy Transfer

The only remaining parameter that we need to specify for the model is the energy transfer probability function P(E,E'). The magnitude of the average energy transferred per collision will affect the fall-off behaviour of the reaction and consequently we need appropriate estimates of this parameter.

Note also that the strong collision approximation is not an adequate description in nearly all cases and it is much preferable to use the weak collision model. This is easily achieved with the

programs of Gilbert (1983a), and the ease of implementation is such that there is no reason why all such calculations should not use this technique.

There are several approaches to calculating the value of the average energy transferred per collision, $\langle \Delta E \rangle$. We can estimate it from similar molecules in similar bath gases, but this is not generally reliable.

Recently, considerable effort has been invested in producing a theory for prediction of the form and parameters of P(E,E') (Gilbert, 1984; Lim, et al., 1986). This has taken a semi-empirical form (Gilbert, 1984) and an a priori form (Lim, et al., 1986) and has been successful in reproducing experimental data within the reliability estimates of the data. However, this is not yet universally available for use.

The final way is to fit the fall-off data of a similar experiment with an appropriate form of P(E,E') and value of $\langle \Delta E \rangle$. Fortunately, extensive data compilations indicate that small changes in the reactant such as loss of an hydrogen atom have little effect on the energy transfer parameters (Tardy, et al., 1977; Quack, et al., 1977; Greenhill, et al., 1986b). So energy transfer parameters which are suitable for CH_3OH should also be suitable for the radicals CH_3O and CH_2OH and data obtained from experimental work on CH_3OH (Spindler, et al., 1982) has been used for CH_3O and CH_2OH.

Further work on energy transfer has also indicated that the pressure dependence of k_{uni} depends, not upon the complete

functional form of P(E,E'), but on only one measure of this (Troe, 1977; Gilbert, et al., 1983; Gilbert, 1983b). The most convenient measure is the average downward energy transferred $\langle \Delta E_{down} \rangle$ (Gilbert, 1983b).

$$\langle \Delta E_{down} \rangle = \int_o^{E'} (E'-E)\ P(E,E')\ dE / \int_o^{E'} P(E,E')dE \qquad 5.5$$

Because of this insensitivity to the functional form of P(E,E'), we can choose any convenient form for it such as exponential down or gaussian down. This can then be used to obtain the value of $\langle \Delta E_{down} \rangle$ by fitting the fall off data at appropriate temperatures.

The data of Spindler, et al., (1982) has been fitted in this way using the model described here but choosing the value of r^+ to reproduce their reported high pressure parameters. Note that the value of $\langle \Delta E_{down} \rangle$ obtained is independent of the products of the reaction. The value of $\langle \Delta E_{down} \rangle = 750 cm^{-1}$ for the temperature range 1600-2000K was obtained in this way for collision with Ar.

The reasonableness of this value needs to be determined before calculations are performed using it. No prior data for methanol are available but methyl isocyanate has a $\langle \Delta E_{down} \rangle = 500 cm^{-1}$ at 500K with He as a bath gas (Tardy, et al., 1977). Methyl isocyanate has a lower average vibrational energy and a higher dipole moment and consequently its collisions can be expected to both be more oriented and less able to transfer energy than methanol. If two systems have the same overall collision rate, then the collisions in the system

with the larger attractive force will have a smaller value of $\langle \Delta E_{down} \rangle$, as the orientation will be more defined as so fewer vibrational modes will be 'exposed' to the collision partner. (Gilbert and McEwan, 1985)

Application of the biased random walk model for P(E,E') of Lim and Gilbert (1986) predicts a value of $\langle \Delta E_{down} \rangle = 1100 cm^{-1}$ for methanol. This value is quite high but the theory is not quantitative for molecules with less than about 16 degrees of freedom. A value of 750 cm^{-1} for $\langle \Delta E_{down} \rangle$ would thus appear to be quite reasonable at 2000K.

At other temperatures of interest predictions of $\langle \Delta E_{down} \rangle$ are also necessary. Hippler, et al., (1985) have found that the temperature dependence of $\langle \Delta E \rangle$, the overall average energy transferred per collision, is quite small. Brown, et al., (1983) have determined that the temperature dependence of $\langle \Delta E_{down} \rangle$ is small and corresponds roughly to a $T^{1/2}$ dependence. Assuming this temperature dependence in the form

$$\langle \Delta E_{down} \rangle = 750 \ (T/2000)^{1/2} \ cm^{-1} \qquad 5.6$$

then a calculated value of approximately 200 cm^{-1} for $\langle \Delta E \rangle$ was obtained at all temperatures between 300 and 2000K. Equation 5.6 gave values of $\langle \Delta E_{down} \rangle$ (cm^{-1}) of 290 at 300K, 410 at 600K, 530 at 1000K and 750 at 2000K. These values were used for both CH_2OH and CH_3O as they were expected to be suitable as discussed previously.

5.5 Results

The calculations were carried out for the temperature range 300 - 2000K, and the pressure range 10^2 - 10^6 Pa (ca. 1 - 10^4 Torr), these covering the range of interest in practical systems. Results of the calculations are given in Table 5.2, as follows. (i) The high-pressure Arrhenius parameters for reactions R5.1 and R5.2 (given as the value at the intermediate temperature of 1000K, the temperature dependence of the Arrhenius parameters being insignificant). (ii) The low-pressure Arrhenius parameters for reactions R5.1 and R5.2, expressing the low-pressure rate coefficient as $k_0 = A_0 \exp(-E_A/RT)$ (these are given as separate Arrhenius parameters for each of the temperature ranges 300 - 600K, 600 - 1000K and 1000 - 2000K, since as is well known, the low-pressure limiting rate cannot be accurately represented by an Arrhenius form over a very wide temperature range). (iii) For representative temperatures, the pressure at which the rate coefficient assumes half of its high-pressure value ($p_{1/2}$), and various quantities summarizing the fall-off behaviour (described below). Fall-off curves are given in Figs. 5.1 and 5.2 for all temperatures. The predicted values for the high-pressure A factors are similar to those reported (Hase, et al., 1982; Sugawara, et al., 1981) for the thermal decomposition of C_2H_5, which supports the physical reasonableness of the computations.

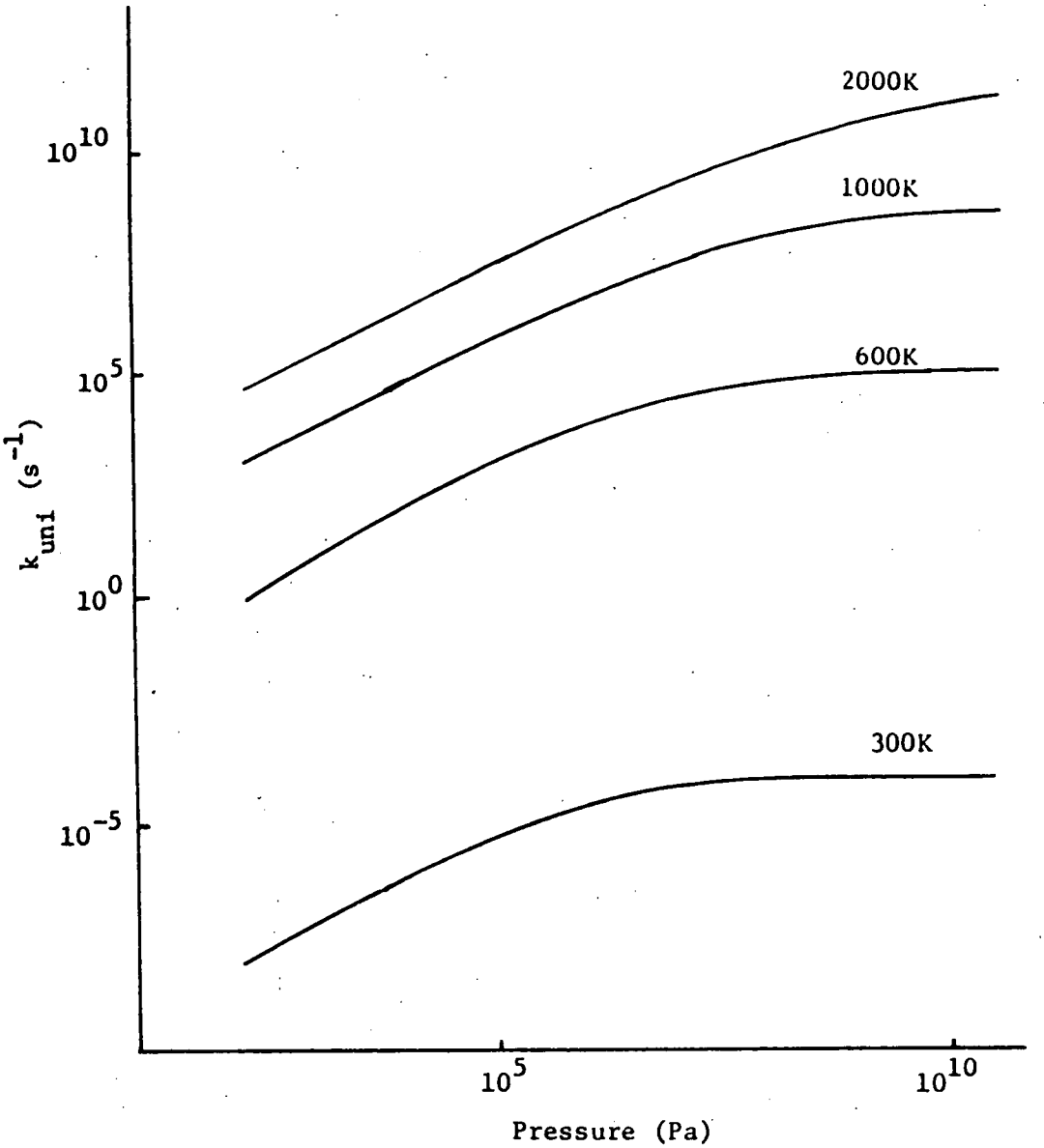

Figure 5.1 Fall-off Curves for the Unimolecular Dissociation of Methoxy Radical

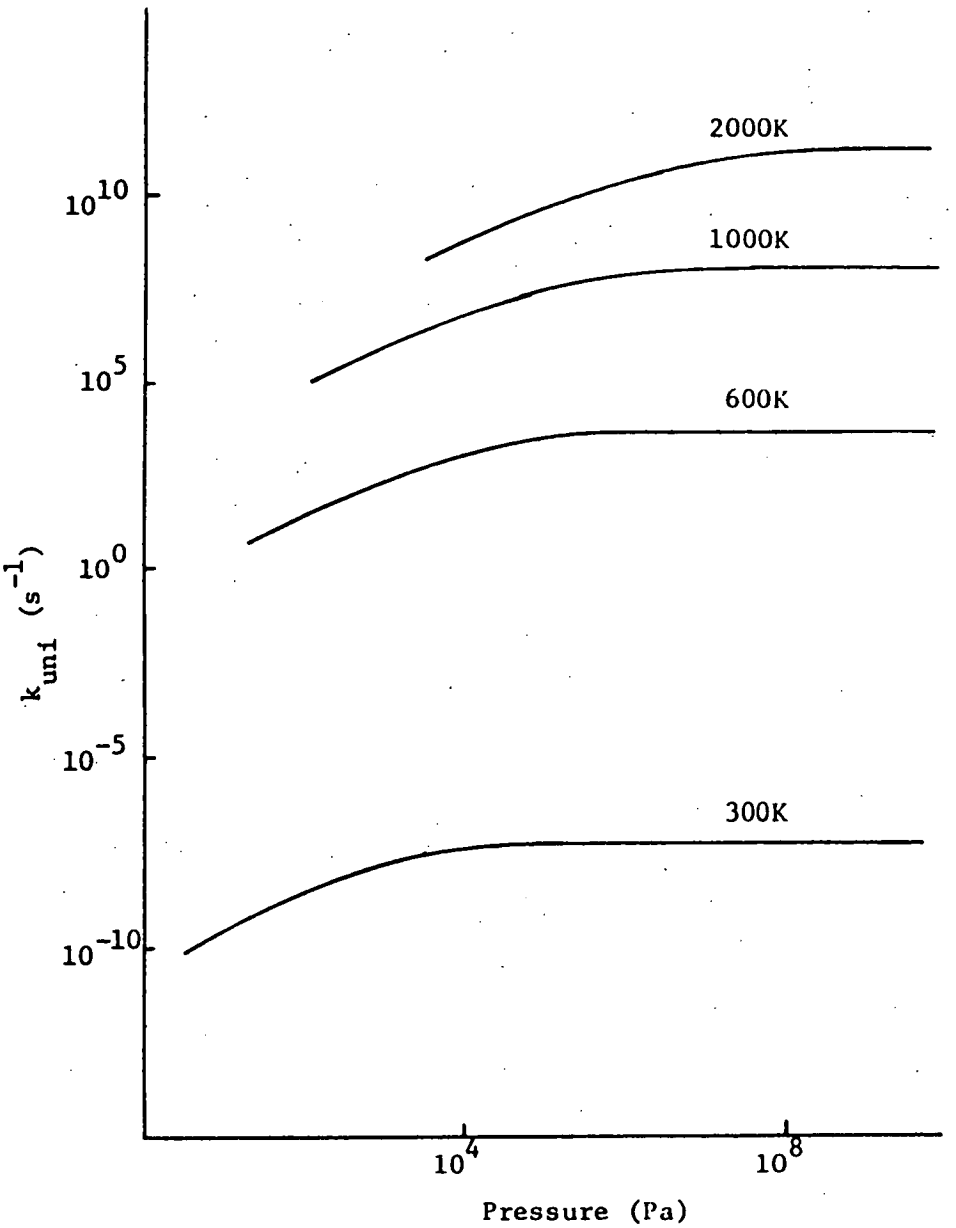

Figure 5.2 Fall-off Curves for the Unimoleclar Dissociation of the Hydroxymethyl Radical.

At a given temperature, the pressure dependences of the rate coefficients as obtained by the solution of the master equation (such as those shown in Figs. 5.1 and 5.2) can be most compactly summarized as follows (Troe, 1979; Gilbert, et al., 1983). One defines the dimensionless "Lindemann-Hinshelwood" factor F_{LH} at each pressure by:

$$F_{LH} = (k_0[M]/k^{\infty}) \; / \; (1 + k_0[M]/k^{\infty}) \qquad 5.7$$

where [M] is the concentration of bath gas at that pressure, k_0 the (second-order) low-pressure limiting rate coefficient, and k the high-pressure limiting rate. It has been shown (Gilbert, et al., 1983) that the unimolecular rate coefficient at any pressure, as obtained by exact solution to the master equation can be approximated by:

$$k_{uni}/k^{\infty} = F_{LH} \, F \qquad 5.8$$

where the dimensionless "combined broadening factor" F at any pressure is given by:

$$\log F(k') = \frac{\log F_{cent}}{1 + \left[\frac{\log(k') + c}{N - d\{\log(k') + c\}}\right]^2} \qquad 5.9$$

where the parameters c, N and d are given by:

$c = -0.4 - 0.67 \log F_{cent}$, $N = 0.75 - 1.27 \log F_{cent}$, $d = 0.14$

and $k' = k_0[M]/k^{\infty}$ (i.e., k' is a dimensionless pressure).

Table 5.2 Calculated Rate Parameters.

$CH_2OH \text{ ---> } CH_2O + H$

High Pressure $k_{uni}(T) = 10^{14.5}\exp(-14915K/T)$

Fall-off and Low Pressure Regime

T	p(1/2)	β_c	F_{cent}	A_o	E_a
K	Pa			$cm^3 s^{-1}$	kJ mol^{-1}
300	4.0×10^5	0.19	0.78		
				$10^{-6.3}$	119
600	2.3×10^6	0.16	0.63		
				$10^{-7.4}$	106
1000	1.6×10^6	0.10	0.55		
				$10^{-8.8}$	79
2000	4.2×10^8	0.04	0.50		

Table 5.2 cont.

CH_3O ---> CH_2O + H

High Pressure $k_{uni}(T=1000K) = 10^{14.5}\exp(-12990K/T)$

Fall-off and Low Pressure Regime

T	p(1/2)	β_c	F_{cent}	A_o	E_a
K	Pa			cm^3s^{-1}	kJ mol^{-1}
300	$3.7x10^6$	0.24	0.73		
				$10^{-7.4}$	98
600	$3.4x10^7$	0.16	0.64		
				$10^{-8.1}$	90
1000	$3.0x10^8$	0.10	0.55		
				$10^{-9.2}$	70
2000	$7.3x10^9$	0.06	0.48		

F_{cent} is given by the product of the strong and weak collision broadening factors F^{sc} and F^{wc}. The values of F_{cent} for each temperature [determined from exact numerical solution of equation 5.1] are given in Table 5.2. The value of k_{uni} (and hence k_{rec}) at any pressure may be explicitly calculated from equations 5.7-5.9. If required, these expressions can be used to calculate apparent Arrhenius parameters at any given pressure.

A further useful quantity to examine is the collision efficiency. For a given unimolecular reaction, one defines the collision efficiency β_c as the ratio of the true low-pressure

limiting rate [from solution of equation 5.1 in the low-pressure limit] to that calculated from the strong collision formula; the values of β_c are given in Table 5.2 for representative temperatures. Note that the value of β_c is not actually required in evaluating k_{uni} at any given pressure using eqs. 5.7-5.9; values of β_c are merely given in Table 5.2 for comparison purposes.

5.6 Discussion.

5.6.1 Unimolecular Dissociation of Methoxy

The decomposition of the methoxy radical is predicted to be in the fall-off regime over the entire range for which calculations were performed, i.e, from 300 to 2000K at pressures between 10^2 to 10^6 Pa (0.75 - 0.75x10^4 Torr). Over the range 1000 - 2000K and 10^3 - 10^5 Pa, the apparent activation energy (as determined from the slope of an Arrhenius plot at a fixed pressure) did not show significant variation (from 61.3 to 61.0 kJ mol^{-1}); however, the calculated apparent A factors at a given pressure varied from 2x10^7 to 2x10^9 s^{-1}. The most significant result is that the calculated rate coefficients at elevated temperatures are significantly higher than those used by Westbrook and Dryer (1979): for example, at 1000K and 1.3x10^5 Pa (10^3 Torr), the difference is a factor of 70. Some Arrhenius plots comparing the rate coefficients as used by Westbrook and Dryer and those calculated here at 1.3x10^5 Pa are shown in

Figure 5.3; this pressure is typical of that used in the modelling studies by Westbrook and Dryer.

The high pressure activation energy obtained from the RRKM calculation is 108 kJ mol^{-1} at 1000K. The apparent activation energies calculated from the fall-off data will of course be less than this because of the depletion in the populations of the energy states close to the critical energy (Gilbert and Ross, 1972); that is, the highest energy states below the critical energy have severely non-equilibrium populations. This effect is greatest for small collision efficiencies. At 1000K, the collision efficiency is 0.10, and at 2000K this falls to $\beta_c = 0.05$. It is obvious that in modelling studies fall-off behaviour must be taken into account for these dissociations.

5.6.2 Unimolecular Dissociation Of Hydroxymethyl

Similar comments apply to the results for the dissociation of the hydroxymethyl radical. The apparent activation energies at the different pressures are up to 40 kJ mol^{-1} below the high pressure activation energies, and show a strong temperature dependence. The collision efficiencies are also very low, β_c having values at 1000K of 0.11, and at 2000K, $\beta_c = 0.06$. As before the results indicate a very large difference between our calculated values and the rate parameters used by Westbrook and Dryer. Figure 5.4 compares the rate coefficients at 1.3×10^5Pa from the present calculations and from Westbrook and Dryer, (1979), in an Arrhenius plot.

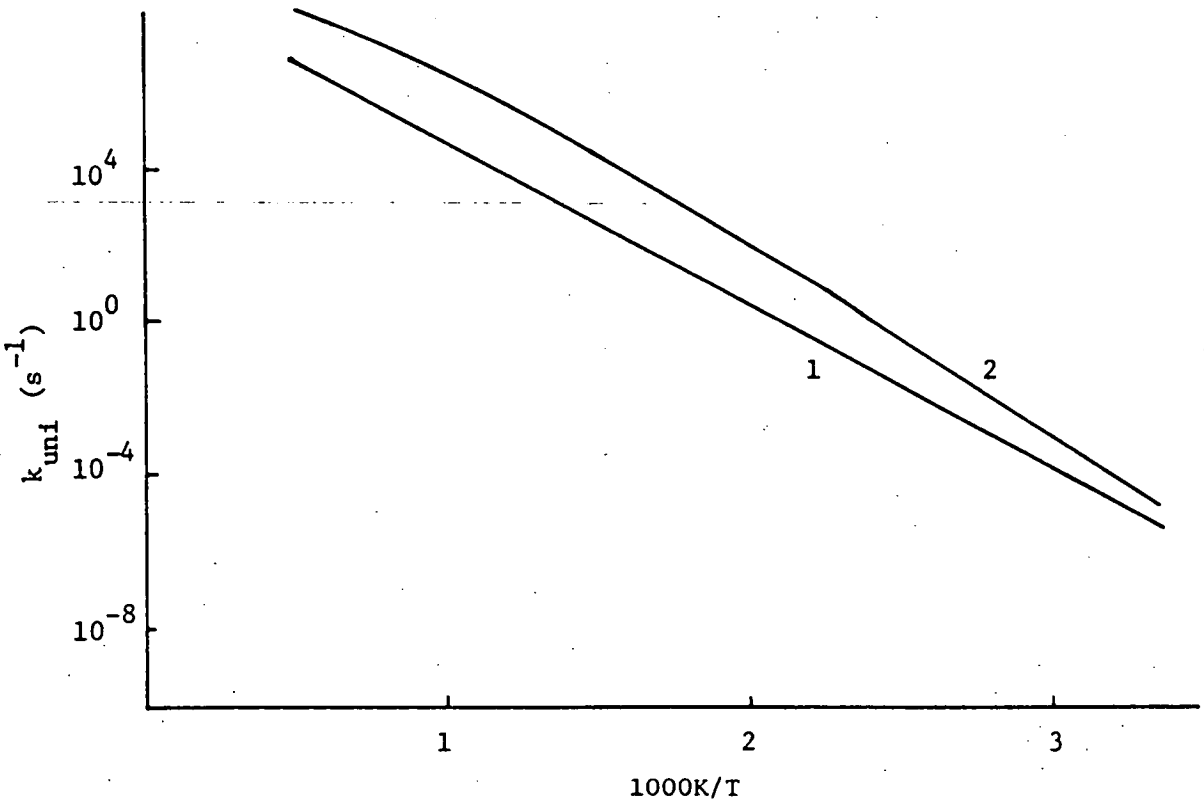

Figure 5.3 Arrhenius Plots of CH_3O Dissociation at 1.3×10^5 Pa. (1) Westbrook and Dryer (2) This Work.

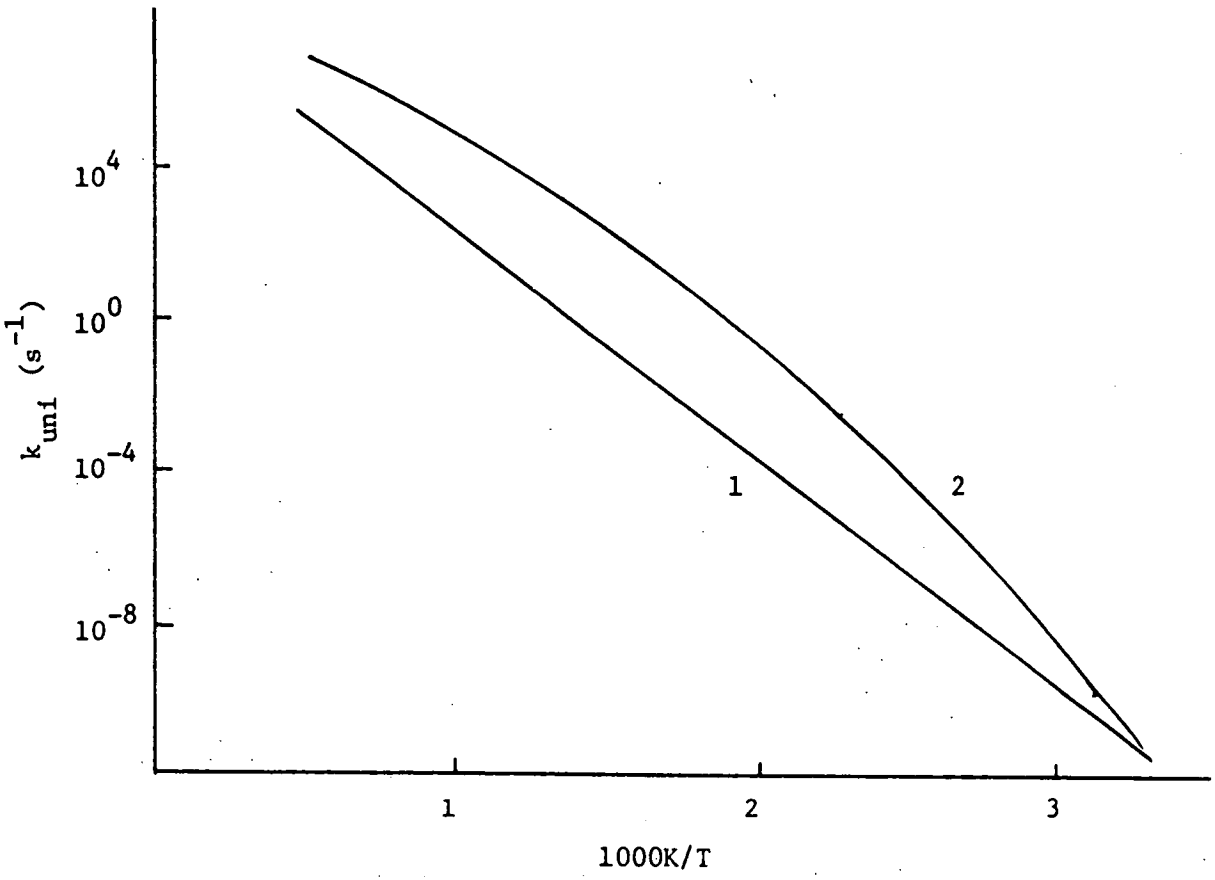

Figure 5.4 Arrhenius Plot of CH_2OH Dissociation at 1.3×10^5 Pa.

(1) Westbrook and Dryer

(2) This Work.

5.7 Conclusions

Some ab initio estimates of the rates of some reactions which are likely to be important in both high temperature oxidation of methanol and the systems used in the study of the elementary kinetics of methanol have been made. RRKM theory and solution of the master equation have enabled us to examine the validity of some rate coefficients currently in use (Westbrook and Dryer, 1979); our studies show that these earlier values are likely to be quite incorrect. Fall-off effects play an important role in the values of their rate coefficients at commonly-used pressures and temperatures.

An important area for future work is to employ the rate parameters generated in this theoretical study in modelling studies of the type pioneered by Westbrook and Dryer.

5.8 References

Benson, S.W., "Thermochemical Kinetics", 2nd Edn., Wiley, New York, 1976.

Benson, S.W., Canad. J. Chem., 1983, 61, 881.

Brown, T.C., Taylor, J.A., King, K.D. and Gilbert, R.G., J. Phys. Chem., 1983, 87, 5214.

Bunker, D.L., Patengill, M., J. Chem. Phys., 1968, 48, 772.

Cobos, C.J., Troe, J., J. Chem. Phys., 1985, 83, 1010.

Forst, W., "Theory of Unimolecular Reactions", Academic Press, New York, 1973.

Garett, B.C., Truhlar, D.G., J. Am. Chem., Soc., 1979, 101, 4534.

Gilbert, R.G., Quantum Chemistry Program Exchange, 1983a, 3, 64.

Gilbert, R.G., Chem. Phys. Letts., 1983b, 96, 259.

Gilbert, R.G., Luther, K. and Troe, J., Ber. Bunsenges. Phys. Chem., 1983, 87, 169.

Gilbert, R.G. and McEwan, M.J., Aust. J. Chem., 1985, 38, 231.

Gilbert, R.G. and Ross, I.G., J. Chem. Phys., 1972, 57, 2299.

Gilbert, R.G., J. Chem. Phys., 1984, 80, 5501.

Gorin, E., J. Chem. Phys., 1939, 7, 263, 642.

Greenhill, P.G., O'Grady, B.V., Gilbert, R.G., Aust. J. Chem., 1986a, 39, 1929.

Greenhill, P.G., Gilbert, R.G., J. Phys. Chem., 1986b, 90, 3104.

Hase, W.L., J. Chem. Phys., 1976, 64, 2442; idem., Acc. Chem. Res., 1983, 16, 258.

Hase, W.L., Schlegel, H.B., J. Phys. Chem., 1982, 86, 3901.

Hippler, H., Lindemann, L., Troe, J., J. Chem. Phys., 1985, 83, 3906.

Holbrook, K.A., Chem. Soc. Reviews, 1983, 12, 163.

Lim, K.F., Gilbert, R.G., J. Chem. Phys., 1986, 84, 6129.

Quack, M. and Troe, J., in "Gas Kinetics and Energy Transfer", vol. 2, p 175, Eds. P.G. Ashmore and R.J. Donovan, The Chemical Society, London, 1977.

Quack, M. and Troe, J., Ber. Bunsenges. Phys. Chem., 1974, 78, 240; 1975, 79, 170.

Rai, S.N., Truhlar, D.G., J. Chem. Phys., 1983, 79, 6046.

Robinson, P.J. and Holbrook, K.A., "Unimolecular Reactions", Wiley, London, 1972.

Spindler, K. and Wagner, H.Gg., Ber. Bunsenges. Phys. Chem., 1982, 86, 2.

Sugawara, K., Okazaki, K., Sato, S., Bull. Chem. Soc. Japan, 1981, 54, 2872.

Tardy, D.C. and Rabinovitch, B.S., Chem. Rev., 1977, 77, 369.

Troe, J., J. Chem. Phys., 1977a, 66, 4758.

Troe, J., J. Chem. Phys., 1977b, 66, 4745.

Troe, J., J. Phys. Chem., 1979, 83, 114.

Troe, J., J. Chem. Phys., 1981, 75, 226.

Westbrook, C.K. and Dryer, F.L., Combustion Science and Technology, 1979, 20, 125.

Chapter 6.

Recombination Reactions: Variational Transition State Theory and The Gorin Model.

6.1 Introduction.

The formulation of predictive theories is always a subject for intensive research in chemistry and physics and this is particularly so in the area of chemical dynamics. The use of kinetic modelling in this work has required the inclusion of rate constants which are not well known and to date have only been estimated.

The mechanism for methanol combustion developed from experimental studies performed here and by other workers (Meier, et al. 1984; Hagele, et al. 1984) contains aproximately twenty reactions which could be expected on theoretical grounds to have no barrier to reaction. That is, the potential energy associated with the reaction is due only to the change in enthalpy. These reactions are usually simple fission reactions of stable molecules to two radicals and the reverse of these, the recombination of two radicals to form a stable molecule.

In this case, the reactions of interest are the following;

$$H + CH_2OH \text{ -----> } CH_3OH$$

$$H + CH_3O \text{ -----> } CH_3OH$$

These will be important at lower temperatures where there are significant concentrations of hydrogen atoms and even at considerably higher temperatures. (Hoyermann, et al. 1981a,b). As well as these reactions for which there is no direct experimental work, the recombination of CH_3 radicals

$$CH_3 + CH_3 \text{ -----> } C_2H_6$$

has been studied. This has been recently reinvestigated (Macpherson, et al. 1985) and should provide a good first test of any theory.

To provide us with these rate constants work has been performed in the area of the prediction of termolecular recombination rate constants using variational transition state theory (VTST). (Garrett and Truhlar, 1984). A new technique for the estimation of these rate coefficients has been developed using VTST, the Gorin model, (Gorin, 1939) and elements of the statistical adiabatic channel model. (Quack and Troe, 1974; 1975; Troe, 1981). It has been tested on the recombination of methyl radicals and used to predict the rates of recombination of methoxy and hydroxymethyl radicals with hydrogen atoms.

This chapter consists of the following sections. In sections 6.2 and 6.3 brief derivations of conventional transition state theory and micricanonical transition state theory in its RRKM form will be given. Section 6.4 provides a simple explaination of the relationship between k_{ter} and k_{uni}, and how microscopic reversibility allows us to obtain a simple way of calculating k_{ter} from k_{uni}. Section 6.5 describes how the Gorin model has been applied physically to the calculations described.

Section 6.6 describes the technique developed here for calculation of the recombination rate coefficients by both canonical and microcanonical treatments. Section 6.7 tabulates the parameters and results of the calculations for the three reactions specified. The results are discussed and compared with experiment where possible in section 6.8.

6.2 Transition State Theory.

The most rigorous and dynamically correct theory of reaction rates is transition state theory. The assumptions inherent in the theory are the most well defined of any of the rate theories and have been rigorously tested. (Pechukas, 1982; Truhlar, Hase, Hynes, 1983)

The use of the theory requires that we be able to define an n-1 dimensional surface in the n dimensional phase space which defines the molecular potential surface, such that trajectories which reach this surface cross it only once and do not return to the reactant region.

The rate constant is essentially the convolution of this surface with the total number of trajectories possible on the molecular potential surface.

In early applications of the theory (Laidler and King, 1983, and references therein), the dividing surface or transition state was usually at some fixed value of the coordinates used to describe the potential energy surface (usually curvilinear). This resulted in overestimation of the rate constant as it was not possible to distinguish those trajectories which recross the surface from those which crossed only once. This led to the development of counting schemes which attempted to minimise the effect of multiple counting of trajectories.

The problems associated with the positioning of the transition state also depend upon the reactive system being investigated. Bimolecular processes in general have well defined energy barriers between reactants and products. This naturally creates a bottleneck in the phase space at which the transition state barrier is generally placed. Conceptually this is correct and reasonable, however it still leads to overestimation of the rate due to overcounting and tunnelling effects. Some progress has been made in the development of quantum theories which attempt to overcome these problems. (Miller, Schwartz, and Tromp, 1983; Bowman, Ju, and Lee, 1982; Truhlar, Isaacson, Skodje, and Garrett, 1982; Garrett, and Truhlar, 1979a).

These problems apply also to those types of unimolecular reaction such as rearrangements which have significant energy barriers. The position of the transition state surface is intuitively obvious but once again rate constants are predicted to be too large.

For systems where there is no definable energy barrier such as in recombination reactions or their reverse, unimolecular dissociations with a "simple fission" mechanism, and some ion-molecule reactions, the problem is greater as there is no intuitive position in which to place the barrier.

This has been overcome by the introduction of a variational criterium. (Garrett, and Truhlar, 1984, 1979b; Rai, and Truhlar, 1983; Truhlar, and Isaacson, 1982). The greatest problem with the theory is that the rate is always overestimated, so our object is always to minimise the calculated rate coefficient. To do this we

must define those properties which enable the calculation to be performed and also decide on a strategy for the solution of the problem in terms of the nature of the system. Two approaches are available which obtain results from reasonable models. They are the canonical and microcanonical treatments.

There are two distinct ways in which we may derive the conventional Transition State Theory (TST) formula. The first and the original technique was based on an equilibrium assumption between reactants and the activated complex. (Eyring, 1935, 1938; Glasstone, Laidler, and Eyring, 1941) This has several versions in which the reaction coordinate has been treated as either a vibration or as a translation. The result is the same in either case.

The second technique is derived from classical mechanics (Mahan, 1974; Miller, 1976; Garrett, and Truhlar, 1979c; Smith, 1980) and is the one that we will follow here as it is consistent with the treatment in the next section on the derivation of microcanonical transition state theory (μTST) or RRKM (Rice-Rampsperger-Kassel-Marcus) theory.

Statistical mechanics provides the Boltzmann distribution to describe the probability distribution of molecules with different energies in an ensemble.

$$\frac{n_i}{n} = \frac{g_i e^{-\varepsilon_i/kT}}{\sum_i g_i e^{-\varepsilon_i/kT}} \qquad 6.1$$

The fundamental assumption here is that all molecules with the same energy are equally probable in an ensemble. The denominator is the partition function and we shall see that it is of fundamental importance in the expression of TST.

The classical equivalent of this probability is that all elements of equal volume of the phase space described by the position, q, and the momentum, p, of particles in the classical system have an equal probability of containing a phase space point. If there are N particles in the system then there are 6N coordinates which must be specified and the phase space element corresponding to these is

$$d\tau_{6N} = dq_1 \cdots\cdots dq_{3N} dp_1 \cdots\cdots dp_{3N}$$

(using the notation of Smith, 1980). The probability is then

$$d^{6N}P = \frac{\exp(-H/kT)\, d\tau_{6N}}{\int \exp(-H/kT)\, d\tau_{6N}} \qquad 6.2$$

Comparison of the denominators of 6.2 and 6.1 indicate that the phase space integral and the partition function are analogous quantities, however, they are dimensionally incompatible. The partition function is a number and the units of the phase integral are (length x momentum)^{3N}. It has been shown that the ratio of the phase integral to the partition function is h^{3N}. This results in exact correspondence between 6.1 and 6.2 and may be expressed explicitly as

$$d^{6N}P = \frac{\exp(-H/kT)\, d\tau_{6N}/h^{3N}}{\int \exp(-H/kT)\, d\tau_{6N}/h^{3N}} \qquad 6.3$$

We now consider the equilibrium constant in terms of the partition functions and the phase space integrals.

The equilibrium constant in terms of concentrations is

$$K_c = \frac{\prod_i [\text{Product}]_i}{\prod_i [\text{Reactant}]_i} \qquad 6.4$$

Now the total number of particles in a system, $\sum_i n_i$, is given by

$$\sum_i n_i = \prod_i [\text{Species}]_i V \qquad 6.5$$

where V is the total volume.

Also the equilibrium constant can be specified in terms of the Σn_i,

$$K_c = \frac{\Sigma n_{i,\text{Products}}}{\Sigma n_{i,\text{Reactants}}} = \frac{\Pi\Sigma\, g_i \exp(-\varepsilon_i/kT)}{\Pi\Sigma\, g_i \exp(-\varepsilon_i/kT)} \qquad 6.6$$

or as the product of the partition functions for each species. Furthermore, by dividing by the volume we get the following for K_c

$$K_c = \frac{\Pi\,(Q_j/V)}{\Pi\,(Q_i/V)} . \exp(-\Delta\varepsilon_o/kT) \qquad 6.7$$

where the Q_i and Q_j are the partition functions for the reactants and products respectively, and $\Delta\varepsilon_o$ is the difference between the zero point energies of the products and reactants.

We now return to equation 6.3 and consider the probability of finding the system in a volume of phase space lying on a dividing surface S^*.

$$d^{6N}P^* = \frac{\exp(-H/kT)\, d\tau_{6N}/h^{3N}}{\int^{S^*} \exp(-H/kT)\, d\tau_{6N}/h^{3N}} \qquad 6.8$$

This is the first assumption of TST that any element of phase space on a surface with the same energy is equally likely to contain a phase space point. Now because the integral in the denominator is a surface integral then it can be placed in any region of the phase space. If it were in the reactant space then we would have

$$d^{6N}P = \frac{\exp(-H_R/kT)\, d\tau^R_{6N}/h^{3N}}{\int^R \exp(-H_R/kT)\, d\tau^R_{6N}/h^{3N}} \qquad 6.9$$

where the surface is now R and H_R is the energy at R. Further, since the system is adiabatic then $H=H_R$ and combining 6.8 and 6.9 gives

$$d^{6N}p^{*} = \frac{n^{+}}{\sum_{1} n_{i,\text{Reactants}}} = \frac{\exp(-H/kT)\,d\tau_{6N}/h^{3N}}{\int^{R}\exp(-H_R/kT)\,d\tau^{R}_{6N}/h^{3N}}$$

Here, n^{+} denotes the number of particles at the dividing surface. Invoking 6.5 gives

$$n^{+} = \prod_{1} [\text{Reactants}]_i \frac{\exp(-H/kT)\,d\tau_{6N}/h^{3N}}{\int^{R}\exp(-H_R/kT)\,d\tau^{R}_{6N}/h^{3N}/V} \qquad 6.10$$

Recognising that the denominator on the right hand side is the partition function per unit volume for the reactants we get

$$n^{+} = \prod_{1} [\text{Reactants}]_i \frac{\exp(-H/kT)\,d\tau_{6N}/h^{3N}}{\prod_{1} (Q_i/V)} \qquad 6.11$$

To this stage we have not been required to invoke any equilibrium assumptions between reactants and any system at the transition state. The reactants are in internal thermodynamic equilibrium and all flux through the dividing surface in one direction is regarded as reactive flux. This is the third fundamental assumption of TST. (The second is that the dynamics are adiabatic.)

Now we must consider the motion along the reaction coordinate, q_1, perpendicular to the dividing surface. This motion is assumed to be separable and the incremental rate of reaction through an element of phase space, $d\tau_{6N}$, at S^{*} is dn^{+}/dt.

$$dn^{+}/dt = \prod_{1} [\text{Reactants}]_i \frac{(dq_1/dt)\exp(-H/kT)\,dp_1 d\tau_{6N-2}}{h^{3N}\prod_{1} (Q_i/V)} \qquad 6.12$$

The coordinates p_1 and q_1 have been separated from the remaining coordinates.

We can also separate the Hamiltonian into its two components, along the reaction coordinate, and the system less one degree of freedom.

$$H = p_1^2/2\mu_1 + H'$$

H′ is thus the energy of the transition state. We can also write the momentum as follows

$$p_1 = \mu_1 (dq_1/dt)$$

The rate becomes

Rate

$$= \prod_i [\text{Reactant}]_i \frac{\int^{S^*} \int_0^\infty p_1/\mu_1 \exp(-(p_1^2/2\mu_1 + H')/kT) dp_1 d\tau_{6N-2}}{Vh^{3N-1} \prod_i (Q_i/V)}$$

$$= \prod_i [\text{Reactant}]_i \frac{1/\mu_1 h \int_0^\infty p_1 \exp(-p_1^2/2\mu_1 kT) dp_1 \int^{S^*} \exp(-H'/kT) d\tau_{6N-2}}{Vh^{3N-1} \prod_i (Q_i/V)}$$

$$= \prod_i [\text{Reactant}]_i \frac{1/\mu_1 h [-\mu_1 kT \exp(-p_1^2/2\mu_1 kT)]_0^\infty \int^{S^*} \exp(-H'/kT) d\tau_{6N-2}}{\prod_i (Q_i/V) \cdot Vh^{3N-1}}$$

$$= \prod_i [\text{Reactant}]_i \frac{kT/h \{\int^{S^*} \exp(-H'/kT)/Vh^{3N-1}\}}{\prod_i (Q_i/V)} \qquad 6.13$$

The term in braces is clearly the partition function of the transition state and we can evaluate it as in 6.7. Thus the rate coefficient is

$$k(T) = \frac{kT}{h} \left[\frac{Q^+/V}{\prod_i Q_i/V}\right] \exp(-\Delta\varepsilon_o^+/kT) \qquad 6.14$$

where the partition functions are the total functions including both translational and internal components. Now the volume only relates to the translational component and the translational and internal functions are truely separable.

Finally we note for the two cases of 1) a unimolecular process and 2) a bimolecular process that the following holds.

For both 1) and 2)

$$Q^+/V = (Q_T^+/V)\ Q_{INT}$$

$$\prod_{reactant} Q/V = \prod_{reactant} Q_T/V \cdot \prod_{reactant} Q_{INT}$$

For 1) For a unimolecular reaction Q_T^+/V and $\prod_{react} Q_T/V$ are clearly equivalent and we obtain

$$k_{uni}(T) = kT/h\ (Q_{INT}^+/Q_{INT})\ \exp(-\Delta\varepsilon_o/kT) \qquad 6.15$$

For 2) For a bimolecular reaction

$$(Q_T^+/V)/\prod_i (Q_T/V)_i = 1/(Q_T/V)$$

where $Q_T/V = (2\pi\mu kT/h^2)^{3/2}$ and describes the relative motion of the two reactants. The usual exprssion of the TST formula is

$$k(T) = kT/h\ \frac{Q^+}{Q_a Q_b}\ \exp(-E_o/kT) \qquad 6.16$$

Evaluation of the Q's is usually by assumption of separability of the individual components and use of the classical statistical mechanical formulae.

6.3 Microcanonical Transition State Theory.

In this section we will briefly describe how microcanonical transition state theory (μTST) may be obtained in its RRKM (Rice, Rampsberger, Kassel, and Marcus) form from the exact classical expression for k(E).

6.3.1 The Exact Classical Rate

The rate constant k(E) is defined as the probability per unit time of a molecule with internal energy E forming product in the absence of collisions. The exact classical rate constant is

$$k(E) = \frac{\lim_{\tau\to\infty} 1/\tau \int_0^\tau dt \iint dpdq\ \delta[E-H]\ \delta[q-q_p]\ p/m\ \chi[p,q,t]}{\iint dpdq\ \delta[E-H]} \qquad 6.17$$

Where H(p,q) is the complete Hamiltonian for the system,

$q=q_p$ defines a surface in the product region crossed once only by trajectories which start in the reactant region,

p is the momentum perpendicular to the surface P,

χ=1 if a trajectory through P for given (q,p) at time t started in the reactant valley,

=0 otherwise.

This may be derived in the following way.

Consider an element of phase space, $dp_Q dq_Q$, then the total area of this space accessible at a given energy is

$$\iint dp_Q dq_Q\ \delta[H-E].$$

The normalized probability of a particular element $dp_Q dq_Q$ is thus

$$\frac{dp_Q dq_Q\ \delta[E-H]}{\iint dp_Q dq_Q\ \delta[E-H]}$$

Now k(E) is the average, over phase space, of the reciprocal of the mean time that a given trajectory takes to cross P; that is,

$$k(E)=\lim_{\tau\to\infty} 1/\tau \int d\tau\ N_n(E,t) \qquad 6.18$$

where $N_n(E,t)$ is the normalized probability per unit time for passage to product <u>at time t.</u> The number of trajectories per unit time through a given element is p/m. We only require those

trajectories which pass through $q=q_p$ so the number per unit time which pass through a particular element of the surface P is

$$p/m\ \delta[q-q_p].$$

So the normalized probability per unit time for passage over a particular element of phase space at $q=q_p$ is

$$N_n(dp,dq_p) = \frac{dpdq\ \delta[E-H]\ p/m\ \delta[q-q_p]}{\iint dpdq\ \delta[E-H]}$$

For all elements such that $q=q_p$ for passage in either direction we have

$$N_n(p,q_p) = \frac{\iint dpdq\ \delta[E-H]\ p/m\ \delta[q-q_p]}{\iint dpdq\ \delta[E-H]}$$

Finally, the probability $N_n(E,t)$ is obtained by only counting those trajectories which start in the reactant region.

$$N_n(E,t) = \frac{\iint dpdq\ p/m\ \delta[E-H]\ \delta[q-q_p]\ \chi[p,q,t]}{\iint dpdq\ \delta[E-H]} \qquad 6.19$$

Combining 6.18 and 6.19 recovers equation 6.17. From this exact expression we may now obtain the RRKM expression by making certain assumptions.

6.3.2 The RRKM Formulation.

The RRKM or μTST formula is

$$k(E) = \int_{E_0}^{E} \rho^+(E^+)dE^+/h\rho(E) \qquad 6.20$$

Here E_0 is the critical energy or the energy at the saddle point and $\rho^+(E^+)$ is the density of states of the system at the activated complex. We observe two things.

(1) Given a potential, it is always possible to determine the density of states and,

(2) the potential for the activated complex is as for the entire molecule at the coordinate $q=q_T$, where q_T is the coordinate defining the activated complex or more generally, a surface $S(q)=0$.

If we now consider the classical expression 6.17, it is apparent that the integral over P (the surface) is a surface integral and is independent of its position. It simply counts the trajectories that start in the reactant region and proceed to the product region regardless of where P is placed defining these regions. Thus 6.17 holds regardless of the position of the surface.

Next, we perform a coordinate transfer to reaction coordinates. These are curvilinear and are defined along a line joining the reactant and product valleys perpendicular to T the dividing surface. We define the coordinate s as the distance along this reaction pathway from T, and the coordinate $\underset{\sim}{u}$ as a vector (in a multidimensional system) defining the distance perpendicular to the path. Associated with these are the corresponding momenta p_s and $p_{\underset{\sim}{u}}$. The surface T is defined as s=0.

If we evaluate at s=0 where p_s is perpendicular to T then we get the exact probability for passage through the surface.

$$N(E,t)= \int_{-\infty}^{\infty}\int_{-\infty}^{\infty} dp_{\underset{\sim}{u}} d\underset{\sim}{u} \int_0^{\infty} dp_s \; \delta[E-H(...s=0)] \; \chi[...s=0] \; p_s/m \qquad 6.21$$

The integral over ds has been eliminated by evaluating at s=0, since

$$\int_{-\infty}^{\infty} f(s) \; \delta(s=0) ds = f(s=0)$$

We now make our first assumption that every trajectory that reaches T originated in the reactant region and terminates in the product region. Thus $\chi=1$ in equation 6.21.

$$N(E,t)= \int_{-\infty}^{\infty}\int_{-\infty}^{\infty} dp_{\underset{\sim}{u}} d\underset{\sim}{u} \int_0^{\infty} dp_s \; \delta[E-H(p_{\underset{\sim}{u}}, p_s, \underset{\sim}{u}, s=0)] \; p_s/m \qquad 6.22$$

The second assumption is that we can assume that 6.18 is ergodic. This implies that the system behaves randomly (decays uniformly in time) and that the time average may be replaced by an appropriate energy average

$$1/\tau \int_0^\tau N(E,t)\ dt \ \text{---}> \ \int N(E,E^*)\ldots dE^*$$

E^* is the energy of the trajectory above E_0 at s=0.

This equivalence of a time and an energy average may be explained in the following way. Consider two ensembles of n and n^2 particles at an energy E. The ensemble of n particles may be followed for a time period to observe the nature of the energy configuration due to randomisation. Consider the second ensemble as n ensembles of n particles. At any instant in time the n ensembles will represent n configurations due to randomisation which is exactly the information obtained from the time average.

The energy E^* is specified and at s=0 the Hamiltonian has the following simple form

$$H(p,q)_{s=0} = p_s^2/2m + p_u^2/2m + V(s=0,u) \qquad 6.23$$

which is separable into a (p_u,u) term and a p_s term. Specifying E^* as the energy above E_o at s=0 gives us the following relationships

$$E^* = p_u^2/2m + V(s=0,u) - E_o \qquad 6.24$$

$$E = E_o + E^* + p_s^2/2m \qquad 6.25$$

The expression for the time averaged probability including normalization by a δ-function in E^* is

$$1/\tau \int_0^\tau N(E,t)\ dt = \int_0^{E-E_o} dE^* \{ \int_{-\infty}^{\infty}\int_{-\infty}^{\infty} dp_{\underset{\sim}{u}} du_{\underset{\sim}{u}}\ \delta[E^* - p_u^2/2m - V(s=0,u) + E_o] \} \times$$

$$\int_0^\infty dp_s\ p_s/m\ \delta[E - E_0 - E^* - p_s^2/2m] \qquad 6.26$$

Using a change of integration variable, the second part of 6.26 may be rewritten as

$$\int_0^\infty \delta[E-E_0-E^*-p_s^2/2m]\ dp_s{}^2/2m$$

since $dp_s^2/2m = p_s/m\ dp_s$. This is identically unity as it is a δ-function. ($\int\delta[x-a]dx = 1$).

We use the following quantum mechanical result to evaluate the remaining term in 6.26 and the denominator in 6.17.

In the classical limit

$$h^n \sum_i \langle i|\hat{f}|i\rangle \approx \iint dpdq\ f(p,q) \qquad 6.27$$

This is summed over all quantum states $|i\rangle$ (normalized) and n is the dimensionality of the system. Note that f on the right hand side is the classical quantity and $\hat{f}$ on the left hand side is the appropriate quantum operator.

Now the density of states $\rho(E)$ for a Hamiltonian H with eigenvalues E_i is $1/\Delta E$ x No. of states between E and $E+\Delta E$.
Thus we have

$$\rho(E) = \sum_i 1/\Delta E \int_E^{E+\Delta E} \delta(E-E_i)dE \qquad 6.28$$

The integral is unity only at $E=E_i$, (when an eigenvalue is a state) and zero otherwise. It then counts the number of states between E and $E+\Delta E$. So

$$\rho(E) = \sum_i 1/\Delta E \int_E^{E+\Delta E} \langle i|\delta(E-H)|i\rangle dE \qquad 6.29$$

since $\delta(E-H)|i\rangle = \delta(E-E_i)|i\rangle$ where $\delta(E-H)$ is the δ-function operator. Taking the limit as $\Delta E \to 0$ of 6.29

$$\lim_{\Delta E\to 0} \int^{E+\Delta E} f(E)dE \approx \Delta E f(E)$$

giving

$$\rho(E) = \sum_i \langle i|\delta(E-H)|i\rangle \qquad 6.30$$

which is in the form of equation 6.27 and in the classical limit

$$\rho(E) = 1/h^n \iint dpdq\ \delta[E-H(p,q)] \qquad 6.31$$

This result implies that the density of states is $1/h^n$ times the total classically accessible area of phase space at energy E. From equation 6.26 we get

$$\int_{-\infty}^{\infty}\int_{-\infty}^{\infty} dp_u d\underset{\sim}{u}\ \delta[E_o + E^* - p_u^2/2m - V(s=0,u)] = h^{n-1}\rho^+(E_o + E^*) \qquad 6.32$$

where one dimension has been removed by evaluating at s=0 and $\rho^+(E_o+E^*)$ is the density of states of the activated complex where

$$H(p,q)_{s=0} = p_u^2/2m + V(s=0,\underset{\sim}{u}) \qquad 6.33$$

Applying a change of variable $E^+ = E_o + E^*$ and rewriting 6.26 gives

$$1/\tau \int_0^{\tau} N(E,t)\ dt = h^{n-1}\int_{E_0}^{E} dE^+\rho(E^+) \qquad 6.34$$

The denominator of 6.17 can be evaluated in the same way giving

$$\iint dpdq\ \delta[E-H(p,q)] = h^n\rho(E) \qquad 6.35$$

The combination of 6.17, 6.34 and 6.35 gives the required result

$$k(E) = \int_{E_0}^{E} \rho^+(E^+)dE^+/h\rho(E) \qquad 6.36$$

6.4 Microscopic Reversibility and k_{ter}/k_{uni}.

The time reversibility of the Schrödinger Equation which governs all processes devolves the principle of microscopic reversibility upon all processes. It is manifested in the equilibrium constant expressions and in the necessity that the forward and reverse processes of an elementary reaction must follow the same detailed path.

It is stated thus (Smith, 1980); "..., the probabilty of a transition per unit time between a fully specified state of the reactants and a fully specified state of the products is independent of the direction in which time is chosen to move,.."

If we consider the following reaction

$$AB \underset{k_{ter}}{\overset{k_{uni}}{\rightleftharpoons}} A + B$$

then this principle allows us to relate k_{uni} and k_{ter} via the equilibrium constant.

$$K_c = \frac{k_{uni}}{k_{ter}} \qquad 6.37$$

Implicit in this equation is the knowledge that the microscopic processes involved in this (apparently) simple process, for example, energy transfer, activation and deactivation, are also explicitly related by microscopic reversibility.

From equation 6.7 we have

$$\frac{k_{ter}}{k_{uni}} = \frac{\prod_i (Q_i/V)}{\prod_j (Q_j/V)} \exp(\varepsilon_0/kT)$$

$$= \frac{Q_{AB}}{Q_A Q_B} \exp(\Delta E_0/RT) \qquad 6.38$$

where ΔE_0 is the difference in molar zero point energy between the products A, B and the reactant AB.

We note that this is similar in form to the expression for a bimolecular reaction from transition state theory so we separate the partition functions into translational and internal components and obtain

$$\frac{k_{ter}}{k_{uni}} = \frac{Q_{AB}^{INT}}{Q_A^{INT} Q_B^{INT}} \frac{1}{(Q_V/T)} \exp(\Delta E_0/RT)$$

$$= \left[\frac{2\pi\mu kT}{h^2}\right]^{-3/2} \frac{Q_{AB}^{INT}}{Q_A^{INT} Q_B^{INT}} \exp(\Delta E_0/RT) \qquad 6.39$$

where the first term is the expression for the translational partition function for the relative motion of A and B, and μ is the reduced mass. Equation 6.39 provides a simple way to calculate k_{ter} from k_{uni}.

6.5 The Gorin Model

The greatest problem in transition state theory and RRKM theory is the specification of the transition state itself. For unimolecular and termolecular processes, the properties which change during reaction are the vibrational frequencies and the rotational moments of the moieties.

If we consider a unimolecular dissociation process, the frequencies associated with the bond breaking must be transformed into other forms. As the bond lengthens the stretch (reaction coordinate) transforms into translational separation of the products. The bending moments must gradually become 'looser' and become the rotational components of the energy of the products on separation. However, at intermediate stages the moieties must look like loosely attached rotors whose motion is hindered by being still bonded to each other.

This is essentially the problem addressed by Gorin (1939) and further developed by Benson (1976, 1983, 1985). However, a number of

studies have cast doubt on the theoretical basis of this model (Garrett and Truhlar, 1979b; Rai and Truhlar, 1983; Cohen and Pritchard, 1985) for bimolecular processes. We believe that the physical description is still useful in describing the processes involved in specifying the transition states. There is no explicit need to postulate the presence of a centrifugal barrier at 2.5 to 3.0 times the normal bond length provided there is an adequate description of the interatomic forces which will describe the geometry of the transition state and thus the motions of the hindered rotors.

We assume only that the properties of the complex AB^+ (from the reaction A + B --> AB) may be described by a combination of the properties of the separated moieties A and B, in particular their vibrational frequencies. The remaining degrees of freedom (rotation in the separated species and bending vibrations in the product) described by hindered rotors whose hindrances are calculated with the atoms of the A and B moieties being described as hard spheres.

We use the method described by Benson (1976) to determine the parameters of the hindered motion. The moiety dissociating (or recombining) is placed at the appropriate distance r^+, and allowed to rotate in two dimensions until its atoms come into van der Waals contact with the atoms of the substrate. The solid angle thus subtended is used to calculate the moment of the hindered rotor.

The problem with this is that the hindered rotors do not tighten to the bending vibrations required in the recombined product. (Garrett and Truhlar, 1979-2; Rai and Truhlar, 1983). This

is the major reason for the unsuitability of this model. We develop later a technique which allows us to overcome these problems.

6.6 Treatments To Obtain Termolecular Rate Coefficients.

In this section the description of the method by which the calculation of termolecular recombination may be performed is given for both the microcanonical and canonical cases. As we will see, while initially the procedures are the same, they rapidly diverge at the point where specification of the transition state(s) is performed. The procedure for the microcanonical approach is flow charted in appendix 7 for those wishing a step by step guide to the technique.

The first step in the procedure is to calculate the minimum energy path of the recombination using a standard classical trajectory calculation. Such programs are commercially available. (Hase, 1983). To do this the potential under which the moieties interact must be defined. The potential may be split into three components, 1) the intramolecular potentials of the moieties, 2) the non-bonding intermolecular potential, and 3) the bonding intermolecular potential.

$$V = V_{INT,A} + V_{INT,B} + V_{A,B} + V_{BOND} \qquad 6.40$$

The intramolecular potential is most easily described by a valence force field approximated by harmonic vibrational modes of the moieties. For the recombination of a polyatomic radical and an atom, this consists of the force constants for the harmonic vibrational modes of the polyatomic; for example, the methoxy or

hydroxymethyl radical. The frequencies of the vibrations can be obtained from spectroscopic or ab initio sources or from a semi-empirical source derived from a large body of data. (Benson, 1976)

The non-bonding intermolecular potential consists of the interaction between the non-bonding atoms on the different moieties. For CH_3O + H it is the interaction between the H atom and the C and H atoms of the methoxy radical. Any sort of interaction may be used such as Lennard-Jones, exponential attraction or repulsion or electrostatic. It is only necessary to give a physically reasonable description. For the reactions studied here, the interaction chosen was a Lennard-Jones(12-6) soft sphere potential.

The bonding intermolecular potential could again be any type of atom-atom interaction with a potential minimum at the equilibrium bond distance and a depth equal to the dissociation energy. It is not necessary in this case that the potential represent the true distance dependence of the energy for the bond because the dynamics of the trajectory are not needed. We are only calculating a trajectory from initial position and momentum coordinates; (NSELT=0 in program MERCURY, Hase 1983); not a collision of two particles where impact parameters and scattering angles are required.

The results of this trajectory calculation are a set of geometries of the recombining moieties (ostensibly bonded via the bonding interaction). These geometries are then minimised to yield the lowest energy conformations and a normal coordinate analysis performed to obtain the vibrational frequencies of the recombined specimen. It is possible to adjust the output to provide geometries which cover the range of s values (intermolecular distance

characterised by the distance between the atoms forming the bonds) of interest.

We note that some of the features of the Gorin model are implicitly included; that is, the intramolecular potentials of the two moieties. It is at this point that the two treatments, canonical and microcanonical, diverge.

6.6.1 Canonical Treatment.

In the canonical treatment, the variational criterium minimises the rate coefficient, $k^{GT}(T,s)$, with respect to s, the reaction coordinate. Canonical variational transition state theory is identifiable with the maximisation of the free energy of activation. (Garrett and Truhlar, 1979b; Rai and Truhlar, 1983). The generalized thermodynamic formulation of transition state theory is,

$$k^{GT}(T,s) = kT/h\ K^{o} \exp(-\Delta G^{GT,0}(T,s)/RT) \qquad 6.41$$

and it is obvious that minimisation of $k^{GT}(T,s)$ requires the maximisation of $\Delta G^{GT,0}(T,s)$. Here K^{o} is the reciprocal of the standard state concentration. (K^{o} = 1 $cm^{3}molecule^{-1}$).

This is achieved by calculating the internal partition functions for the activated complex from the frequencies from the normal coordinate analysis and the moment of inertia of the transition state at various s. The formulae for the partition

functions are,

$$q^r = \frac{\pi^{1/2}}{\sigma}\left[\frac{8\pi^2 I_m kT}{h^2}\right]^{3/2} \qquad 6.42$$

$$q_i^v = (1-\exp(-h\nu_i/kT))^{-1} \qquad 6.43$$

$$q^v = \prod_i q_i^v \qquad 6.44$$

Where I_m is the overall moment of inertia ($= I_x I_y I_z$) and the i refer to the individual vibrational frequencies.

The total internal partition function Q_{AB}^{+}, is thus

$$Q_{AB}^{+} = q^e q^v q^r \qquad 6.45$$

and the free energy is

$$\Delta G = -nRT \ln Q_{AB}^{+} \qquad 6.46$$

q^e is the electronic partition function and is described by the spin degeneracy. The largest value of ΔG corresponds to the s of the transition state and the high pressure rate constant, k_{ter}, may be calculated from the following relations.

The rate coefficients k_{ter} and k_{uni} are related by microscopic reversibility and we may rewrite 6.39 as follows;

$$\frac{k_{ter}}{k_{uni}} = \exp(H_o/k_B T)(Q_{AB}/Q_A Q_B)[(2\,k_B T/h^2)M_A M_B/(M_A+M_B)]^{-3/2} \qquad 6.47$$

where the M's are the molecular weights of the reactants and the Q's are the partition functions. H_o is the difference in zero-point energy between AB and infinitely separated A and B. In the high pressure limit, transition state theory provides an expression for

k^{∞}_{uni} from 6.15;

$$k^{\infty}_{uni} = (k_B T/h)(Q^{+}_{AB}/Q_{AB})\exp(-E_o/k_B T) \qquad 6.48$$

where E_o is the critical energy for reaction and Q^{+}_{AB} is the internal partition function for the activated complex. Combining these two equations and evaluating in convenient units gives the following expression for the high pressure limiting termolecular rate coefficient;

$$k_{ter} = 1.11 \times 10^{-10} T^{-1/2} A\left[\frac{M_A + M_B}{M_A M_B} A\right]^{3/2}\left[\frac{Q^{+}_{AB}}{Q_A Q_B}\right]\exp([\Delta H_o - E_o]/k_B T) \qquad 6.49$$

where the masses are in a.m.u., and k_{ter} is in $cm^3 s^{-1}$. The term $(\Delta H_o - E_o)$ is now the difference between the zero-point energy difference of the reactants and the critical energy of the reaction. This completes the canonical description.

6.6.2 Microcanonical Treatment

In microcanonical variational transition state theory the transition state for each energy, E, is placed at that s where the microscopic rate, k(E), is a minimum. Since we have from equation 6.20

$$k(E) = \int_{E_0}^{E} \rho^{+}(E^{+})\,dE^{+}/h\rho(E)$$

$$\equiv N(E)/h\rho(E) \qquad 6.50$$

where N(E) is the sum of states of the activated complex, we need to minimise the N(E). To do this we need to be able to calculate the density of states, $\rho^{+}(E)$, of the activated complex.

As stated previously, the development of the microcanonical treatment is identical to the canonical treatment up to the normal mode analysis of the activated complex.

We wish to calculate the density of states at various s. From the normal coordinate analysis we note that the frequencies obtained consist of some which have evolved from the infinitely separated A and B moieties and some very low frequencies which are linear combinations of the hindered internal rotors. The application of a normal mode analysis is inappropriate and an alternative description is required. This is provided by the Gorin model and these modes are replaced by hindered internal rotors. It has been shown that this treatment successfully reproduces the thermodynamic properties of such systems. (Benson, 1976; 1983).

The hindrance of these rotors is determined from the geometry of the species as described in section 6.5. The moments of inertia for the hindered rotors are found in the following way. Each moiety is treated in the normal way and the moments are calculated by diagonalization of the inertia tensor. This gives three moments for each moiety, I_1, I_2, I_3 (unless one is an atom.) Two of these moments will be the same or nearly the same and these two represent the two dimensional motion of the rotor about the moiety's symmetry axis. The moment is thus

$$I_A = (I_1 I_2)^{1/2}.$$

For the case when both moieties are polyatomic then there are two such moments for the internal rotors, one for each moiety.

In the case where one moiety is an atom, there is only one moment in total. The procedure is as before for the polyatomic moiety and the moment is the same. The moment of the atom is about the centre of mass of the polyatomic giving

$$I_B = mr_B^2$$

The final moment for the hindered rotor is then

$$I_{HR} = I_A I_B / (I_A + I_B)$$

The hindrance of the rotors as described by the solid angle θ (see section 6.5) is used to adjust the moments of inertia in the following way. The solid angle subtended is

$$\Delta\Omega/4\pi = (1-\text{Cos}\theta)/2$$

and the moment of the hindered rotor, I_{HR}, is replaced by $I_{HR}(\Delta\Omega/4\pi)$.

This completes the specification necessary to enable the calculation of the $\rho^+(E,s)$. This is done for several s in the region of interest.

At large s, where the hindrances are small ($\theta > 1$ Radian), the density of states is well behaved as a function of s and $\ln(\rho^+(E))$ decreases approximately linearly with s. However, at small s the density of states calculated in this way decrease very rapidly and fall below the $\rho(E)$ at $s = r_{eq}$, the equilibrium bond length as shown in figure 6.1. This is due to the very rapid tightening of the hindrance as the moieties come close together.

It is useful to note that if we perform a normal coordinate analysis on the structures at small s frequencies are obtained which

are identifiable with bending modes of the product. However, these are strongly anharmonic as they are the sum of Lennard-Jones potentials between the non-bonding atoms near their minima. This naturally renders such an analysis inapplicable and as well as this, since the atom-atom distances are so small, any attempt to separate the motions into hindered rotors is quite unreasonable.

The consequence of this is that a different technique is required to determine the density of states at smaller s.

It is reasonable to assume that because the dynamics of recombination are a 'smooth' and continuous process; that is, there are no discontinuities or other non-continuous attributes of the potential surface, that the other properties, for example, $\rho^+(E)$, should also be continuous over the region of interest. Also, the recombined molecule is at a relative minimum in energy to the reactants and it should not be unreasonable to assume that the properties associated with the recombined moiety are also at a minimum.

The procedure that has been devised is this. The density of states at $r = r_{eq}$ is well defined (stable molecule). The density of states, $\rho^+(E,s)$, can be calculated as the density of states of the stable molecule with the bond formed 'frozen out' or held rigid. This reduces the molecular degrees of freedom by one and identifies it with a transition state.

The $\rho^+(E,r_{eq})$ and $\rho^+(E,s)$ (large s) are known and we assume for any energy, E, that the $\rho^+(E,s)$ can be interpolated between $s = r_{eq}$ and $s = s_G$ where s_G is some separation where the Gorin model holds.

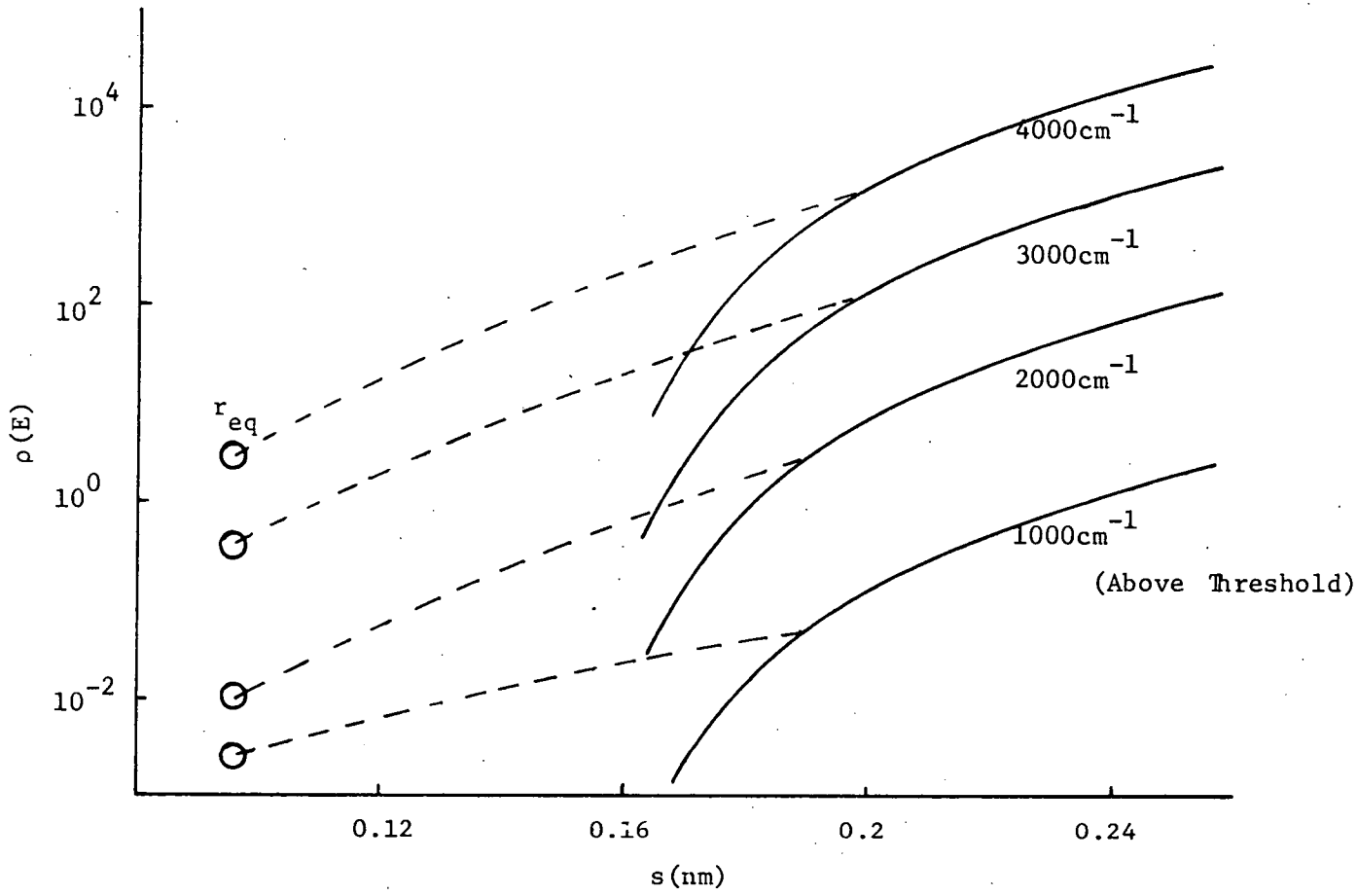

Figure 6.1 Density of States, ρ(E), as a Function of Bond Length, s.
(———) Calculated (Gorin), (------) Interpolated.

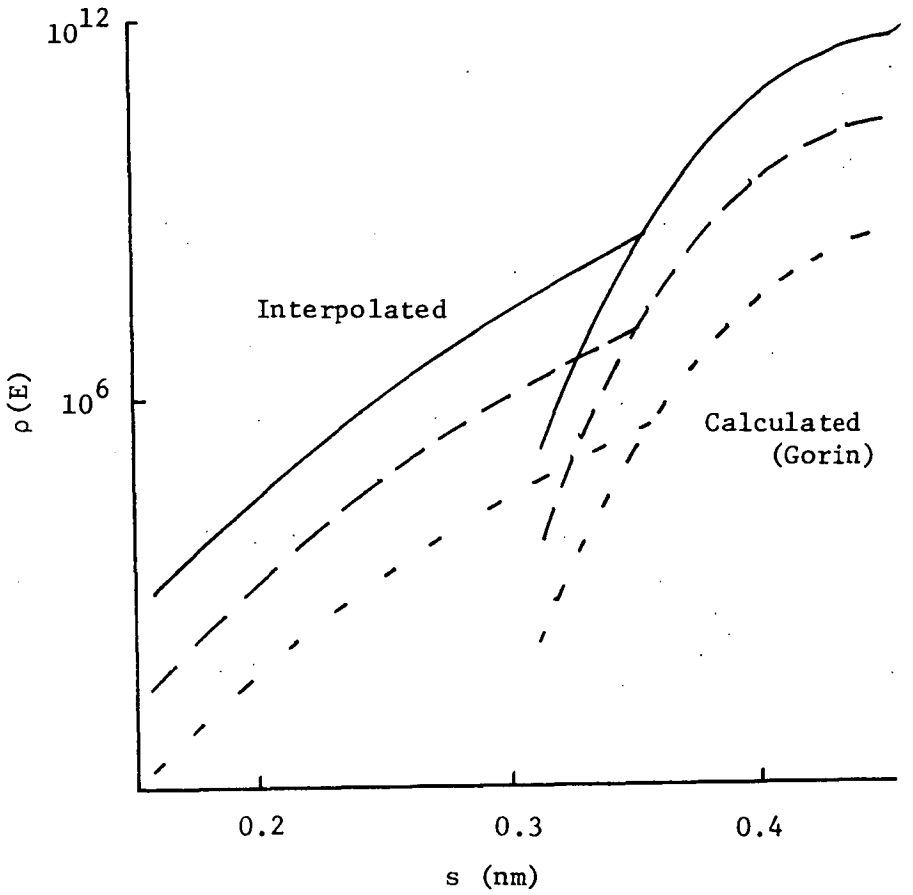

Figure 6.2 Density of States as a Function of Bond Length. CH_3 Recombination.

An example of the interpolation is shown in figure 6.2 for methyl radical recombination. The interpolation assumes $\ln(\rho^+)$ to be linear in $\ln(s_o-s)$ where s_o is a suitable value of s (0.4nm in this case). The interpolation was performed between $s = r_{eq}$ and $s = s_G$ (0.35nm in this case). The choice of interpolation technique is not critical as errors associated with slight inaccuracies in the density of states will be less important in the integration of them to get the sum of states, N(E).

This method can be compared with the statistical adiabatic channel model (Quack and Troe, 1974; 1975; Troe, 1981). It is obvious that the intention of this procedure and the SAC model are similar. However, here the ρ's are interpolated rather than the eigenvalues. This is a more straight forward approach which uses the fact that to calculate the sum of states it is the density of states that is required rather than the potentials. We believe that this procedure is susceptible to fewer errors as there is no parameterization involved.

Having calculated the $\rho^+(E,s)$'s, $\rho^+(E)$ is found as that $\rho^+(E,s)$ where the sum of states is a minimum. This is different and not equivalent (necessarily) to minimizing the density of states as has been done. (Wong, and Marcus, 1971). It is possible thus to have a different transition state (different s) for each energy, E. (Bunker and Pattengill, 1968; Truhlar and Garrett, 1984).

The specific microscopic rate coefficient, k(E), may then be calculated in the usual way from 6.50

$$k(E) = \int_{E_0}^{E} \rho^+(E^+)dE^+/h\rho(E) \qquad 6.50$$

where E_0 is for that particular energy, E, the value of the local minimum of the potential at the specific s for which the $\rho^+(E)$ was calculated. To obtain the thermal rate coefficient only those values of k(E) with E greater than the dissociation energy are included as it is not possible for molecules to dissociate with less than this energy. This has been implemented using programs which are commercially available. (Hase, 1983; Gilbert, 1983)

The final step is to calculate the termolecular recombination rate coefficients from the unimolecular rate coefficients using equation 6.30.

This completes the microcanonical specification.

6.7 Results.

Three reactions were considered for application of The theory.

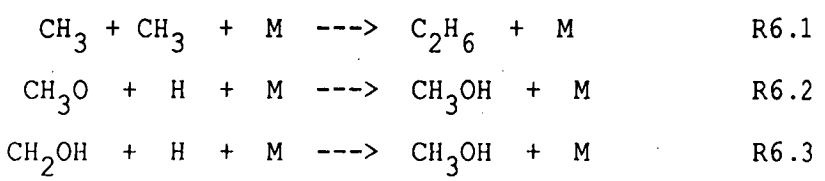

$$CH_3 + CH_3 + M \rightarrow C_2H_6 + M \qquad R6.1$$

$$CH_3O + H + M \rightarrow CH_3OH + M \qquad R6.2$$

$$CH_2OH + H + M \rightarrow CH_3OH + M \qquad R6.3$$

The recombination of methyl radicals was chosen as the test of the theory as good recent experimental results have been obtained for this reaction. (Macpherson, et al., 1985)

The other two reactions were chosen because of their relevance to alcohol combustion and alcohol kinetics. Up to 15% reformation of methanol has been predicted by these reactions in a flow reactor study. (Hoyermann, et al., 1981a)

6.7.1 The Recombination of Methyl Radicals

The recombination of methyl radicals was studied using both the canonical and the microcanonical approach. The canonical treatment illustrated here is neither complete nor rigorous. It is included only for completeness in describing the development of the microcanonical treatment. It is, of course possible to apply the interpolation technique to densities of states calculated for the potential described and to subsequently calculate the partition functions from the interpolated densities of the states, and thus the free energies for the canonical calculation. This was not done as it was not necessary for the subsequent development of the microcanonical theory.

The result obtained using the canonical approach described here is thus not a proper and rigorous test of canonical transition state theory and no such rigorous test was intended.

a) Canonical Treatment.

The potential describing the reaction was formulated as in section 6.6. The C-C interaction was described by a standard Morse potential. The parameters a, b and c in tables 6.1, 6.3 and 6.5 are the coefficients in a cubic equation of the form -

$$\beta(r)/\beta_o = ax^3 + bx^2 + cx + 1 \quad \text{where } x=(r/r_e-1)$$

This enables all of the potentials used in this work to be expressed as a Morse-type function with an r dependent β. The parameters are given in table 6.1 for the entire potential used.

The potential we have used has not been refined or optimized in any way with respect to the trajectory calculation. The valence force field description has been refined to reproduce as closely as possible all frequencies of the methyl radical especially the out of plane and in plane bending modes.

TABLE 6.1 CH_3 + CH_3 Potential.

Frequencies	3162 3162 3044 1396 1396 580	
Lennard-Jones	C_{12}	C_6
C-H	21082	-56.58
H-H	6436.1	-22.87
Bonding Interaction	C-C	
	Morse	Hase
$beta_o$	1.814	1.814
a	0.0	0.1711
b	0.0	0.054
c	0.0	-0.0618
D_o	366.0	366.0
r_e	1.53	1.53
Range	$0 \rightarrow \infty$	$0 \rightarrow \infty$

The rate constant was calculated using equation 6.49. We need to know the internal partition functions for the transition state and for the reactants, and the value of the $\Delta H_o - E_o$ term. The partition functions are easily determined using the formulae of statistical thermodynamics (Atkins, 1983), and equations 6.42-6.44, and a knowledge of the vibrational frequencies and moments of

inertia of the appropriate species. The reactants are usually well characterised species and these properties are well known either from spectroscopic data or from empirical interpolation techniques (Benson, 1976).

The frequencies and moments of the transition state are obtained by a normal coordinate analysis of the maximum free energy geometry from the trajectory calculation. This is performed with the reaction coordinate "frozen out" so that there are only 3N-7 degrees of freedom (excluding rotational and translational components). The resultant vibrational frequencies can then be used to determine the vibrational partition function.

The $\Delta H_o - E_o$ which we will call E_{or}, may be described as the energy barrier to reaction and is found by subtracting the critical energy for reaction from the zero point energy difference of the reactants and transition state. The critical energy here is the difference in energy between the equilibrium potential and the potential at $r=r^+$ of the potential function describing the bond broken or formed. In this case the potential is the simple Morse function described for the C-C bond.

The zero-point energy difference was calculated from the frequencies using standard statistical thermodynamics formulae (Atkins, 1983).

High Pressure Rate Constants.

The high pressure recombination rate coefficient at 300K was found to be $9.0 \times 10^{-11} cm^3 s^{-1}$. This result was calculated for a C-C

bond distance of 0.365 nm, which was the geometry with the highest free energy from those calculated in the trajectory calculation. The variation of ΔG as a function of r is shown in figure 6.3. It is apparent from this plot that this is not in actual fact the geometry with the maximum free energy and thus not the true transition state. The maximum of the curve is -23.2 kJ $mole^{-1}$ at r=0.375 nm. This gives a value of 10955.31 for the internal partition function of the transition state and a value of 8.2 x $10^{-11} cm^3 s^{-1}$ for the recombination rate coefficient if we assume that the exponential factor does not change. This is not realistic as the critical energy changes from 6.69 kJ $mole^{-1}$ to 5.53 kJ $mole^{-1}$ when r^+ is increased to 0.375 nm, and the frequencies of the activated complex are not known.

This result is approximately a factor of two higher than the experimental results available at this time, but recent work by Macpherson, et al. (1985) has indicated that these experimental results should be revised upwards by approximately 50%.

b) Microcanonical Treatment.

The microcanonical treatment of this reaction has differed slightly from the canonical because of the use of a revised potential for the C-C bond. This was obtained from an ab initio potential used by Duchovic and Hase (1985) to investigate methane dissociation. This is a "stiff Morse" oscillator and is compared with the standard Morse in figure 6.4. This stiff Morse has a β

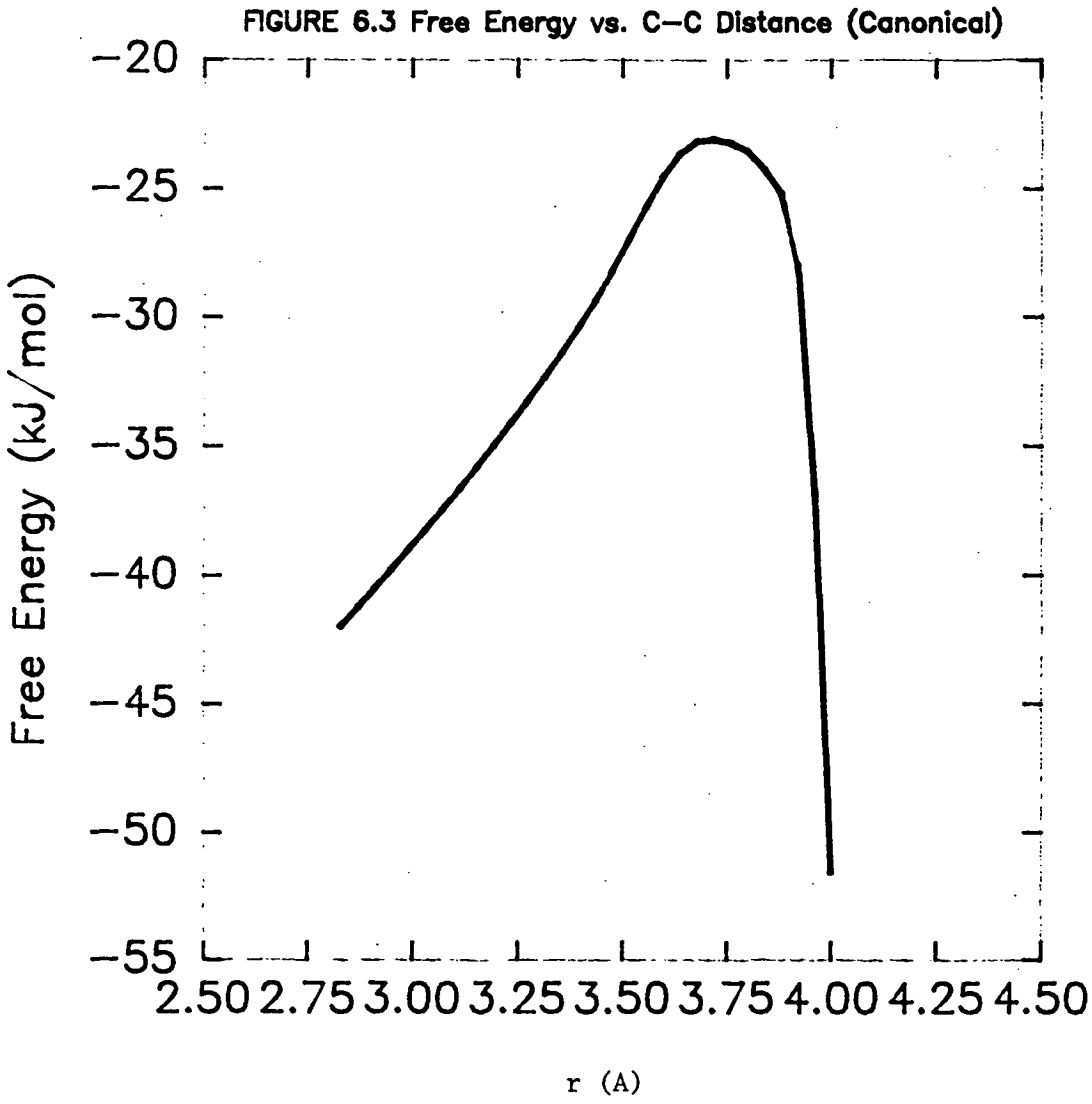

Figure 6.3 Free Energy, ΔG, as a Function of C-C Bond Distance. For Calculation of k(T) by Canonical Method.

parameter which is a function of the bond length and can be expressed dimensionlessly as;

$$\beta(r)/\beta_o = 0.1711x^3 + 0.054x^2 - 0.0618x + 1 \qquad 6.51$$

Here β_o is the Morse parameter calculated at r_e and $x = (r/r_e - 1)$. The assumption inherent in the use of this expression is that equation 6.51 is valid for similar and related reactions in its dimensionless form. This is known as the corresponding states hypothesis. (Adamson, 1973; Atkins, 1983)

High Pressure Rate Constants.

The results for this reaction are given in table 6.2 along with the experimental results of Macpherson, et al. (1985). The agreement obtained is very satisfactory considering that we have used no adjustable parameters. The temperature dependence predicted is stronger than that observed but not excessively different. Agreement between the data and the predicted rate constants could be obtained by adjusting the C-C bond potential in an empirical manner but this was not considered necessary.

TABLE 6.2 Methyl Recombination k_{ter}.

Temperature (K)	Recombination Rate Coefficients High Press. (10^{-11} cm^{3}s^{-1})	
	Calculated	Experimental
300	6.8	6.5±0.2
450	3.1	5.6±0.4
600	2.5	5.1±0.3

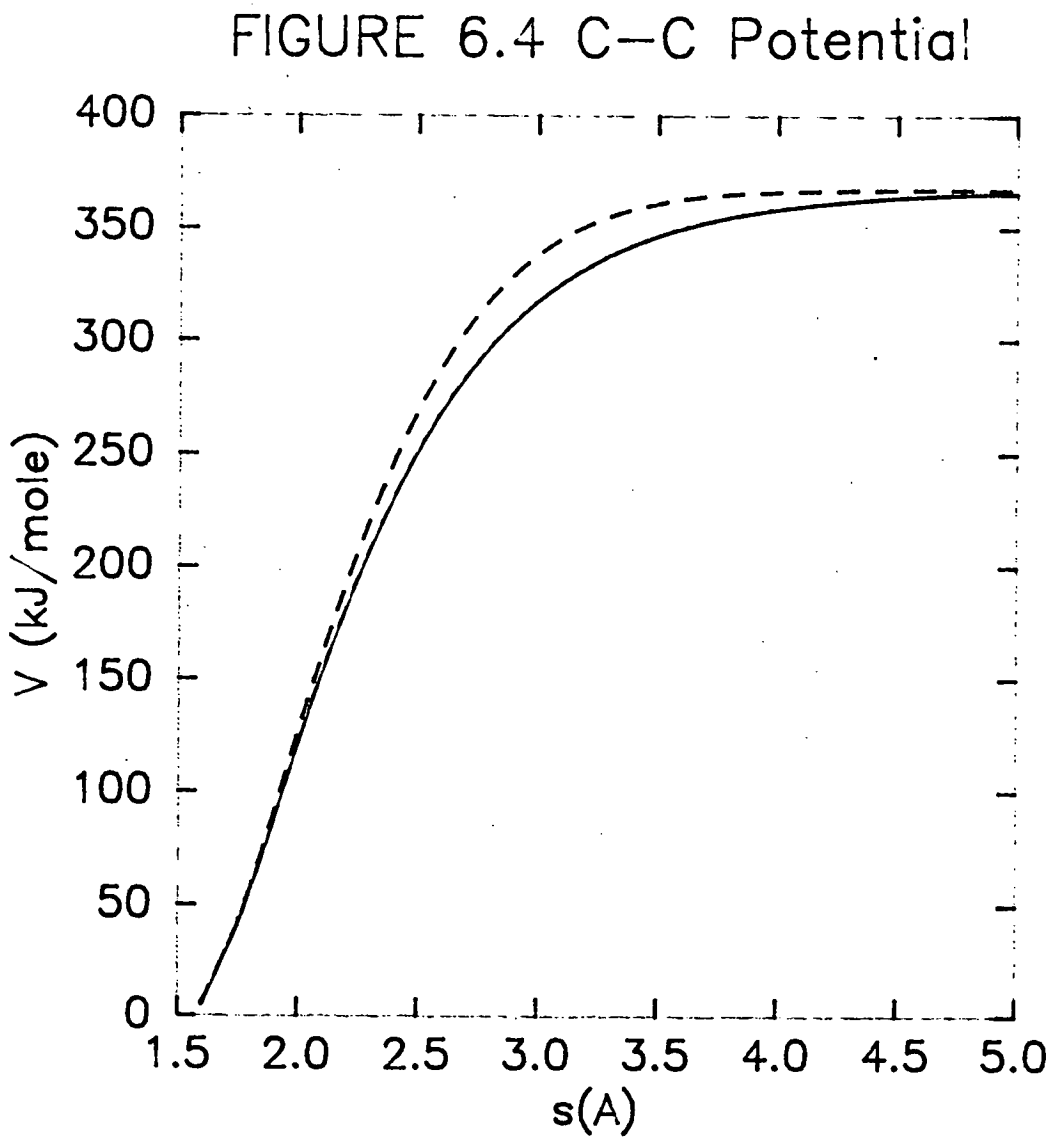

Figure 6.4 C-C Potentials for Methyl Radical Recombination.

——— Morse

– – – Hase, (ab initio)

6.7.2 The Recombination of Methoxy Radicals and Hydrogen Atoms.

The recombination of methoxy radicals with hydrogen atoms has only been studied using the microcanonical approach as it has a much superior theoretical basis and more diverse application.

The potential describing the recombination has been formulated according to the treatment of section 6.6. The frequencies for

TABLE 6.3 CH_3O + H Potential.

Frequencies	3320 3311 3216 1657 1599 1582 1159 1064 717		
Lennard-Jones		C_{12}	C_6
C-H		21082	-56.58
H-H		6436.1	-22.87
Bonding Interaction	O-H		
		Morse	Hase	Buenker
$beta_o$		2.34888	2.34888	2.34888
a		0.0	0.1711	0.0
b		0.0	0.054	0.64144
c		0.0	-0.0618	-0.06888
D_o		436.8	436.8	436.8
r_e		0.9625	0.9625	0.9625
Range		0 → ∞	0 → ∞	1.625 → 3.5

methoxy were taken from the paper of Colwell, Amos and Handy (1984), and the parameters for the Lennard-Jones atom-atom potentials from Hirschfelder, Curtiss and Bird (1954).

Three potentials for the O-H bond were considered. They were a standard Morse, the derived dimensionless stiff Morse of Duchovic and Hase (1985), (see also Greenhill and Gilbert, 1986), and the ab initio surface of Buenker, et. al. (1984). The standard Morse was constructed using an O-H stretching frequency of 3679 cm^{-1} (Arbrow-van der Veen and Leyte, 1972). The O-H dissociation energy was taken as 436.8 $kJmol^{-1}$. All the parameters for the potentials are described in table 6.3. Figure 6.5 is a plot of the potentials used for this reaction.

High Pressure Rate Coefficients.

The results for each potential are given in table 6.4 in units of cm^3s^{-1} and plotted in figure 6.6

TABLE 6.4 High Pressure Recombination Rate Coefficients Methoxy

Temperature (K)	Recombination Rate Coefficients ($10^{-11}cm^3s^{-1}$)		
	Morse	Hase	Buenker
300	243.3	8.6	4.1
600	83.5	5.3	2.6
1000	26.4	3.2	1.6
1500	9.1	1.9	1.0
2000	4.3	1.3	0.7

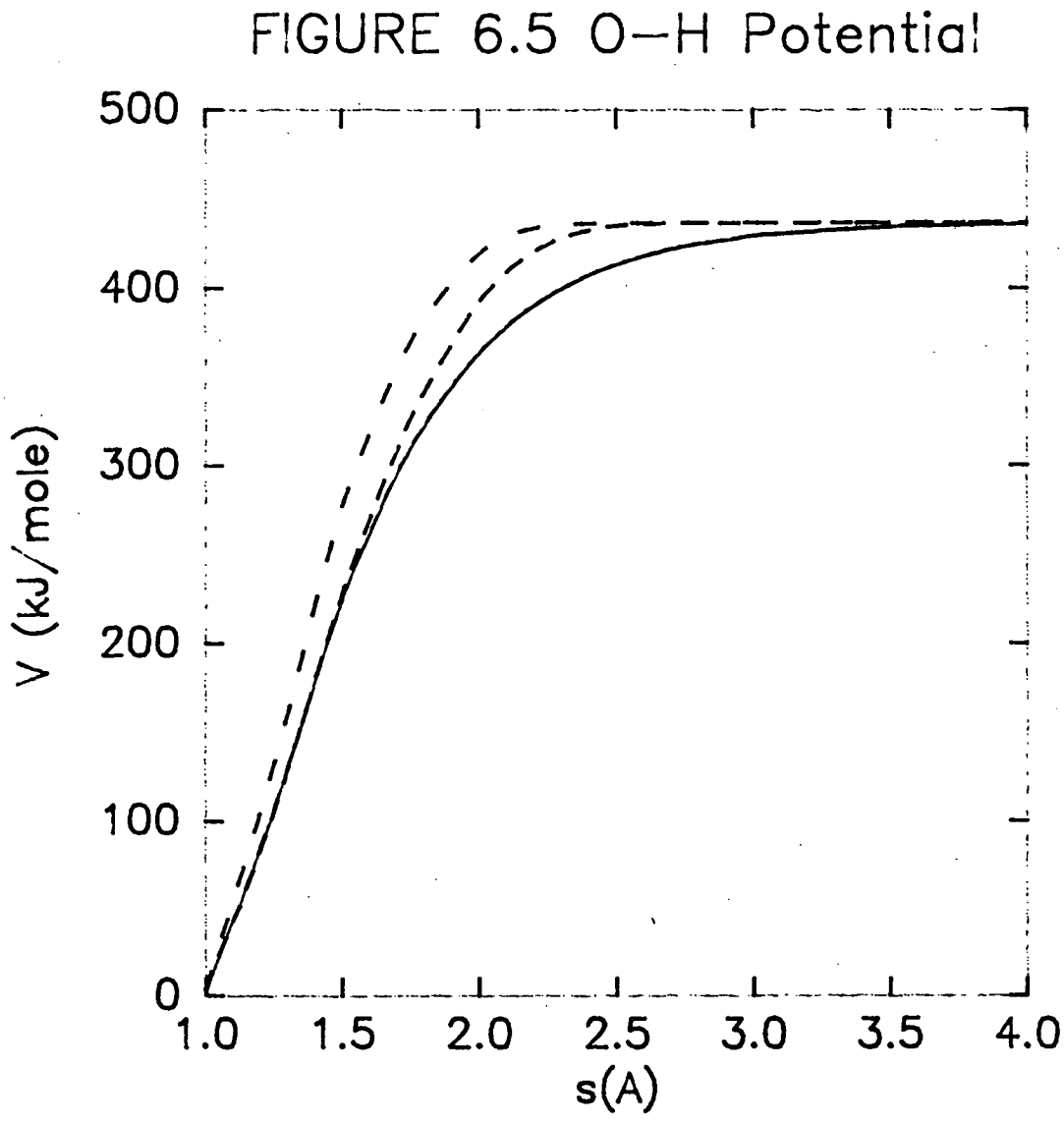

Figure 6.5 O-H Potentials for H + Methoxy Radical Recombination.

——— Morse

- - - Buenker

---- Hase

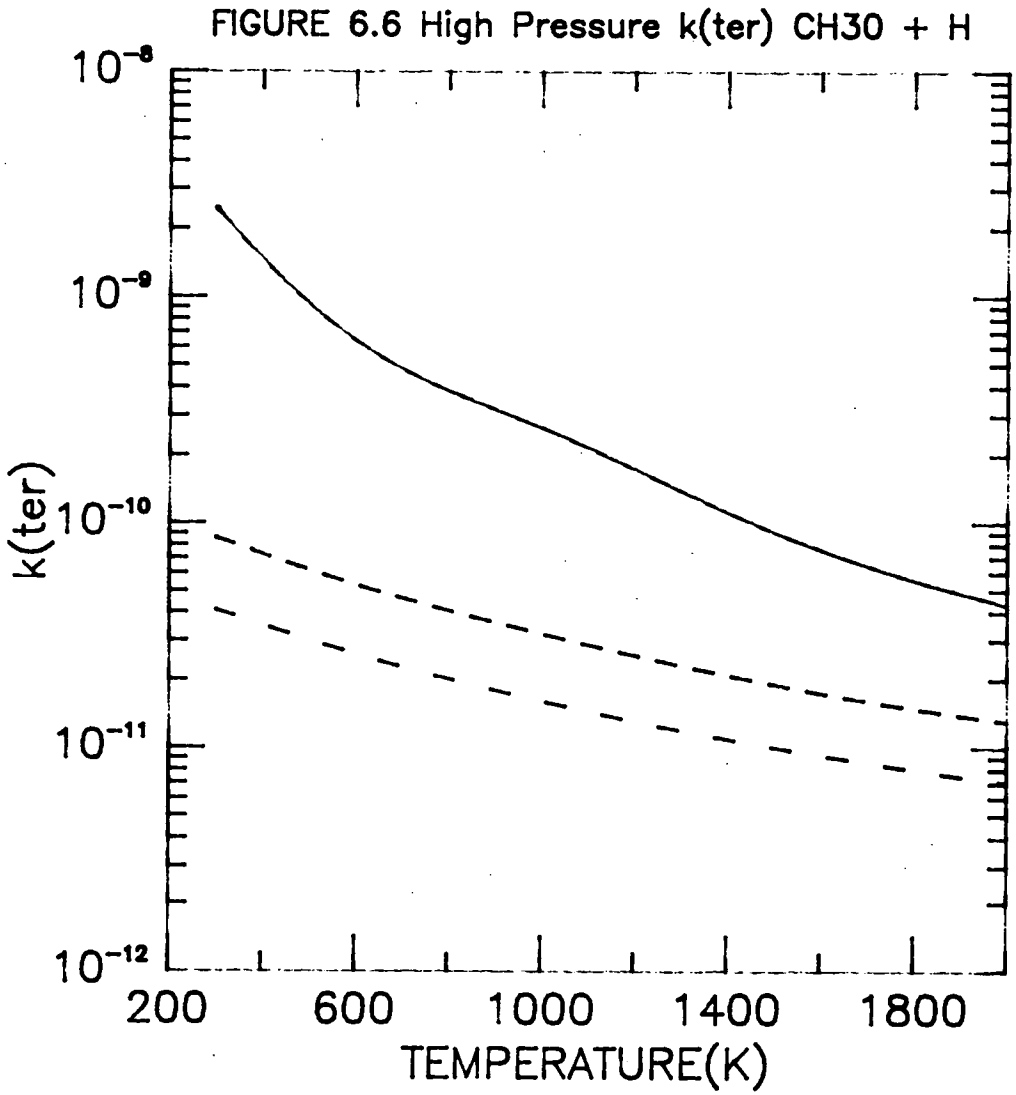

Figure 6.6 High Pressure Recombination Rate Coefficients for H + Methoxy Radicals.

——— Morse

– – Buenker.

– – – Hase.

Comparison of the results shows that the Morse potential provide rate coefficients which are much too large and approximately an order of magnitude larger than the collision frequency at room temperature. The other potentials give results which are more reasonable. The rate coefficients from the Hase potential are approximately a factor of five lower than the collision frequency at room temperature and those from the Buenker potential a further factor of two lower. All three results show a negative temperature dependence over the range studied with the most severe dependence predicted by the Morse potential.

6.7.3 The Recombination of Hydroxymethyl Radicals and Hydrogen Atoms.

This reaction has been studied under the influence of three potentials for the C-H bond from the same sources as for the recombination of CH_3O and H. The potential for the trajectory was formulated as in section 6.6.

The frequencies for hydroxymethyl were taken from the work of Saebø, Radom and Schaefer III (1983), and the Lennard Jones (12-6) parameters were as for methoxy. The Morse curve was constructed using a C-H stretching frequency of the average of the three C-H frequencies from Saebø, et al. of 3000, 2960, and 2883 cm^{-1}. The C-H dissociation energy was calculated to be 393.3 $kJmol^{-1}$. All the parameters are given in table 6.5 and the potentials are plotted in figure 6.7.

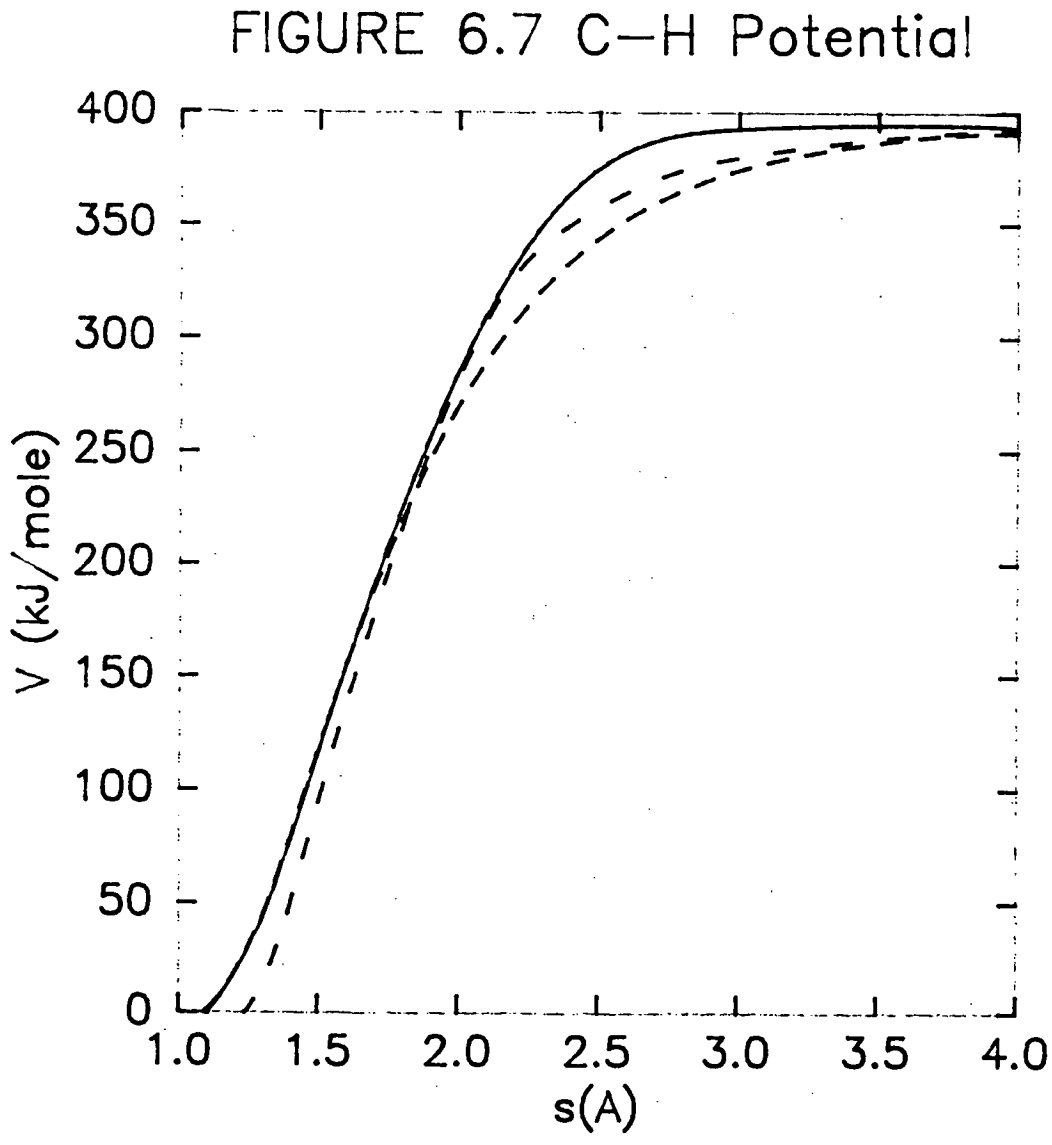

Figure 6.7 C-H Potentials for H + Hydroxymethyl Radical Recombination.

--- Morse

– – Buenker

—— Hase

High Pressure Rate Coefficients.

The high pressure rate coefficients are tabulated in table 6.6 and plotted as a function of temperature in figure 6.8.

As observed for the recombination of methoxy radicals with

TABLE 6.5 CH_2OH + H Potential.

Frequencies 3650 2960 2883 1459 1334 1183 1048 569 420			
Lennard-Jones		C_{12}	C_6
O-H		21082	-56.58
H-H		6436.1	-22.87
Bonding Interaction C-H			
	Morse	Hase	Buenker
$beta_o$	1.9486	1.9486	1.9486
a	0.0	0.1711	0.0
b	0.0	0.054	-0.03129
c	0.0	-0.0618	0.13468
D_o	393.3	393.3	393.3
r_e	1.094	1.094	1.094
Range	0 → ∞	0 → ∞	1.9 → 4.0

hydrogen, the Morse potential provides rate coefficients which are much too high; approximately two orders of magnitude greater than the collision frequency at room temperature. The results from the two ab initio potentials are much lower but in contrast to reaction R6.2 the Buenker potential provides results which are also greater than the collision frequency.

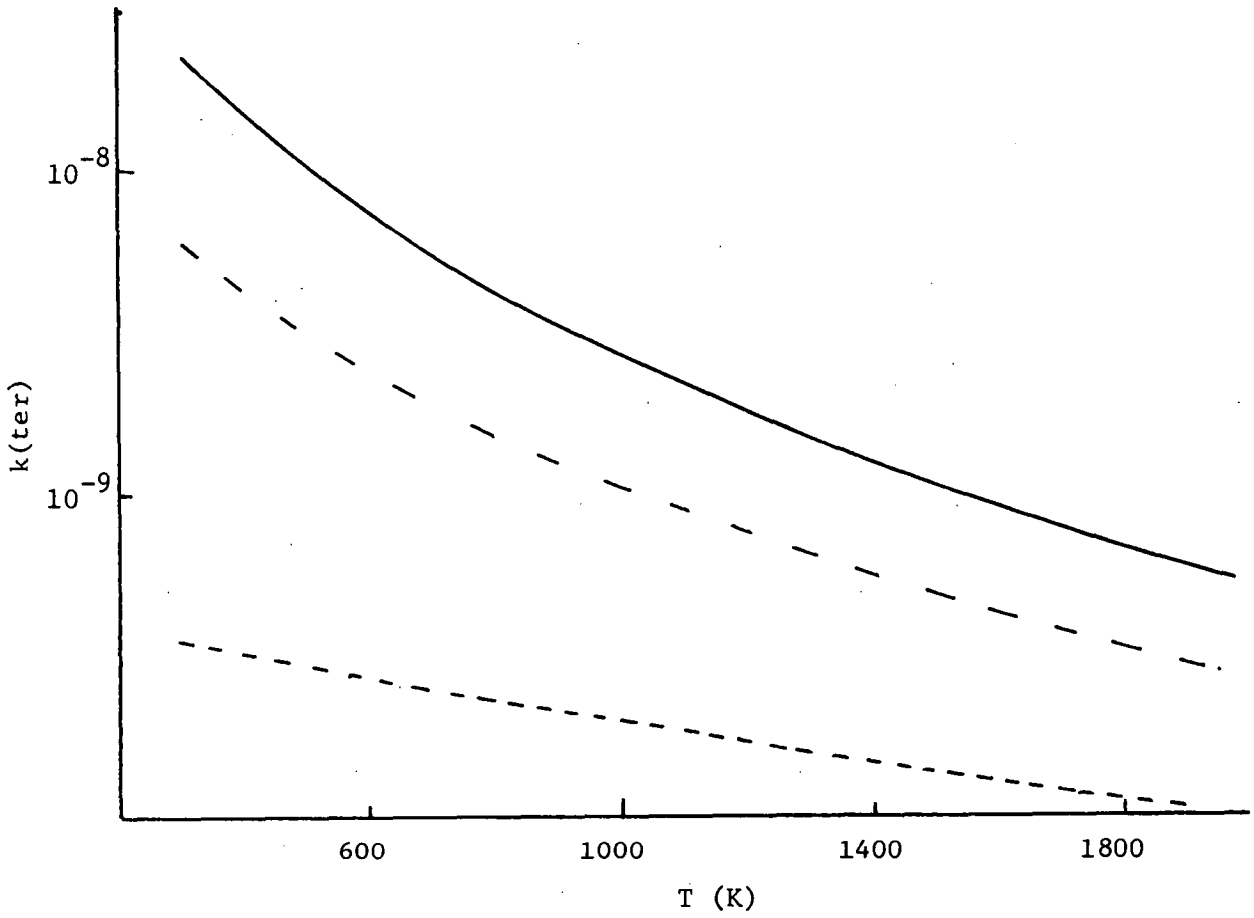

Figure 6.8 High Pressure Recombination Rate Coefficients for H + Hydroxymethyl Radicals. (——) Morse, (- -) Buenker, (- - -) Hase.

TABLE 6.6 High Press. Recomb. Rate Coefficients Hydroxymethyl

Temperature (K)	Recombination Rate Coefficients ($10^{-10}cm^3s^{-1}$)		
	Morse	Hase	Buenker
300	221.8	3.5	58.9
600	71.5	2.7	23.2
1000	26.2	2.0	10.4
1500	10.2	1.4	4.7
2000	5.2	1.0	2.7

6.8 Discussion.

6.8.1 Methyl Radical Recombination - Canonical.

The rate coefficient calculated at 300K is 40% higher than the experimental value of $6.5 \times 10^{-11}cm^3s^{-1}$. This difference, considering the level of theory used, is not highly significant and agreement is quite satisfactory. However, considering that the free energies were calculated from a normal coordinate analysis of the transition state and this is not really appropriate (see section 6.6.2), then the validity of this result must be doubtful.

Certain features of the treatment are still valid though. Firstly, it indicates that a canonical transition state can be determined from minimisation of the free energy. It also indicates

that at room temperature, the transition state occurs at considerably smaller s than that which would be predicted by the Gorin model.

6.8.2 Methyl Radical Recombination - Microcanonical.

The agreement within a factor of two at all the studied temperatures and almost within the experimental error at 300K is highly pleasing.

The transition state which contributes most to the rate of recombination at 450K of s = 0.35nm is much smaller than that predicted from the Gorin model (s = 0.43nm). Lesser contributions come from states that are even smaller at higher energies above the threshold energy. This provides further evidence that the Gorin model is based on inconsistencies and false premises. (Garrett and Truhlar, 1979 (1); Rai and Truhlar; Bunker and Pattengill; Hase, 1983 (2); Duchovic and Hase)

Also the prediction that many transition states are capable of contributing to the thermal rate indicates that these should be taken into consideration when such calculations are performed, particularly at higher temperatures where the transition states for higher energies become more important. This spread of transition states is also largely responsible for the negative temperature dependence obtained. While canonical transition state theory can predict a negative temperature dependence as shown by Hase (1972, 1976) it is necessary to include states below the threshold which counts regions of phase space which are not formally reactive.

This description is not totally valid and using the microcanonical approach provides a much more rigorous technique without any necessity to include empirical perturbations in the theory to provide agreement with experiment.

It is also interesting to compare this treatment with one by Wardlaw and Marcus who have calculated the density of states for the transition states using semi-classical methods on a non-separable potential. Such calculations are complex and computationally difficult for large systems.

In the technique developed here, the programs required for the calculation are commercially available (Hase, 1983 (1); Gilbert, 1983) and will run at a relatively low cost on most computers. The total procedure is quite simple and does not require transformations to action-angle coordinates or other inconveniences.

Computationally it is not much more difficult than a standard RRKM calculation.

6.8.3 Methoxy/Hydroxymethyl + Hydrogen Recombination.

The rate constants obtained are plotted in figures 6.6 and 6.8. The difference in the results for each reaction appears to be attributable to the different values of the potentials in the region of the transition state. The Morse potential has energies which are significantly lower than the dissociation energy (critical energy, E_o) over the range of s values associated with transition states than do the other potentials. It is apparent that even though the densities of states at energies which are less than E_o are excluded

as contributors to the thermal rate, the effect on the densities of states is pronounced. The result is that $\int_{E_o}^{E} \rho^{+}(E)dE$ is larger than that which is calculated from the other potentials. This results in a very high rate constant. The accuracy of the rate constants calculated is thus very dependent upon the accuracy of the potential used.

While the positions predicted for the transition states do not vary considerably from potential to potential there does appear to be a slight bias towards larger transition states for potentials which give larger k^{∞}_{ter} values at those energies close to threshold (which will contribute most to the thermal rate.)

The transition states are plotted as a function of energy for each of the potentials in figures 6.9 and 6.10. For reaction R6.2

$$CH_3O + H + M \longrightarrow CH_3OH + M \qquad R6.2$$

the predicted transition states are generally smaller than that predicted by the Gorin model of approximately 0.28nm for the Hase and Buenker potentials, but the effect is not as pronounced as for the recombination of methyl radicals.

For reaction R6.3

$$CH_2OH + H + M \longrightarrow CH_3OH + M \qquad R6.3$$

the Morse and Buenker potentials predict transition states at approximately the Gorin prediction of 0.31nm but the Hase potential (which provides more plausible rate constants which are less than the collision frequencies) predicts a slightly tighter transition state at approximately 0.29nm.

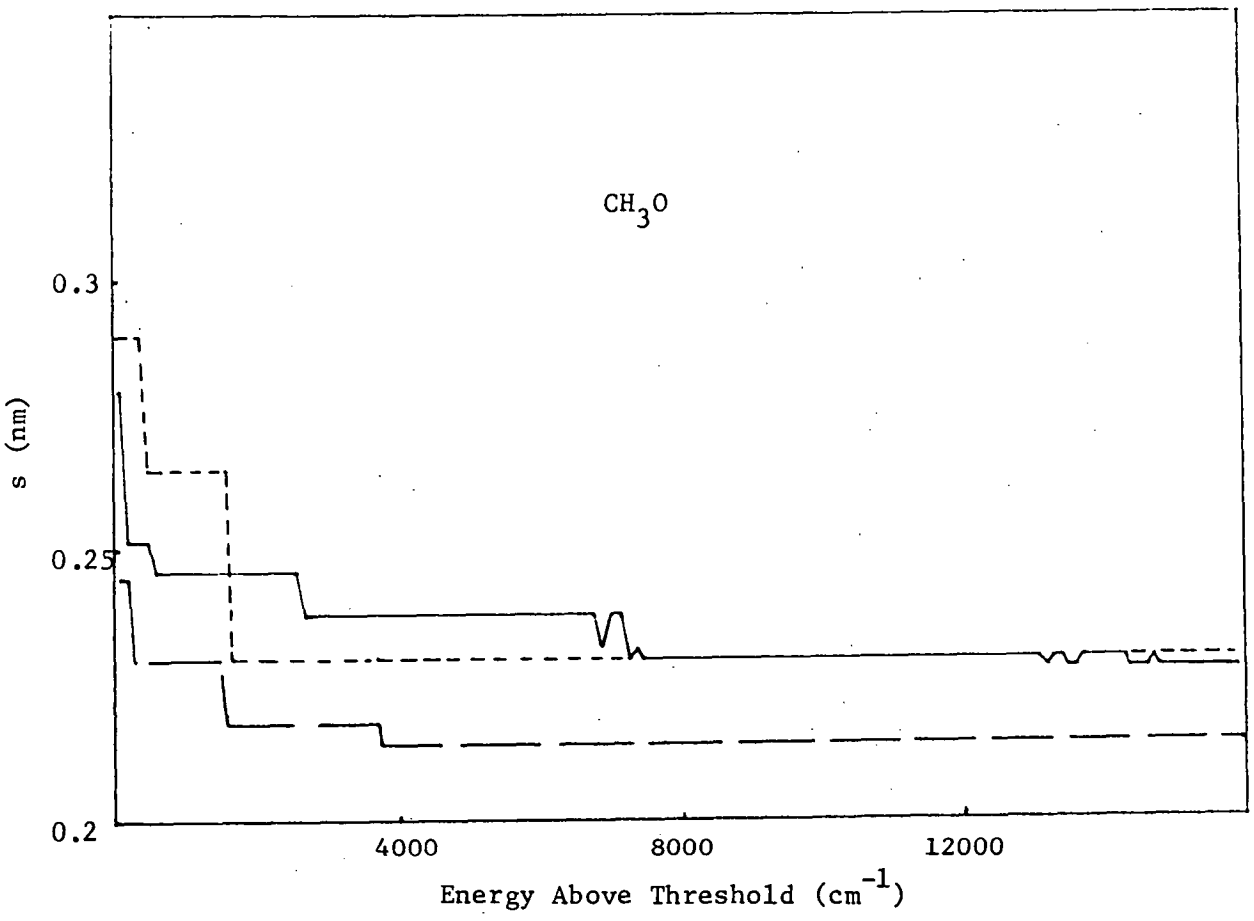

Figure 6.9 Position of the Transition State as a Function of Energy Above Threshold.

---- Morse

— — Buenker

——— Hase

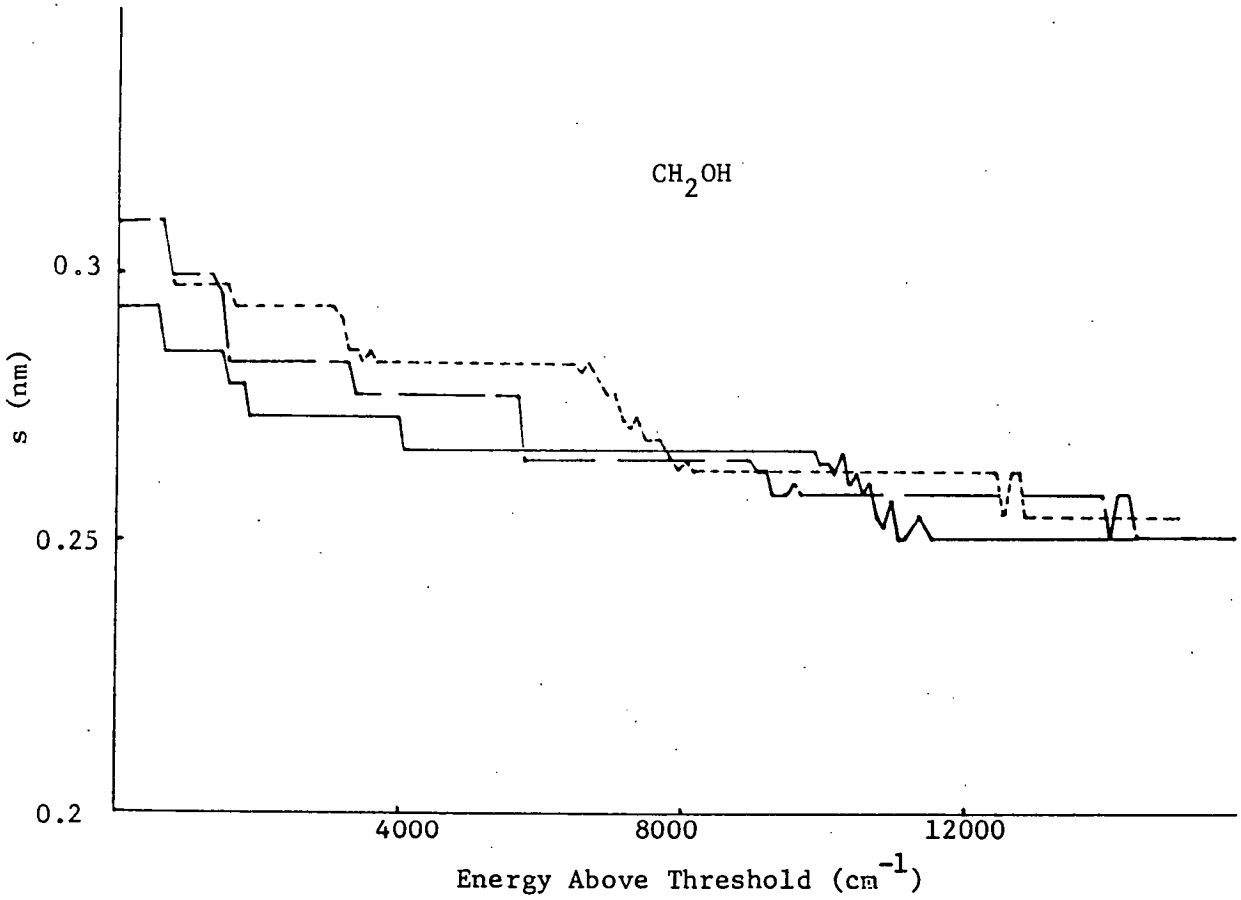

Figure 6.10 Position of the Transition State as a Function of Energy Above Threshold.

---- Morse

— — Buenker

——— Hase

Pressure Dependence

The pressure dependences of the recombinations have been calculated and are displayed in figures 6.11 and 6.12 for the Hase potential only. The rate constants calculated indicate that under typical experimental conditions such as used by Hoyermann et al. (1981a,b), the contribution to H atom loss could be the order of 5-50 s^{-1} and at higher pressures, such as is common in photolysis experiments, considerably higher.

The relative high pressure rates of recombination for the two reactions of approximately $k^{\infty}_{R7.3}/k^{\infty}_{R7.2} = 5$ is due largely to the difference in E_o values of 393.3 $kJmol^{-1}$ (C-H) and 436.8 $kJmol^{-1}$ (O-H).

6.9 Summary and Extensions

The theory has been used to successfully predict the rate constant for the recombination of CH_3 radicals and predictions have been made for the recombinations of H atoms with CH_2OH and CH_3O. Although the results for these two reactions appear to be high when compared with the experimental evidence of Hoyermann, et al. (1981a,b), this can be attributed to a lack of knowledge of the potential at large separation of the bond being formed.

The adaptation of the physical Gorin model and the calculation of the density of states by interpolation have enabled implementation of microcanonical variational transition state theory

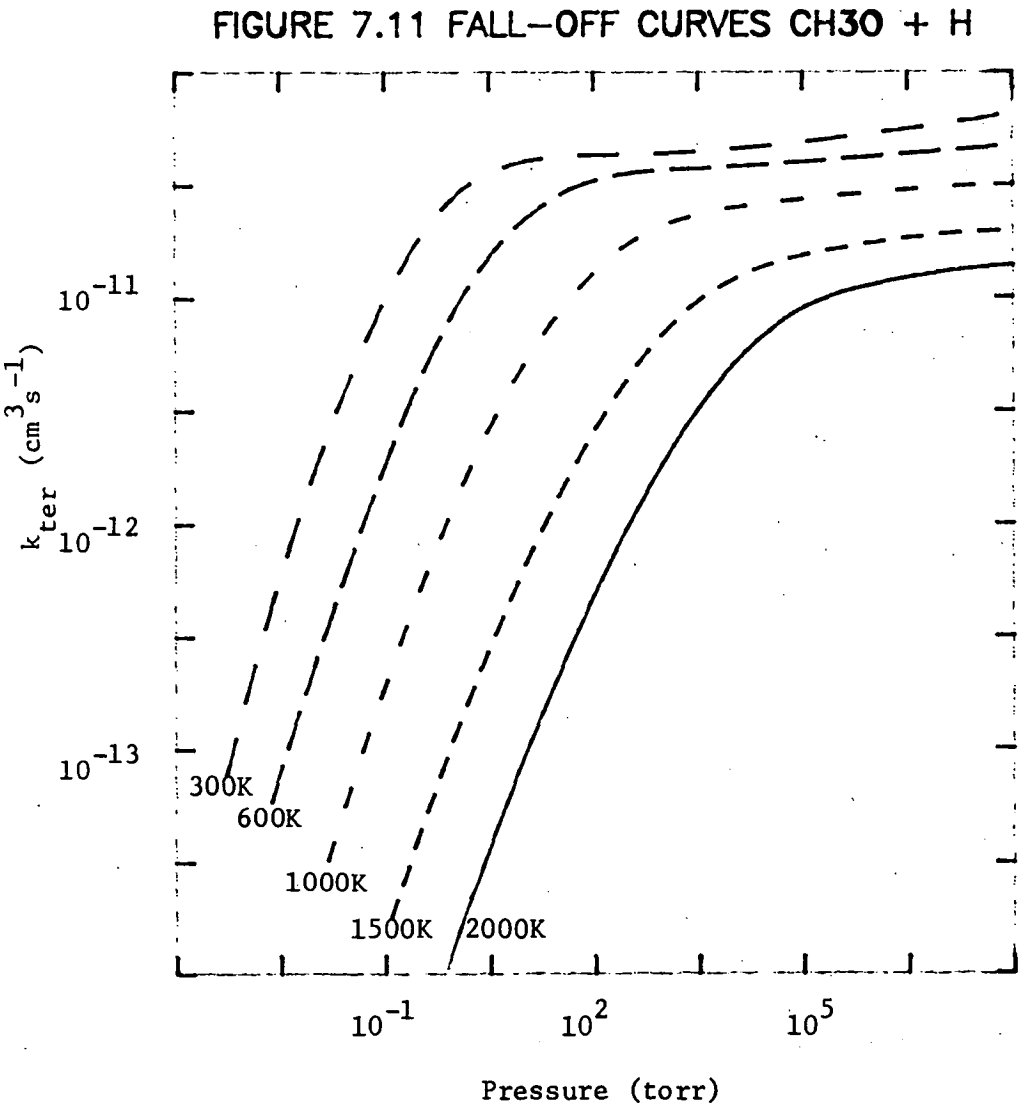

Figure 6.11 Fall-off Curves for the Recombination of H + CH_3O From the Hase Potential.

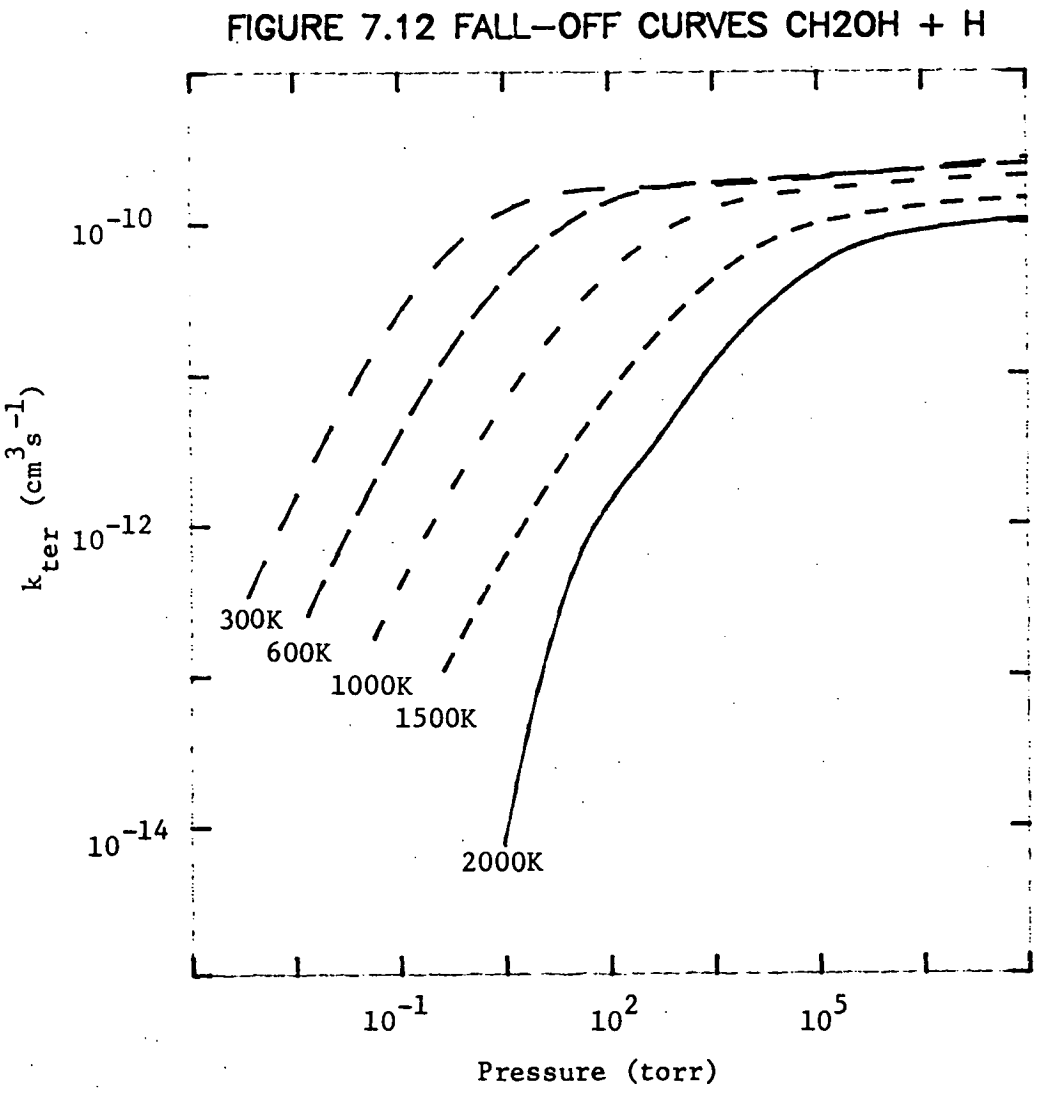

Figure 6.12 Fall-off Curves for the Recombination of H + CH_2OH From the Hase Potential.

in a totally *a priori* manner to termolecular reactions without barriers.

Transition state theory is applicable to all reactions provided the transition state can be described. Corrections for such things as quantum mechanical tunneling and electronically non-adiabatic reactions can be made (Smith, 1980) but they are not simple and at this stage it is not envisaged that the theory developed here could be extended to these phenomena.

However, extension to unimolecular reactions with barriers is contemplatable and formally only requires a knowledge of the potential in the region of the interaction. This is, naturally, a more difficult problem than reactions without barriers but it should be possible. Logically, a further extension is to bimolecular reactions and similar comments apply to these as to unimolecular reactions with barriers.

Initially, though it is necessary that the theory be extensively validated for other reactions without barriers.

One final aspect is that if the technique proves to be valid and provides accurate predictions than it should be possible, for certain classes of reactions, to reverse the process and refine the potential surfaces in the critical regions. However, this will only be valid if the technique is unambiguous in its predictions. That is, only if different potentials do not give the same results.

It could in no way replace *ab initio* calculations or experimental evidence as it could only provide features in the critical region from which the transition states are drawn.

6.10 References

Adamson, A.W., 'A Textbook Of Physical Chemistry', Academic Press, New York, 1973.

Atkins, P.W., 'Physical Chemistry', 2nd Edition, OUP, London, 1983.

Benson, S.W., 'Thermochemical Kinetics' 2nd. Edn. (John Wiley: New York 1976).

Benson, S.W., Can. J. Chem., 1983, **61**, 881.

Benson, S.W., J. Phys. Chem., 1985, **89**, 4366.

Bowman, J.M., Ju, G-Z., and Lee, K.T., J. Phys. Chem., 1982, **86**, 2232.

Cohen, L.K., and Pritchard, H.O., Can. J. Chem., 1985, **63**, 2374.

Duchovic, R.J., and Hase, W.L., J. Chem. Phys, 1985, **82**, 3599; 1985, **83**, 3448.

Garrett, B.C. and Truhlar, D.G., J. Am. Chem. Soc., 1979a, **101**, 4534.

Garrett, B.C. and Truhlar, D.G., J. Phys. Chem., 1979b, **83**, 1079.

Garrett, B.C. and Truhlar, D.G., J. Phys. Chem., 1979c, **83**, 1052.

Gilbert, R.G., QCPE, 1983, **3**, 64.

Gorin, E., J. Chem. Phys, 1939, **7**, 263; 1939, **7**, 642.

Greenhill, P.G., and Gilbert, R.G., J. Phys. Chem., 1986, 90, 3104.

Hase, W. L., QCPE, 1983, **3**, 14. (1)

Hase, W. L., Acc. Chem. Res., 1983, **16**, 258. (2)

Hase, W. L., J. Chem. Phys, 1972, **57**, 730.

Hase, W. L., J. Chem. Phys, 1976, **64**, 2442.

Hoyermann, K., Sievert, R., and Wagner, H.Gg., Ber. Bunsenges. Phys. Chem., 1981, **81**, 149.

Hoyermann, K., loftfield, N.S., Sievert, R., and Wagner, H.Gg., 18th Symp. (Intl.) Combustion, 1981, 831.

Isaacson, A.D., and Truhlar, D.G., J. Chem. Phys, 1982, **76**, 1380.

Laidler, K.J., and King, M.C., J. Phys. Chem., 1983, **87**, 2656.

Macpherson, M.T., Pilling, M.J., and Smith, M.J.C., J. Phys. Chem., 1985, **89**, 2268.

Mahan, B.H., J. Chem. Ed., 1974, **51**, 709.

Miller, W.H., Acc. Chem. Res., 1976, **9**, 306.

Miller, W.H., Schwaartz, S.D., and Tromp, J.W., J. Chem. Phys., 1983, **79**, 4889.

Pechukas, P., Ber. Bunsenges. Phys. Chem., 1982, **86**, 372.

Quack, M., and Troe, J., Ber. Bunsenges. Phys. Chem., 1974, **78**, 240; 1975, **79**, 170;

Rai, S. N. and Truhlar, D. G., J. Chem. Phys., 1983, **79**, 6046.

Smith, I.W.M., 'Kinetics And Dynamics Of Elementary Gas Reactions', Butterworths, London, 1980.

Troe, J., J. Chem. Phys., 1981, **75**, 226.

Truhlar, D.G., and Garrett, B.C., Ann. Rev. Phys. Chem., 1984, **35**, 159.

Truhlar, D.G., Isaacson, A.D., Skodje,R.T., and Garrett, B.C., J. Phys. Chem., 1982, **86**, 2252.

Wardlaw D.M., and Marcus, R.A., J. Chem. Phys., 1985, **83**, 3462.

Wong, W.H., and Marcus, R.A., J. Chem. Phys., 1971, **55**, 5625.

Chapter 7.

7.1 Final Remarks.

Five reactions of considerable importance to methanol combustion and one of importance to ethanol combustion have been investigated. This has improved our knowledge of the combustion phenomenon.

The reactions are.

$$CH_3OH + OH \longrightarrow CH_3O/CH_2OH + H_2O \qquad R7.1$$

$$CH_3CH_2OH + OH \longrightarrow CH_3CH_2O/CH_3CHOH + H_2O \qquad R7.2$$

$$CH_3O + M \longrightarrow CH_2O + H + M \qquad R7.3$$

$$CH_2OH + M \longrightarrow CH_2O + H + M \qquad R7.4$$

$$CH_2OH + H + M \longrightarrow CH_3OH + M \qquad R7.5$$

$$CH_3O + H + M \longrightarrow CH_3OH + M \qquad R7.6$$

The rate coefficients of reactions R7.1 and R7.2 have been determined in the temperature ranges 255K - 703K and 260K - 460K respectively. As indicated, alternate pathways are present which have not been taken into account in any of the modelling studies performed to date. The production of CH_3O at higher temperatures in R7.1 needs to be explicitly taken into account as it has a very different reactivity with O_2 when compared with the reactivity of CH_2OH with O_2.

The decomposition processes R7.3 and R7.4 have been studied using an easily implemented form of RRKM theory incorporating a modified Gorin model. The procedure has been fully described to make it more accessible and tractable to use. These two reactions have

been shown to be more important than previously assumed with rate constants up to 70 times those originally used in modelling.

Reactions R7.5 and R7.6 have been investigated as they might be expected to be important in systems where there are large numbers of H atoms. They have been found to be very fast and of some significance at low to intermediate temperatures, particularly at higher pressures.

The nature of these reactions has lead to the development of an a priori technique which will have application to any reaction where the potential surface in the region of the bond breaking or reformation. To date it has only been applied to reactions R7.5 and R7.6 and the recombination of methyl radicals as these reactions are examples of simple fission transition states without barriers.

The technique utilises microcanonical transition state theory and a modified Gorin model. The conventional problem of the description of the transition states in reactions without barriers has been overcome by representing the change from external rotations of the reactants to internal bending modes of the products by a novel interpolation.

This procedure is considerably simpler to implement than classical trajectory calculations or quantum mechanical calculations and yet can be performed with only a knowledge of molecular parameters of reactants and products and the potential surface along the minimum energy path for the reaction.

APPENDIX A.

Experimental First Order Rate Constants.

Table A.1. Experimental First Order Rate Constants Methanol

T K	[MeOH] $x10^6$M	P mmHg	k_{1st} s^{-1}	S s^{-1}
260	6.66	100	3384.1	8.6
			4192.4	15.0
			4061.3	16.8
			3684.5	11.0
			3987.0	13.1
			3712.9	11.6
			4162.8	16.4
			4180.4	16.5
	12.65	101	4728.7	45.7
			4743.6	24.0
			5747.2	20.7
			6758.2	27.9
			4756.1	33.1
			7076.9	37.6
			5036.3	19.9
			5159.5	19.7
			5691.2	23.4
			6681.4	21.0
			6279.8	20.8
			6267.0	23.3
	18.735	75	6743.2	29.6
			8184.7	27.0
			7826.4	36.1
	25.23	101	9622.1	63.8
			9471.9	86.2
			9862.5	62.0
			9858.2	80.2
			10255.5	75.0

T K	[MeOH] $x10^6$M	P mmHg	k_{1st} s^{-1}	S s^{-1}
292	1.0581	100	1427.2	4.7
			1531.0	5.5
			1414.4	4.7
			1335.5	3.4
			1326.8	4.2
	2.8849	51	2575.5	11.7
			1935.6	12.6
			1588.8	14.4
			2160.8	16.3
			1795.3	12.0
	5.686	100	3173.9	14.7
			3274.4	14.7
			4178.6	25.6
			3398.6	20.4
			3439.4	17.5
	14.394	101	7701.1	62.5
			9798.8	62.4
			9833.4	90.3
			7503.6	65.5
			7504.0	65.0
			9049.1	63.0
	22.098	101	9673.2	166.5
			13336.1	162.4
			9090.0	139.3
300	3.154	50	2014.1	24.6
			1705.7	47.2
			1170.2	18.2
			1715.6	24.0
			2172.2	39.2
			2960.0	65.4

T K	[MeOH] x10^{6}M	P mmHg	k_{1st} s^{-1}	S s^{-1}
	6.308	100	2719.6	18.0
			3988.1	23.1
			3420.8	32.6
			3370.4	24.9
			2581.5	20.8
			3114.5	28.8
	26.49	100	11179.2	142.4
			16569.2	583.7
			12347.0	240.4
			13262.4	266.5
			11242.6	226.0
			12087.7	224.3
	52.98	100	32313.6	1001.0
	53.33	100	27453.0	1477.9
	53.51	100	22426.5	998.5
331	4.762	100	2494.9	6.1
			2113.6	5.1
			2430.8	13.0
			2316.2	10.9
			1919.9	6.8
			2107.9	7.1
	9.835	100	4986.9	18.1
			5482.2	23.4
			5562.1	23.9
			5738.9	29.2
			6883.9	45.8
			5995.6	27.8
	14.761	75	8237.4	40.2
			9298.6	23.1
			11557.9	83.1

T	[MeOH]	P	k_{1st}	S
K	$x10^6$M	mmHg	s^{-1}	s^{-1}
			10327.6	73.8
			10594.5	216.0
	19.622	100	13644.1	88.0
			11247.7	57.4
			13847.3	156.9
			12697.1	72.2
			10814.1	103.8
			12326.9	200.7
REANALYSE 362K DATA				
362	4.44	102	1932.6	7.0
			2322.0	6.4
			2255.4	6.8
			2190.2	10.2
			2105.4	8.4
			2094.1	10.0
	8.993	100	5673.4	20.0
			5419.5	28.5
			6252.5	24.8
			5194.3	48.7
			6980.7	39.3
			5747.7	20.8
			5713.6	21.7
			6016.0	27.0
			8444.7	45.0
			6586.5	34.4
			6307.2	24.8
	13.456	75	11958.9	81.4
			11494.8	62.5
			13154.2	73.4
			9057.9	73.6

T K	[MeOH] x10^{6}M	P mmHg	k_{1st} s^{-1}	S s^{-1}
			13490.4	102.4
			9200.3	123.5
	17.941	100	12545.0	149.9
			12198.7	179.9
			13165.3	190.2
			11596.7	113.7
			10886.3	126.2
453	0.683	100	2340.6	5.7
			2373.1	5.5
			1607.0	3.2
			1364.4	3.2
			1235.0	3.2
	2.542	99	3445.3	13.6
			3877.1	11.8
			3378.4	10.7
			2885.7	10.2
			2142.3	5.4
	5.087	100	5260.9	35.5
			6316.2	49.6
			6431.6	28.8
			5997.9	40.0
			7579.8	69.8
	9.186	100	8585.4	34.8
			8952.9	36.5
			10354.3	55.4
			8054.9	56.7
			8805.6	87.0
465	0.666	100	3788.9	13.9
			3828.7	17.4

T K	[MeOH] x10^{6}M	P mmHg	k_{1st} s^{-1}	S s^{-1}
			3738.1	21.4
			3184.6	19.4
			3848.3	18.1
	2.476	100	5863.3	30.2
			5061.4	31.7
			5371.3	21.9
			5997.5	28.9
			6288.0	32.0
	5.005	101	6691.9	43.9
			7522.6	74.0
			6562.1	45.0
			7688.1	77.5
			7765.7	43.4
	8.949	100	10645.8	102.9
			11435.0	62.4
			9920.1	54.8
			9572.6	49.9
			10814.2	77.6
570	0.538	99	4435.6	25.1
			4028.3	31.3
			4095.3	24.4
			3449.8	25.5
			3838.5	13.1
	2.040	101	5455.1	49.0
			5323.1	57.1
			5516.2	36.7
			6752.8	38.8
			6193.0	44.7
	4.043	100	8176.0	74.3
			10004.0	63.2

T K	[MeOH] $x10^6$M	P mmHg	k_{1st} s^{-1}	S s^{-1}
			8950.2	63.9
			7232.8	58.0
			6874.3	68.5
	7.301	101	11617.6	172.7
			11971.6	316.6
			12622.1	299.9
			13362.2	294.1
			9560.8	276.4
597.5	0.518	99	1970.7	9.3
			1450.4	7.1
			876.6	6.0
			975.9	3.7
			976.3	3.6
	1.927	100	3815.9	17.7
			4716.6	20.8
			4693.8	28.4
			3968.9	14.7
			4259.7	23.3
	3.857	102	5540.5	28.5
			6327.2	51.7
			5925.7	45.8
			5572.4	60.9
			5341.6	62.9
	6.965	90	13759.5	295.1
			10395.5	97.6
			11282.6	242.2
			9318.4	46.7
			10192.9	83.3

T K	[MeOH] x10^{6}M	P mmHg	k_{1st} s^{-1}	S s^{-1}
669	0.458	99	4991.1	69.1
			4510.4	98.4
			4096.9	37.1
			3540.7	51.6
			4002.1	32.1
	1.721	100	5303.4	55.0
			6151.1	82.7
			8557.9	189.4
			5758.9	42.7
			6400.6	61.7
	3.479	101	8297.9	96.5
			10750.2	144.0
			9455.1	122.6
			9047.9	324.0
			7621.1	94.0
	6.220	100	17702.4	220.5
			11052.2	309.6
			17598.3	230.5
			13320.1	369.3
803	0.193	50	1363.6	47.7
			1384.4	20.6
			1349.4	21.0
			1946.1	45.8
			1627.0	36.2
	0.385	100	2234.0	23.3
			2533.0	18.6
			2372.6	17.4
			2160.6	13.5
			2835.7	30.7

T	[MeOH]	P	k_{1st}	S
K	$x10^6$M	mmHg	s^{-1}	s^{-1}
	1.434	100	5678.8	123.7
			6410.8	142.1
			5538.4	111.1
	2.870	101	8091.2	243.6
			9686.4	213.4
			12436.0	555.1

Table A.2 Experimental First Order Rate Constants For OH + CD_3OH

T K	$[CD_3OH]$ $x10^6$M	P mmHg	k_{1st} s^{-1}	S s^{-1}
293	1.729	102	1598.2	9.4
			1566.1	20.5
			1179.5	13.4
			1174.0	11.0
	6.815	108	2882.7	19.5
			2674.6	19.7
			3454.2	54.2
			3321.6	39.0
			3359.2	30.1
	13.046	101	4474.8	40.3
			4631.7	53.6
			4260.0	73.1
			5872.7	104.2
			5041.9	38.5
	23.282	103	7058.4	79.0
			7582.0	72.2
			8054.5	63.1
			8609.5	142.2
			9333.4	87.6

Table A.3 First Order Rate Constants For OH + Ethanol

T K	[EtOH] $x10^6$ M	P mmHg	k_{1st} s^{-1}	S s^{-1}
255	0.619	50	2126.7	13.5
			1714.5	8.1
			2066.4	11.4
			2249.9	21.8
			2150.7	11.5
			1911.3	8.1
	1.239	100	3475.0	8.0
			3029.5	13.0
			3251.7	21.8
			3291.6	15.7
			3070.0	15.2
			2746.0	11.3
	2.478	200	5798.6	22.5
			5091.9	32.5
			5765.3	23.8
			6378.3	34.6
			5983.6	26.3
			5932.0	31.3
	3.955	75	9877.2	116.8
			7864.6	139.9
	5.273	100	8402.0	113.9
			11618.0	154.0
			12545.5	216.8
			13041.9	309.5
			12132.4	424.7
273	0.579	50	2222.0	17.6
			2049.8	7.8
			2013.4	11.3
			1982.7	11.4

T K	[EtOH] x10^{6}M	P mmHg	k_{1st} s^{-1}	S s^{-1}
			1920.9	7.6
			1576.6	7.1
	1.157	100	3395.2	7.5
			4136.7	13.9
			3289.4	10.1
			3866.7	14.5
			3004.7	10.7
			2978.6	10.0
	3.475	70	8145.5	42.0
			9358.6	39.9
			9175.9	52.6
	5.063	102	12726.7	135.4
			12444.1	137.5
			13427.5	279.1
			13054.8	144.7
289	0.227	100	1220.5	7.2
			1669.5	9.3
			1618.7	8.9
			1267.4	6.7
			1164.2	5.5
			1164.2	5.5
			1164.7	5.3
			920.5	5.1
			912.0	3.9
			1013.6	5.1
	2.836	103	7283.9	51.8
			7011.9	42.2
			8722.0	61.9
			7408.1	52.9

T K	[EtOH] x10^{6}M	P mmHg	k_{1st} s^{-1}	S s^{-1}
			9051.4	71.6
			10208.6	62.3
			8876.5	51.3
			8753.9	47.3
			7542.5	40.7
			9192.2	42.0
	4.642	100	10553.3	70.4
			17772.7	452.9
			17828.1	275.3
			18693.3	608.8
			18563.8	617.4
			12879.4	183.0
			7910.2	246.6
			14455.9	265.6
			15693.2	408.7
			17575.0	305.5
293	1.066	100	3686.7	8.1
			3959.5	14.9
			3963.4	15.9
			3740.1	17.5
			3316.5	8.4
			3216.7	6.6
	1.817	170	5592.9	18.3
			6875.7	64.8
			6392.5	82.7
			6526.9	38.8
			6001.0	43.9
			6208.3	83.2
	2.203	51	5732.5	94.5
			6731.7	45.6

T K	[EtOH] x10^{6}M	P mmHg	k_{1st} s^{-1}	S s^{-1}
			6174.2	54.2
			7294.0	56.3
			7431.2	62.2
	3.240	75	7269.7	56.1
			10576.2	91.4
			10159.0	170.6
			8126.9	63.8
			11233.3	166.9
			9983.3	73.1
	3.982	76.5	7087.6	45.6
			10458.4	75.1
			9272.5	57.9
			7972.7	82.7
			10823.3	87.7
	4.335	100	12409.4	291.1
			13442.5	330.7
			12335.6	148.8
			12650.8	128.8
			13886.6	122.6
	5.241	100	11392.2	88.3
			13012.8	82.3
			14496.4	121.3
			13091.9	105.5
	5.40	125	15117.6	64.5
			14352.5	65.8
331	0.470	50	1906.4	6.3
			2070.0	8.7
			2265.4	11.9
			2303.3	9.2
			2100.2	9.5

T K	[EtOH] x10^{6}M	P mmHg	k_{1st} s^{-1}	S s^{-1}
			1979.4	7.3
	0.957	102	3386.8	8.0
			3662.6	32.0
			3354.2	18.2
			4253.2	26.4
			3526.6	18.6
			3187.3	19.9
	2.302	60	8427.1	79.1
			7213.7	55.7
			8143.9	32.2
			7818.1	62.8
			8790.3	49.1
	3.837	100	10576.3	109.9
			10515.1	135.4
			12716.8	92.1
			12170.6	148.1
			13674.6	330.0
			10050.3	122.7
360	0.432	50	1866.1	9.1
			1980.9	14.7
			1890.3	7.6
			1832.4	7.2
			2081.8	8.2
			1752.3	9.5
	0.864	100	3446.4	17.1
			3376.9	15.1
			3694.4	16.8
			3890.5	28.7
			3488.1	17.0
			2676.2	15.3

T K	[EtOH] x10^{6}M	P mmHg	k_{1st} s^{-1}	S s^{-1}
	2.117	60	8223.2	61.2
			7386.8	48.3
			7145.5	41.2
			7782.3	118.4
			7186.9	61.4
			6374.7	31.1
	3.528	100	13632.5	17.1
			9556.9	156.7
			10579.0	68.4
			10298.7	70.2
			10755.3	130.3
			11766.3	97.1
369	0.180	101	1476.0	10.0
			1291.7	10.5
			1056.8	6.3
			1475.9	9.9
			1117.3	5.5
			1476.0	11.7
			1039.2	8.7
			906.0	5.4
			854.5	5.4
			934.9	5.5
	2.160	100	7097.0	52.6
			8375.3	61.6
			8291.2	83.2
			7045.2	55.8
			11013.1	123.1
			8823.6	72.7
			9327.0	74.8
			9198.1	67.6

T K	[EtOH] x10^{6}M	P mmHg	k_{1st} s^{-1}	S s^{-1}
			9965.9	168.9
			6745.3	68.0
	3.642	100	16707.5	240.1
			18803.1	216.3
			18739.8	281.6
			13825.0	260.2
			13824.9	260.2
			18743.1	268.9
			17276.5	383.9
			20426.5	452.7
			11638.6	250.1
			13148.0	146.6
459	0.143	100	1786.7	14.3
			1632.7	12.5
			1580.9	11.6
			1437.6	11.5
			1360.3	7.4
			1360.1	7.7
			1043.2	5.1
			1075.8	7.3
			1042.8	5.3
	1.736	100	5807.5	69.8
			8166.7	104.8
			5807.3	70.1
			7984.6	66.4
			9587.5	111.6
			9846.9	93.4
			9229.2	89.3
			9133.0	105.5
			9128.6	105.9

T K	[EtOH] $x10^6$ M	P mmHg	k_{1st} s^{-1}	S s^{-1}
			6381.7	81.5
	2.928	100	11284.9	140.5
			14324.0	157.5
			12401.8	196.2
	2.977	101	11344.6	196.8
			15087.6	315.5
			9621.1	176.7
			12758.3	289.8
			11882.7	498.3
			9473.3	217.6

APPENDIX B.

Preparation of Dimethyl Ether.

APPENDIX B.

Preparation of Dimethyl Ether.

A three neck flask was fitted with a nitrogen inlet, a tall stillhead, and a dropping funnel. A trap fitted with teflon taps on inlet and outlet was immersed in liquid nitrogen and connected to the stillhead via an adapter. 40 ml. of conc. H_2SO_4 was put in the flask and a slow N_2 purge started. Methanol (B.D.H. Analar), 40 ml., was added dropwise to the H_2SO_4 with stirring. The mixture was heated to 80 C with a water bath and a further 50-100ml CH_3OH added over about 4 hours with stirring. Dimethyl ether distilled from the mixture and condensed in the trap.

The product was transferred to a vacuum line and distilled trap to trap twice. GC/MS analysis indicated that CH_3OCH_3 was formed with approximately 2% contamination by CH_3OH.

APPENDIX C.

Calculation of Recombination Rate Coefficients by μVTST.

Appendix C.

Calculation of Recombination Rate Coefficients by μVTST.

The following flowchart gives a brief step by step guide to the implementation of μVTST as treated in this thesis. The two major programs for the trajectory calculation and for the RRKM calculation are available from Quantum Chemistry Program Exchange (Q.C.E.P.) as referenced in the text and at the end of this appendix.

Three other small programs are required to link the usage of the main programs. They are programs to

a) calculate the moments of hindered rotors

b) perform the interpolation of the densities of states to get the $\rho^{+}(E,S)$

c) apply the variational criterium and select the final $\rho^{+}(E)$ from the $\rho^{+}(E,S)$.

μVTST Flowchart

1/ Define potential of molecule

2/ Determine MEP - Program MERCURY

3/ Perform a normal co-ordinate analysis at various s on MEP.

4/ Reject low frequencies from NCA.

5/ Calculate moments of hindered rotors.

6/ Combine ν's with hindered rotors and do RRKM calculation to obtain ρ's.

7/ Calculate ρ's for stable molecule.

8/ Choose some $\mathbf{s}$ where the Gorin model is valid.

9/ Interpolate ρ's between $\mathbf{s}_G$ and $\mathbf{s}_{eq}$.

10/ Apply variational criterium to $\rho^+(E,\mathbf{s})$ and minimise $N(E,\mathbf{s})$ to find $\rho^+(E)$.

11/ Calculate

$$k(e) = \int_{E_o}^{E} r^+(E^+)dE^+ hr(E)$$

where E_o is the value of the bonding potential at that $\mathbf{s}$.

12/ Calculate k(T) from k(E) but only include those k(e) where E > dissociation energy.

13/ Calculate k_{ter} from k_{uni}.

PROGRAM DESCRIPTION

1. Program Mercury:

QCEP, 1983, 3, 14. This program is a classical trajectory calculation program which has the provision for a number of different options.

The program is used in three ways in this treatment. Firstly it is used to calculate the minimum enery path (MEP) of a collection of atoms under the influence of a predefined potential, and from a set of predefined position and momentum coordinates. (NSELT=0). The output is a set of atomic coordinates at regular time intervals after t=0. This should be done so that the range of internuclear distances between the bonding atoms is sufficient to include the Gorin model bondlength. (Approximately 2.8 times the normal bondlength).

Secondly it is used to minimise the geometry of the moieties calculated initially. This gives a geometry which is totally relaxed and equilibrated

These equilibrated geometries are then used as the input for the normal coordinate analysis which is also performed by this program. This normal coordinate analysis is performed under the constraint imposed by the predefined potential.

This program has not been altered in any way.

Programs FALLOFF and MASTER:

Q.C.E.P., 1983, 3, 64. These two programs comprise the package necessary for the calculation of thermal unimolecular rate coefficients, k(T), from a knowledge of the nature of the transition state and the reactant. THe microscopic rate coefficients,k(E), are calculsated using RRKM theory (FALLOFF) and falloff effects are taken into account using the mastyer equation (MASTER).

FALLOFF has been slightly modified to provide the densities of states and k(E) for the reactant as well as the transition state as output. This output file is used as input for the interpolation program.

MASTER has not been modified.

Program HINDROT:

This program was used to calculate the hindrance angle, θ, as described in Sections 5.3, 6.5, and 6.6.2. The input is the atomic coordinates from the geometry minimisation performed with program MERCURY. Simple goemetrical formulae are used to calculate θ from the atomic coordinates.

Program INTERP:

This program initially interpolates the densities of states between the equilibrium geometry and the geometry of a suitable Gorin model bondlength.

The interpolation relation used here assumes that $\ln(\rho^+)$ is linear in $\ln(s_o - s)$ where $s_o = 0.4$ nm and s is varied between $s = 0.35$ nm and $s = r_{eq}$.

The result is a two dimensional matrix of the density of states as a function of E and s, $\rho^+(E,S)$.

Program MICRO:

From the matrix obtained above are selected the $\rho^+(E)$ as those $\rho^+(E,s)$ which satisfy

$$\rho^+(E) = \min\left[\int_{E_o}^{E} \rho^+(E,s)\,dE^+\right] \quad \text{for all } s.$$

The k(E) are then calculated from

$$k(E) = \int_{E_o}^{E} \rho^+(E)\,dE^+ / h\rho(E)$$

where E_o is the value of the interatomic bonding potential at the s where the $\rho^+(E)$ was selected.

The final output consists of the $\rho^+(E)$ and the k(E) calculated as above but only including those $\rho^+(E)$ and k(E) where E is greater than the bond dissociation energy. This file constitutes the input file for the program MASTER.

APPENDIX D

Publications:

"Gas/Wall Collision Efficiencies In Very Low Pressure Experiments".
Paul G. Dick*, Robert G. Gilbert, and Keith D. King, Int. J. Chem. Kinet., 1984, 16, 1129 - 1137.
(*This paper was published under my former surname).

"The Rate Constant of the Reaction of Hydroxyl Radicals With Methanol, Ethanol and (D_3)Methanol."
Paul G. Greenhill and Barry V. O'Grady, Aust. J. Chem., 1986, 39, 1775 - 1787.

"Recombination Reactions: Variational Transition STate THeory and the Gorin Model".
Paul G. Greenhill and Robert R. Gilbert, J. Phys. Chem., 90, 3104 - 3106.

"Theoretical Prediction of CH_3O and CH_2OH Gas Phase Decomposition Rate Coefficients".
Paul G. Greenhill, Barry V. O'Grady and Robert G. Gilbert, Aust. J. Chem., 1986, 39, 1929 - 1942.

Gas/Wall Collision Efficiencies in Very Low-Pressure Pyrolysis Experiments

PAUL G. DICK
Department of Chemistry, University of Tasmania, G.P.O. Box 252C, Hobart, Tasmania 7001, Australia

ROBERT G. GILBERT
Department of Theoretical Chemistry, University of Sydney, N.S.W. 2006, Australia

KEITH D. KING
Department of Chemical Engineering, University of Adelaide, Adelaide, S.A. 5001, Australia

Abstract

A readily applicable empirical formula is obtained for the collisional efficiency for energy transfer between a highly vibrationally excited reactant and a seasoned (usually quartz) wall, in terms of the molecular weight, potential well depth and dipole moment of the reactant. This expression is used to examine corrections due to nonunit wall collision efficiency in the high-pressure rate parameters obtained from very low-pressure pyrolysis experiments. It is found that these corrections are up to ca. ±5 kJ/mol in the high-pressure activation energy and a factor of ca. 2 in the high-pressure frequency factor, for molecules with molecular weight less than ca. 100 and where experiments are carried out at temperatures exceeding 1000 K.

Introduction

The technique of very low-pressure pyrolysis (VLPP) is particularly suited for the determination of rate parameters in unimolecular systems [1]. Accurate interpretation of VLPP experiments requires certain information on the gas/wall collisional energy transfer process. In this article we derive an empirical expression for predicting the requisite energy transfer information to the rather limited accuracy needed for the interpretation of VLPP data.

A unimolecular rate coefficient as obtained from a VLPP experiment is in the fall-off regime, and provided it is not too far towards the low-pressure limit, high-pressure data can be extracted from the results.

International Journal of Chemical Kinetics, Vol. 16, 1129–1137 (1984)
 CCC 0538-8066/84/091129-09$04.00

It has been demonstrated [2] that under favorable circumstances the derived high-pressure parameters are as accurate as those from other techniques. The observed rate coefficient as a function of temperature is used to determine the microscopic rate of reaction as a function of energy, $k(E)$, and thus the high-pressure and other rate parameters (termolecular rate coefficients, enthalpies of formation of free radical products, and information about the collisional energy transfer in the excited reactant/bath gas system [2–5]).

Since the amount of energy transferred in gas/wall collisions is large in these systems (ca. 5×10^3 cm^{-1}), details of the collisional energy transfer probability distribution function are unimportant [6] and the thermal rate coefficient can be calculated from the gas/wall collisional efficiency, $\beta_w(T)$ (defined in the usual way [6]):

$$(1) \quad k_{\text{uni}} = \int g(E)k(E)\,dE \,/\, \int g\,(E), g(E) = \frac{\omega_w \beta_w}{\omega_w \beta_w + k(E)} \rho(E) \exp(-E/k_B T)$$

where $\rho(E)$ is the density of states and ω_w the gas/wall collision frequency.

The gas/wall collision efficiency can be determined experimentally only in a limited number of cases. Current data are given in Table I. The first set of results are from the "variable encounter method" (VEM) [7]; the second from multiple channel pressure-dependent VLPP [3–5]. The last datum is cycloheptatriene, where $k(E)$ is known from other experiments [8] and thus β_w is calculated by fitting to the observed VLPP rate coefficients [9].

The primary object of this article is to use the available data on $\beta_w(T)$ to determine a functional form for this quantity which should be applicable in a wide range of systems. This form should preferably be in terms of readily obtainable parameters of the molecule (such as the molecular weight and the Lennard-Jones potential well depth) which ought to reflect the energy transfer dynamics with a seasoned wall (when the highly vibrationally excited reactant is colliding with an environment that consists essentially of molecules of structure similar to itself but anchored to the wall). This formula is an improvement of earlier work on this problem [10], which obtained an expression for $\beta_w(T)$ in terms of the normal boiling point (T_B, equivalent to the Lennard-Jones well depth ε) alone; data subsequently obtained have necessitated this improvement.

There are currently no *a priori* theories for gas/seasoned surface energy transfer which would permit β_w to be reliably estimated, and indeed given the complexity of the problem it seems unlikely that any will be developed in the immediate future. It is therefore necessary,

TABLE I. Experimental $\beta_w(T)$, dipole moments $(p)/10^{-30}$ C m, and values of T' (K) fitted to data and calculated from eqs. (2) and (3).

Molecule	Ref.	$\beta_w(T)$	p	T'(expt)	T'(calc)
Cyclobutane	7	0.62(800), 0.48(900), 0.38(1000), 0.30(1100)	0	526	515
Methylcyclopropane	7	0.48(800), 0.33(950), 0.24(1100)	0.5	453	550
Cyclopropane-d_6	7	0.66(800), 0.51(900), 0.43(1000), 0.36(1100)	0	582	656
Cyclopropane	7	0.70(800), 0.58(900), 0.49(1000), 0.42(1100)	0	644	631
Nitromethane	7	0.70(800), 0.58(900), 0.50(1000), 0.42(1100)	11.3	646	768
Chloroethane-2-d_1	2	0.9(975), 0.5(1200)	6.8	870	726
Chlorocyclobutane	3	0.8(930), 0.4(1150)	7.0	729	760
Bromoethane	2	0.85(900), 0.4(1150)	6.8	863	856
Bromoethane-d_4	2	0.8(1000), 0.6(1200)	6.8	830	875
Cycloheptatriene	see text	0.5(1100)	1.3	721	677

for the important purpose of being able to interpret VLPP data, to develop an empirical expression for this quantity. Although earlier work used a two-parameter function to represent the temperature dependence of β_w [2], we find that a suitable one-parameter empirical functional form is given by:

$$\beta_w(T) = min\{1, 0.64 \tanh^{-1}(T'/T)\}. \tag{2}$$

Here *min* means minimum value. Values of the quantity T' are given in Table I, and fits of eq.(2) to data in this table are shown in Figure 1. Note that the value of T' is approximately the temperature above which β_w begins to deviate significantly from unity.

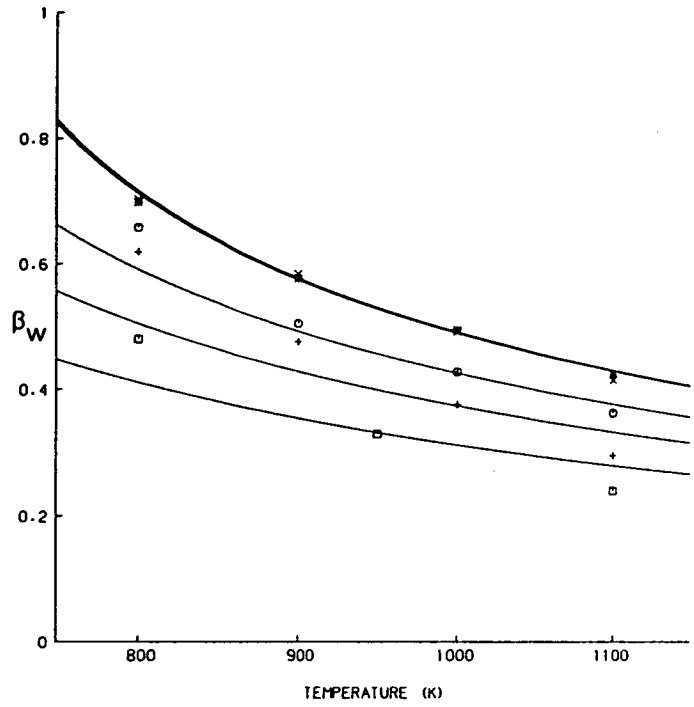

Figure 1. Collision efficiency as function of temperature for (bottom to top) methylcyclopropane, cyclobutane, cyclopropane-d_6, cyclopropane, and nitromethane. Lines: calculated from eq. (2) with fitted T' values of Table I; points: experimental values. Last five molecules in Table I (covering smaller temperature range) not included since experimental points lie virtually on top of fitted lines.

An examination of the values of T' given in Table I reveals that (i) the values of T' cover a comparatively small range, and (ii) there is a significant variation in the T' values for the same reactant when deuterated and undeuterated. Observation (i), when taken in conjunction with the fact that the reactants in Table I cover moderately wide ranges of molecular properties, suggests that a straightforward statistical treatment based on a linear regression should be able to provide an adequate treatment for the data. To be more specific, one assumes that the T' values can be expressed in terms of a linear combination of appropriate variables which should reflect the interaction and dynamics of the reactant/seasoned surface system.

Observation (ii) shows that a simple correlation of T' with ε alone is insufficient, since the difference in deuterated and undeuterated T' values is much greater than predicted by a simple boiling point correlation [10] (deduced when data for deuteration effects were not avail-

able). Since deuteration affects both the mass and vibrational frequencies of the molecule, one or both of these quantities must appear in a more generally applicable formula for β_w.

Since T' is a positive definite quantity, one can put $T' = q^2$, and assume, from observation (i) above, that q can be written as a linear combination of a set of variables, which express the dynamics of the system under study. The linear coefficients can be determined from the data by the χ^2 test [11].

We next consider the variables which may reflect the dynamics of the collision. The earlier theory gave β_w in terms of nonlinear functions of ε (through T_B, with the relation [12] $\varepsilon = 1.15T_B$); thus ε and perhaps higher powers (ε^2, etc.) may be considered as possibly independent parameters. Observation (ii) indicates that the reactant mass (m) and the average vibrational frequency can both be considered as reflecting the dynamics in a significant way. The dipole moment K of reactant is another possibly important quantity. By application of the χ^2 test to the data of Table I, it was found that m, ε, ε^2, and p (whose values are given in Table I) form a suitable set of independent variables in the linear regression. This yields

$$(3) \quad T' = (75.2 + 0.0832m + 0.493p - 0.345T_B + 0.506 \times 10^{-3}T_B)^2$$

Here m is in atomic mass units, p is in 10^{-30}C m, and T_B and T' are in K; eq. (3) has been expressed in terms of T_B rather than ε for convenience, assuming $\varepsilon = 1.15T_B$. The T' values computed using eq. (3) are also given in Table I. It should be noted that the data given in Table I were obtained by two different techniques: The lower temperature results using VEM and the higher temperature ones using VLPP. Different systematic errors may therefore be present in these two data sets. The VLPP-derived data were therefore given a greater weight in the fitting.

Equations (2) and (3) give the desired expression for $\beta_w(T)$. While the lack of information as to the basic nature of the gas/seasoned surface interaction potential and dynamics has precluded any physical model as a guide in obtaining these formulas, the statistical treatment employed should ensure their validity over the range of molecular parameters covered by the data used to obtain the fit, and indeed somewhat beyond this range. Indeed, these limits cover most cases of interest in interpreting VLPP data, since, for example, heavier molecules are expected to have a value of T' so large that $\beta_w \approx 1$ over the temperature range for which VLPP reactors may be used (i.e., up to ca. 1250 K); the same applies for molecules with greater dipole moments and boiling points.

Because of the unknown errors in the data from which eq. (3) was obtained, this expression is itself subject to some uncertainty. Hence

the values of the coefficients and the choice of independent variable are not unique. However, providing the new χ^2 is still small, choosing (say) an additional independent variable gives T' values which predict new β_ω which differ from the old only within the accuracy required for interpreting VLPP data, viz. a variation in the predicted β_ω of ca. 10%. This is simply because variables such as the molecular weight, the Lennard-Jones well depth, and the number of vibrational frequencies are interrelated. One can thus state confidently that, within the range of molecular parameters specified above, eqs. (2) and (3) enable one to estimate $\beta_\omega(T)$ to within an accuracy suitable for interpretation of conventional VLPP data.

Corrections for Nonunit Wall Collision Efficiency

We now employ eqs. (2) and (3) to determine corrections to high-pressure Arrhenius parameters (A_∞ and E_∞) deduced from VLPP data for a representative range of systems, as given in Table II. The original experimental VLPP rate coefficients were refitted by a nonlinear least-squares method using RRKM theory and with $\beta_\omega(T)$ calculated from the above expressions.

The reactions in Table II were chosen to illustrate cases where nonunit β_ω effects may be important. In all of them the calculated value of T' is significantly less than the temperatures of the experiment (i.e., $\beta_\omega < 1$). Note that although reactions with low critical energies may have low T', if the critical energy is sufficiently low then the VLPP experiment will be carried out at a comparatively low temperature (of the order of T' or lower), so that $\beta_\omega \simeq 1$ for such cases. For this reason, no low E_∞ data are included. Included are some bond fission reactions (decomposition of neopentane, 1,1-dimethylhydrazine, and ethylbenzene) where the E_∞ has been used to deduce enthalpies of formation of free radical products. It should be noted that the data fit for 1,1-dimethylhydrazine gives computed rate coefficients at the lower temperatures which are significantly less than those reported; this is indicative of a surface reaction, so the high-pressure parameters in Table II were obtained using only the rate coefficients reported at higher temperatures.

It is important to consider the values of k_{uni}/k_∞ (i.e., how far the reaction is in the fall-off regime, k_∞ being the high-pressure limiting rate coefficient) at the same time as considering β_ω corrections, since the lower k_{uni}/k_∞, the less the sensitivity of the data to the high-pressure parameters. Conversely, the VLPP data are most sensitive to nonunit β_ω the lower k_{uni}/k_∞. Values for k_{uni}/k_∞ are also shown in Table II for the highest and lowest temperatures in each study.

TABLE II. Corrections to high-pressure parameters arising from nonunit β_w.

Reactant	Ref.	E_∞ (kJ mol^{-1})		$\log_{10}(A_\infty/s^{-1})$		T range (K)	$\frac{k_{uni}}{k_\infty}$ range	T' (K)	β_w range
		$\beta_w=1$	β_w from eq.(3)	$\beta_w=1$	β_w from eq. (3)				
Ethylbenzene	15	304	307	15.3	15.7	1050-1240	0.2-0.05	825	0.7-0.5
Neopentane	16	338	334	17.3	17.3	1040-1260	0.06-0.008	585	0.4-0.3
Ethyl vinyl ether	17	182	179	11.5	11.4	760-1060	0.6-0.2	620	0.7-0.4
Cyclobutane	14	274	253	16.5	14.9	950-1300	0.06-0.004	515	0.4-0.3
1,1-Dimethyl-hydrazine	18	237	226	17.2	17.1	930-1080	0.0003-0.00006	610	0.5-0.4

It is seen from Table II that the β_w corrections to the high-pressure parameters are usually small: typically no more than ± 5 kJ/mol in E_∞ and about a factor of 2 in A_∞. The exceptions are cyclobutane and 1,1-dimethylhydrazine. For these cases, the values of T' are low and the data cover a particularly wide temperature range. Moreover, these molecules are well into the fall-off regime under the experimental conditions. Thus while there is a large change in the fitted E_∞ and A_∞ because of nonunit β_w, the error in these quantities is also large (although not quite as large as the β_w corrections). Note that the new set of high-pressure parameters for cyclobutane gives better agreement with previous studies [13] than did the original VLPP estimates [14]. Generally, other nonunit β_w corrections are of the order of the uncertainty in E_∞ and A_∞. Corrections to E_∞ are comparatively small in the important cases of bond fission reactions, which are used to deduce radical enthalpies of formation. In all the cases in Table II, the E_∞ values for such processes are large, and while the β_w values deviate significantly from unity, the reactions are sufficiently high in the fall-off regime to be only moderately sensitive to the β_w correction. Bond fission reactions with low values for E_∞ will have a negligible β_w correction for VLPP data, since, although the T' values for such reactants

[9] B. J. Gaynor, R. G. Gilbert, K. D. King, and J. C. Mackie, *Int. J. Chem. Kinet.*, **8**, 695 (1976).
[10] R. G. Gilbert, *Int. J. Chem. Kinet.*, **14**, 447 (1982).
[11] P. R. Bevington, "Data Reduction and Error Analysis for the Physical Sciences," McGraw-Hill, New York, 1969.
[12] J. O. Hirschfelder, C. F. Curtiss, and R. B. Byrd, "Molecular Theory of Gases and Liquids," Wiley, New York, 1964.
[13] C. T. Genaux, F. Kern, and W. D. Walters, *J. Am. Chem. Soc.*, **75**, 6196 (1953).
[14] P. C. Beadle, D. M. Golden, K. D. King, and S. W. Benson, *J. Am. Chem. Soc.*, **94**, 2943 (1972).
[15] D. A. Robaugh and S. E. Stein, *Int. J. Chem. Kinet.*, **13**, 445 (1981).
[16] A. C. Baldwin, K. E. Lewis, and D. M. Golden, *Int. J. Chem. Kinet.*, **11**, 529 (1979).
[17] M. Rossi and D. M. Golden, *Int. J. Chem. Kinet.*, **11**, 715 (1979).
[18] D. M. Golden, R. K. Solly, N. A. Gac, and S. W. Benson, *Int. J. Chem. Kinet.*, **4**, 433 (1972).

Received November 11, 1983
Accepted March 5, 1984

Aust. J. Chem., 1986, 39, 1775–87

The Rate Constant of the Reaction of Hydroxyl Radicals with Methanol, Ethanol and (D_3)Methanol

Paul G. Greenhill and Barry V. O'Grady

Chemistry Department, University of Tasmania,
P.O. Box 252C, Hobart, Tas. 7001.

Abstract

The rate coefficients for hydrogen abstraction by hydroxyl radicals from methanol and ethanol have been determined in the temperature ranges 260–803 K and 255–459 K respectively. Flash photolysis combined with resonance absorption detection of OH was used to obtain results which may be described by the Arrhenius expressions:

$$\text{Methanol} \qquad k(T) = (8{\cdot}0 \pm 1{\cdot}9) \times 10^{-12} \exp[-(664 \pm 88)\text{K}/T] \text{ cm}^3 \text{ s}^{-1} \qquad (1)$$

$$\text{Ethanol} \qquad k(T) = (1{\cdot}25 \pm 0{\cdot}24) \times 10^{-11} \exp[-(360 \pm 52)\text{K}/T] \text{ cm}^3 \text{ s}^{-1} \qquad (2)$$

The results obtained for methanol are in excellent agreement with results obtained by other workers, but the Arrhenius parameters for ethanol are markedly different to those obtained in the only other study of the temperature dependence of this reaction.

The rate constant for reaction with (D_3)methanol has been determined at 293 K:

$$(D_3)\text{Methanol} \qquad k(293) = 5{\cdot}0 \pm 0{\cdot}2 \times 10^{-13} \text{ cm}^3 \text{ s}^{-1} \qquad (3)$$

The presence of an isotope effect confirms that the predominant process is abstraction of hydrogen from the carbon rather than the oxygen.

The results obtained for the reaction with ethanol were analysed by using a 21 reaction scheme to determine the effect of $[OH]_0$ and secondary reactions on $k(T)$. The simulations indicate that secondary reactions involving OH are relatively unimportant in determining the bimolecular rate coefficients found in this study.

Introduction

The reactions of hydroxyl radicals have been shown to be key reactions in the oxidation of hydrocarbons and other fuels and in the chemistry of the lower atmosphere.[1–3] However, despite their importance few measurements of the rate constants have been made over an extended temperature range.

[1] Atkinson, R., Darnall, K. R., Lloyd, A. C., Winer, A. M., and Pitts, J. N., Jr, *Adv. Photochem.*, 1979, **11**, 375.
[2] Baulch, D. L., and Campbell, I. M., 'Gas Kinetics and Energy Transfer' Vol. 4, p. 137, Chem. Soc. Specialist Periodical Reports, 1981.
[3] Westbrook, C. K., and Dryer, F. L., *Combust. Sci. Technol.*, 1979, **20**, 125.

0004-9425/86/111775$02.00

One group of compounds of interest in both atmospheric and combustion chemistry is the alcohols. Recent investigations of the reaction of OH with methanol:[4–8]

$$OH + CH_3OH \rightarrow CH_2OH + H_2O \quad (1a)$$

$$\rightarrow CH_3O + H_2O \quad (1b)$$

have shown that the reaction has an activation energy lower than that predicted by the modelling of high temperature flame,[9] flow reactor[10] and shock tube[11] studies.

Both Hagele[5] and Meier[6] have reported the branching ratio of reaction (1) and conclude that (1a) is the dominant process at room temperature. Confirmatory evidence for this observation may be had by studying the reaction between OH and CD_3OH. If k_1 shows an isotope effect then reaction (1a) is indicated as being the favoured channel.

The corresponding reaction of OH with ethanol has been investigated to an even lesser degree:

$$OH + CH_3CH_2OH \rightarrow CH_2CH_2OH + H_2O \quad (2a)$$

$$\rightarrow CH_3CHOH + H_2O \quad (2b)$$

$$\rightarrow CH_3CH_2O + H_2O \quad (2c)$$

Three direct studies using flash photolysis/resonance absorption,[7] flash photolysis/resonance fluorescence[8] and discharge flow/laser induced fluorescence[12] respectively and one relative rate study[4] have yielded rate constants at room temperature which range from 1.76 to 3.65×10^{-12} cm^3 s^{-1}. Only one of these studies has addressed the temperature dependence of the reaction.[12]

We present here the results of a study of the temperature dependence of the reaction of OH with methanol and ethanol, and of the reaction of OH with (D_3)methanol at room temperature.

Experimental

All experiments were performed by using the flash photolysis/resonance absorption technique. The reaction vessel consisted of Suprasil tubing of 30 mm diameter and approximately 1 m length surrounded by a coaxial Pyrex tube 40 mm in diameter. The annular space formed was enclosed by sealing in two circular stainless steel electrodes each with a small hole bored in it for the admission of the fill gas. A reaction zone 43 cm long was defined by internal windows fused into the reaction vessel approximately 25 cm from each end. This arrangement allowed the total reaction volume to be heated in an electric furnace while at the same time keeping the flash electrodes outside the furnace. The temperature of the furnace could be maintained to ± 5 K and

[4] Campbell, I. M., McLaughlin, D. F., and Handy, B. J., *Chem. Phys. Lett*, 1976, **38**, 362.
[5] Hagele, J., Lorenz, K., Rhasa, D., and Zellner, R., *Ber. Bungsenges. Phys. Chem.*, 1983, **87**, 1023.
[6] Meier, U., Grotheer, H. H., and Just, Th., *Chem. Phys. Lett.*, 1984, **106**, 97.
[7] Overend, R., and Paraskevopoulos, G., *J. Phys. Chem.*, 1978, **82**, 1329.
[8] Ravishankara, A. R., and Davis, D. D., *J. Phys. Chem.*, 1978, **82**, 2852.
[9] Vandooren, J., and Van Tiggelen, P. J., 18th Symp. (Intl) On Combustion, 1980, p. 473.
[10] Aronowitz, D., Santoro, R. J., Dryer, F. L., and Glassman, I., 17th Symp. (Intl) On Combustion, 1979, p. 633.
[11] Bowman, C. T., *Combust. Flame*, 1975, **25**, 343.
[12] Meier, U., Grotheer, H. H., Riekert, G., and Just, Th., *Chem. Phys. Lett.*, 1985, **115**, 221.

the temperature of the reactant gas mixture was measured by a chromel–alumel thermocouple. The photolysis flash was generated in a flowing stream of nitrogen at about 5 Torr pressure with an Applied Photophysics capacitor bank 150–03. Typical flash energies were in the range 300–400 J with an effective flash duration (time elapsed until the flash had decayed to a level low enough not to interfere with recording of the OH decay profile) under the conditions of the experiment of 70–80 μs.

The OH radicals were generated by the photolysis of water vapour in most experiments. The effect of using a different OH radical precursor was tested by using nitric acid for several experiments at room temperature.

The reactant gas mixtures were prepared manometrically from water, alcohol and argon in two stages. Initially, a mixture containing a known percentage (about 4–5%) of alcohol in argon was prepared and stored in a 10-l. glass bulb. This was used as the source of reactant which was mixed with water vapour and further diluted with argon to give the required reactant concentrations. These mixtures were stored and were allowed to mix for 48 h before use. The final mixtures contained $5–200\times10^{14}$ cm^{-3} methanol or $1\cdot4–35\times10^{14}$ cm^{-3} ethanol in 100 Torr of 0·5–1% H_2O in argon. The reaction vessel was filled to a pressure of 100 Torr immediately before photolysis. No significant difference or trend in k_{1st} was observed by either repetitively flashing the same mixture or refilling after each flash. Normally no fill was photolysed more than five times.

The hydroxyl radicals were detected by absorption of lines of the (0,0) band of the $A^2\Sigma - X^2\Pi$ transition from a microwave discharge through a 5% water/argon mixture at 1 Torr pressure. A single pass of the collimated beam from the lamp passed through the cell and was focused on the entrance slit of an Unicam SP500 quartz prism monochromator fitted with a Hamamatsu photomultiplier (R212UH) wired for fast response. The monochromator was centred on the emission maximum at about 308·1 nm. This resulted in acceptance of the $Q_1 3$ line as well as the $Q_1 2$ (308·00 nm), $Q_1 4$ (308·33 nm) and the $P_1 1$ (308·17 nm) lines with a slit width of 0·1 mm.

The conversion of the observed I values (where I is the intensity of the transmitted 308 nm radiation) into relative hydroxyl radical concentrations was made by using Beer's law in its usual form:

$$\log(I_0/I) = \epsilon_{OH}[OH]l$$

or

$$[OH]_{rel} = \text{constant}[\log(I_0/I)]$$

Other workers have suggested that Beer's law should be used in the form

$$\log(I_0/I) = (\epsilon_{OH}[OH]l)^{\gamma}$$

where γ is a constant. In the present work, γ was found to be $1\pm0\cdot1$ for $I > 70\%\ I_0$.

The signal from the photomultiplier, following photolysis of the reaction mixture, was stored in a Datalab DL 905 transient recorder (1024×8 bit words) and then transferred to a microcomputer for processing. The I_0 value was determined by running the transient recorder in either the pre-trigger mode and recording the unattenuated resonance lamp signal for 100 ms before the flash or in the A/B mode, which enabled the sweep time B near the end of the reaction time to be increased over the sweep time A used during the reaction, and recording the signal when [OH] = 0.

Early in the work it was found that the transient recorder was susceptible to overloading from the scattered light signal generated by the photolysis flash resulting in slow response times. To prevent this large signal affecting the transient recorder a 6·5 V cut off diode was placed between the photomultiplier and the transient recorder.

The observed I against time curve was truncated to remove points which may be affected by the tail of the flash and points when the noise on the signal overlapped the I_0 value. The signal-to-noise ratio was typically 10–15 to 1. A typical absorption profile with and without ethanol is shown in Fig. 1.

The initial OH concentration was estimated from the initial absorption of the resonance radiation and the oscillator strength of the $A^2 - X^2$ transition in the same manner as other workers.[7,13] For absorptions observed in this work and a pathlength of 43 cm, we estimate typical initial OH concentrations in the range $1–3\times10^{13}$ cm^{-3}.

[13] Overend, R. P., Paraskevopoulos, G., and Cvetanović, R. J., *Can. J. Chem.*, 1975, 53, 3374.

It was not possible in this work to obtain any conclusive experimental evidence of the effect of varying OH concentrations. With the single shot methodology employed, any significant reduction in $[OH]_0$ would have reduced the absorption to a level where the observation and analysis of decays would be unreliable.

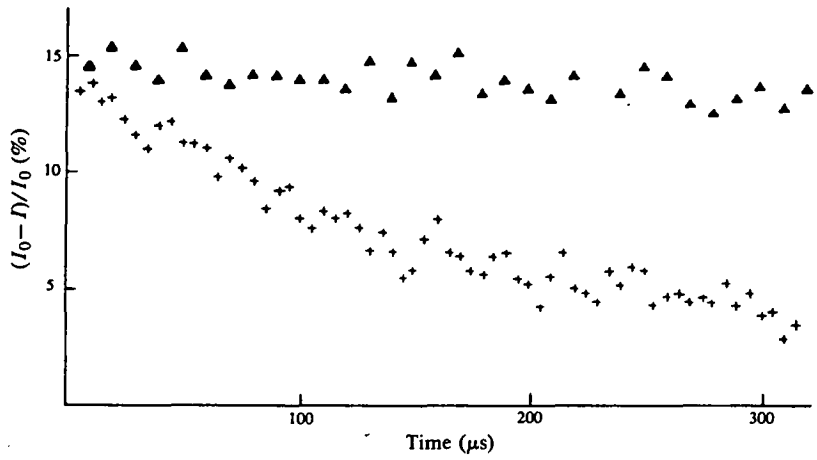

Fig. 1. Typical OH absorption profiles for +, [EtOH] $1{\cdot}70\times10^{15}$ cm^{-3}; ▲, no ethanol.

Reagents

Alcohols were Aldrich Chemicals spectrophotometric grade (99·9%+). Methanol and ethanol were redistilled and stored over molecular sieve. Prior to making reaction mixtures, the alcohols were degassed by bulb-to-bulb distillation and the middle fraction used for making up the reaction mixtures.

High Purity Argon (99·99% min.) from C.I.G. was used without further purification. Water was distilled and degassed by successive freeze, pump, thaw cycles before use.

Nitric acid was prepared by vacuum distillation from a 1 : 2 mixture of concentrated nitric and sulfuric acids and condensed in a liquid nitrogen trap.

Results

In an excess of alcohol the rate law for the reaction between OH and an alcohol can be written as

$$d[OH]/dt = -k_{1st}[OH]$$

where k_{1st} is a pseudo-first-order rate constant given by $k_{bim}[ROH]+k_s$. The constant k_s includes all losses of OH by secondary processes. As the alcohols have hydrogen atoms in different environments, k_{bim} will represent the sum of the rate constants for the different reaction channels. A plot of ln[OH] against time yields k_{1st} for a particular alcohol concentration and a second plot of k_{1st} against alcohol concentration will give k_{bim}.

Values of the pseudo-first-order rate constant and its variance were calculated by using linear least-squares techniques[14] applied to the variation of $\ln[OH]_{rel}$ with time.

[14] Cvetanović, R. J., Overend, R. P., and Paraskevopoulos, G., *Int. J. Chem. Kinet., Symp. 1*, 1975, 249.

The bimolecular rate constant was determined from weighted linear least-squares analysis of k_{1st} as a function of alcohol concentration.

Much of the criticism of the photolysis technique used here stems from the non-selectivity of the photolysis flash, i.e. the wide wavelength range of radiation emitted by the flash lamp. It is important to know whether the reactant is photolysed and if so what products and quantities of products are formed. We performed experiments involving photolysis of an alcohol/argon mixture in the absence of water vapour to determine if (i) there was any production of OH by direct photolysis of the alcohol, and (ii) if there were any other products formed during the photolysis which may interfere with the reactions under study.

No absorption of the OH resonance radiation was observed indicating that OH was not formed from photolysis of the alcohols. This result is in agreement with the observation that ultraviolet photolysis of the alcohols leads to O–H fission rather than C–O fission.[15] Samples of the post-photolysis mixture were taken for analysis by gas chromatography/mass spectrometry. After five photolysis flashes on the same mixture, products produced consisted less than 0·5% of the total reactant concentration. This level of impurity is too low to affect the observed rate constants. The *m/e* values for these minute levels of impurities were consistent with them being aldehydes.

Methanol

Typical plots of $\ln[OH]_{rel}$ against time, k_{1st} against [MeOH] and $\ln k_{bim}$ against $1/T$ are given in Figs 2, 3 and 4 respectively.

Over the temperature range from 260 to 803 K the rate coefficient $k_1(T)$ $(= k_{1a} + k_{1b})$ is well represented by

$$k_1(T) = (8{\cdot}0 \pm 1{\cdot}9) \times 10^{-12} \exp[-(664 \pm 88)\text{K}/T]\ \text{cm}^3\ \text{s}^{-1} \qquad (1)$$

The error limits are one standard deviation.

This gives a value at 298 K of $0{\cdot}86 \times 10^{-12}$ cm^3 s^{-1}. The temperatures and corresponding rate coefficients are given in Table 1 for all the studied temperatures.

(D_3)Methanol

At 293 K the rate constant for reaction of OH with CD_3OH was found to be:

$$k(293) = 5{\cdot}0 \pm 0{\cdot}2 \times 10^{-13}\ \text{cm}^3\ \text{s}^{-1} \qquad (3)$$

This gave on overall isotope effect at 293 K of $k_H/k_D = 1{\cdot}65$. Fig. 5 is a plot of k_{1st} as a function of $[CD_3OH]$.

Based on the branching ratios determined by Hagele[5] and Meier,[6] we can calculate a true isotope effect for abstraction from the carbon. We have taken the average of the three branching ratios quoted in these reports which gives $k_{1b}/(k_{1a} + k_{1b}) = 0{\cdot}18$. The corrected isotope effect for H/D abstraction from carbon in methanol is thus $2{\cdot}1 \pm 0{\cdot}2$.

[15] Buenker, R. J., Olbrich, G., Schuchmann, H.-P., Schürmann, B. L., and von Sonntag, C., *J. Am. Chem. Soc.*, 1984, **106**, 4362, and references therein.

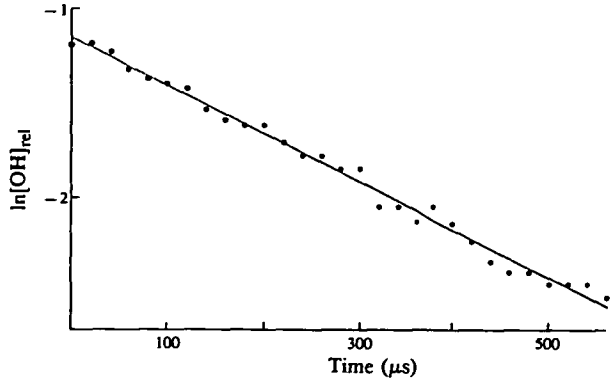

Fig. 2. Plot of $\ln[OH]_{rel}$ against time for [MeOH] 2.01×10^{15} cm^{-3}

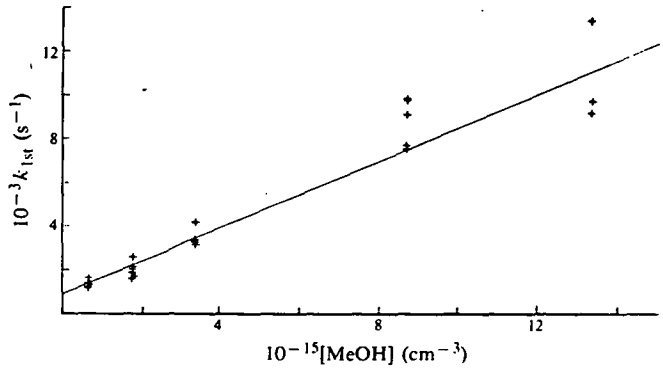

Fig. 3. Pseudo-first-order rate constant as a function of methanol concentration. T 292 K.

Table 1. Experimental values of k_{bim} for the reaction $OH + CH_3OH \rightarrow$ products and for $OH + C_2H_5OH \rightarrow$ products

	$OH + CH_3OH \rightarrow$ products				$OH + C_2H_5OH \rightarrow$ products		
T (K)	$10^{12}k_{bim}$ (cm^3 s^{-1})	$10^{12}\sigma(k)^A$ (cm^3 s^{-1})	Number of expts	T (K)	$10^{12}k_{bim}$ (cm^3 s^{-1})	$10^{12}\sigma(k)^A$ (cm^3 s^{-1})	Number of expts
260	0·54	0·04	28	255	2·84	0·15	25
292	0·76	0·04	21	273	3·40	0·14	19
300	0·75	0·08	21	289	3·80	0·24	30
331	1·13	0·05	22	293	3·40	0·17	26
362	1·44	0·06	26	331	4·26	0·19	23
453	1·44	0·09	20	360	4·26	0·18	24
465	1·35	0·08	20	369	5·21	0·36	30
570	2·06	0·17	20	459	5·63	0·48	28
597·5	2·67	0·24	20				
669	2·79	0·25	19				
803	5·76	0·59	18				

[A] One standard deviation.

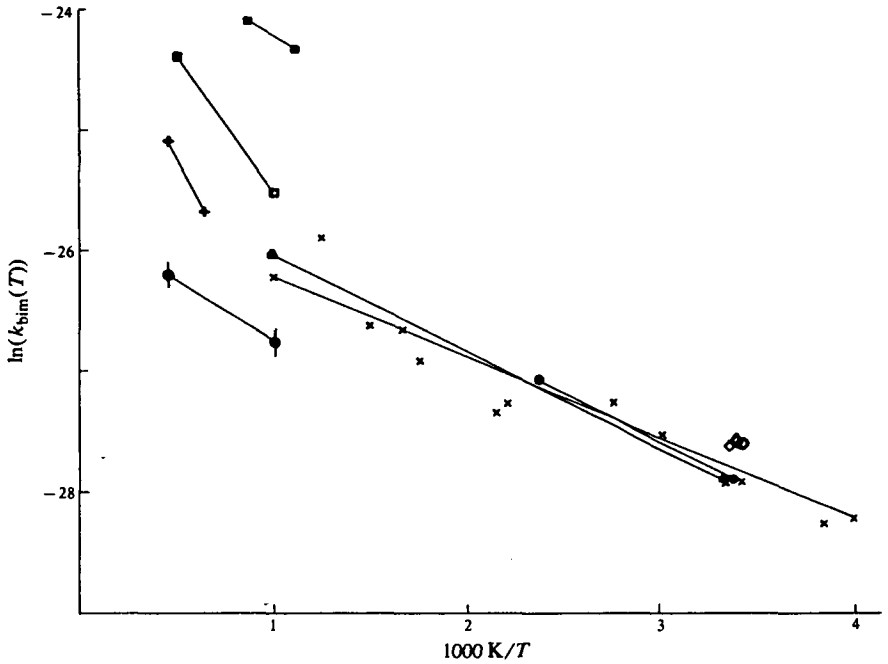

Fig. 4. Arrhenius plot of all data on OH + methanol reaction: ■, ref. 10; □, ref. 9; +, ref. 11; ⧫, ref. 3; ◆, ref. 6; ●, ref. 5; ◇, ref. 4; △, ref. 7; ○, ref. 8; ×, this work.

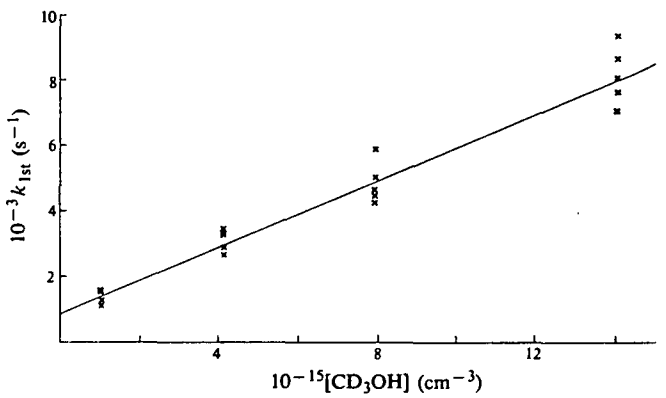

Fig. 5. Pseudo-first-order rate constant as a function of (D_3)methanol concentration. T 293 K.

Ethanol

Typical plots of $\ln[OH]_{rel}$ against t, k_{1st} against $[C_2H_5OH]$ and $\ln k_{bim}$ against $1/T$ are shown in Figs 6, 7 and 8 respectively.

Over the temperature range covered in this study the rate coefficient $k_2(T)$ $(= k_{2a} + k_{2b} + k_{2c})$ is well represented by

$$k_2(T) = (1{\cdot}25 \pm 0{\cdot}24) \times 10^{-11} \exp[-(360 \pm 52)\text{K}/T]\ (\text{cm}^3\ \text{s}^{-1}) \qquad (2)$$

which gives a value at 298 K of $0{\cdot}37 \times 10^{-11}$ cm^3 s^{-1}. Table 1 lists the experimental rate coefficients and the corresponding temperatures.

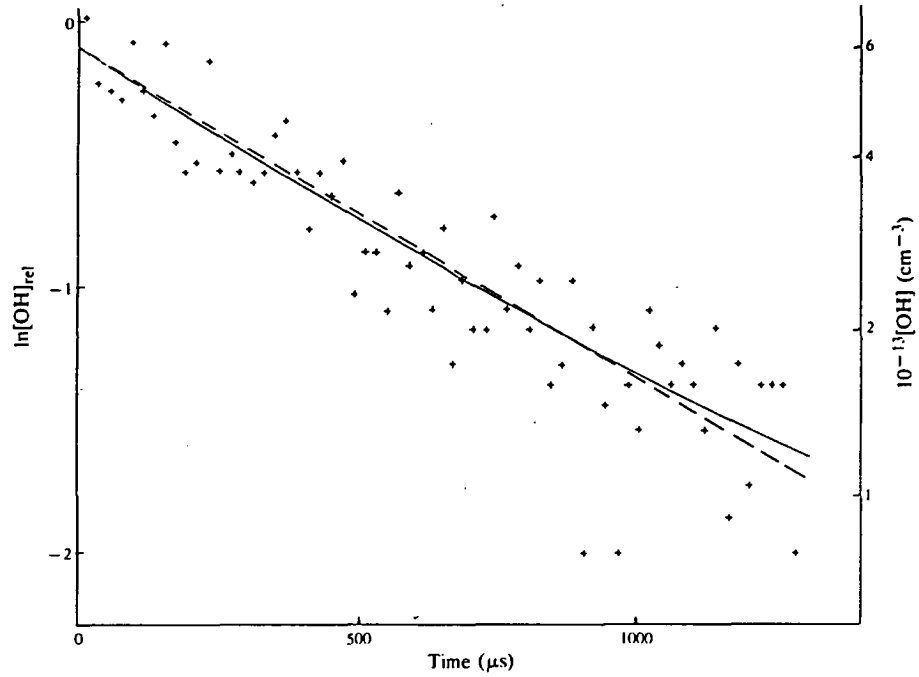

Fig. 6. Plot of $\ln[OH]_{rel}$ as a function of time for ethanol: +, observed points; ---, linear fit for k_1; —, modelled [OH] with $[OH]_0$ 6×10^{13} cm^{-3}; [EtOH] 1.37×10^{14} cm^{-3}.

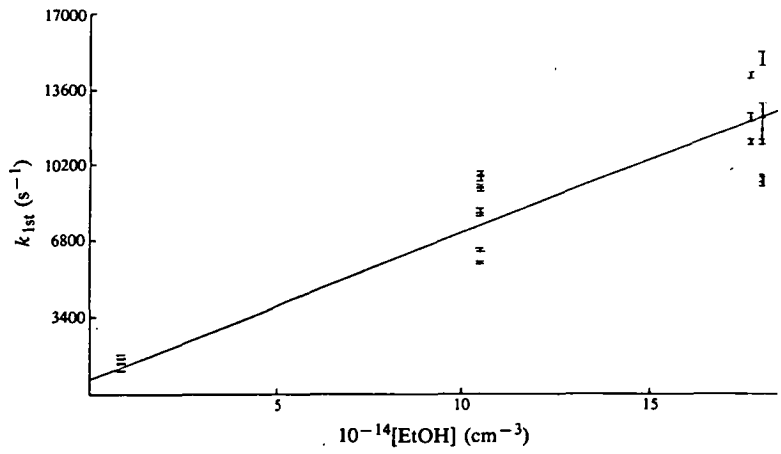

Fig. 7. Pseudo-first-order rate constant as a function of ethanol concentration. T 459 K.

Discussion

Methanol

The results obtained for the overall rate constant for the reaction of OH with methanol are in excellent agreement with two recent studies of the temperature dependence of this reaction.[5,6] The rate constants determined in this work are tabulated along with the results from the literature in Table 2 and plotted in Fig. 4.

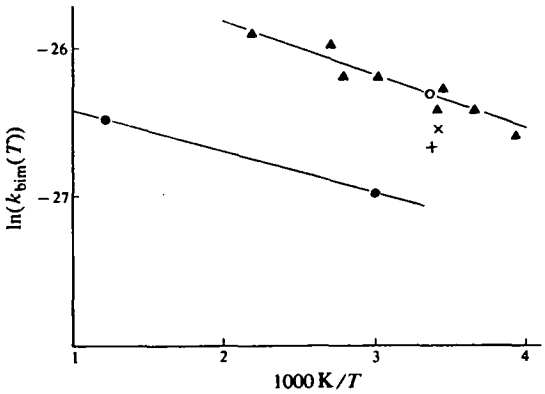

Fig. 8. Arrhenius plot of all data from the ethanol + OH reaction:
o, ref. 7;
+, ref. 4;
×, ref. 8;
•, ref. 12;
▲, this work.

Table 2. Comparison of rate coefficients of $OH + CH_3OH \rightarrow$ products

$10^{12} k_1$ ($cm^3 s^{-1}$)	$10^{11} A$ ($cm^3 s^{-1}$)	E_a/R (K)	T (K)	Ref.
0·79[A]	1·2±0·3	810±50	295–420	5
1·06±0·10			296	7
1·00±0·10			298	8
0·76[A]	1·1±0·3	798±45	300–1000	6
0·95±0·10			292	4
0·86[A]	0·80±0·19	664±88	250±803	this work

[A] 298 K.

The agreement obtained between this work and the published results indicates that the technique that we have employed is suitable and provides satisfactory results for systems involving the reactions of hydroxyl radicals. It is reasonable to suppose that the same technique can provide satisfactory results for the OH + ethanol system.

(D_3)Methanol

This is the first reported result for this reaction. The presence of an isotope effect indicates that the predominant process in hydroxyl radical attack on methanol is reaction (1a). This result is in agreement with the branched mechanism reported in refs[5,6].

The isotope effect for hydroxyl radical reactions has been little studied but the results obtained here is similar to that observed for H_2–D_2[16] (3·2), HCl–DCl[16,17] (2·0) and C_6H_6–C_6D_6[18] (1·4). On the other hand the value of 11 obtained by Gordon and Mulac[19] for CH_4–CD_4 appears to be abnormally high. These reactions obviously merit further study.

[16] Smith, I. W. M., and Zellner, R., *J. Chem. Soc., Faraday Trans. 2*, 1973, **70**, 1045.
[17] Husain, D., Plane, J. M. C., and Xiang, C. C., *J. Chem. Soc., Faraday Trans. 2*, 1984, **80**, 713.
[18] Lorenz, K., and Zellner, R., *Ber. Bunsenges. Phys. Chem.*, 1983, **87**, 629.
[19] Gordon, S., and Mulac, W. A., *Int. J. Chem. Kinet., Symp. 1*, 1975, 289.

Ethanol

Comparison with the results of other workers in Table 3 and Fig. 8 shows a marked difference in the rate coefficients quoted. The result obtained here is in good agreement with the highest result in the group of room temperature results but a factor of 2 higher than the results of Meier *et al.*

Table 3. Comparison of rate coefficients of $OH + C_2H_5OH \rightarrow$ products

$10^{12} k_2$ ($cm^3 s^{-1}$)	$10^{12} A$ ($cm^3 s^{-1}$)	E_a/R (K)	T (K)	Ref.
3.74 ± 0.37			296	7
2.62 ± 0.36			298	8
1.75^A	4.4 ± 1.0	274 ± 90	300–1000	12
2.99 ± 0.33			292	4
3.7^A	12.5 ± 2.4	360 ± 52	250–459	this work

[A] 298 K.

Table 4. Reaction mechanism and rate coefficients

No.	Reaction	A ($cm^3 s^{-1}$)	E_a (kJ mol^{-1})	Ref.
(2b)	$CH_3CH_2OH + OH \rightarrow CH_3CHOH + H_2O$	3.73×10^{-12}	0.0^A	B
(2c)	$CH_3CH_2OH + OH \rightarrow CH_3CH_2O + H_2O$	4.63×10^{-13}	0.0^A	B
(3)	$CH_3CH_2OH + H \rightarrow CH_3CH_2H_2O$			
(4)	$CH_3CH_2OH + H \rightarrow CH_3CHOH + H_2$	2.0×10^{-11}	33.8^C	
(5)	$CH_3CH_2OH + \rightarrow CH_3CH_2O + H_2$			
(6)	$2CH_3CHOH \rightarrow$ products	1.0×10^{-11}	0.0	12
(7)	$2CH_3CH_2O \rightarrow$ products	1.0×10^{-11}	0.0	12
(8)	$CH_3CHOH + CH_3CH_2O \rightarrow$ products	1.0×10^{-10}	0.0	12
(9)	$CH_3CH_2O + OH \rightarrow CH_3CHO + H_2O$	3.0×10^{-10}	0.0	12
(10)	$CH_3CHOH + OH \rightarrow CH_3CHO + H_2O$	3.0×10^{-10}	0.0	12
(11)	$CH_3CH_2O + H \rightarrow CH_3CHO + H_2$	1.0×10^{-10}	0.0	—[D]
(12)	$CH_3CHOH + H \rightarrow CH_3CHO + H_2$	1.0×10^{-10}	0.0	—[D]
(13)	$CH_3CH_2O \rightarrow CH_3CHO + H$	1.47×10^{-9} [E]	—	19
(14)	$CH_3CHOH \rightarrow CH_3CHO + H$	1.13×10^{-6} [E]	—	19
(15)	$CH_3CHOH + H \rightarrow CH_3CH_2OH$	1.16×10^{-11}	−0.39	19[F,G]
(16)	$CH_3CH_2O + H \rightarrow CH_3CH_2OH$	4.73×10^{-12}	−0.06	19[F,G]
(17)	$CH_3CHO + OH \rightarrow$ products	6.9×10^{-12}	-2.16^H	
(18)	$CH_3CHO + H \rightarrow$ products	2.24×10^{-11}	13.8^I	
(19)	$2OH \rightarrow H_2O + O$	1.83×10^{-12}	0.0^H	
(20)	$2OH \rightarrow H_2O_2$	2.13×10^{-12}	$0.0^{F,H}$	
(21)	$H + OH \rightarrow H_2O$	7.72×10^{-15}	$-3.64^{F,H}$	

[A] Activation energies omitted and rate constant expressed as a pre-exponential factor only at 300 K.
[B] This work.
[C] 'Handbook of Bimolecular and Termolecular Gas Reactions' Vol. 1 (Ed. J. A. Kerr) (CRC Press: Boca Raton, Florida, 1981).
[D] Estimated.
[E] s^{-1} at 300 K.
[F] Calculated for total pressure = 100 Torr.
[G] Arbitrarily half methanol rate.
[H] From *J. Phys. Chem. Ref. Data*, 1982, **11**, 327.
[I] Whytock, D. A., Michael, J. V., Payne, W. A., and Stief, L. J., *J. Chem. Phys.*, 1976, **65**, 4871.

The reason for the present disparity is unclear. The initial hydroxyl radical concentration in the present work is somewhat higher than that used by Meier and this may lead to a greater contribution by secondary reactions to the observed OH decay.

The effect of OH radical concentration can be assessed by modelling the reaction process with a suitable set of elementary reactions.

Table 4 specifies the reaction scheme used in this study and the rate coefficients used. Some features of this mechanism are as follows. The scheme includes two reactions, (15) and (16), which will be of importance in a system such as the experimental arrangement employed here that contains significant levels of hydrogen atoms. The rates of reactions (15) and (16) were taken from a theoretical prediction of the rate coefficients of the corresponding methanol species calculated by application of RRKM theory with a Gorin model.[20] It is assumed that the recombinations are slower than those calculated for the methanol reactions. The unimolecular decomposition of the radicals was assumed to be as slow as those of the corresponding methanol species at these temperatures.[20] The rates of OH reaction with the secondary species were also those obtained by Meier *et al.*[12] Only two pathways for OH attack on ethanol have been included, one on the hydroxy group and one on the C 1 carbon. Attack on the C 2 carbon is a minor pathway[12] when compared with the alternatives and in this study we have included it within the rate coefficients of the other pathways.

The majority of the secondary reactions (for example, reactions involving species produced from the initial products) have no influence on the model as they are of such low concentration. They have been included for completeness. In most of the modelling performed in this work, the secondary reactions with unknown rate parameters have been given rate coefficients which are in the order of the collision frequencies. This should have the effect of maximizing any contribution of the secondary reactions to the modelled profiles and in effect be a 'worst possible case'.

The program used was modified from one used by Ellis and Gilbert to model sound propagation in reacting systems.[21] It uses the Gear algorithm[22] to solve the stiffly coupled differential equations representing the reactions occurring after identifying the independent species and thus the independent equations. Initial conditions for reactant species were selected assuming that photolysis produced effectively instantaneous concentrations of the radicals and did not disturb the thermal or temperature equilibrium of the system.

To test the effect of the initial concentration of OH, that is, the necessity for pseudo-first-order conditions, the initial OH concentrations were varied up to a level where they were comparable to the lowest reactant concentrations used. In this situation there is a significant loss of ethanol and it is no longer valid to assume pseudo-first-order conditions. This results in plots of ln[OH] *v.* t which are curved, the degree of curvature being dictated by the change in ethanol concentration.

Calculation of k_{1st} at varying alcohol concentrations with such high $[OH]_0$ results in plots of k_{1st} as a function of [ROH] which have two quite distinct regions. At low [ROH], where [ROH]/[OH] $\approx$ 1, there is high curvature as the plot moves towards the origin. Analysis to obtain the bimolecular rate constant would produce results

[20] Greenhill, P. G., O'Grady, B. V., and Gilbert, R. G., unpublished data.
[21] Ellis, R. J., and Gilbert, R. G., *J. Acoust. Soc. Am.*, 1977, **62**, 245.
[22] Gear, C. W., 'Numerical Initial Value Problems in Ordinary Differential Equations' (Prentice-Hall: New York 1971).

which were much too high. However, when [ROH]/[OH] ≫ 1 the plots are almost linear with an intercept that is dictated by the $[OH]_0$ and results which are close to the true rate coefficients. Such intercepts were observed in this work.

The results of the computation indicate that even under conditions when $[OH]_0 = 0{\cdot}5[EtOH]_{min}$ it would be difficult to detect curvature in the experimental ln[OH] *v.* *t* plots. Fig. 6 is a superposition of the modelled OH profile at an ethanol concentration of $1{\cdot}37\times10^{14}$ cm^{-3} and an $[OH]_0$ of 6×10^{13} cm^{-3} on the experimental plot. However, attempts to fit the observed decays with functions other than a linear one produced cumulative errors which were greater than for a linear fit. This tends to indicate that the initial OH concentration in the experimental work is in fact lower than that used in these modelling studies.

It is important to note that the modelled results indicate only a slight curvature of the ln[OH] *v.* *t* plot under conditions which could never be regarded as pseudo-first order. More importantly, they produce the observed first-order decay of OH very closely. At higher concentrations of ethanol the modelled decays are even more linear and reproduce the observed decays almost exactly.

Results obtained at varying $[OH]_0$ are displayed in Fig. 9. What is particularly important is that these plots are linear within the experimental error for [ROH]/[OH] ratios greater than 10 even at very high $[OH]_0$. But any rate constants obtained without an analysis of the effect of [OH] and secondary reactions would be in error even though k_{1st} varies linearly with alcohol concentration.

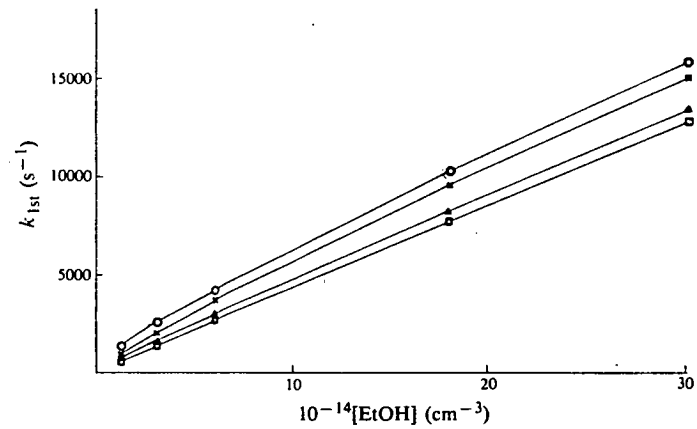

Fig. 9. The effect of $[OH]_0$ on the pseudo-first-order rate constant: o, 6×10^{13}; ×, 2×10^{13}; ▲, 5×10^{12}; □, 2×10^{12} cm^{-3}.

The observed k_{bim} increases by up to 20% at an initial OH concentration of 6×10^{13} cm^{-3} over the true value for the rate constant. At the estimated $[OH]_0$ for this work and across the temperature range of the experiments, we calculated an average downward correction of 14·5% to the observed k_{bim} is required to obtain the true bimolecular rate coefficients.

This analysis indicates that to reproduce the results of Meier *et al.*[12] (i.e. k_{bim} a factor of 2 lower than these experiments indicate), then the observed pseudo-first-order rate constants at the higher ethanol concentrations would have to be reduced by a factor of 2 also. There is no question of the conditions being not pseudo-first order at these concentrations where the [EtOH]/[OH] ratio was the order of 100.

An attempt has been made to reproduce the results observed in this work by using the results obtained by Meier *et al.* The rate constants determined were put into

the model developed for the current work and simulations were run for varying OH radical concentrations and reactant concentrations. The first-order rate constants in this work cannot be reproduced by using the rate coefficients determined by Meier *et al.* even at very high $[OH]_0$ and very fast secondary reaction rate coefficients. Such a high initial [OH] would naturally result in the observed decays being strongly affected by nearly all reactions other than the one of interest, but such a calculation illustrates the point that the conventional criticism of underestimation of the $[OH]_0$ is not valid in this case.

The reason for the disparity between results obtained in this work and that of Meier *et al.* is not clear but one further possibility is apparent. The pseudo-first-order rate constants obtained in Meier's work were all in the region of 0 to 700 s^{-1} and the majority of the results had values less than 400 s^{-1}. These compare with k_{1st} values between 1000 and 15000 s^{-1} from our work. The relative magnitude of our first-order rate constants is of course a result of the relatively high reactant concentrations used but it is highly unlikely that the measured concentrations in this work are significantly in error. Recent work[23] on the reaction of OH with HBr using the discharge flow technique has concluded that the most likely source of error in such experiments was the incorrect determination of the HBr concentration. Discrepancies of up to a factor of two were observed. This was attributed to wall absorption and similar comments may apply here.

Conclusion

In the present work with flash photolysis–resonance absorption, the temperature dependence of the overall rate constant for hydrogen abstraction from methanol and ethanol by OH [reactions (1a)–(2c)] was found to be as given in equations *(1)* and *(2)*. Our results for methanol are in good agreement with those of other workers. For the reaction with ethanol there is agreement with some literature values but discrepancies with the only other study of the temperature dependence.

It is clear that further work is required to explain the discrepancy between the discharge flow results and the flash photolysis results.

Acknowledgments

We wish to acknowledge the award of a Commonwealth Postgraduate Scholarship to P.G.G. and valuable discussions with Associate Professor R. G. Gilbert.

Manuscript received 20 December 1985

[23] Ravishankara, A. R., Wine, P. H., and Wells, J. R., *J. Chem. Phys.*, 1985, **83**, 447.

Recombination Reactions: Variational Transition State Theory and the Gorin Model.

Paul G Greenhill

Department of Chemistry, University of Tasmania, GPO Box 252c, Hobart, Tasmania 7001, Australia

and Robert G Gilbert*

School of Chemistry, University of Sydney, NSW 2006, Australia

Submitted to the Journal of Physical Chemistry

Abstract

An easily-implemented means is given of calculating recombination rate coefficients using microcanonical variational transition state theory (μVTST) employing the potential function implicit in the Gorin model. The technique involves interpolation of the density of states of the activated complex between those at large values of the reactant coordinate and those at the stable product geometry. The use of μVTST plus interpolation overcomes the problem of inconsistencies inherent in the Gorin model as usually applied. Computational requirements are comparable to those for a conventional Gorin calculation. Applied to the recombination of methyl radicals, the results agree with current data, including the negative temperature dependence; this last is seen to arise in part because of contributions to the thermal rate from different transition states (present, because of μVTST, at different internal energies).

Introduction

Predictions of rate coefficients for recombination reactions (or their reverse, unimolecular dissociations with a "simple fission" transition state) are often carried out using the Gorin model.[1] This easily-applied theory contains parameters fitted to a large body of data and thus is moderately reliable for reactions related to those with which it has been parametrized. However, there are serious doubts about the validity of its theoretical basis.[2] On the other hand, variational transition state theory[3] (VTST) is theoretically rigorous, and is clearly the method of choice when using transition state theory. However, it is not easy to apply, especially to reactions involving many atoms. Similar problems arise with another sophisticated variational approach, the statistical adiabatic channel model[4] (although important steps forward here have recently appeared[5]).

We here show how microcanonical VTST can be readily applied to any system by employing the potential function that is implicit in the Gorin model. The main part of our treatment is to show how the problem of the change in character of the vibrational modes (from rotors to harmonic oscillators), which renders application of VTST difficult,[6] can be overcome. We do this by interpolating the density of states of the activated complex between two regions where it is easily calculated: moderate distances (where the complex can be represented as harmonic normal modes plus hindered rotors) and at the equilibrium geometry of product. The present technique enables

the mathematically rigorous microcanonical VTST to be implemented using readily available programs, and the computational requirements are not much more than those needed for a conventional Gorin calculation.

The Gorin model[1] involves two important assumptions. The first is the location of the activated complex at a centrifugal barrier: this assumption appears to be incorrect;[2] the success of the model despite this shortcoming is perhaps due to its parametrization to fit a large array of data. The second assumption is that the properties (especially the density of states) of the complex $AB^{\dagger}$ (for the reaction A+B→AB) can be calculated by assuming that $AB^{\dagger}$ has the vibrational frequencies of the separate A and B moieties, with the other degrees of freedom being internal rotors whose percent hindrances are found by treating each atom in A and B as hard spheres. It has been shown[2] that this does not yield a tightening of the hindered internal rotations to a proper bending vibration. It will be shown below that this objection can be overcome by use of the interpolation technique given in the next section.

It should be noted that this second assumption does in fact lead to a switch from hindered rotors to bending vibrations. It is equivalent to assuming that the potential consists of the sum of (1) a valence-force-field for the A and B moieties; (2) Lennard-Jones interactions between each non-bonded atom in A and B except for the two atoms where the bond will form; and (3) an appropriate interaction (Morse, say) for the atoms in A and B between which the bond forms.

This potential permits a tightening of the incipient bending vibration, because the non-bonding interactions cause the free rotors to become bends, albeit anharmonic ones, at close distances. The problem is that while this is qualitatively correct, the quantitative values of the bending frequencies so found are wrong; as stated, we shall overcome this by a novel interpolation method. While more precise μVTST calculations with similar potentials have been carried out,[6] such calculations would require considerable computational effort in systems involving many atoms. The innovations introduced here, while breaking no new theoretical ground, enable μVTST to be very easily implemented.

Method

In μVTST,[3] the transition state at each energy E is placed at that point on the reaction path where the sum of states of the activated complex is a minimum. One thus needs to determine the density of states of the complex as a function of the reaction coordinate s: $\rho_s^{\dagger}(E)$.

The present technique is as follows; up to a certain point, the development is quite standard.[2,3]

(1) The reaction coordinate is determined as the path of minimum energy, found as described elsewhere:[2] by running a trajectory starting at large s, with the translational energy set to zero every few time steps. This is readily implemented

with a publicly available program.[7]

(2) For each s, it is necessary to determine the density of states of the activated complex. The first step here is a normal mode analysis, with the reaction coordinate (s) held fixed. Note that this requires a determinination of the equilibrium geometry for each fixed value of s. This can be carried out with the same software as used for finding the reaction path.[7] With the assumed potential, this analysis yields a set of normal modes whose frequencies directly evolve from those of infinitely-separated A and B, plus some very low frequencies. Each of the latter corresponds to some linear combination of hindered internal rotors. A normal mode analysis for these is inappropriate. In our first innovation, we replace these low frequencies by hindered internal rotors: it is well established[1] that this is successful in reproducing the thermodynamic properties (and hence the densities of states) of systems with such degrees of freedom. The percent of hindrance of these rotors are determined from the geometry of each moiety with each atom represented by a hard sphere, with the moments of inertia then found in the usual way by diagonalization of the inertia tensor. One thus obtains two moments of inertia for each of A and B (assuming for convenience that neither are monatomic) plus a fifth reduced moment of inertia ($I = I_a I_b/(I_a+I_b)$ corresponding to torsional motion around the incipient bond (here I_a and I_b are the moments of inertia of A and B respectively around this bond axis[1]). Of course, given the vibrational frequencies plus moments of inertia of internal (hindered) rotors, evaluation of the density of states is straightforward.

(3) For small s, the frequencies from the normal mode analysis corresponding to these hindered rotors become larger, as the moieties come into close contact. While the frequencies now resemble those of bending vibrations, the potential is strongly anharmonic: specifically, it is a sum of Lennard-Jones potentials near their minimua. This strong anharmonicity renders a normal mode analysis invalid. Moreover, the contact between the moieties is now so close that a separation into hindered rotors is quite inapplicable. One cannot then use a normal mode analysis, with or without hindered rotors.

This problem has been overcome[6] by evaluating ϱ_s^T using essentially exact semi-classical methods on the non-separable potential. However, such calculations are complex, and difficult for large systems. In the second innovation of the present treatment, the problem of finding ϱ_s^T in this close interaction region is obviated as follows.

We note that $\varrho_s^T(E)$ is known precisely at short distances: when s is the <u>equilibrium</u> A-B distance, r_e. At $s = r_e$, ϱ_s^T is the density of states of the stable AB product calculated with the formed bond held rigid. Figure 1 shows $\varrho_s^T(E)$ for the recombination of two methyl radicals ($A = B = CH_3$), calculated as in (1) and (2) and with $\varrho_s^T(E)$ at the equilibrium distance found as just described using ethane force constants. The breakdown at smaller s of the method given in (1) and (2) is clearly seen: the values of ϱ^T so calculated fall orders of magnitude below the values at the equilibrium distance, which

is obviously physically incorrect. However, it is not unreasonable to suppose that, for each E, one can approximately interpolate $\varrho_s^{\dagger}(E)$ between the "well-behaved" values at large s and the equilibrium distance value (when $s = r_e$). A suitable interpolation is illustrated in Figure 1. The particular interpolation illustrated takes $ln(\varrho^{\dagger})$ to be linear in $ln(s-s_0)$ (where s_0 is some suitable value of s; s_0 = 0.4 nm in this case); the linearity is assumed to be obeyed between $s = r_e$ and a chosen value of s (s_c =0.35 nm in this case). Another interpolation procedure could require that the slope of $ln(\varrho^{\dagger})$ be continuous between s_c and r_e. Obviously, any number of reasonable interpolation methods for obtaining a continuous $\varrho^{\dagger}$ between s_c and r_e can be devised. The choice of interpolation method is not critical, since errors will be reduced by the integration required to yield the sum of states from $\varrho_s^{\dagger}(E)$.

This interpolation approximation enables $\varrho_s^{\dagger}(E)$ to be found very easily. One then finds $\varrho^{\dagger}(E)$ as the value of $\varrho_s^{\dagger}(E)$ at that s where the sum of states is a minimum. As is well known,[3] this may yield a different location of the transition state for each E.

The interpolation method is in the spirit of the statistical adiabatic channel model,[4] except that instead of potentials, we interpolate the density of states of the complex. This takes advantage of the fact that it is the sum of states ($\int \varrho^{\dagger}(E)\, dE$) rather than potentials that is actually required in the calculation of reaction rates.

Using the $\rho_s^T(E)$ so obtained, the specific (microscopic) rate is then calculated as in standard μVTST, i.e., from:

$$k(E) = \int_0^E \rho^T(E_+)\, dE_+ \;/\; h\rho(E)$$

where $\rho(E)$ the density of states of reactant and the lower bound in the integration is, for that value of E, the local minimum in the potential at the particular value of s where the sum of states is least. The thermal rate coefficient is found by only including k(E) values of E above the dissociation energy of AB.

This procedure is easily implemented using readily available programs,[7,8] and the computational requirements are not much more than that for the Gorin method.

Application

We illustrate the method for the reaction $CH_3 + CH_3 \rightarrow C_2H_6$. The frequencies of CH_3 and C_2H_6 are well known, and their potential functions can be accurately represented in terms of bond stretches, bends, torsions and wags. The non-bonded interactions between the atoms of each moiety are taken to be those of the corresponding inert gases (He and Ne Ar), using the usual combining rules. For the dissociation energy we take the value of 367 kJ mol^{-1} quoted by Wardlaw and Marcus;[6] as is well known,[9] the high-pressure recombination rate coefficient is not sensitive to this quantity. The only

unknown quantity in the potential is the interaction between the two carbon atoms. It was found that representing the C-C potential by a Morse interaction (with a β value chosen to yield the correct C-C vibrational frequency and dissociation energy at the equlibrium distance r_e) did not give agreement with current experiments.[10] Wardlaw and Marcus[6] have given an empirical expression for this interaction, but of a form that does not lend itself to the simple Gorin-type potential function which it is our object to assume here. We therefore adopt the following approach. For the reaction $H + CH_3 \rightarrow CH_4$, Duchovic and Hase[11] have used an *ab initio* potential for the C-H bond and expressed the potential as what they term a "stiff Morse" oscillator: a Morse potential where the quantity β is a function of bond length r. In dimensionless form, their distance-dependent β can be written:

$$\beta(r)/\beta_0 = 0.1711x^3 + 5.4\times10^{-2}x^2 - 6.18\times10^{-2}x + 1 \quad (1)$$

where β_0 is the Morse parameter calculated at r_e, and $x = [(r/r_e)-1]$. We assume here that eq 1 (which is obtained from an *ab initio* potential, rather than a semi-empirical one) is valid in its dimensionless form for kindred reactions such as that examined here (i.e., we adopt a corresponding states hypothesis). This completes the specification of all the parameters required in the present treatment.

The calculated and experimental[10] values for the high-pressure recombination rate coefficient are shown in Table 1.

The agreement between the present treatment and experiment is regarded as most satisfactory, particularly since the model contains no adjustable parameters. As will be discussed later, the observed negative temperature dependence is reproduced, although the model predicts a slightly stronger dependence than is seen in the data. Exact accord with the data could be obtained by empirically adjusting the C-C interaction potential, but this is not felt to be necessary.

Discussion

It is noteworthy that (at that energy E contributing most to the recombination rate at 450 K) the transition state is found from the $\rho_s^{\dagger}(E)$ to be at s = 0.35 nm. While this value is consistent with other VST calculations,[2,3,11] it is smaller than that in the usual Gorin treatments. This discrepancy may arise from the above-mentioned inconsistencies in the latter.[2]

A most important point (which is a characteristic of a microcanonical treatment) is that, except at low temperatures, a significant range of transition states (over 0.35 to 0.3 nm) contribute to the thermal rate. It is this spread of transition states that is largely responsible for the calculated negative temperature dependence, in accord with experiment.[10] This spread of transition states is an essential feature of μVTST (as distinct from canonical versions which only have a single transition state). This suggests that it is important to employ a microcanonical formulation for reactions of this type; we note that technically this is not much more

difficult than the canonical approach, since only minor coding changes are required in a conventional RRKM program.

The present model is easily applied and combines mathematical rigor with that part of the Gorin model which is physically reasonable. The main aspect of the present development is that (through the interpolation approximation for the density of states) it enables a rigorous calculation of rate coefficients for recombination or simple-fission dissociation reactions to be carried out with virtually the same ease as a Gorin calculation, but without any empirical parameters. If future tests show that acceptable agreement with experiment can be obtained for a wide range of reactions, the methodology would be of significant practical use.

Acknowledgements. Enlightening conversations with Professors Bill Hase and Don Truhlar are gratefully acknowledged, as is the support of the Australian Research Grants Scheme.

TABLE I: Calculated and Experimental[10] High-Pressure Recombination Rate Coefficients.

Temperature (K)	Recombination Rate Coefficient (10^{-11} cm^3 s^{-1})	
	Calculated	Experimental
300	6.8	6.5±0.2
450	3.1	5.6±0.4
600	2.5	5.1±0.3

References

(1) Benson, S.W., "Thermochemical Kinetics", 2nd Edn., Wiley, New York, 1976; *idem.*, Canad. J. Chem., 1983, 61, 881.

(2) Garrett, B.C.; Truhlar, D.G., J. Am. Chem. Soc., 1979, 101, 4534; Rai, S.N.; Truhlar, D.G., J. Chem. Phys. 1983, 79, 6046.

(3) Truhlar, D.G.; Garrett, B.C., Ann. Rev. Phys. Chem. 1984, 35, 159.

(4) Quack, M.; Troe, J., Ber. Bunsenges. Physik. Chem. 1977, 81, 329; *idem.*, Chem. Soc. Spec. Period. Rept. Gas Kinet. Energy Transfer, 1977, 2, 175; Troe, J., J. Chem. Phys., 1983, 79, 6017.

(5) Cobos, C.J.; Troe, J., J. Chem. Phys. 1985, 83, 1010.

(6) Wardlaw, D.M.; Marcus, R.A., J. Chem. Phys. 1985, 83, 3462.

(7) Hase, W.L., Quantum Chem. Prog. Exchange 1983, 3, 14.

(8) Gilbert, R.G., Quantum Chem. Prog. Exchange 1983, 3, 64.

(9) See, for example, Gilbert, R.G.; McEwan, M.J., Aust. J. Chem. 1985, 38, 231.

(10) Macpherson, M.T.; Pilling, M.J.; Smith, M.J.C., J. Phys.

Chem. 1985, 89, 2268.

(11) Duchovic, R.J.; Hase, W.L., J. Chem. Phys. 1985, 82, 3599; Hase, W.L.; Duchovic, R.J., *idem*. 1985, 83, 3448.

Figure Caption

Figure 1. Density of states of complex [as $ln(\rho_s^{\dagger}(E)/cm^{-1})$] as a function of reaction coordinate s, for energies E = 2000 (full line), 3000 (----) and 4000 (···) cm^{-1} above the local potential minimum. Right-hand lines are calculated from normal mode/hindered rotor analysis; left-hand lines are interpolated to the values of $\rho_s^{\dagger}$ at $s = r_e$ (points).

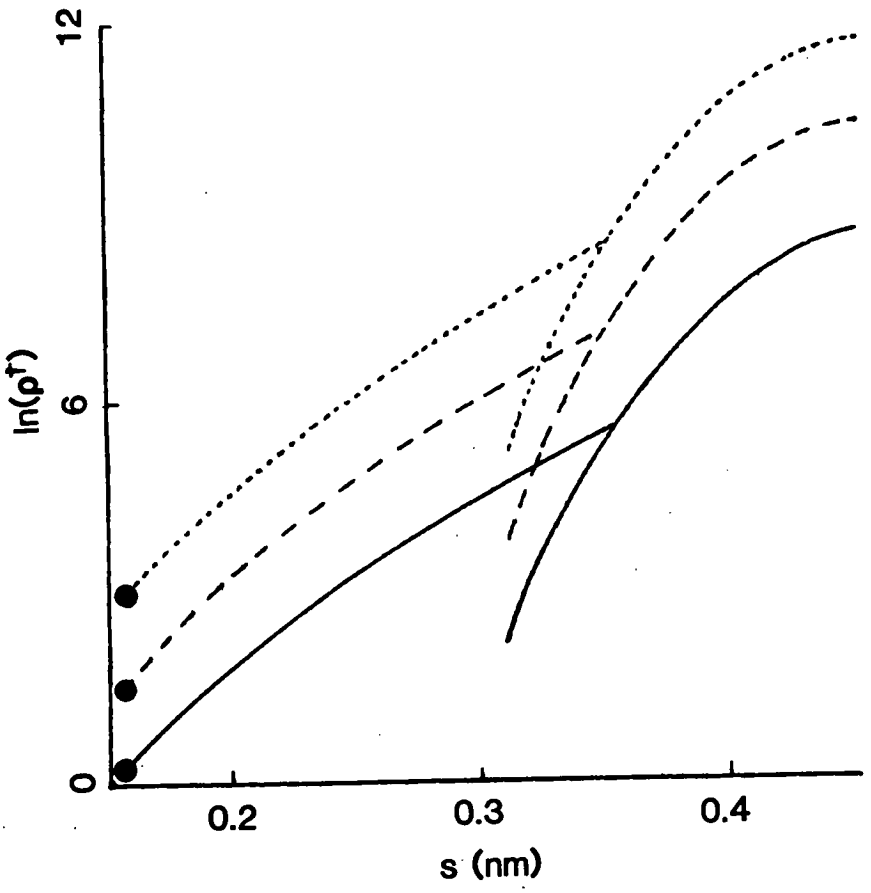
12
6
0
ln(ρ')
0.2
0.3
0.4
s (nm)

Aust. J. Chem., 1986, 39, 1929–42

Theoretical Prediction of CH_3O and CH_2OH Gas Phase Decomposition Rate Coefficients*

Paul G. Greenhill,[A] *Barry V. O'Grady*[A] *and Robert G. Gilbert*[B]

[A] Department of Chemistry, University of Tasmania,
P.O. Box 252C, Hobart, Tas. 7001.
[B] Department of Theoretical Chemistry, University of Sydney, N.S.W. 2006.
Author to whom correspondence should be addressed.

Abstract

Theoretical predictions are made for the pressure and temperature dependences of two reactions involved in methanol combustion: (A) $CH_3O \rightarrow CH_2O + H$ and (B) $CH_2OH \rightarrow CH_2O + H$. The calculations are carried out by using RRKM theory with a Gorin model for the activated complexes, with fall-off effects being taken into account by using the master equation. Results for the high-pressure rate coefficients (s^{-1}) are (A) $3\times10^{14}\exp(-108\text{ kJ mol}^{-1}/RT)$, (B) $7\times10^{14}\exp(-124\text{ kJ mol}^{-1}/RT)$ at 1000 K. For the low-pressure limiting rate coefficient ($cm^3\ s^{-1}$) over the range 600–1000 K (A) $8\times10^{-9}\exp(-90\text{ kJ mol}^{-1}/RT)$; (B) $2\times10^{-8}\exp(-108\text{ kJ mol}^{-1}/RT)$. At 1000 K, the pressure at which the fall-off rate coefficients are one-half of their limiting high-pressure values are 3×10^8 Pa for both reactions. Formulae for inclusion of these reactions (including fall-off effects) over the range 300–2000 K and 10^{-2}–10^6 Pa in modelling complex kinetic schemes are presented.

Introduction

The accurate modelling of complex combustion processes has become routine, using numerical solution of stiffly coupled differential equations in many variables. An important application of this modelling involves exploration of alternatives to petroleum based fuels, which has stimulated interest in the reaction kinetics of alcohols. The improvement in fuel technology which is made possible by such modelling studies is, however, contingent on the accuracy of the rate parameters used. A major problem here is that it is frequently impossible to obtain experimental data on some of the component reactions free from ambiguities induced by uncertainties in the rate parameters for other reactions. However, the present status of the theory of unimolecular and termolecular reactions is such that for many cases of interest one should be able to predict rate parameters to an accuracy quite acceptable for modelling studies. For example, the methods used in the present paper have (with some simplifications, such as ignoring weak collision effects) been used in an extensive theoretical study by Smith and Golden[1] of reactions of stratospheric importance.

In the present paper, we examine reactions which are kinetically significant in the combustion of methanol (which is an important alternative liquid fuel). We carry

* This paper is dedicated to Bob Schoenfeld, formerly Managing Editor of the Australian Journal of Chemistry, whose masterly editorship has made a real contribution to science in Australia.

[1] Smith, G. P., and Golden, D. M., *Int. J. Chem. Kinet.*, 1978, 10, 489.

0004-9425/86/121929$02.00

out theoretical calculations of the appropriate rate parameters, based on techniques which should provide rate coefficients which are accurate to within a factor of two or better. The resulting kinetic parameters will be of use in current overall modelling studies and also in indicating experimental techniques which can later be used for the direct observation of the elementary rates of the reactions studied. An important aspect of the present paper is that the techniques are described in sufficient detail so as to facilitate application to other systems of interest.

In the combustion of methanol, the initiating reactions are:[2]

$$O_2 + CH_3OH \rightarrow CH_2OH + HO_2$$

and (at very high temperatures):

$$CH_3OH \rightarrow CH_3 + OH \quad (1)$$

These are then followed by a large number of free-radical reactions such as

$$CH_3 + HO_2 \rightarrow CH_3O + OH$$

Very little is known about the mechanism and rates of the subsequent reactions of two of the primary products, viz., the methoxy and hydroxymethyl radicals. The fate of these two radicals is still largely uncertain and has not hitherto been addressed either in systems at lower temperatures where elementary bimolecular processes are usually studied or at combustion temperatures. However, it is just these conditions where the fate of these radicals is critical in influencing the distribution of species formed at later reaction times. Several modelling studies over the last ten years[2,3] have tried with varying degrees of success to model the high temperature oxidation of methanol. Now, the formation of the methoxy radical has recently been shown[4] to be the dominant pathway in the attack of hydroxyl radicals on methanol at higher temperatures. In previous studies, loss processes of methoxy and hydroxymethyl were restricted to unimolecular decomposition and bimolecular attack by oxygen. This has led to a number of inconsistencies. For example, the rate parameters used for the unimolecular losses in the study by Westbrook and Dryer[2] (from estimates of the bond dissociation energies) have very low activation energies. These appear to be too low for the processes involved (even though these reactions would in fact be well into the fall-off regime, and thus the activation energies somewhat lower than the critical energies[5]). It is apparent that progress in understanding methanol combustion would be aided by reliable estimates for the rate coefficients for the thermal decomposition of methoxy and of hydroxymethyl:

$$CH_2OH \rightarrow CH_2O + H \quad (2)$$

$$CH_3O \rightarrow CH_2O + H \quad (3)$$

[2] Westbrook, C. K., and Dryer, F. L., *Combust. Sci. Technol.*, 1979, **20**, 125.
[3] Bowman, C. T., *Combust. Flame*, 1975, **25**, 343; Vandooren, J., and Van Tiggelen, P. J., 18th Symp. (Int.) Combustion, 1980, 473; Aronowitz, D., Santoro, R. J., Dryer, F. L., and Glassman, I., 17th Symp. (Int.) Combustion, 1979, 633.
[4] Hagele, J., Lorenz, K., Rhasa, D., and Zellner, R., *Ber. Bunsenges. Phys. Chem.*, 1983, **87**, 1023; Meier, U., Grotheer, H. H., and Just, Th., *Chem. Phys. Lett.*, 1984, **106**, 97.
[5] Gilbert, R. G., and Ross, I. G., *J. Chem. Phys.*, 1972, **57**, 2299.

In this paper we calculate rate parameters *a priori* for these reactions. At present, no direct experimental data on their rate parameters are available. However, the current status of predictive theories for unimolecular and recombination processes is such that *a priori* calculations of the rate coefficients for such reactions should be accurate to within a factor of 2 or better. The techniques which will be used here have not been hitherto applied systematically to the analysis of any of the multitude of reactions involved in combustion systems.

The present paper has two objectives: (i) the actual calculation of the rate parameters involved, and (ii) to set out precisely how these theoretical calculations are carried out (one notes that comparatively little effort is involved in such calculations). It is thus hoped that the current practise of simply 'guesstimating' rate parameters for unknown reactions in multiple reaction systems will be replaced by a more scientific approach.

Theoretical Background and Techniques

Unimolecular decomposition and bimolecular recombination reactions typically make up some two-thirds of the reaction types in complex kinetic modelling schemes. Although we do not consider recombination reactions here, it is useful to note that the rate coefficients for the reactions AB → A+B and A+B → AB are exactly related by microscopic reversibility (e.g.[6,7]):

$$k_{rec}/k_{uni} = 5{\cdot}33\times10^{-21}\frac{Q_{AB}}{Q_A Q_B}\left[\frac{M_A+M_B}{T M_A M_B}\right]^{3/2}\exp(\Delta H_0^\circ/k_B T) \qquad (4)$$

where k_{rec} is the recombination rate coefficient (in $cm^3\ s^{-1}$), k_{uni} the unimolecular rate coefficient (in s^{-1}), the various Q are (internal) partition functions, k_B is Boltzmann's constant, T is the temperature (K), the various M are molecular weights (a.m.u.), and ΔH_0° is the difference in zero point energy between reactant and products. The numerical constant in equation (4) arises from the units employed in evaluating the translational partition function.

The value of k_{uni} at any pressure can be calculated exactly from the solution to the integral eigenvalue master equation (e.g.[8,9]):

$$-g(E)k_{uni} = \omega\int_0^\infty [P(E,E')g(E') - P(E',E)g(E)]\,dE' - k(E)g(E) \qquad (5)$$

where ω is the collision frequency (e.g., gas-kinetic hard sphere or Lennard-Jones), $P(E, E')$ is the probability of collisional excitation from a state with internal energy E' to one with E, $k(E)$ is the microscopic reaction rate at energy E, and the eigenfunction $g(E)$ is the population of molecules with energy E. Equation (5) gives complete account of fall-off effects (i.e., the variation of the rate coefficient from the

[6] Troe, J., *J. Phys. Chem.*, 1979, **83**, 114.
[7] Gilbert, R. G., and McEwan, M. J., *Aust. J. Chem.*, 1985, **38**, 231.
[8] Tardy, D. C., and Rabinovitch, B. S., *Chem. Rev.*, 1977, **77**, 369.
[9] Quack, M., and Troe, J., in 'Gas Kinetics and Energy Transfer' (Eds P. G. Ashmore and R. J. Donovan) Vol. 2, p. 175 (The Chemical Society: London 1977); Holbrook, K. A., *Chem. Soc. Rev.*, 1983, **12**, 163.

high to the low pressure limiting values). As is well known (e.g.[10]), equation (5) has simple limiting forms in the high and low pressure limits.

Given $k(E)$ and $P(E,E')$, the solution to equation (5) can be readily obtained by using a standard technique on a publicly available computer program[11] that has minimal requirements of computer time and storage. Note incidentally that the use of equation (5) in the low pressure limit for reactions which can proceed via several channels has apparently not been presented hitherto; although not employed in the present paper, the requisite expression (which will be of real value in theoretical rate calculations) is derived in the Appendix.

A reliable *ab initio* prediction for $k(E)$ can be made by means of RRKM theory,[12] viz.,

$$k(E) = \int_{E_0}^{\infty} \rho^{\dagger}(E_+)\,\mathrm{d}E_+ / h\rho(E) \qquad (6)$$

Here E_0 is the critical energy for reaction, h is Planck's constant, and $\rho(E)$ and $\rho^{\dagger}(E)$ are the densities of states of the parent molecule (AB) and of the activated complex ($AB^{\dagger}$) respectively. Given the requisite properties of the reactant molecule and of the transition state, $k(E)$ can be readily computed, for example by using standard programs.[10] All that is needed[12] is to specify the following properties of the reactant molecule and of the transition state: the vibrational frequencies (usually all vibrations are assumed harmonic), the moments of inertia of any internal rotations (free or hindered, and the degree of hindrance in the latter case), the overall moment of inertia (and whether or not the rotational degree of freedom along the reaction coordinate is to be treated as active[12-14]) and the symmetry number.

The requisite physical parameters describing the reactant molecule are usually available from spectroscopic, *ab initio* and/or thermodynamic data. In theoretical prediction of rate data, it is essential to ensure that the transition state postulated is of a physically and chemically reasonable form (for example, bond fission implies a loose transition state). The critical energy E_0 can then be estimated from bond enthalpies using extensive tabulated data.[15] For multi-centre activated complexes, reliable semi-empirical means of estimating the requisite parameters of the transition state (and of the parent molecule, if spectroscopic or *ab initio* data are not available) have been developed.[15] The situation with regard to reliable semi-empirical estimation of requisite parameters for a simple fission activated complex (as is the present case) is less simple, as now discussed.

We now turn to the evaluation of rate parameters for reactions (2) and (3). Both have the same type of activated complex, viz., a simple fission. Now, a number of means of calculating the $k(E)$ for such a system have been developed. The simplest is the Benson semi-empirical Gorin approach.[15] However, it has been proven[16-18]

[10] Gilbert, R. G., and Ross, I. G., *Aust. J. Chem.*, 1971, **24**, 1541.
[11] Gilbert, R. G., *Quant. Chem. Program Exch.*, 1983, **3**, 64.
[12] Robinson, P. J., and Holbrook, K. A., 'Unimolecular Reactions' (John Wiley: London 1972).
[13] Forst, W., 'Theory of Unimolecular Reactions' (Academic Press: New York 1973).
[14] Troe, J., *J. Chem. Phys.*, 1977, **66**, 4758.
[15] Benson, S. W., 'Thermochemical Kinetics' 2nd Edn (John Wiley: New York 1976).
[16] Garrett, B. C., and Truhlar, D. G., *J. Am. Chem. Soc.*, 1979, **101**, 4534; Rai, S. N., and Truhlar, D. G., *J. Chem. Phys.*, 1983, **79**, 6046; Bunker, D. L., and Pattengill, M., *J. Chem. Phys.*, 1968, **48**, 772.
[17] Hase, W. L., *J. Chem. Phys.*, 1976, **64**, 2442; *Acc. Chem. Res.*, 1983, **16**, 258.
[18] Greenhill, P. G., and Gilbert, R. G., *J. Phys. Chem.*, 1986, **90**, 3104.

that the theoretical basis for this model is incorrect. A number of theoretically rigorous alternatives to the Gorin model are now available,[16-20] based on variational procedures. However, usually these are relatively difficult to implement. Although two recent advances[18,20] have resulted in a considerable diminution of the problem, standard computer programs for the implementation of variational transition state theory[16-18] or the statistical adiabatic channel model[19,20] are not yet available. Because our aims here include illustrating the implementation of current rate theory using readily available tools (especially standard computer programs), we chose for the present purpose to employ the common Gorin model for the transition state.[15] Extensive semi-empirical rules have been developed for the transition state parameters by comparison with a very large body of data, and thus pragmatically any physical deficiencies of the theory are likely to yield $k(E)$ (by cancellation of errors) which are

Table 1. Rice–Ramsperger–Kassel–Marcus (RRKM) parameters for all reactions
B value is the rotational constant; E_0 is the critical energy

Frequencies (cm^{-1}) (i)	(ii)	Rotations	*B* values (cm^{-1})[A] (i)	(ii)	E_0 (kJ mol^{-1})
		CH_3O (i) and transition state (ii) [reaction (3)]			
3320[B]	2977[G]	ext. inactive	0·876 (1,2)[C]	1·317 (1,2)[C]	100·4
3311[B]	2844[G]	ext. active	5·495 (1,1)[C]	0·745 (1,1)[C]	
3216[B]	1744[G]	internal		110·0 (2,2)[E]	
1657[B]	1503[G]				
1599[B]	1280[G]				
1582[B]	1160[G]				
1159[B]					
1064[B]					
717[B]					
		CH_2OH (i) and transition state (ii) [reaction (2)]			
3650[D]	2977[G]	ext. inactive	0·944 (2,2)[C]	0·755 (2,2)[C]	121·3
2960[D]	2844[G]	ext. active	6·470 (1,1)[C]	2·583 (1,1)[C]	
2885[D]	1744[G]	internal		7·093 (2,2)[F]	
1459[D]	1280[G]				
1334[D]	1160[G]				
1183[D]	1503[G]				
1048[D]					
569[D]					
420[D]					

[A] Parenthetic quantities are symmetry number and dimension respectively.
[B] Methoxy frequencies from Colwell, S. M., Amos, R. D., and Handy, N. C., *Chem. Phys. Lett.*, 1984, **109**, 525.
[C] Calculated from geometry using conventional bond distances.
[D] Hydroxymethyl frequencies from Saebø, S., Radom, L., and Schaeffer, H. F., *J. Chem. Phys.*, 1983, **78**, 845.
[E] Formaldehyde two-dimensional hindered rotation; incorporates hindrance angle $\theta = 28·5°$. Geometry from CH_3O---H transition state.
[F] Formaldehyde two-dimensional hindered rotation; incorporates hindrance angle $\theta = 88·0°$. Geometry from CH_2O---H transition state.
[G] Formaldehyde frequencies.

[19] Quack, M., and Troe, J., *Ber. Bunsenges. Phys. Chem.*, 1974, **78**, 240; 1975, **79**, 170; Troe, J., *J. Chem. Phys.*, 1981, **75**, 226.
[20] Cobos, C. J., and Troe, J., *J. Chem. Phys.*, 1985, **83**, 1010.

of acceptable accuracy for purposes such as combustion modelling. The Gorin model is particularly simple to apply because the requisite parameters are easily available or calculated.

The assumptions in the Gorin model are as follows. The critical energy for recombination for the reactions studied are taken as 8 kJ mol^{-1}, in keeping with theoretical and experimental evidence[21] that the $H+C_2H_4$ recombination has an activation barrier of approximately 8 kJ mol^{-1}. Thus the critical energy for the forward reaction (AB $\rightarrow$ A+B) is given by ΔH_0°+8 kJ mol^{-1}. The transition state is assumed to be made up of two free or hindered rotors whose vibrational frequencies are those of the isolated A and B moieties. In the case of reactions (2) and (3), moiety A is formaldehyde (whose vibrational frequencies and moments of inertia are well known), and moiety B is an H atom; the vibrational frequencies and geometries of the reactants (CH_2OH and CH_3O) are available from spectra and from *ab initio* calculations (see Table 1). The vibrational frequencies for the reactants and activated complexes involved in the present systems are listed in Table 1, along with the sources of each frequency (spectroscopic or *ab initio*).

In addition to the vibrational frequencies, there are some degrees of freedom in the activated complex (corresponding to deformation modes in the parent AB molecule) which are treated as two-dimensional hindered rotors. If either A or B is an atom (as is the case in the systems studied here), one has a single two-dimensional rotor to consider (whose moment of inertia I_r is determined from individual components I_a and I_b as shown below); if both are non-monatomic, one has instead two two-dimensional internal rotors with moments of inertia I_a and I_b.

In the Gorin model, the bond broken has in the activated complex a length $r^\dagger$ separating the two moieties whose value is taken to be the bond length at the centrifugal barrier to recombination. A number of methods for estimating $r^\dagger$ are available.[14,15,22] We adopt here the recipe of Benson[22] which (although obtained using dubious arguments) has been chosen to give agreement with extensive data and should thus be adequate for the present purpose. In this model, $r^\dagger$ is taken to be 2·8 times the normal bond length. It should be noted that the preferred (but more involved) microcanonical variational transition state theory[16–18] yields an $r^\dagger$ which is a function of E (or, in the canonical version, a function of temperature); for reasons explained above, we ignore this refinement here.

The moments of inertia of the two-dimensional hindered rotors whose motion corresponds to the AB deformations are found by allowing the separate A and B moieties to bend until the two come into van der Waals contact. One defines[15] the angle θ as that subtended when these moieties so bend. The equivalent solid angle $\Delta\Omega$ is given by

$$\Delta\Omega/4\pi = (1-\cos\theta)/2 \qquad (7)$$

This factor which takes the hindrance into account is then used to adjust the moment of inertia of the internal rotor(s) by replacing the moment of inertia of the free rotor (I) by $(\Delta\Omega/4\pi)I$.

[21] Hase, W. L., and Schlegel, H. B., *J. Phys. Chem.*, 1982, **86**, 3901; Sugawara, K., Okazaki, K., and Sato, S., *Bull. Chem. Soc. Jpn*, 1981, **54**, 2872.
[22] Benson, S. W., *Can. J. Chem.*, 1983, **61**, 881.

If we have a transition state complex of the form:

A- - - - -B

then both moieties have three principal moments of inertia I_a, I_b and I_c values associated with them such that the two (I_a and I_b) corresponding to the two-dimensional internal rotation about the symmetry axis are identical (or very similar) and the other (I_c) is different. For the case where one of A or B is an atom (as in the systems studied here), the two-dimensional moment of inertia for the free internal rotation is replaced by the reduced moment, I_r, where

$$I_r = I_A I_B/(I_A + I_B) \tag{8}$$

where (if B is the monatomic species) I_A is the moment of top A about its symmetry axis and I_B is the moment of B about the centre of mass of A. Specific illustrations have been given elsewhere.[15] The hindrance [i.e., the angle θ in equation (7)] can be obtained from the hard-sphere geometries analytically or by using solid models. All moments of inertia were calculated exactly from the experimental or *ab initio* geometries. They are listed in Table 1 (where the factor $\Delta\Omega/4\pi$ is included in all D, along with the values of θ.

Finally, in considering the rotational degrees of freedom, it is important to note in cases such as the present (where there is a large difference in the moments of inertia of parent molecule and activated complex) that one of the *external* moments of inertia is 'active', i.e., that it must be treated as an internal degree of freedom; this is simply because[14] the K quantum number in rotation is not conserved in a non-rigid molecule, but can exchange energy with the vibrational degrees of freedom. I_c, the moment of inertia of the overall rotation (of molecule and of activated complex) corresponding to this quantum number, is identified as that one of the three external moments of inertia which is not equal to (or well separated from) the other two.

The values for the various rotational degrees of freedom for the systems under study are listed and explained in Table 1. This completes the specification of the $k(E)$.

We now consider how the collisional energy exchange term $P(E,E')$ can be specified. It is now well established that the convenient strong collision approximation is quite inadequate (even when allowance is made for 'inefficient' collisions through a collision efficiency). One should always use the more physically acceptable weak collision model, and indeed its implementation through an exact solution of the master equation, equation (5), is now very simple. The solution of equation (5) [and evaluation of $k(E)$ through equation (6)] is easily effected through standard programs.[10]

It now remains to consider the form and parameters of $P(E,E')$. The formulation of a general reliable theory for this quantity has been the subject of considerable recent effort. An important step in this direction has been made in the form of the 'biased random walk' theory.[23,24] This theory can be applied either in semi-empirical[23] or *a priori*[24] forms. While the former is trivial to implement, the expressions for

[23] Gilbert, R. G., *J. Chem. Phys.*, 1984, **80**, 5501.
[24] Lim, K. F., and Gilbert. R. G., *J. Chem. Phys.*, 1986, **84**, 6129.

where the dimensionless 'combined broadening factor' F at any pressure is given by

$$\log F(k') = \log F_{cent} / \left(1 + \left[\frac{\log(k') + c}{N - d\{\log(k') + c\}}\right]^2\right) \quad (12)$$

where the parameters c, N and d are given by:

$$c = -0{\cdot}4 - 0{\cdot}67 \log F_{cent} \qquad N = 0{\cdot}75 - 1{\cdot}27 \log F_{cent} \qquad d = 0{\cdot}14 \quad (13)$$

and $k' = k_0[M]/k^\infty$ (i.e., k' is a dimensionless pressure). The values of F_{cent} for each temperature [determined from exact numerical solution of equation (5)] are given in Tables 2 and 3. The value of k_{uni} (and hence k_{rec}) at any pressure may be explicitly calculated from equations (10)–(13). If required, these expressions can be used to calculate apparent Arrhenius parameters at any given pressure.

A further useful quantity to examine is the collision efficiency. For a given unimolecular reaction, one defines the collision efficiency β_c as the ratio of the true low-pressure limiting rate [from solution of equation (5) in the low-pressure limit, as in equation (17) in the Appendix] to that calculated from the strong collision formula; the values of β_c are given in Tables 2 and 3 for representative temperatures. Note that the value of β_c is not actually required in evaluating k_{uni} at any given pressure by means of equations (10)–(13); values of β_c are merely given in Tables 2 and 3 for comparison purposes.

Having given the pressure and temperature dependences of the calculated rate coefficients, we now proceed to discuss the implications of our results.

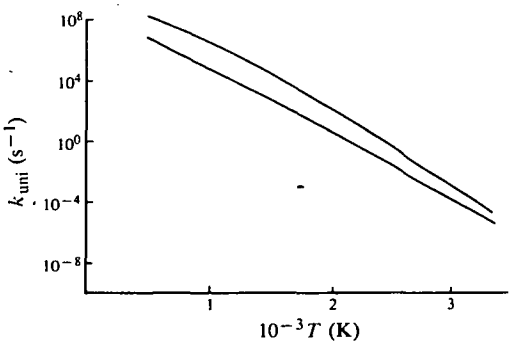

Fig. 3. Temperature dependence of the rate coefficient for $CH_3O \rightarrow CH_2O + H$ at $1{\cdot}3 \times 10^5$ Pa (*c.* at 10^3 Torr) as calculated here (upper curve) and as used by Westbrook and Dryer[2] (lower curve).

Unimolecular Dissociation of Methoxyl

The decomposition of the methoxy radical is predicted to be in the fall-off regime over the entire range for which calculations were performed, i.e., from 300 to 2000 K at pressures between 10^2 to 10^6 Pa ($0{\cdot}75$–$0{\cdot}75 \times 10^4$ Torr). Over the range 1000–2000 K and 10^3–10^5 Pa, the apparent activation energy (as determined from the slope of an Arrhenius plot at a fixed pressure) did not show significant variation (from 61·3 to 61·0 kJ mol^{-1}); however, the calculated apparent A factors at a given pressure varied from 2×10^7 to 2×10^9 s^{-1}. The most significant result is that the calculated coefficients at elevated temperatures are significantly higher than those used by Westbrook and Dryer:[2] for example, at 1000 K and $1{\cdot}3 \times 10^5$ Pa (10^3 Torr), the difference is a factor

of 70. Some Arrhenius plots comparing the rate coefficients as used by Westbrook and Dryer and those calculated here at $1{\cdot}3\times10^5$ Pa are shown in Fig. 3; this pressure is typical of that used in the modelling studies in ref. 2.

The high-pressure activation energy obtained from the RRKM calculation is 108 kJ mol^{-1} at 1000 K. The apparent activation energies calculated from the fall-off data will of course be less than this because of the depletion in the populations of the energy states close to the critical energy;[5] that is, the highest energy states below the critical energy have severely non-equilibrium populations. This effect is greatest for small collision efficiencies. At 1000 K, the collision efficiency is 0·10, and at 2000 K this falls to $\beta_c = 0{\cdot}05$. It is obvious that in modelling studies fall-off behaviour must be taken into account for these dissociations.

Unimolecular Dissociation of Hydroxymethyl

Similar comments apply to the results for the dissociation of the hydroxymethyl radical. The apparent activation energies at the different pressures are up to 40 kJ mol^{-1} below the high pressure activation energies, and show a strong temperature dependence. The collision efficiencies are also very low, β_c having values at 1000 K of 0·11, and at 2000 K, $\beta_c = 0{\cdot}06$. As before, the results indicate a very large difference between our calculated values and the rate parameters used by Westbrook and Dryer. Fig. 4 compares the rate coefficients at $1{\cdot}3\times10^5$ Pa from the present calculations and from ref. 1 in an Arrhenius plot.

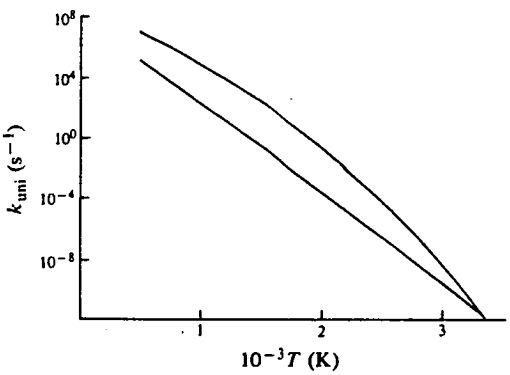

Fig. 4. Temperature dependence of the rate coefficient for $CH_2OH \rightarrow CH_2O+H$ at $1{\cdot}3\times10^5$ Pa (*c.* at 10^3 Torr) as calculated here (upper curve) and as used by Westbrook and Dryer[2] (lower curve).

Conclusions

In the present paper we have made some *ab initio* estimates of the rates of some reactions which are likely to be important in both high temperature oxidation of methanol and the systems used in the study of the elementary kinetics of methanol. RRKM theory and solution of the master equation have enabled us to examine the validity of some rate coefficients currently in use;[2] our studies show that these earlier values are likely to be quite incorrect. Fall-off effects play an important role in the values of their rate coefficients at commonly used pressures and temperatures.

An important area for future work is to employ the rate parameters generated in this theoretical study in modelling studies of the type pioneered by Westbrook and Dryer.

Appendix

We here give (apparently for the first time) the generalization of the low-pressure limit of equation (5) to include multiple channel reactions.

If one has channels $i = 1, 2, \ldots$, then each has a corresponding $k_i(E)$. The $k(E)$ in equation (5) is then the total microscopic rate:

$$k(E) = \sum_i k_i(E) \tag{14}$$

The overall rate coefficient for channel i, $k^i{}_{\text{uni}}$, is then given by

$$k^i{}_{\text{uni}} = \int_0^\infty k_i(E)\, g(E)\, \mathrm{d}E \Big/ \int_0^\infty g(E)\, \mathrm{d}E \tag{15}$$

where the $g(E)$ is evaluated as the eigenfunction in equation (5).

In the low-pressure limit, it is readily shown (e.g.[5]) that equation (5) takes the form:

$$-g(E)k_0 = \int_0^{E_0} [P(E, E')g(E') - P(E', E)g(E)]\, \mathrm{d}E' - g(E) \int_{E_0}^\infty P(E', E)\, \mathrm{d}E' \tag{16}$$

where $k_0 = k_{\text{uni}}/\omega$ is the total low-pressure limiting rate coefficient (expressed for convenience in dimensionless form). In the low-pressure limit, the equivalent of equation (15) for the total rate coefficient from all channels is:

$$k_0 = \int_0^{E_0} g(E) \left(\int_{E_0}^\infty P(E', E)\, \mathrm{d}E' \right) \mathrm{d}E \Big/ \int_0^{E_0} g(E)\, \mathrm{d}E \tag{17}$$

for the i^{th} channel, the low-pressure limiting rate coefficient is given by

$$k_0{}^i = \int_0^{E_0} g(E) \left(\int_{E_0}^\infty P(E', E)\, p_i(E')\, \mathrm{d}E' \right) \mathrm{d}E \Big/ \int_0^{E_0} g(E)\, \mathrm{d}E \tag{18}$$

where here E_0 refers to the critical energy for the i^{th} channel, and the probability of reacting into the i^{th} channel in the low-pressure limit, $p_i(E)$, is given by

$$p_i(E) = k_i(E)/k(E) \tag{19}$$

Equation (19) has apparently not been given hitherto, although its derivation is an obvious generalization of equations (14)–(18).

Acknowledgments

We are pleased to acknowledge helpful discussion with Dr Leo Radom, and some most perceptive comments from Dr Keith Ryan.

Manuscript received 15 May 1985